

(Anti-)(hyper-)nuclei production with ALICE at the LHC

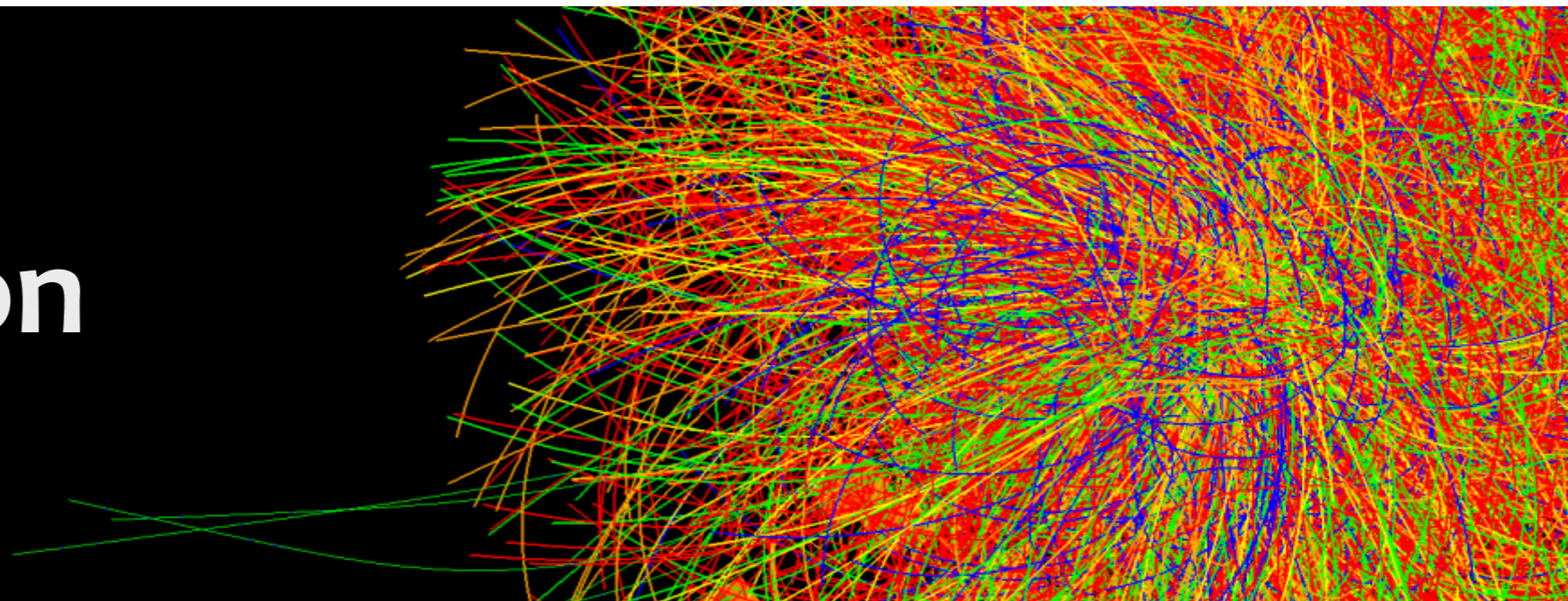
Stefano Trogolo

University and INFN - Torino



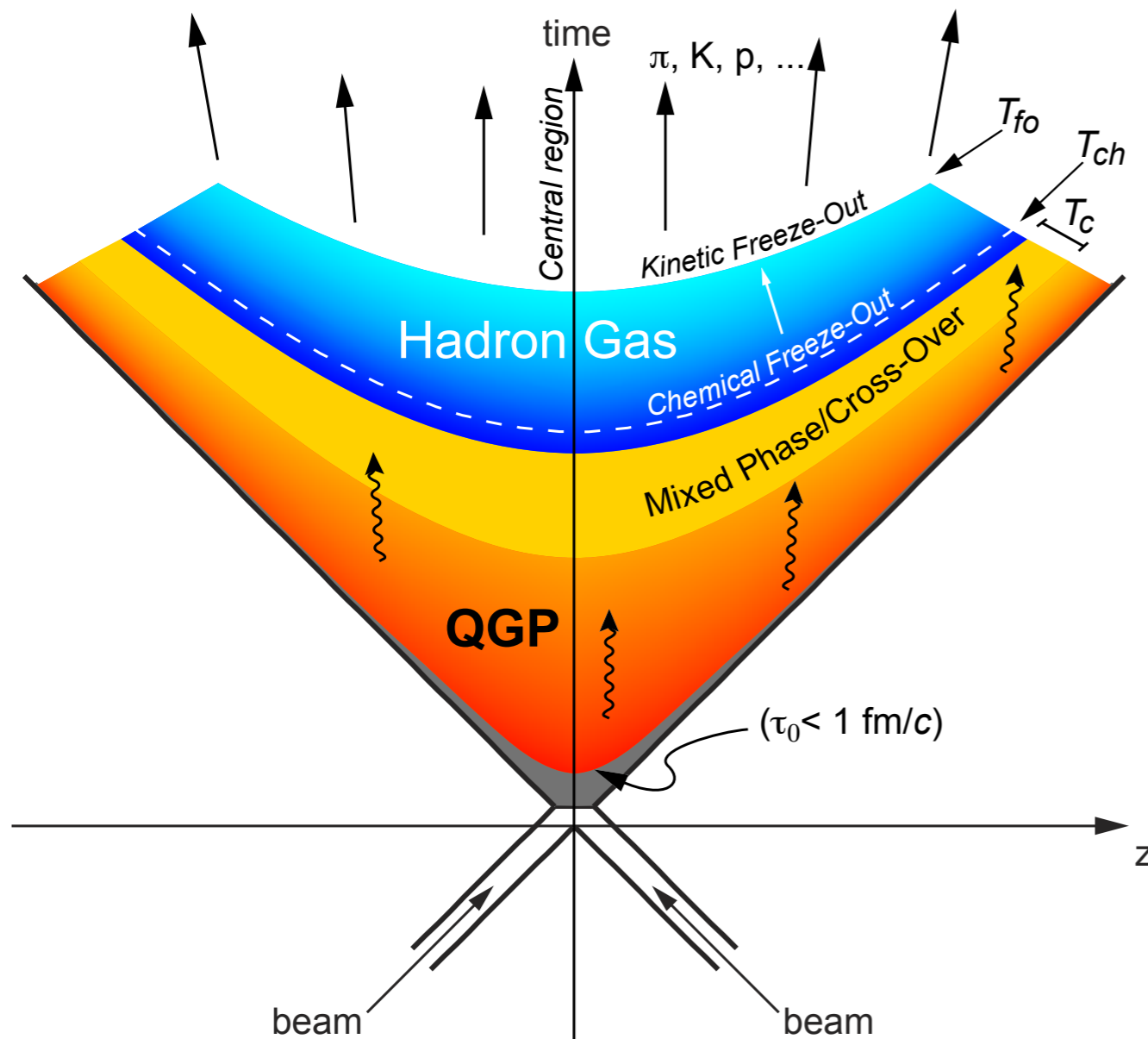
Nuclear Physics Colloquium
Frankfurt University - December 13th, 2018

Introduction



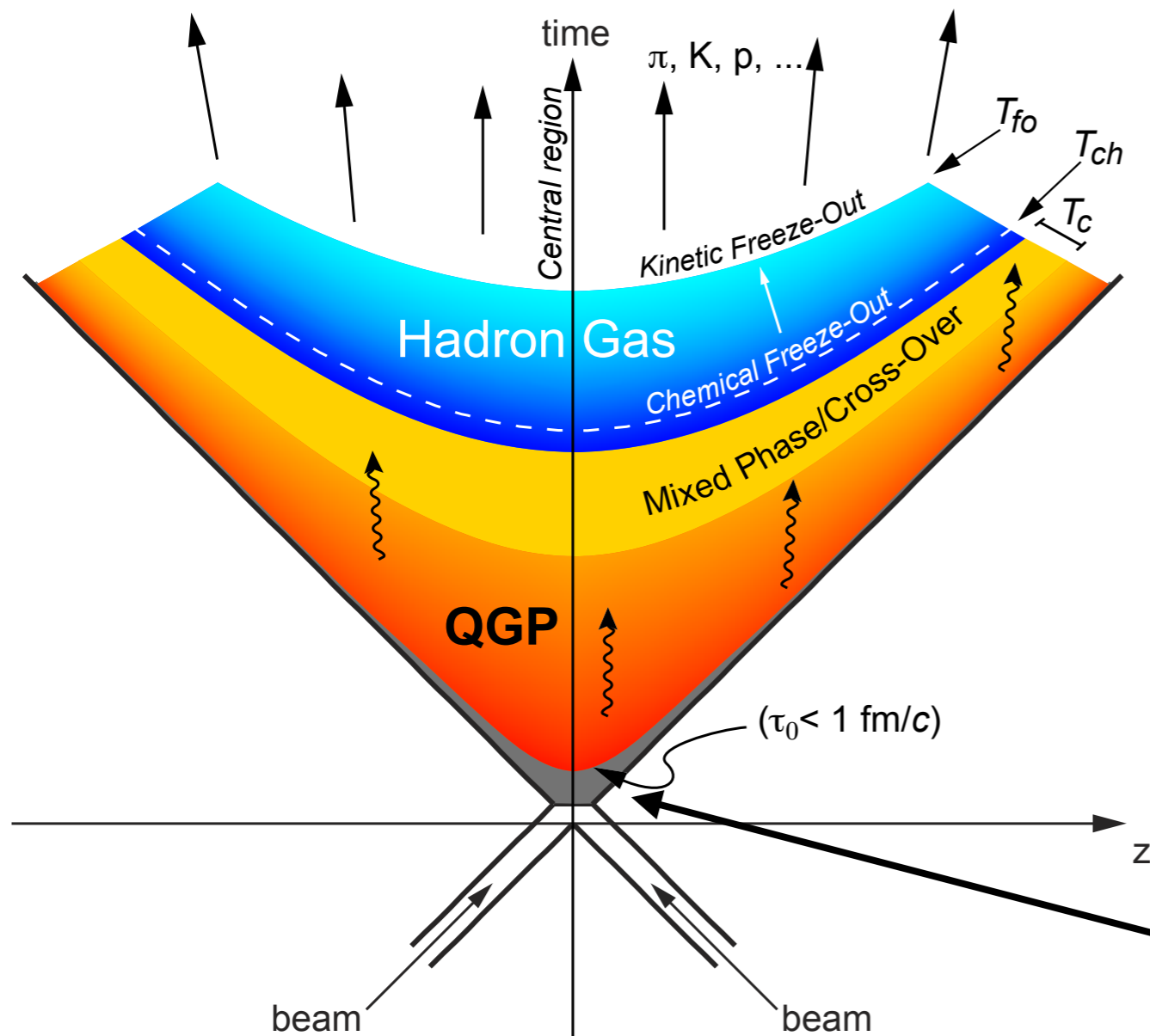
Heavy Ion collisions

- study of hadronic matter under conditions of **high energy density** ($\sim 18 \text{ GeV}/\text{fm}^3$) and **temperature** ($\sim 300 \text{ MeV}$)
- a hot and dense partonic medium is created that undergoes a radial **expansion**
- rapid expansion described using **hydrodynamical** models



Heavy Ion collisions

- study of hadronic matter under conditions of **high energy density** ($\sim 18 \text{ GeV}/\text{fm}^3$) and **temperature** ($\sim 300 \text{ MeV}$)
- a hot and dense partonic medium is created that undergoes a radial **expansion**
- rapid expansion described using **hydrodynamical** models



Thermalization time (LHC) $\tau_0 < 1 \text{ fm}/c$

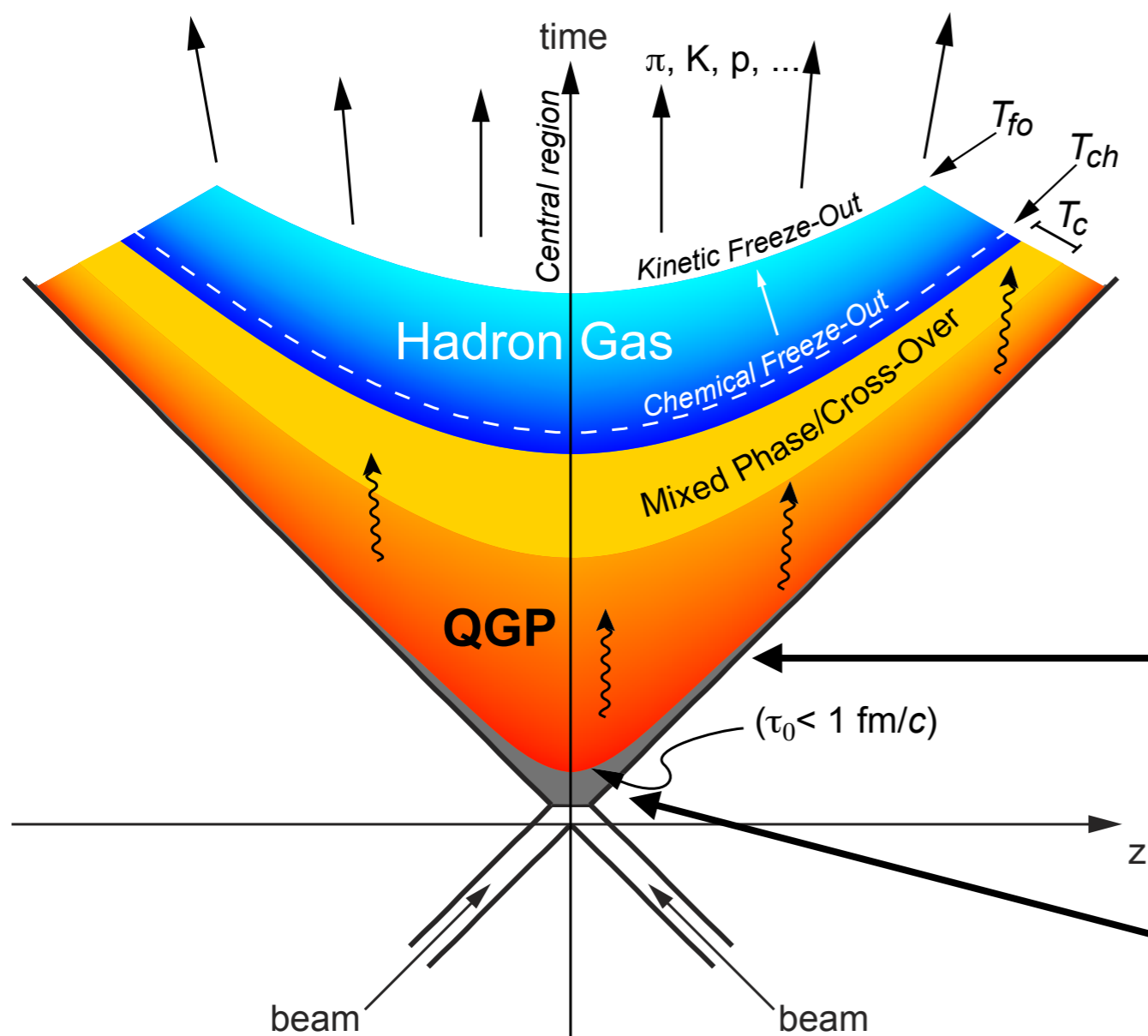
- centre-of-mass energy dependent

Hard processes

- probe the whole evolution of the collision

Heavy Ion collisions

- study of hadronic matter under conditions of **high energy density** ($\sim 18 \text{ GeV}/\text{fm}^3$) and **temperature** ($\sim 300 \text{ MeV}$)
- a hot and dense partonic medium is created that undergoes a radial **expansion**
- rapid expansion described using **hydrodynamical** models



System expansion $1 \text{ fm}/c < \tau < 10 \text{ fm}/c$

- Hydrodynamics laws
- Temp. (T) and energy density (ε) drop down

Thermalization time (LHC) $\tau_0 < 1 \text{ fm}/c$

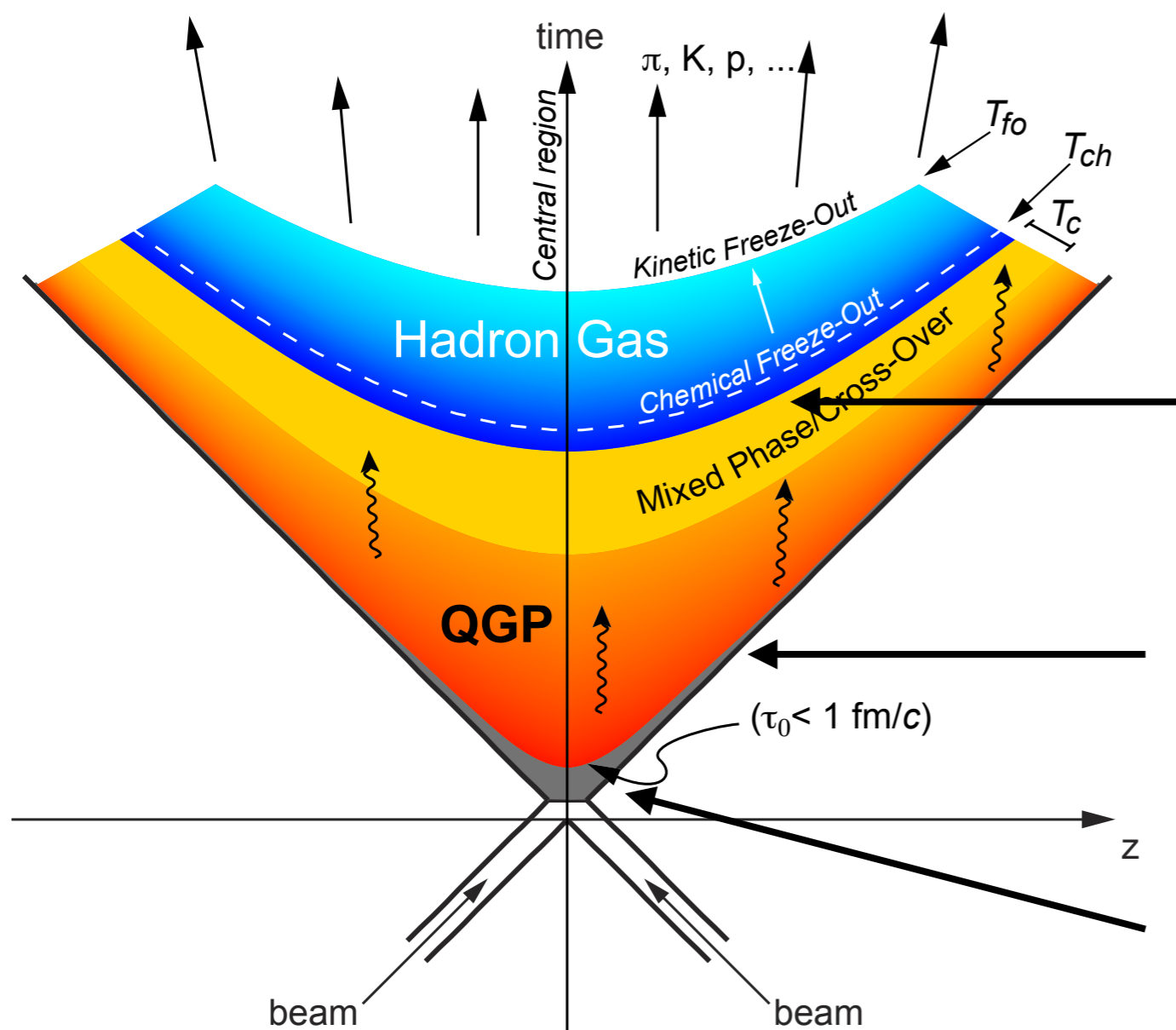
- centre-of-mass energy dependent

Hard processes

- probe the whole evolution of the collision

Heavy Ion collisions

- study of hadronic matter under conditions of **high energy density** ($\sim 18 \text{ GeV}/\text{fm}^3$) and **temperature** ($\sim 300 \text{ MeV}$)
- a hot and dense partonic medium is created that undergoes a radial **expansion**
- rapid expansion described using **hydrodynamical** models



Hadronization

- $T_c \cong 160 \div 170 \text{ MeV}$
- Confinement of quarks and gluons

System expansion $1 \text{ fm}/c < \tau < 10 \text{ fm}/c$

- Hydrodynamics laws
- Temp. (T) and energy density (ε) drop down

Thermalization time (LHC) $\tau_0 < 1 \text{ fm}/c$

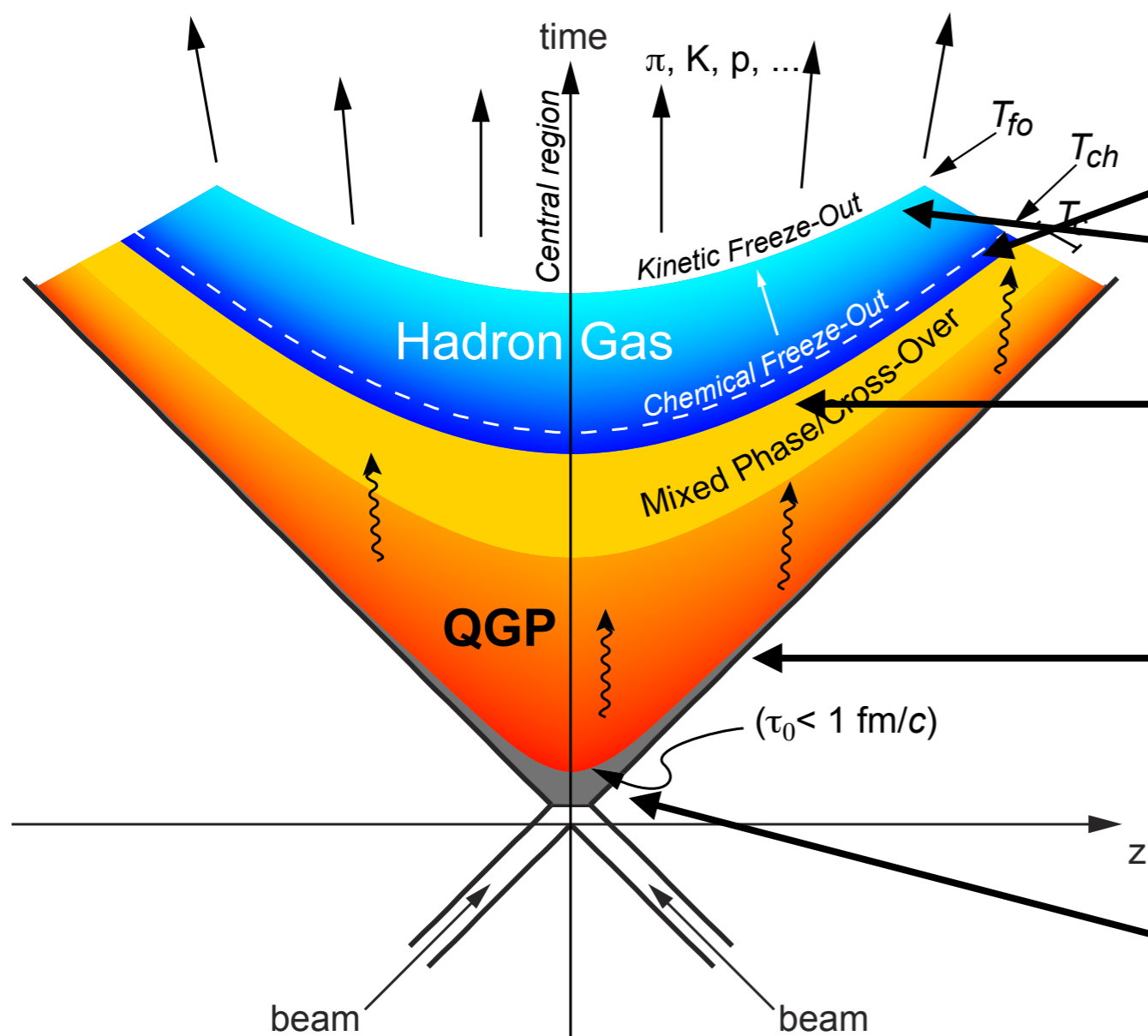
- centre-of-mass energy dependent

Hard processes

- probe the whole evolution of the collision

Heavy Ion collisions

- study of hadronic matter under conditions of **high energy density** ($\sim 18 \text{ GeV}/\text{fm}^3$) and **temperature** ($\sim 300 \text{ MeV}$)
- a hot and dense partonic medium is created that undergoes a radial **expansion**
- rapid expansion described using **hydrodynamical** models



Freeze-out (fo)

- **Chemical**: particle composition is fixed (inel. coll. ceased) $\rightarrow T_{ch} \approx 150 \div 155 \text{ MeV}$
- **Kinetic**: momentum spectra are fixed (elas. coll. ceased) $\rightarrow T_{fo} \approx 110 \div 130 \text{ MeV}$

Hadronization

- $T_c \approx 160 \div 170 \text{ MeV}$
- Confinement of quarks and gluons

System expansion $1 \text{ fm}/c < \tau < 10 \text{ fm}/c$

- Hydrodynamics laws
- Temp. (T) and energy density (ϵ) drop down

Thermalization time (LHC) $\tau_0 < 1 \text{ fm}/c$

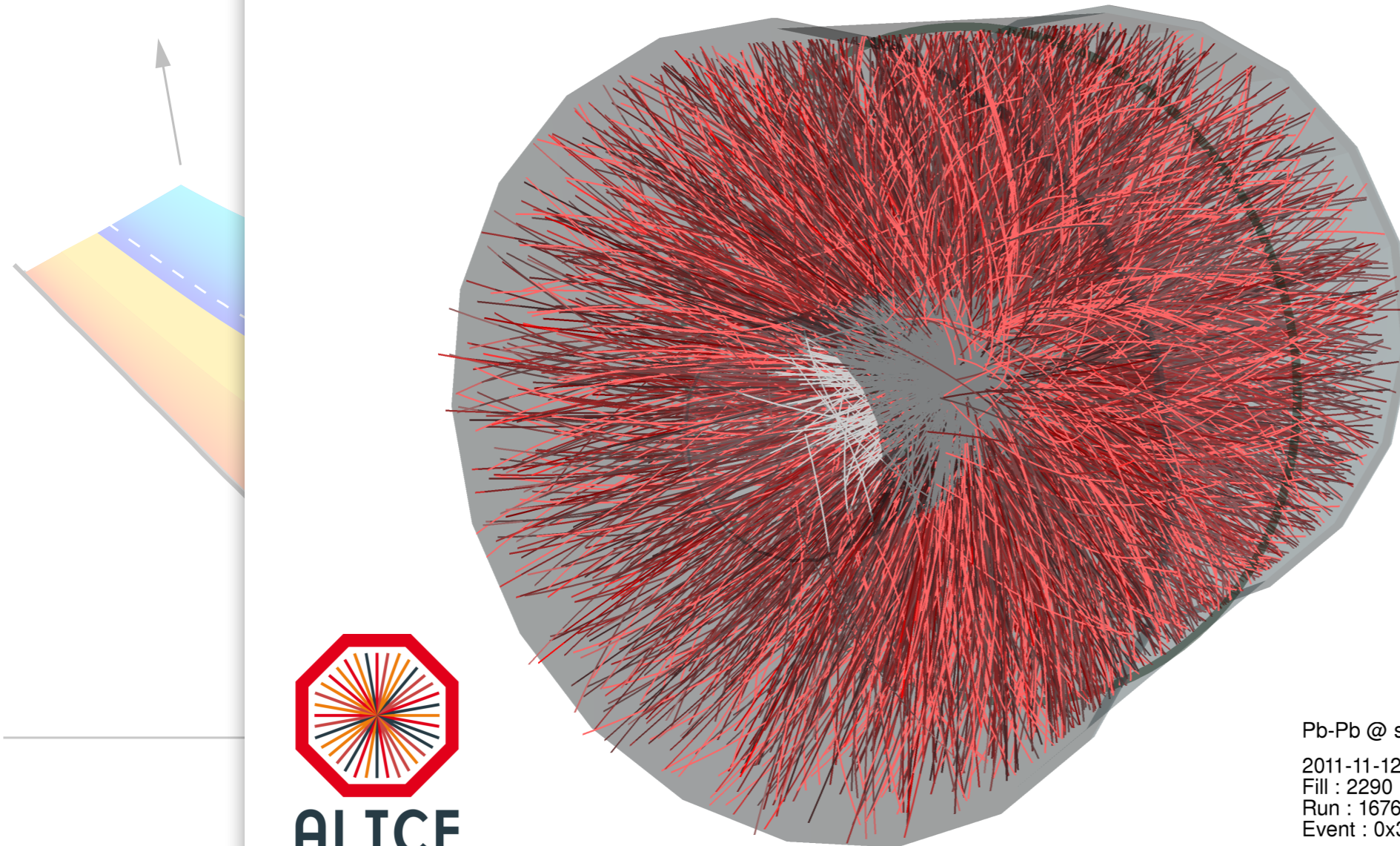
- centre-of-mass energy dependent

Hard processes

- probe the whole evolution of the collision

Heavy Ion collisions

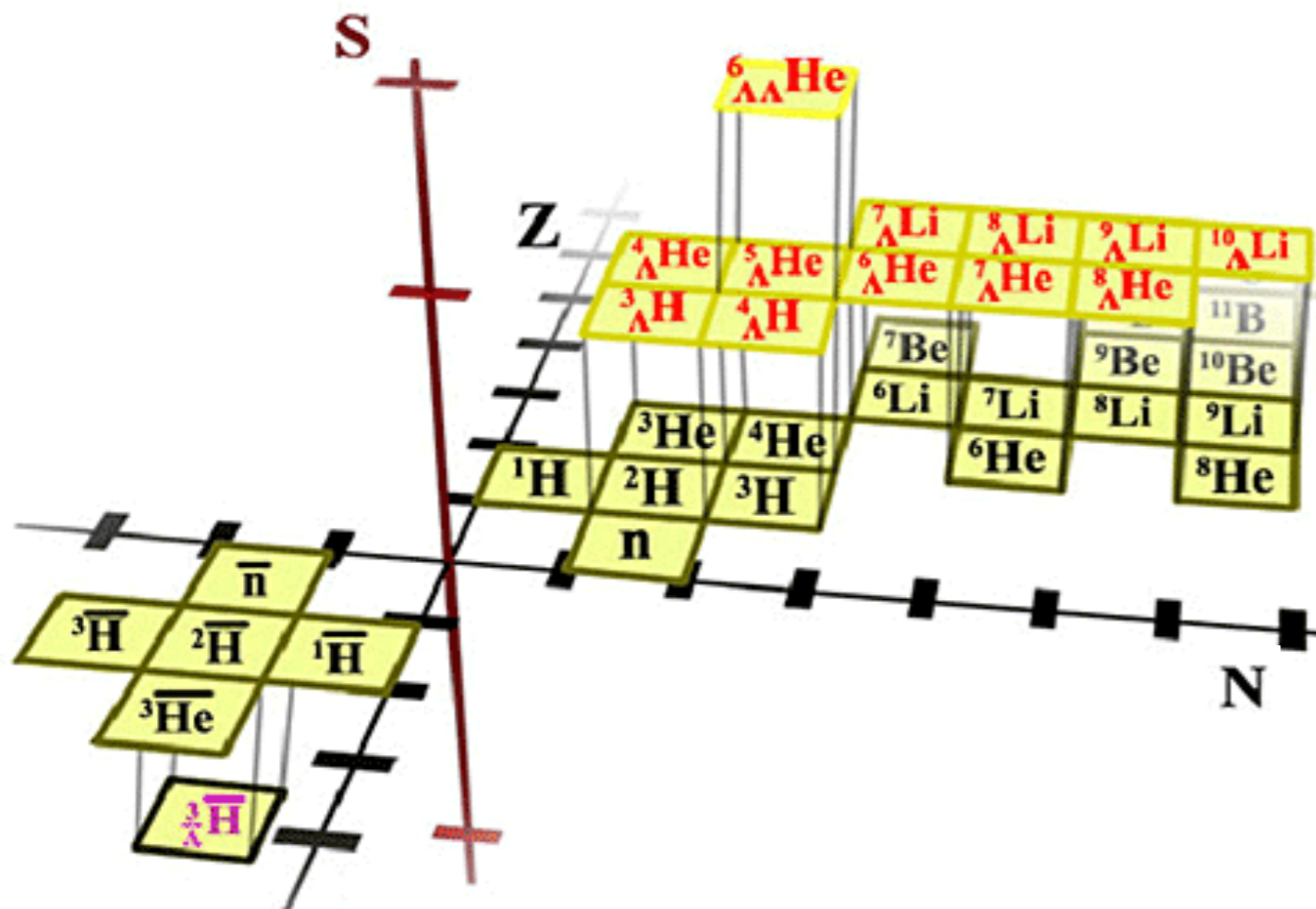
- study of hadronic matter under conditions of **high energy density** ($\sim 18 \text{ GeV}/\text{fm}^3$) and **temperature** ($\sim 300 \text{ MeV}$)
- a hot and dense medium
- rapid expansion



• probe the whole evolution of the collision

Heavy Ion collisions

- study of hadronic matter under conditions of **high energy density** ($\sim 18 \text{ GeV}/\text{fm}^3$) and **temperature** ($\sim 300 \text{ MeV}$)
- a hot and dense partonic medium is created that undergoes a radial **expansion**
- rapid expansion described using **hydrodynamical** models



Soft Probes

- Low p_T ($p_T < 2 \text{ GeV}/c$) **light flavoured** objects coming from the interaction region
- They are produced in the **late stage** of the collision
- Useful to study the **freeze-out** conditions

Light (anti-)(hyper-)nuclei are soft probes and it is interesting to investigate their production in HIC since they are **loosely bound** objects



- [U. W. Heinz, "Concepts of heavy ion physics" \(2004\)](#)
- [C. A. Salgado, "Lectures on high-energy heavy-ion collisions at the LHC" \(2009\)](#)

What is an hypernucleus?

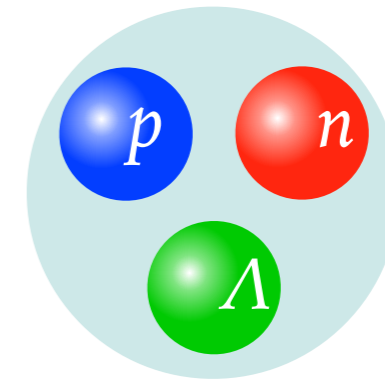
Hypernucleus

a nucleus that contains at least one hyperon in addition to nucleons

First observation in 1952 by Danysz and Pniewski [Phil. Mag. 44 \(1953\) 348](#)

Hypertriton (${}^3_{\Lambda}\text{H}$): bound state of **p**, **n** and **Λ** , is the lightest known hypernucleus

- Mass = $2.99116 \pm 0.00005 \text{ GeV}/c^2$ [1]
- Λ binding energy = $0.13 \pm 0.05 \text{ MeV}$ [1]
- lifetime: world average = $216^{+16}_{-19} \text{ ps}$ [2]
- decay channels: \rightarrow Mesonic (MWD)
 \rightarrow Non Mesonic (NMWD)



Mesonic channels

| Channels | ${}^3\text{He}+\pi^-$ ${}^3\text{H}+\pi^0$ | $d+p+\pi^-$ $d+n+\pi^0$ | $n+p+p+\pi^-$ $n+n+p+\pi^0$ |
|---------------------|---|----------------------------|--------------------------------|
| Branching Ratio [3] | 37,3% | 60,1% | 0,94% |

Study of the production in the accessible decay channels (charged products only)

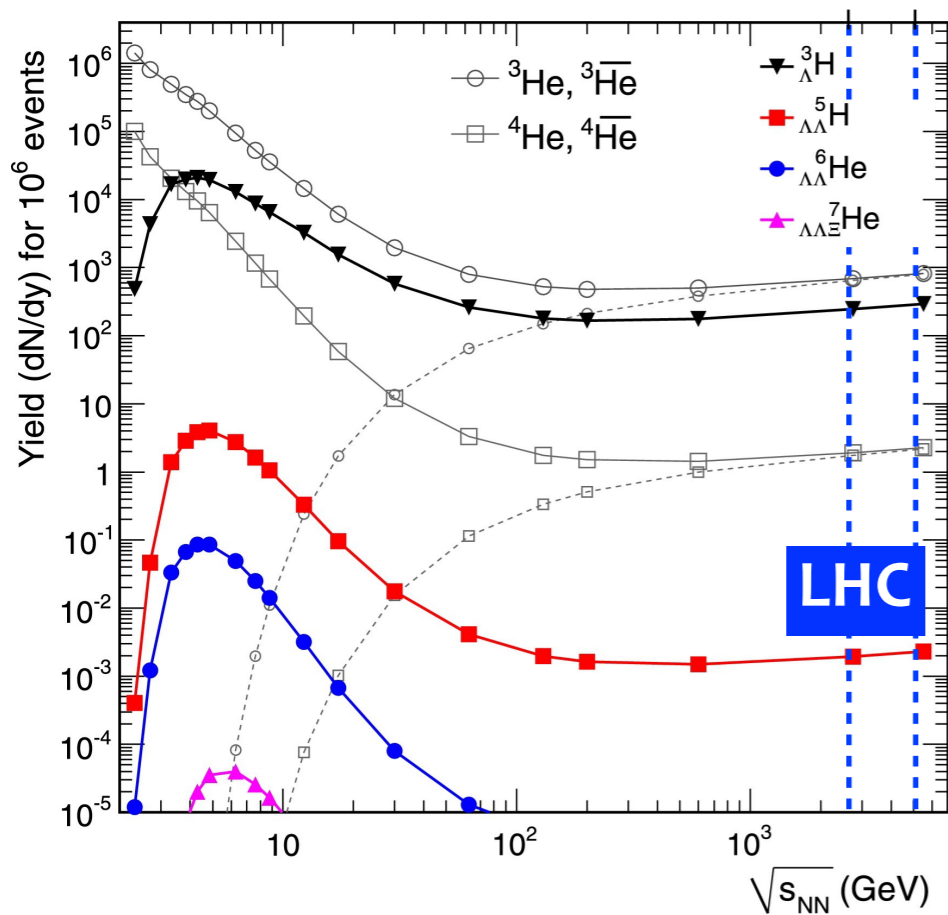
- \rightarrow 2-body (B.R. \cong 25%)
- \rightarrow 3-body (B.R. \cong 41%)

[1] [D.H. Davis., Nucl. Phys. A 754 \(2005\) 3-13](#)

[2] [C. Rappold et al., Phys. Lett. B 728, 543 \(2014\)](#)

[3] [H. Kamada et al., Phys. Rev. C 57 \(1998\) 1595-1603](#)

How (hyper-)nuclei can be produced?

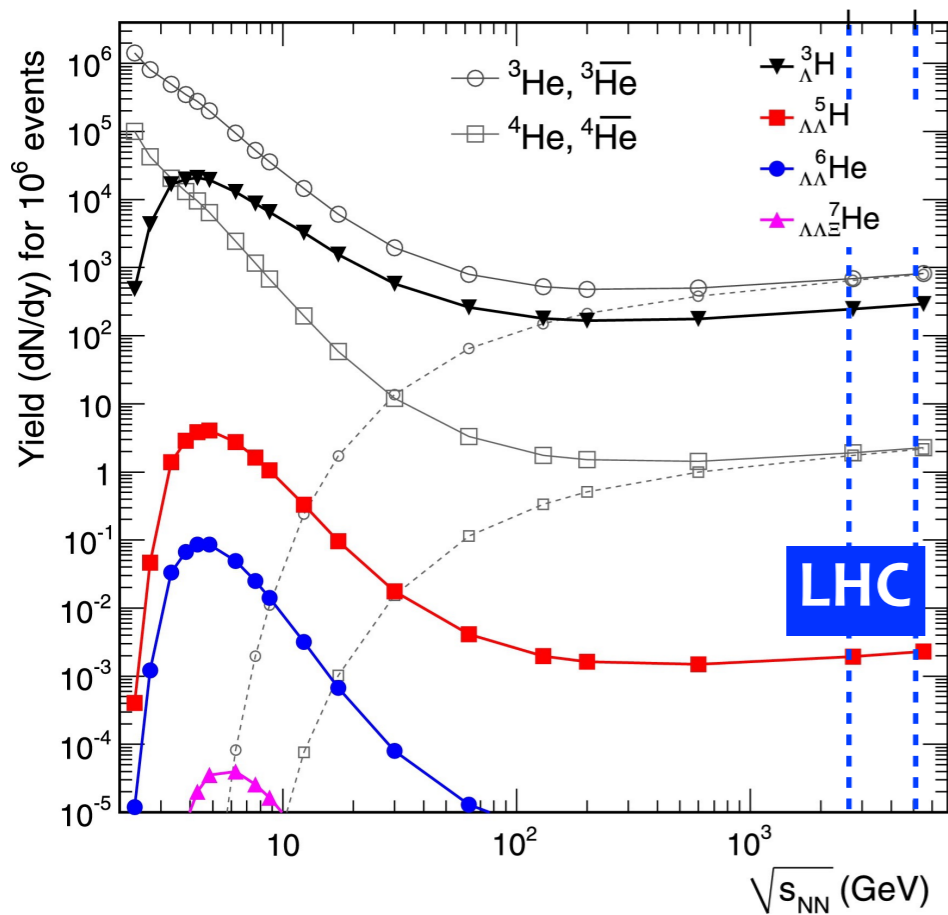


Thermal model

- Hadrons emitted from the interaction region in **statistical equilibrium** once the *chemical freeze-out* temperature is reached
 - Key parameter is *chemical freeze-out* temperature T_{chem}
 - Abundance of a species $\propto \exp(-m/T_{\text{chem}})$
- ➔ For hypernuclei (large m) strong dependence on T_{chem}

[A. Andronic, P. Braun-Munzinger, J. Stachel, H. Stoecker. Phys. Lett. B 697, 203 \(2011\)](#)

How (hyper-)nuclei can be produced?



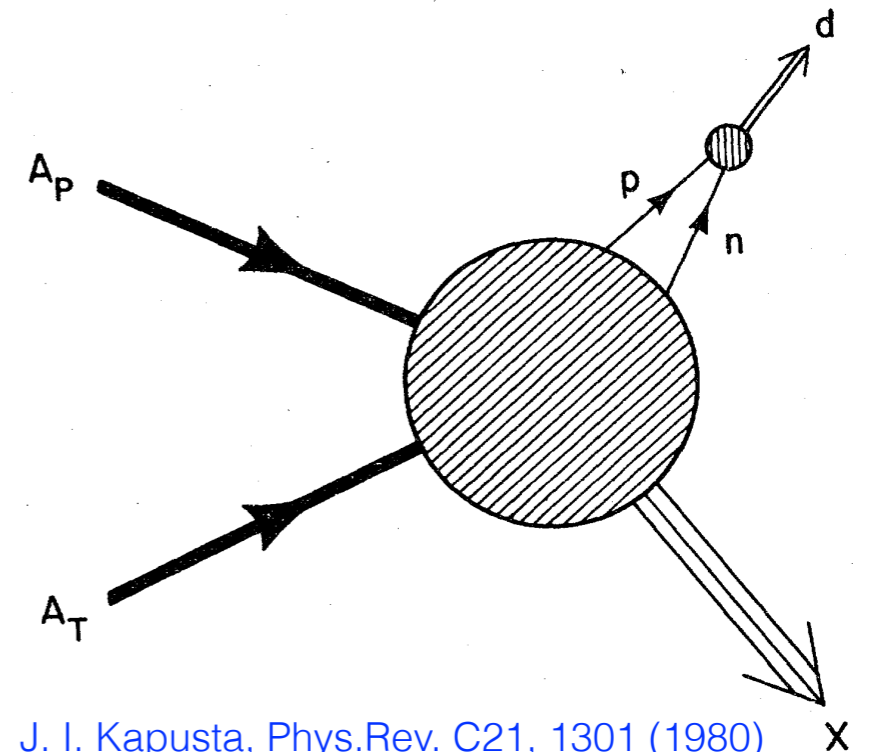
Thermal model

- Hadrons emitted from the interaction region in **statistical equilibrium** once the *chemical freeze-out* temperature is reached
- Key parameter is *chemical freeze-out* temperature T_{chem}
- Abundance of a species $\propto \exp(-m/T_{\text{chem}})$
- ➔ For hypernuclei (large m) strong dependence on T_{chem}

[A. Andronic, P. Braun-Munzinger, J. Stachel, H. Stoecker. Phys. Lett. B 697, 203 \(2011\)](#)

Coalescence model

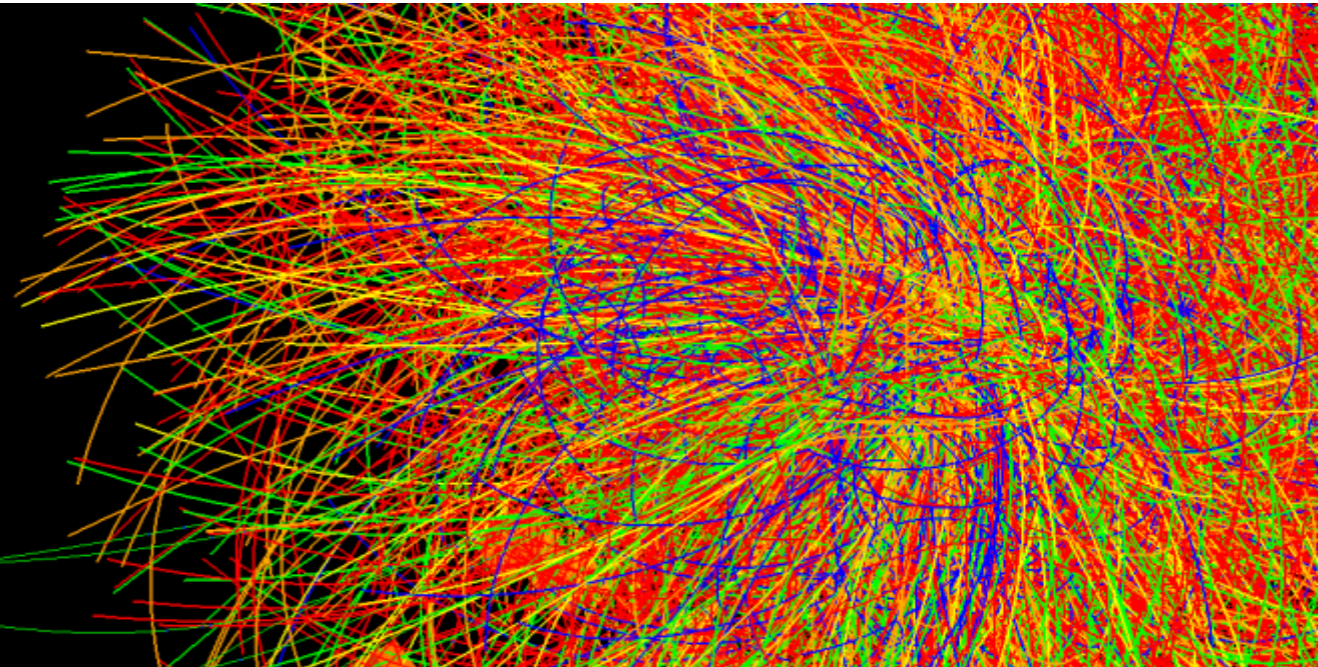
- (Anti-)baryons close in phase space at the *kinetic freeze-out* can form a (anti-)(hyper-)nucleus
- (Anti-)(hyper-)nuclei formed at the *chemical freeze-out*:
 - might **break up**
 - **regenerate** in the time interval between *chemical* and *kinetic freeze-out*



[J. I. Kapusta, Phys. Rev. C 21, 1301 \(1980\)](#)

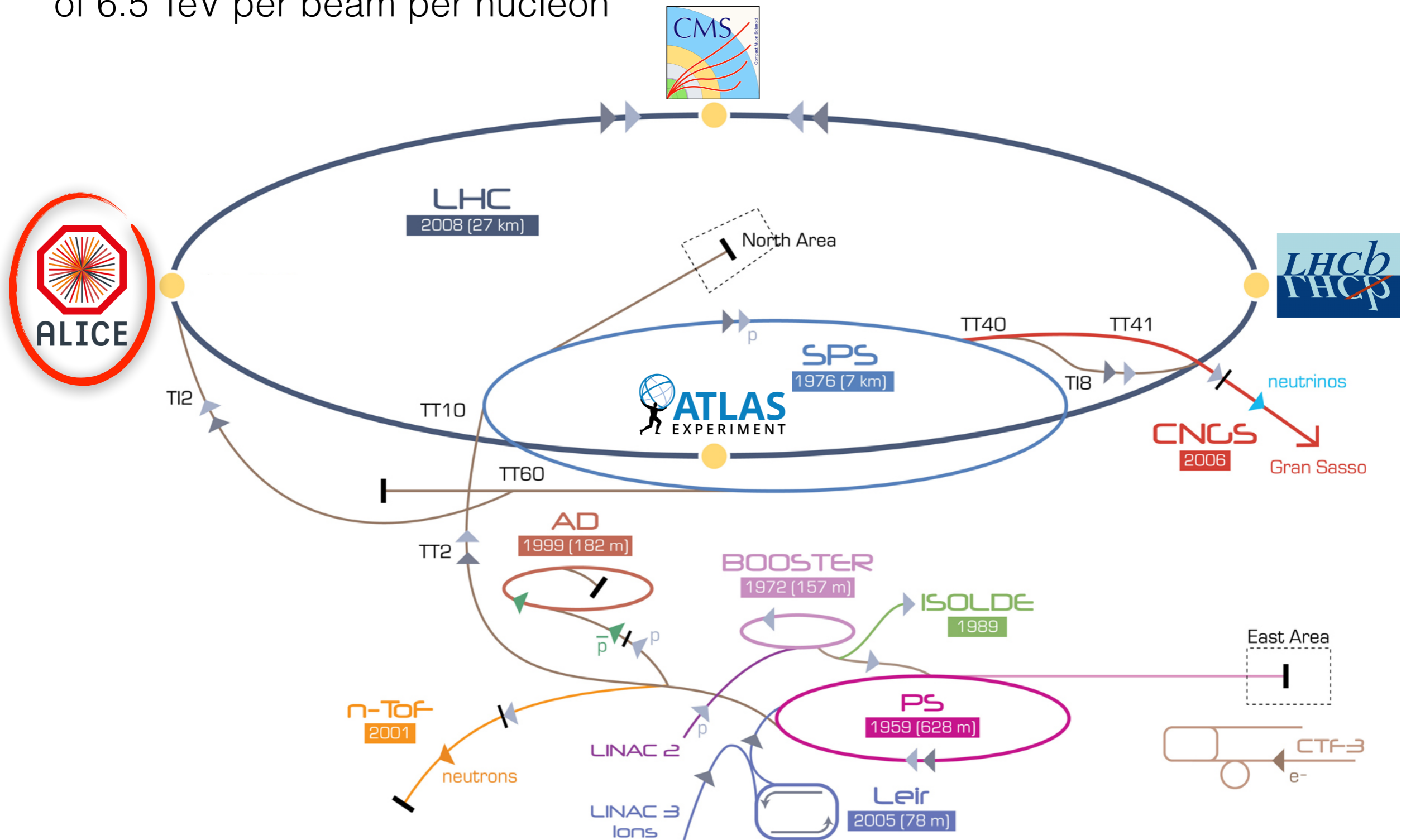
[J. Steinheimer et al. Phys. Lett. B 714, 85-91 \(2012\)](#)

A Large Ion Collider Experiment

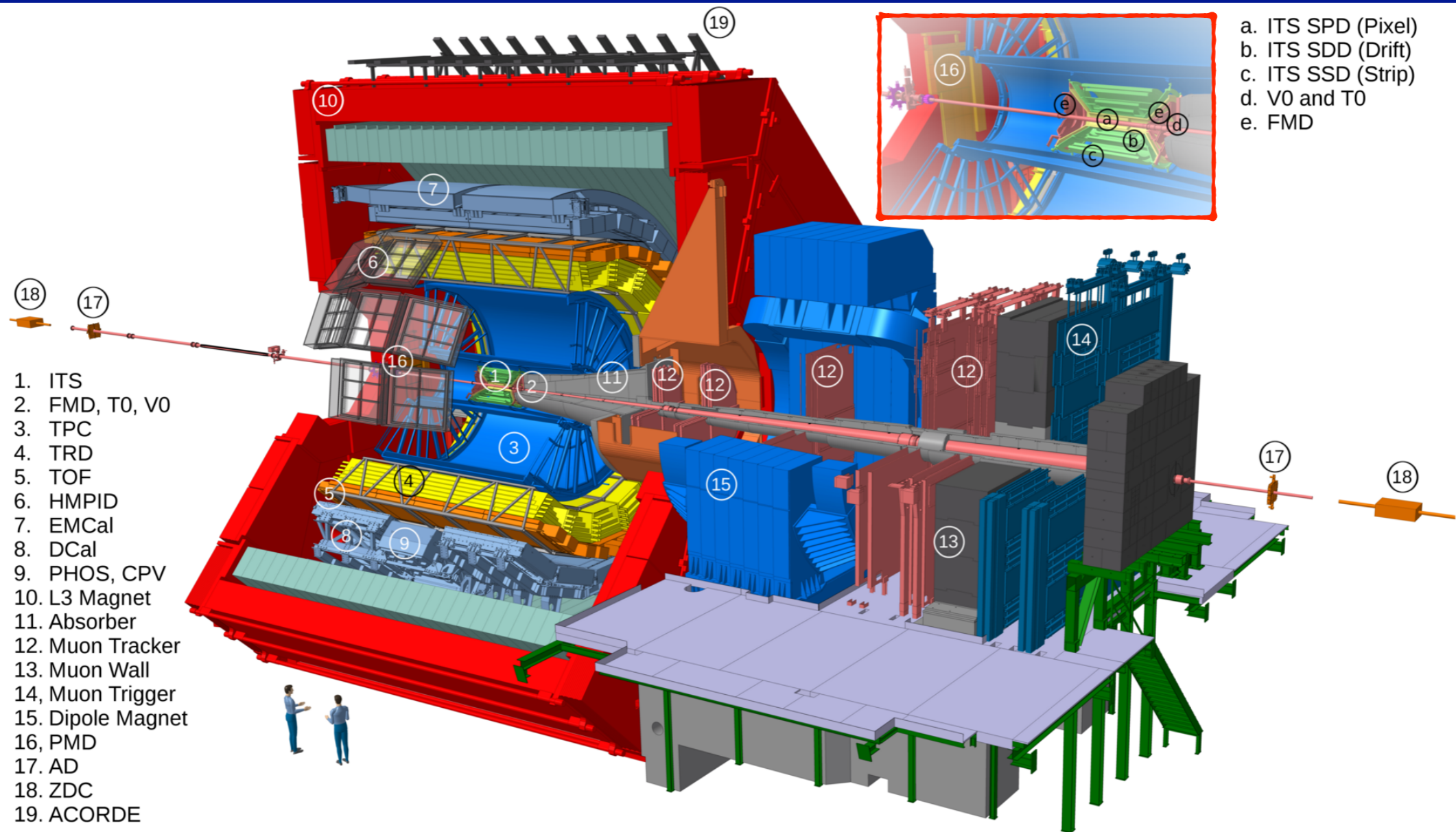


Large Hadron Collider

- In the **LHC** particle beams (protons and Pb ions) are accelerated up to the energy of 6.5 TeV per beam per nucleon

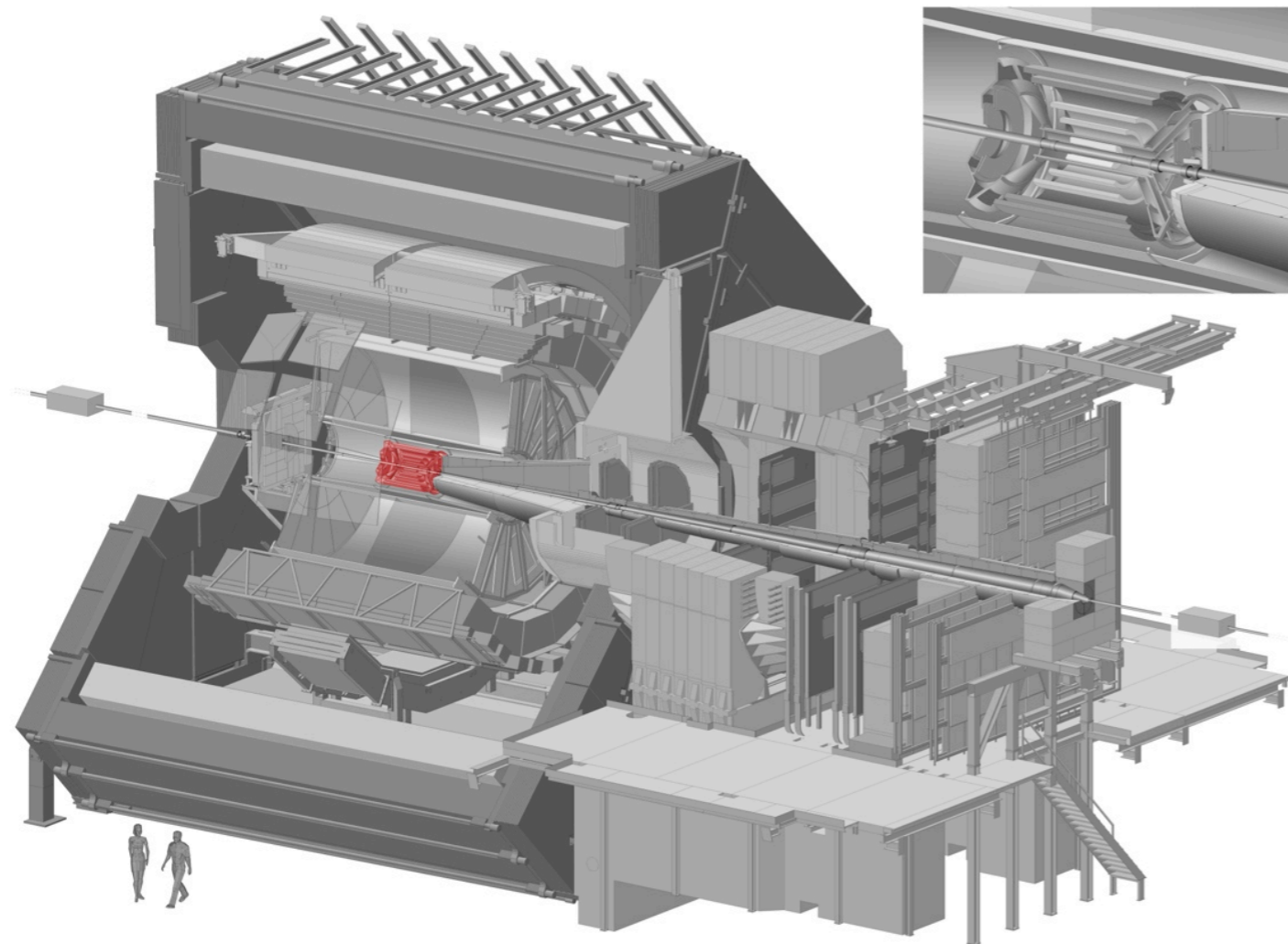


A Large Ion Collider Experiment



- General purpose heavy ion apparatus
- Excellent **particle identification** (PID) capabilities ($\sigma \sim 5-7\%$) and low material budget ($\sim 7.26\% X/X_0$)
- Most suited detector at the LHC to study the (anti-)(hyper-)nuclei production in the collisions

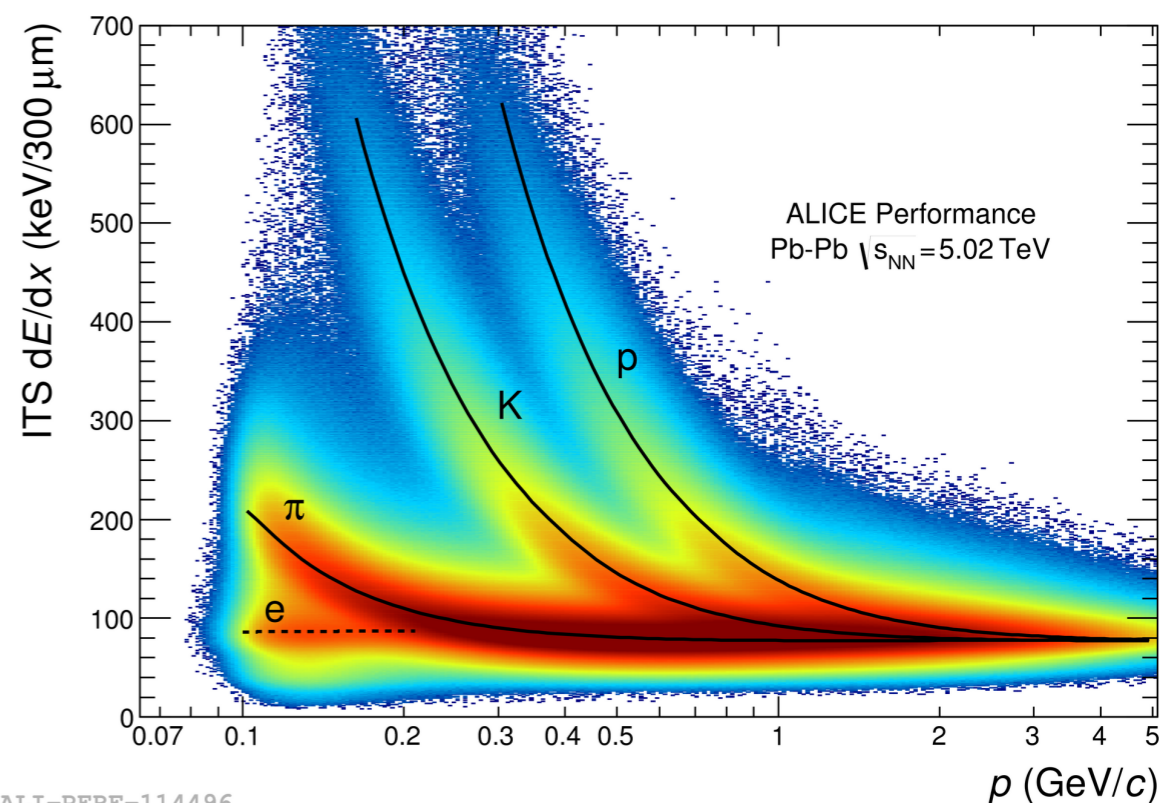
A Large Ion Collider Experiment



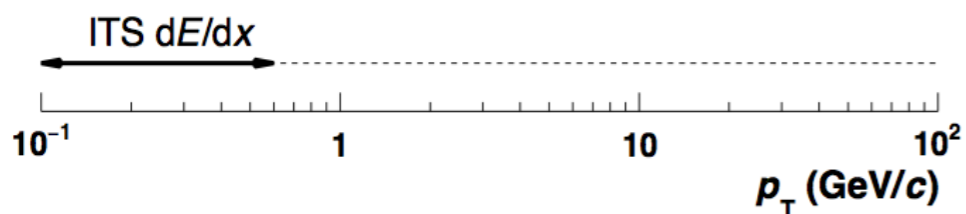
Inner Tracking System

- 6 Layers of silicon detectors
 - Pixel, Drift and Strip detectors
 - $r_{\min} = 3.9 \text{ cm}$, $r_{\max} = 43 \text{ cm}$
 - $|\eta| < 0.9$
- Main purposes:
 - Trigger, vertexing and tracking
 - PID via dE/dx

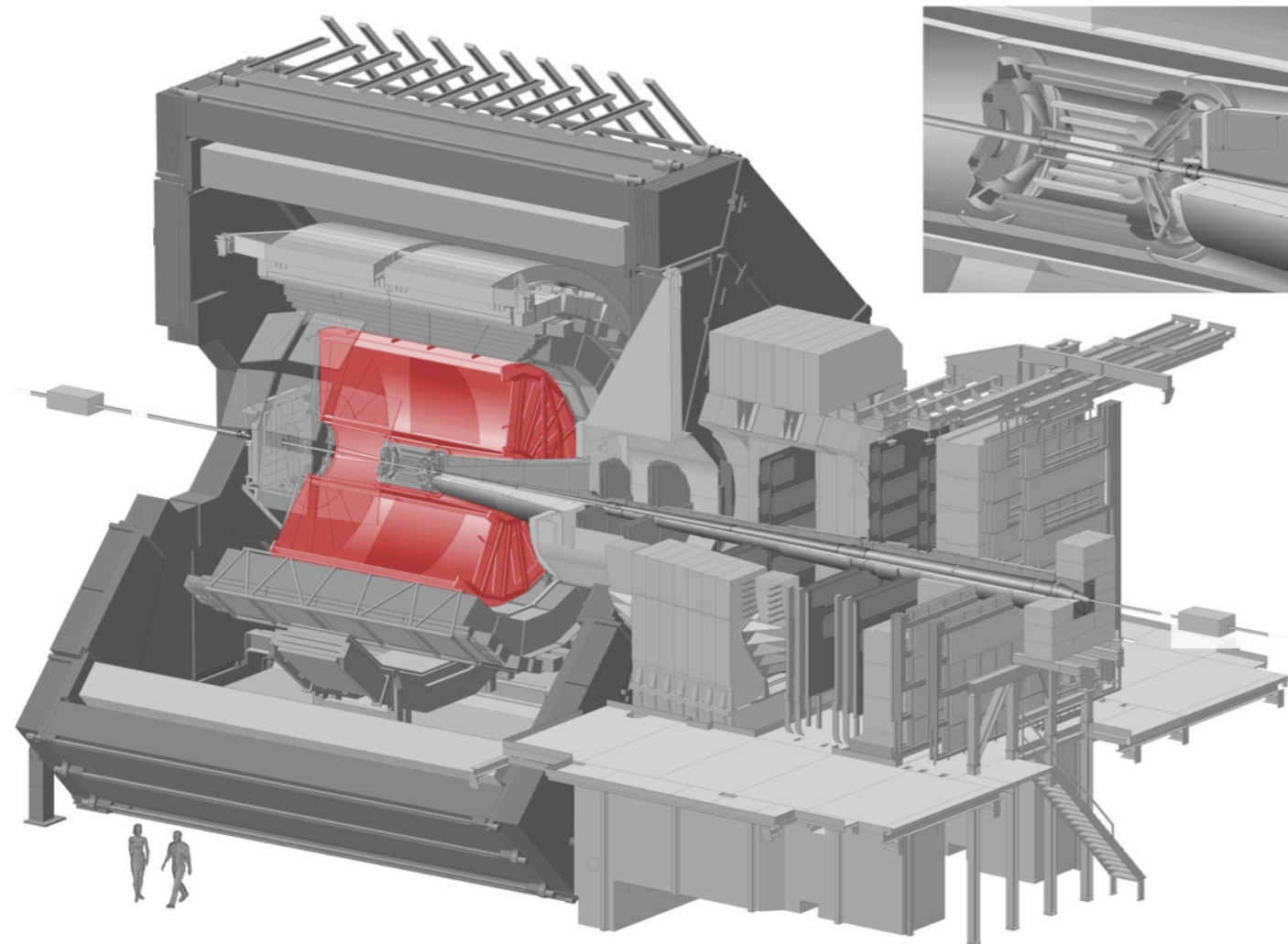
More details on ITS:
[ALICE Collaboration, JINST 5 \(2010\) P03003](#)



ALI-PERF-114496



A Large Ion Collider Experiment

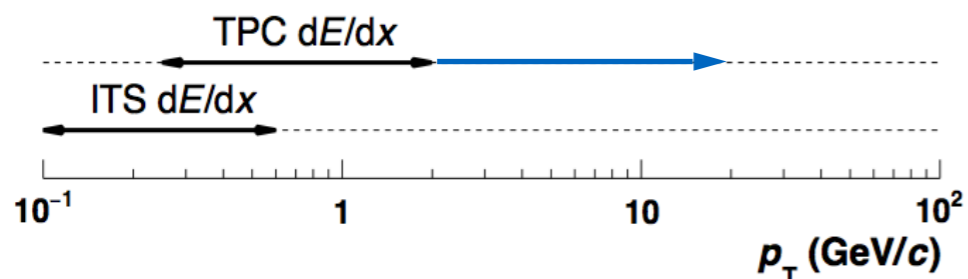


Time Projection Chamber

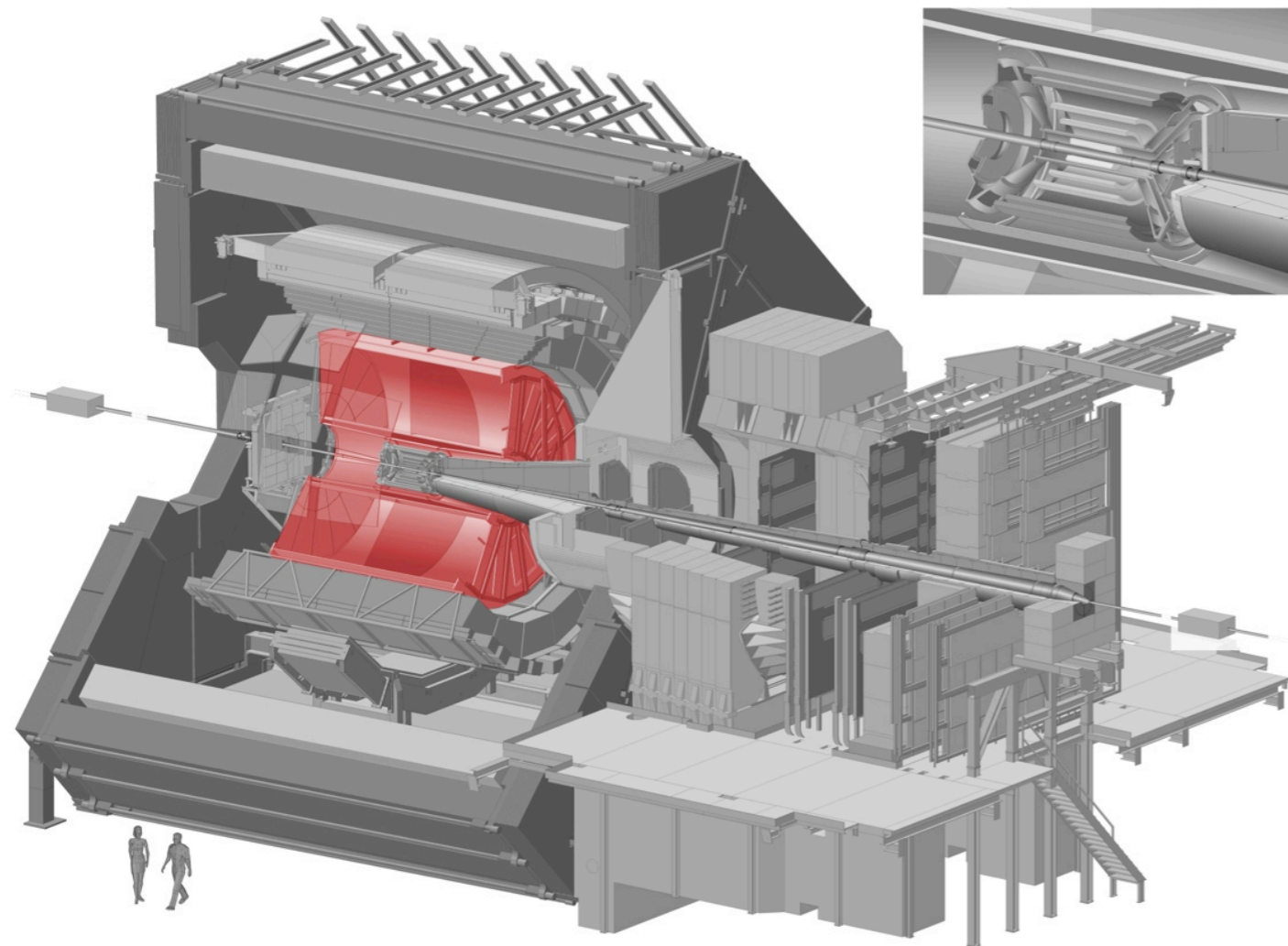
- Gas-filled ionization detection volume
 - 90 m³ of Ne-CO₂ or Ar-CO₂
 - $r_{\min} = 85$ cm, $r_{\max} = 247$ cm
 - $|\eta| < 0.9$
- Main purposes:
 - Tracking and vertexing
 - Weak decay reconstruction (e.g. Λ)
 - PID via dE/dx

More details on TPC:

[J. Alme et al., Nucl. Instrum. Methods A 622 \(2010\) 316-367](#)



A Large Ion Collider Experiment

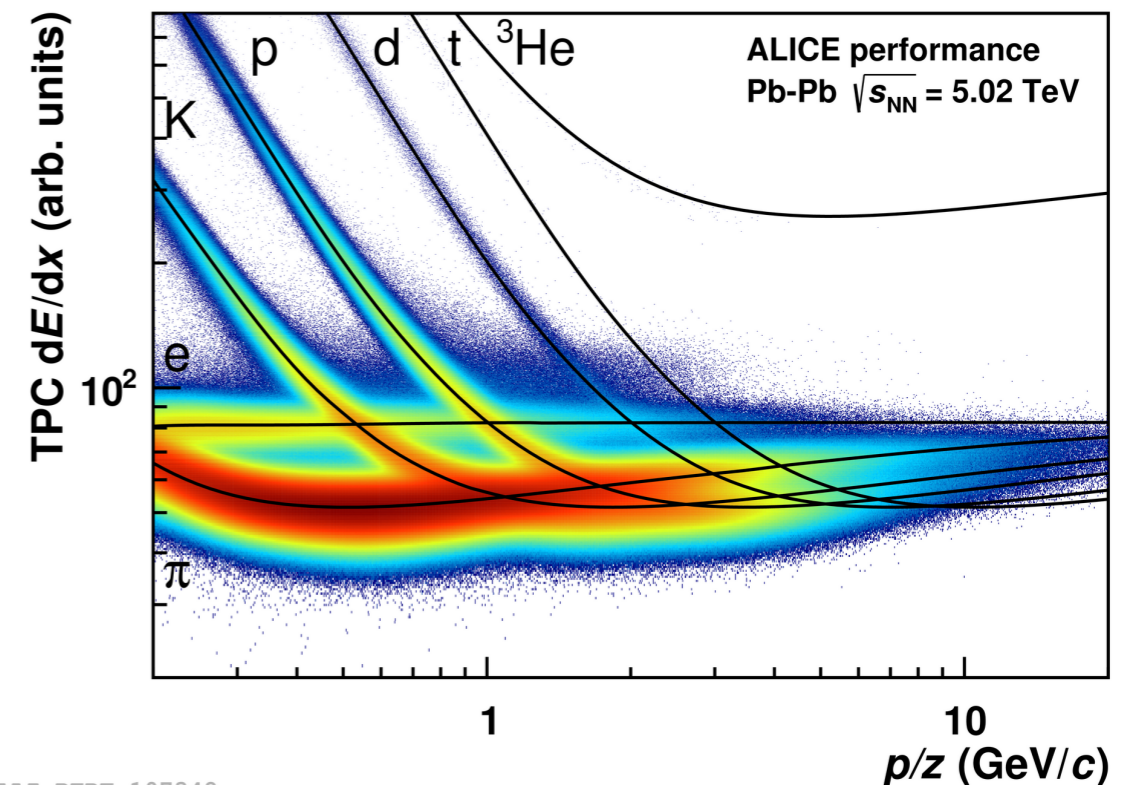


Time Projection Chamber

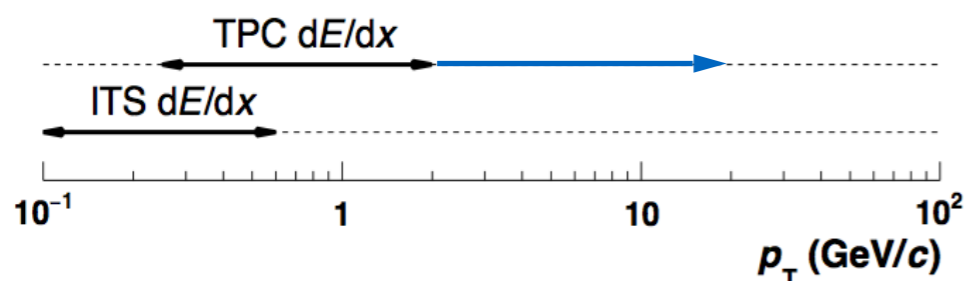
- Gas-filled ionization detection volume
 - 90 m³ of Ne-CO₂ or Ar-CO₂
 - $r_{\min} = 85$ cm, $r_{\max} = 247$ cm
 - $|\eta| < 0.9$
- Main purposes:
 - Tracking and vertexing
 - Weak decay reconstruction (e.g. Λ)

More details on TPC:

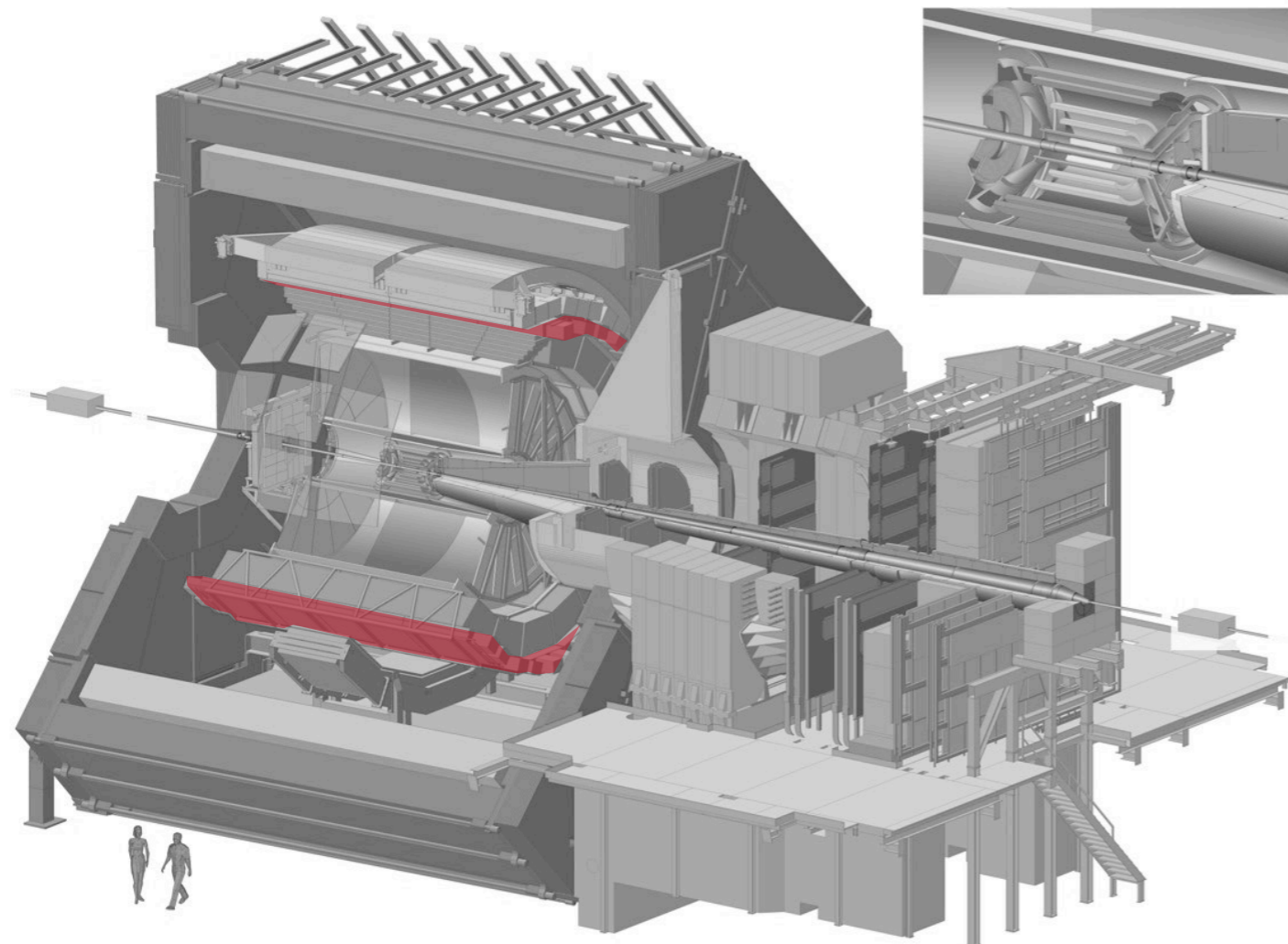
[J. Alme et al., Nucl. Instrum. Methods A 622 \(2010\) 316-367](#)



ALI-PERF-107348



A Large Ion Collider Experiment

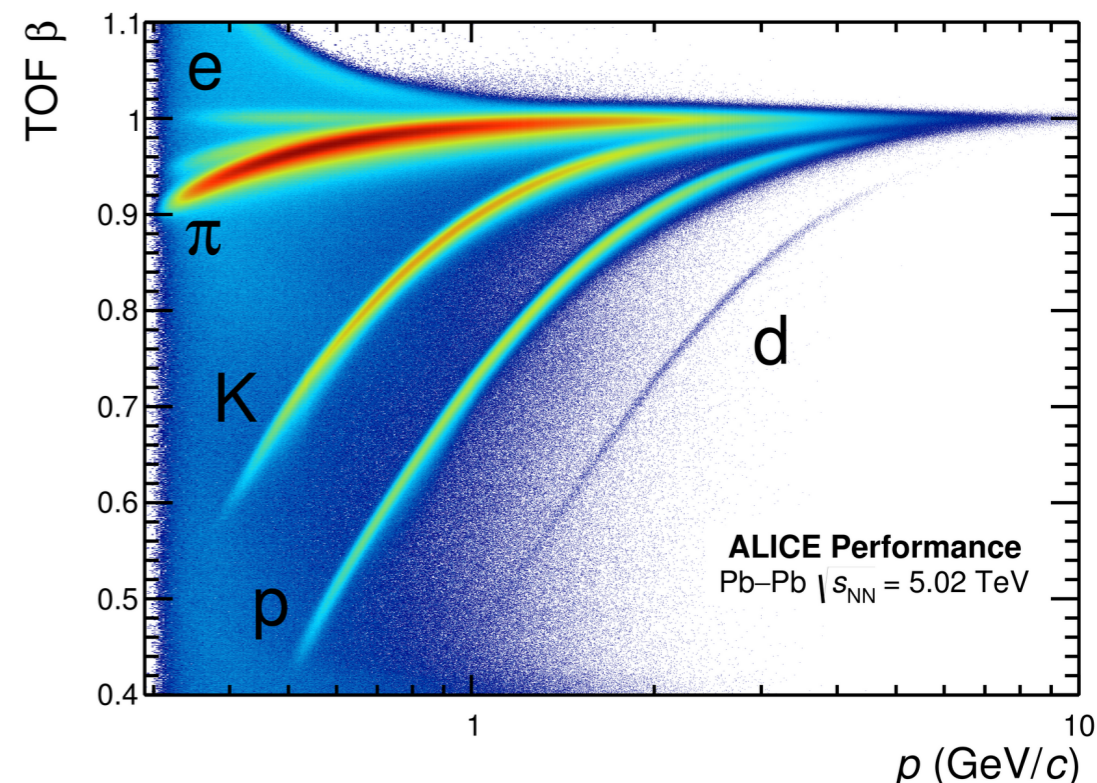
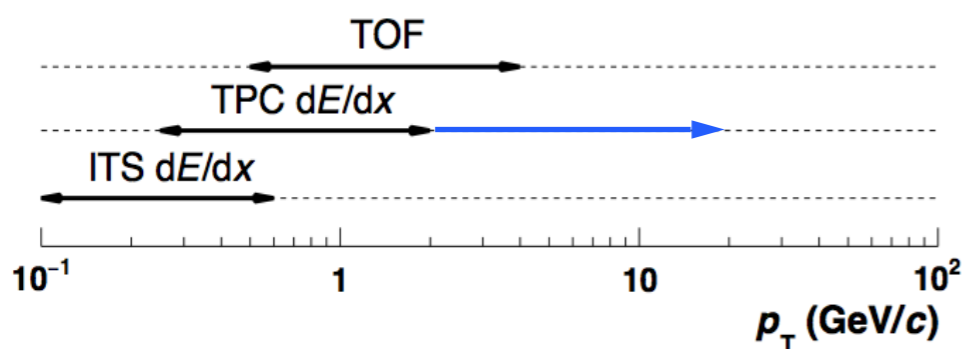


Time-Of-Flight

- Multi-gap resistive plate chambers
 - $r_{\min} = 370$ cm, $r_{\max} = 399$ cm
 - $|\eta| < 0.9$
- PID in the intermediate momentum range:
 - via velocity determination
 - time resolution $\sigma_{\text{TOF}} \sim 80$ ps

More details on TOF:

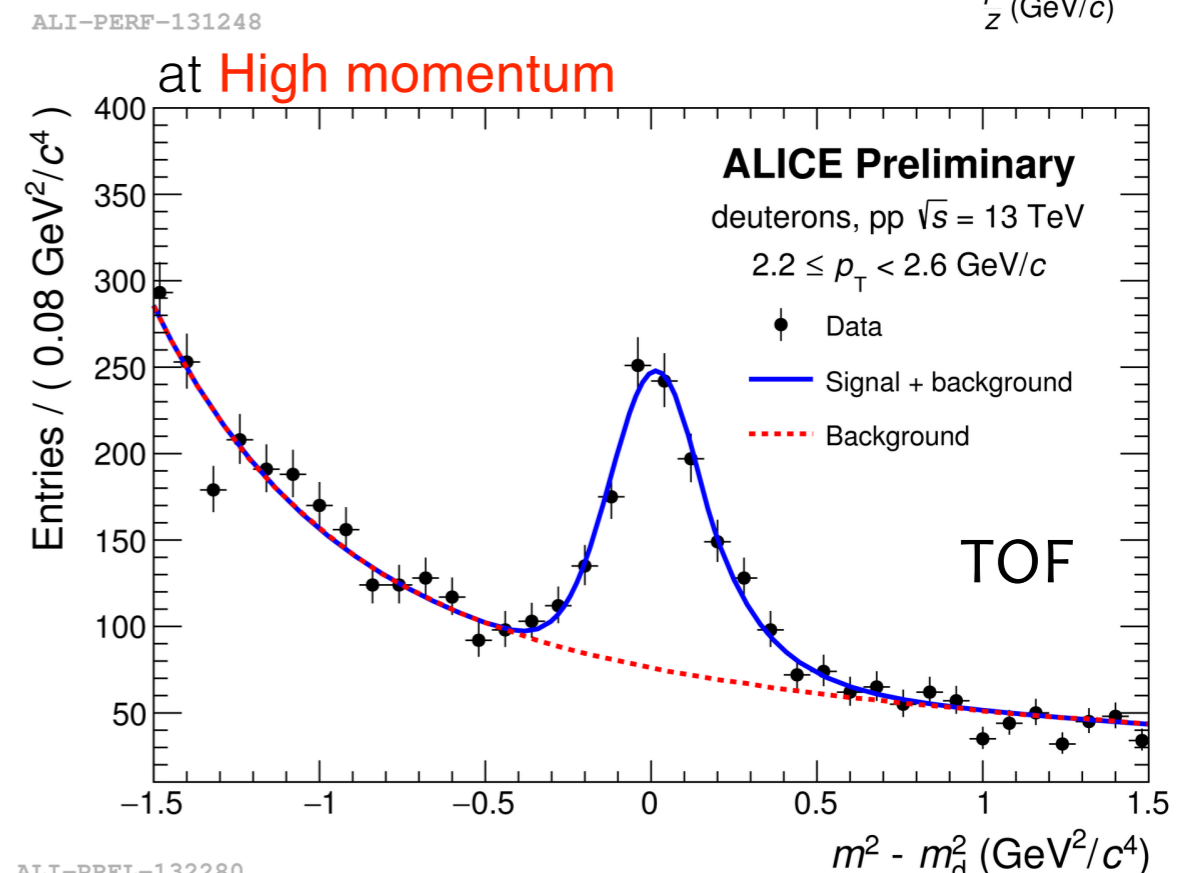
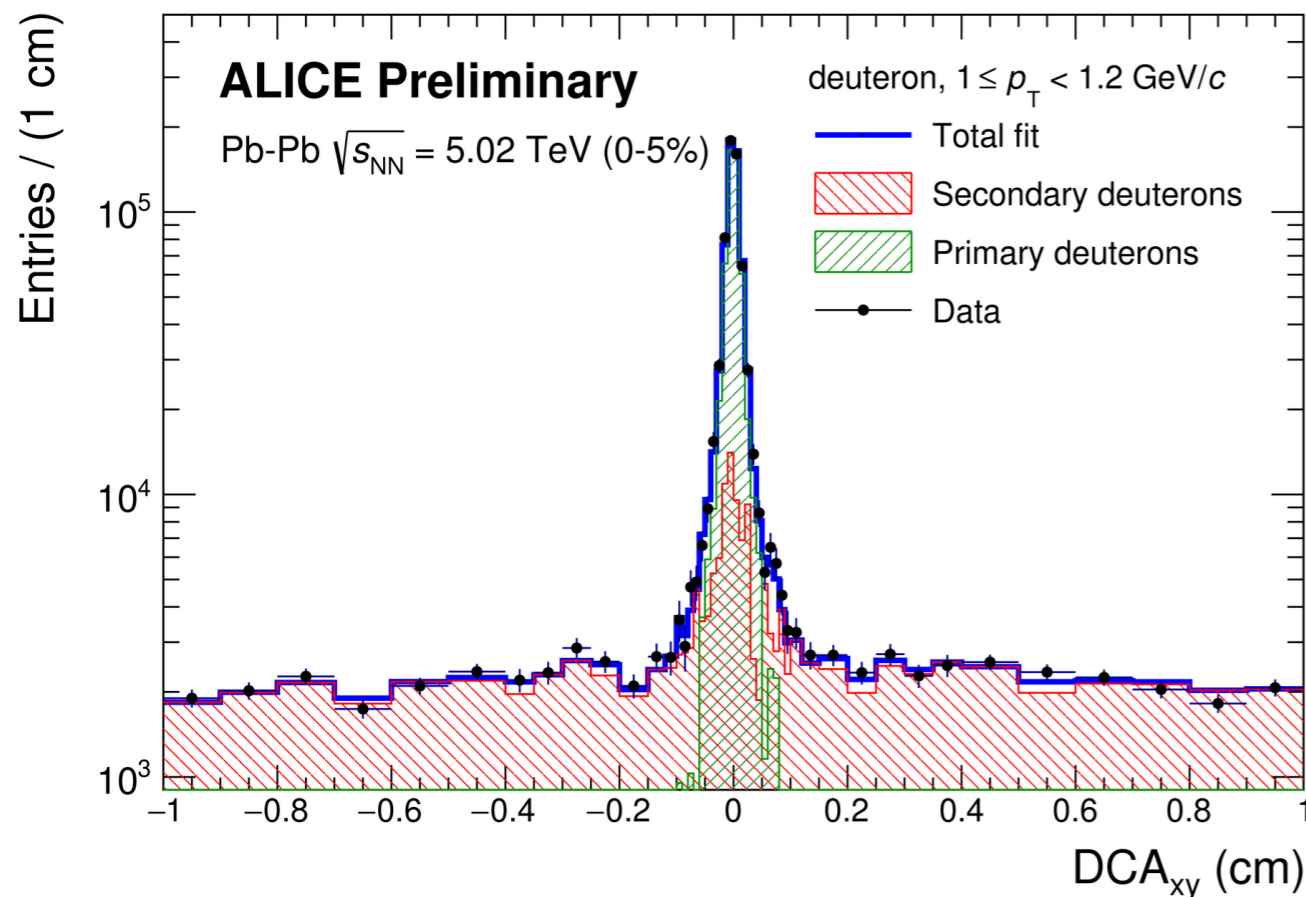
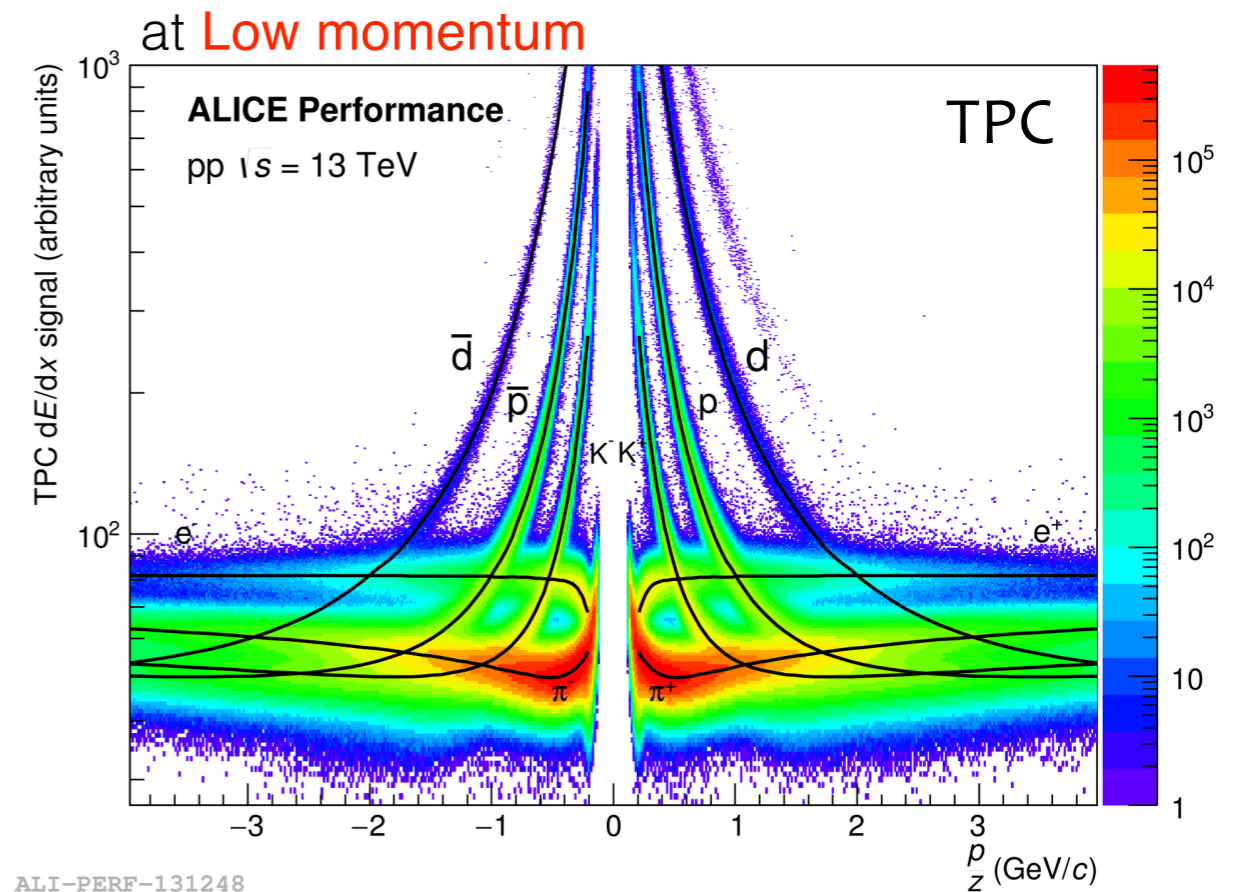
[ALICE Collaboration, JINST 3 \(2008\) S08002](#)



ALI-PERF-106336

Nuclei identification

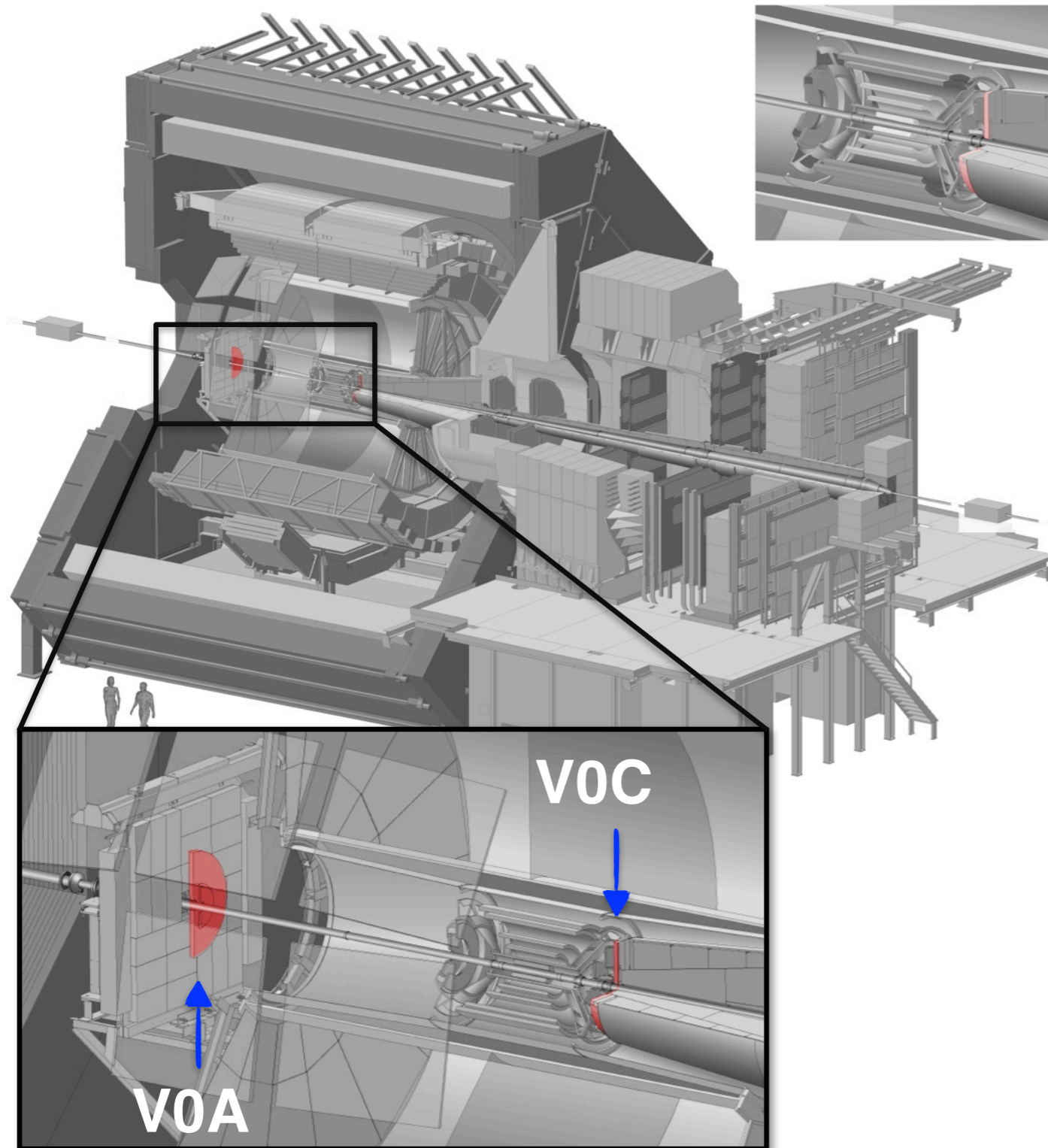
- Nuclei **production** studies performed via:
 - Particle IDentification (TPC, TOF)
 - Topological selection
- Distance-of-Closest-Approach (DCA) distributions used to separate **primary** particles from **secondary** particles (e.g. knock-out from material)



ALI-PREL-130203

ALI-PREL-132280

A Large Ion Collider Experiment

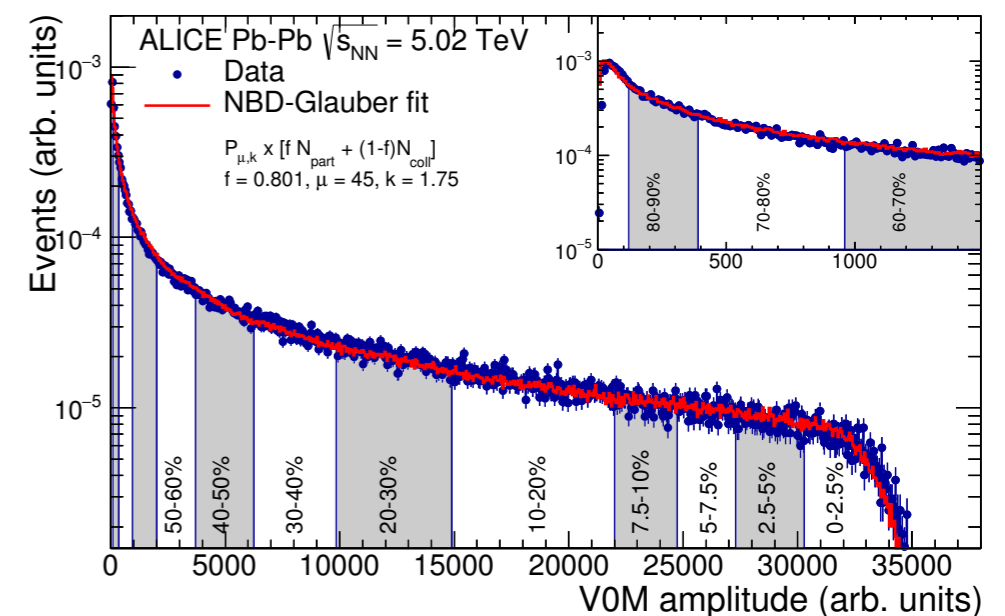


More details on V0:

[ALICE Collaboration, JINST 8 \(2013\) P10016](#)

V-ZERO

- Two arrays of scintillator detectors
 - V0A ($2.8 < \eta < 5.1$) and V0C ($-3.7 < \eta < -1.7$)
- Main purposes:
 - trigger, beam-gas rejection
 - centrality and multiplicity estimator
- Event selection based on total charge deposited in the **V0A** and **V0C** detectors (“V0M”)



Centrality of a collision

Theory

The centrality of the collision is defined by the absolute value of the impact parameter vector \mathbf{b}

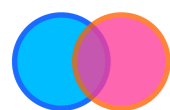
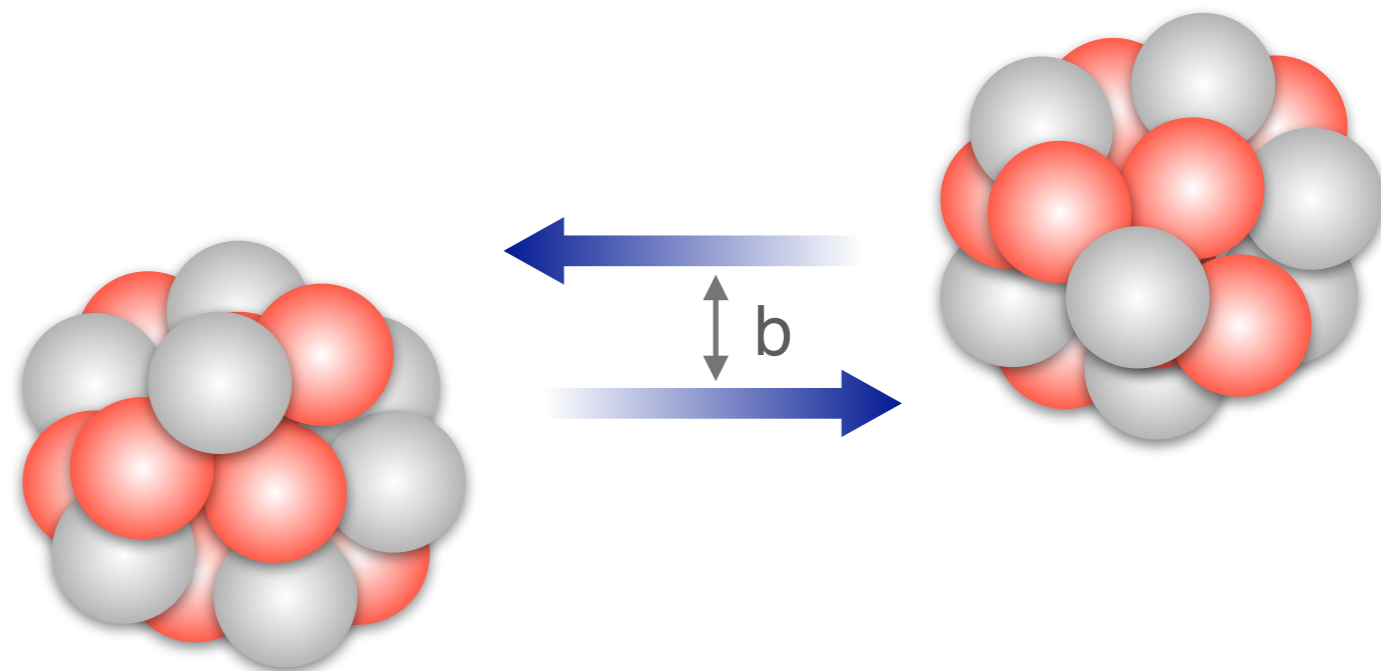
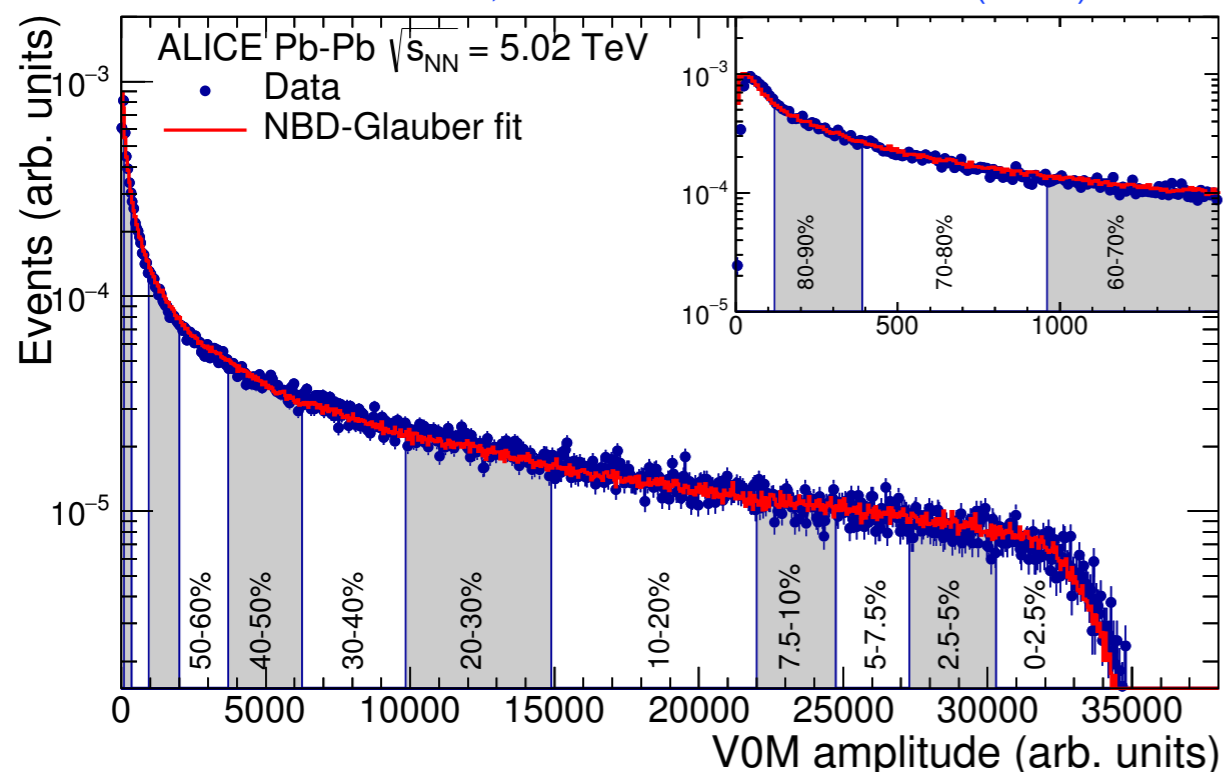
Most central collision \iff Smallest b

Experimentally

It is possible to correlate the charged particle multiplicity to an impact parameter value by fitting data with predictions from Glauber model

- centrality class defined as percentile of the total cross-section

ALICE Collaboration, ALICE-PUBLIC-2015-008 (2015)



Centrality of a collision

Theory

The centrality of the collision is defined by the absolute value of the impact parameter vector \mathbf{b}

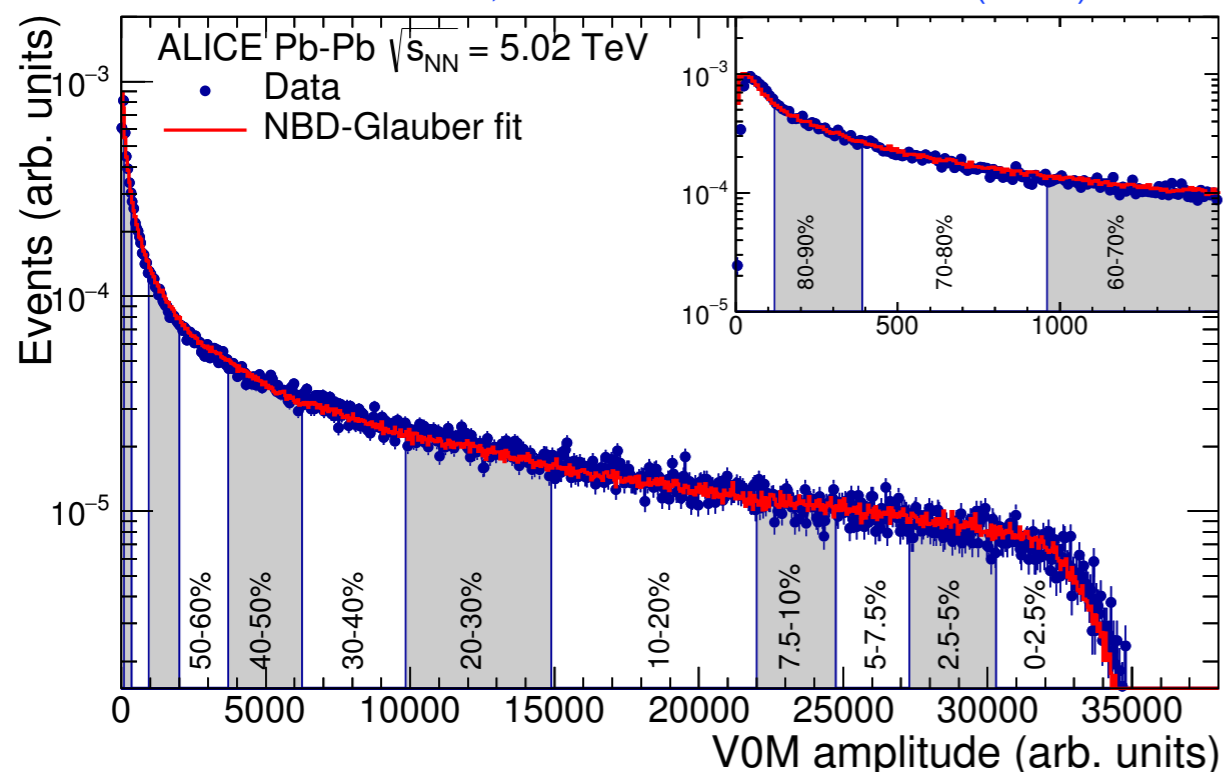
Most central collision \iff Smallest \mathbf{b}

Experimentally

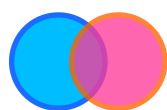
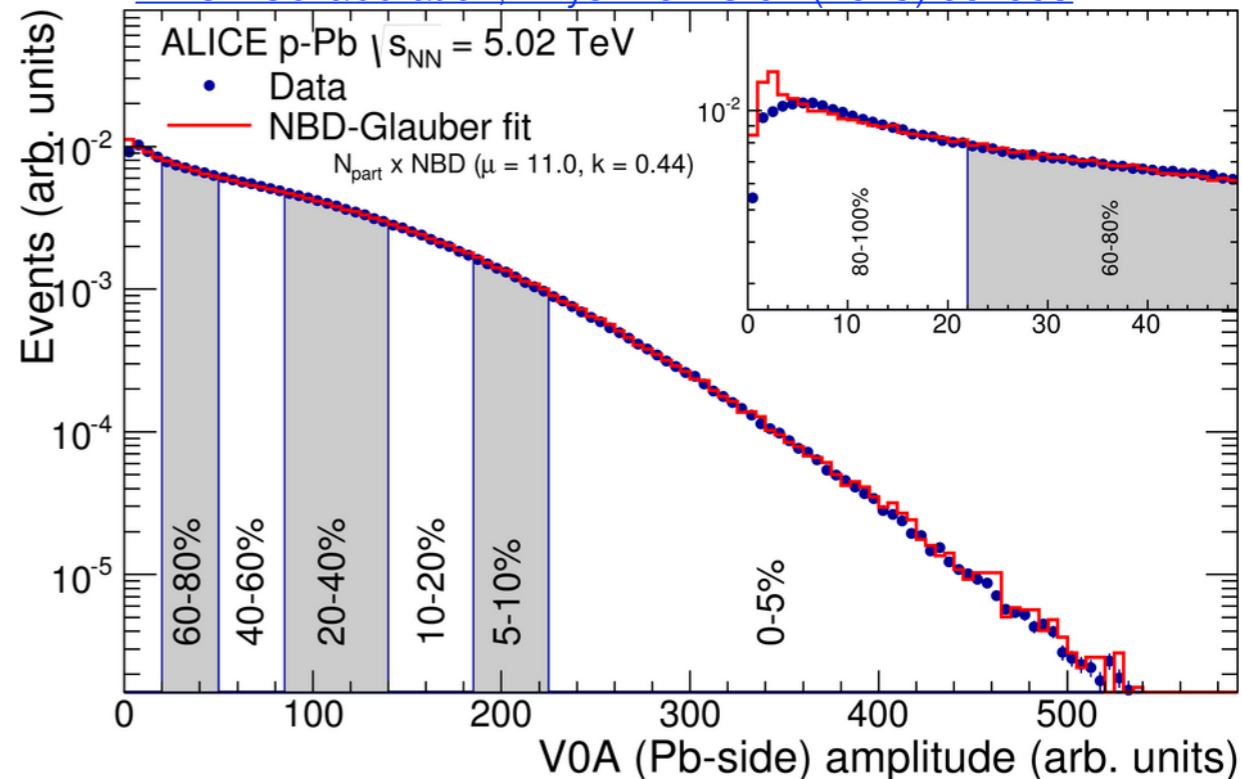
It is possible to correlate the charged particle multiplicity to an impact parameter value by fitting data with predictions from Glauber model

- centrality class defined as percentile of the total cross-section

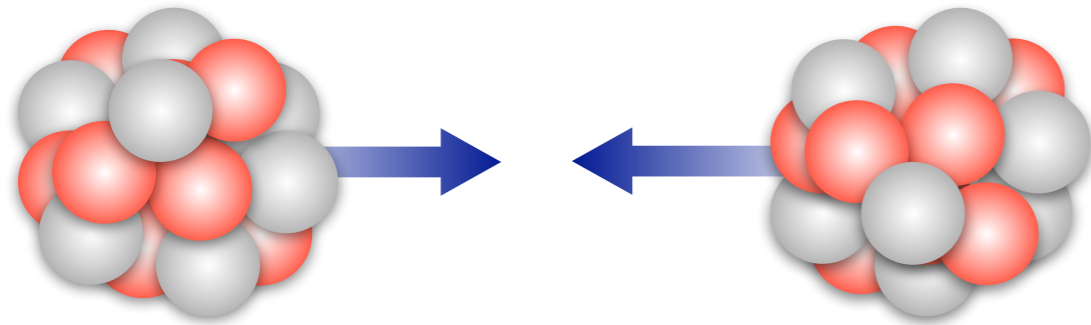
[ALICE Collaboration, ALICE-PUBLIC-2015-008 \(2015\)](#)



[ALICE Collaboration, Phys. Rev. C 91 \(2015\) 064905](#)



Collision systems at the LHC



Pb-Pb

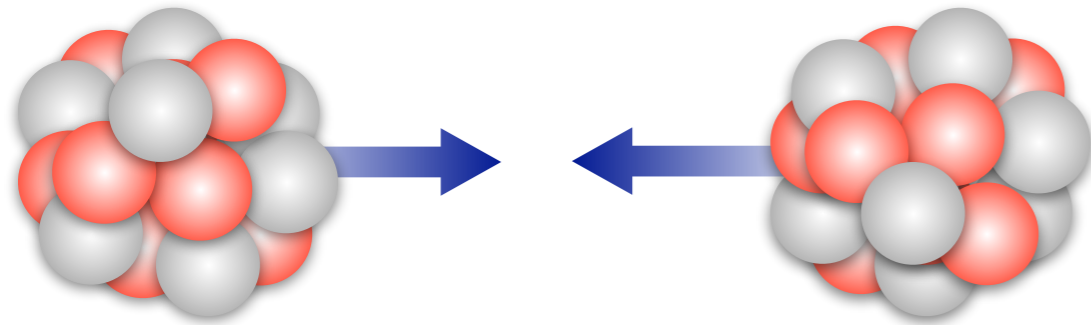
Xe-Xe

| $\sqrt{s_{NN}}$ |
|-----------------|
| 2.76 TeV |
| 5.02 TeV |
| 5.44 TeV |

Study of the hot and dense matter

Study of these **three collision** systems is fundamental to improve our knowledge of **hadronisation** and **strong interaction** at extreme regimes of **energy density**

Collision systems at the LHC



Pb-Pb

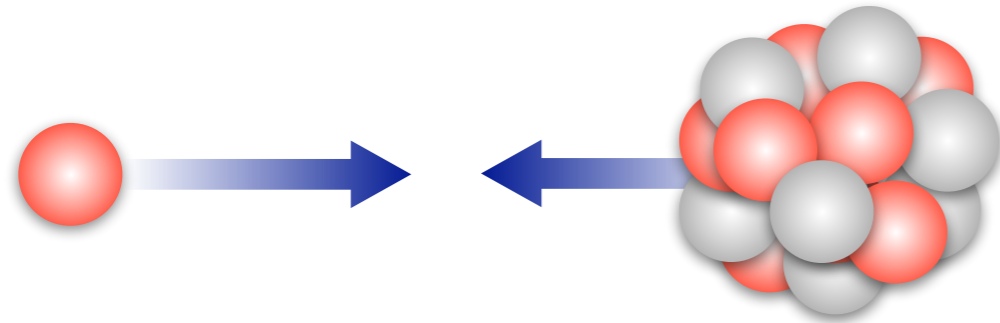
Xe-Xe

$\sqrt{s_{NN}}$

2.76 TeV

5.02 TeV

5.44 TeV



p-Pb

Pb-p

$\sqrt{s_{NN}}$

5.02 TeV

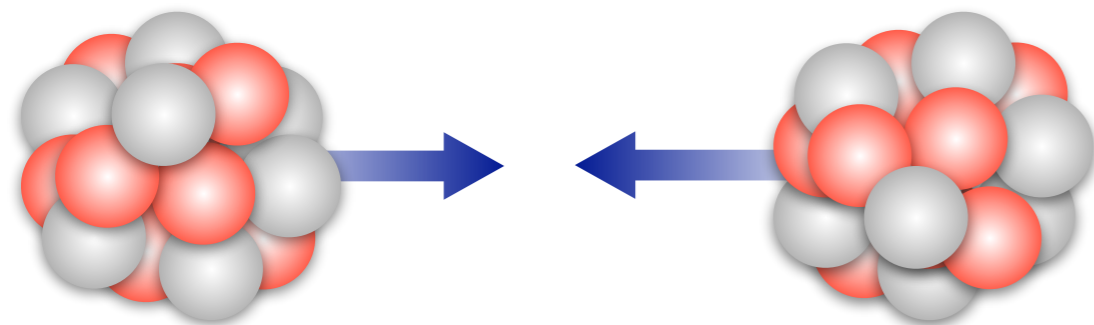
8.16 TeV

Study of the hot and dense matter

Study of nuclear matter effects

Study of these **three collision** systems is fundamental to improve our knowledge of **hadronisation** and **strong interaction** at extreme regimes of **energy density**

Collision systems at the LHC



Pb-Pb

Xe-Xe

$\sqrt{s_{NN}}$

2.76 TeV

5.02 TeV

5.44 TeV

Study of the hot and dense matter



p-Pb

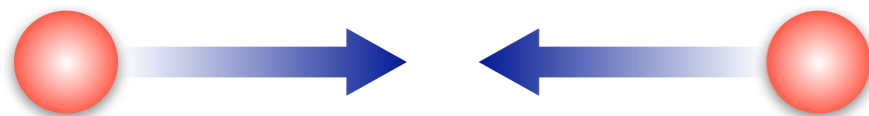
Pb-p

$\sqrt{s_{NN}}$

5.02 TeV

8.16 TeV

Study of nuclear matter effects



p-p

$\sqrt{s_{NN}}$

0.9 TeV

2.76 TeV

5 TeV

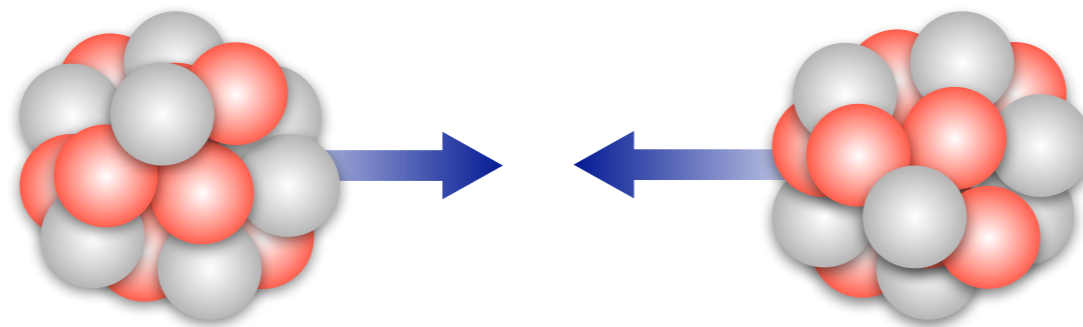
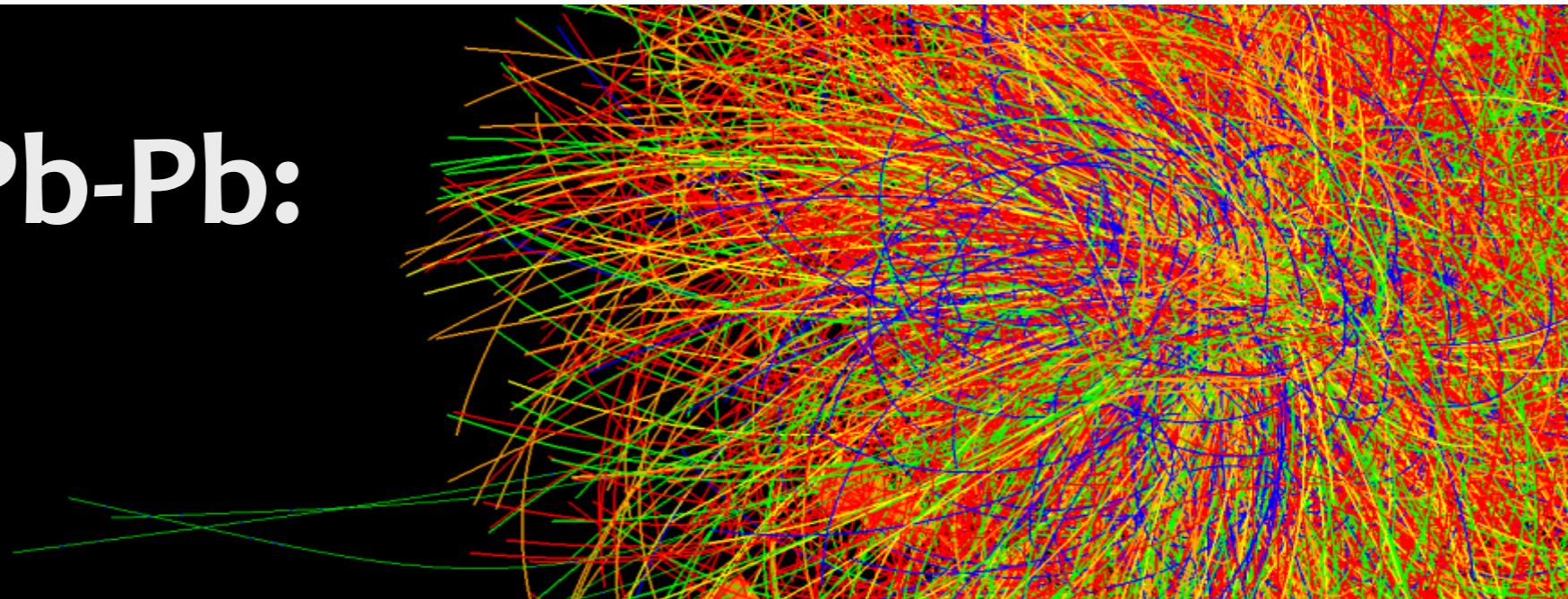
7 TeV

13 TeV

Reference for measurements in other systems

Study of these **three collision** systems is fundamental to improve our knowledge of **hadronisation** and **strong interaction** at extreme regimes of **energy density**

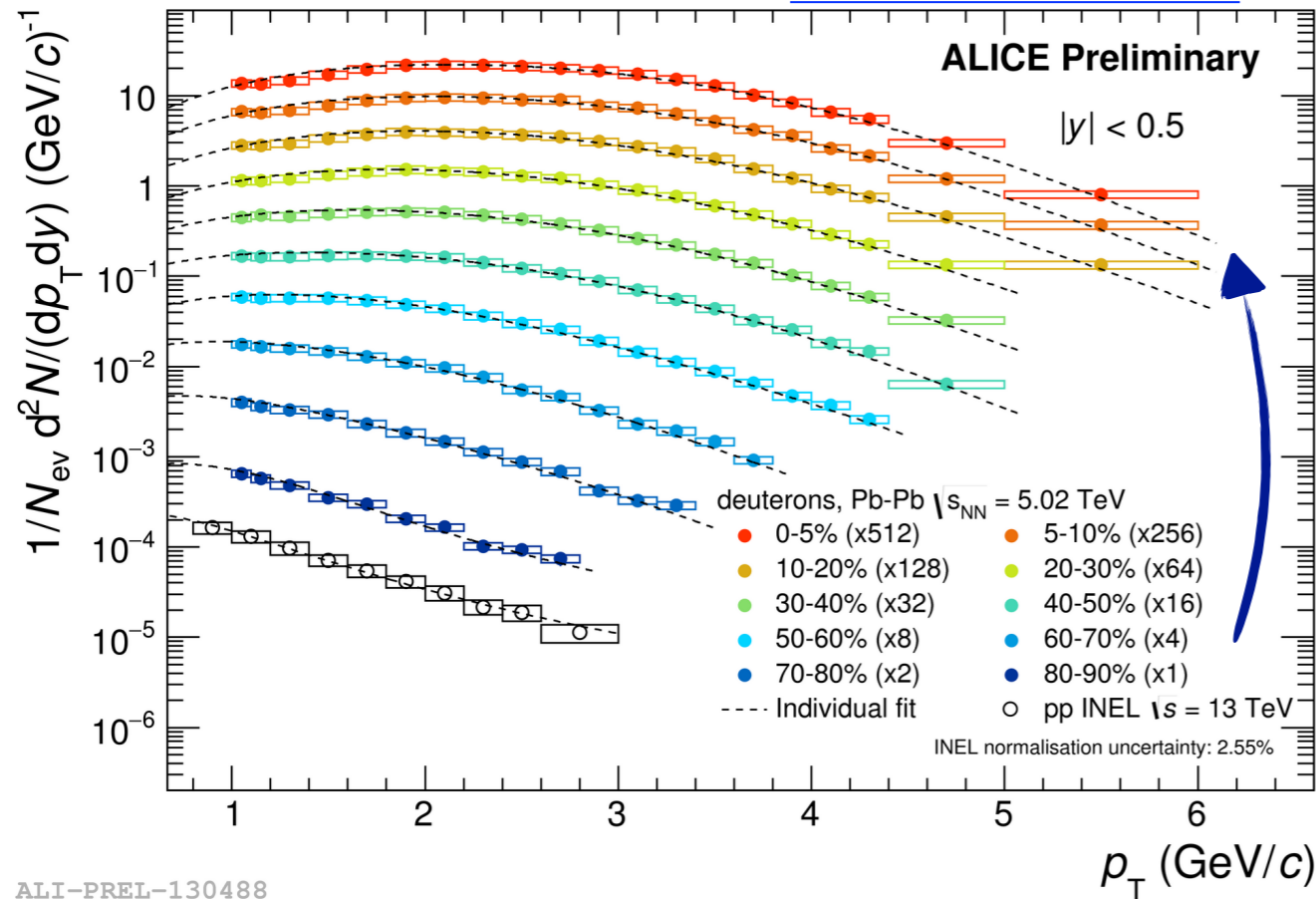
Production in Pb-Pb: *Nuclei*



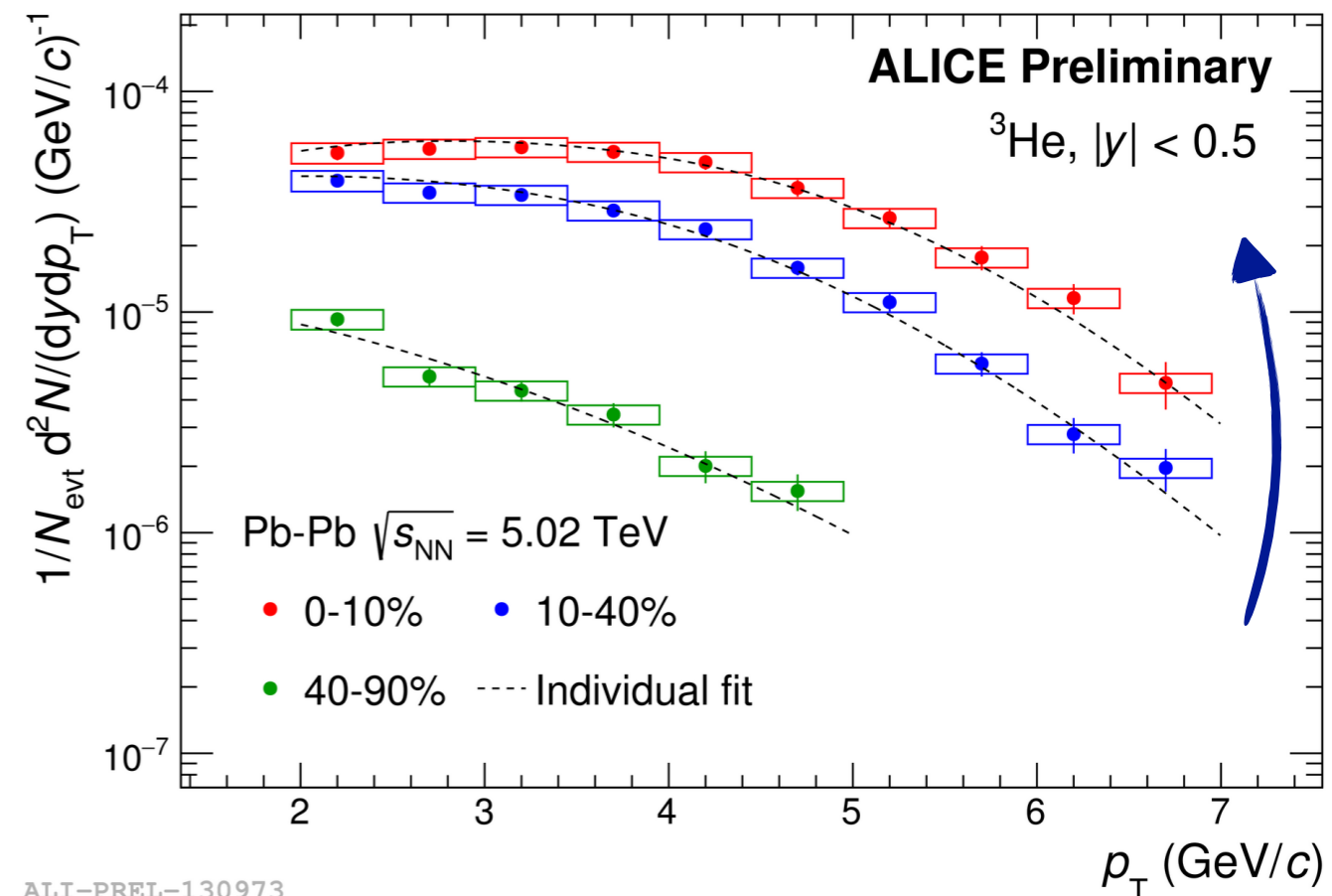
Deuteron and ^3He spectra

$\sqrt{s_{NN}} = 5.02 \text{ TeV}$

ALICE-PUBLIC-2017-006



ALI-PREL-130488



ALI-PREL-130973

- deuteron and ^3He spectra measured as a function of centrality classes
- Pronounced hardening of deuteron and ^3He p_T spectra with increasing centrality → radial flow
- p_T spectra are fitted with the Blast-Wave [4] function → yield extrapolation to unmeasured regions

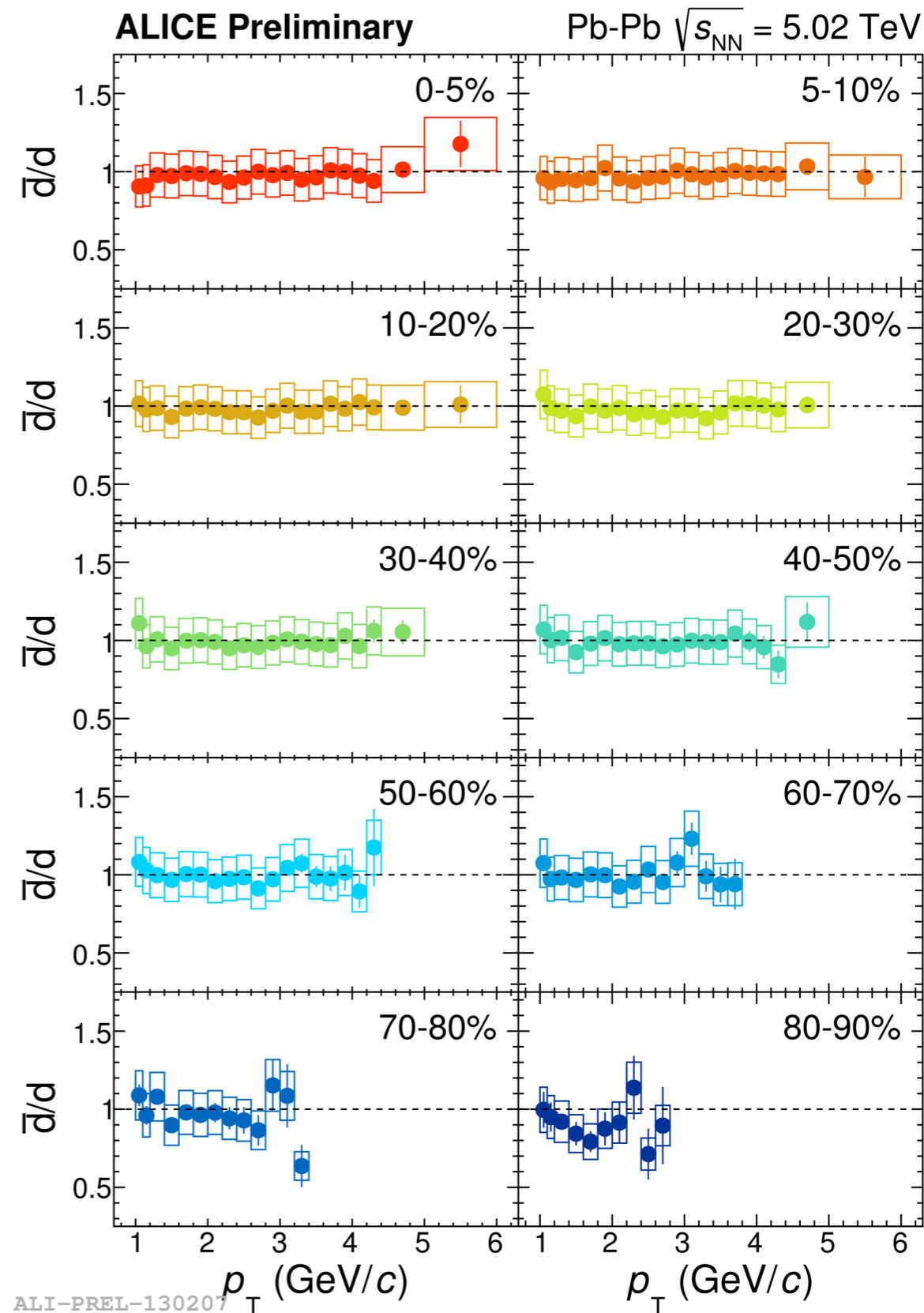
[4] E. Schnedermann et al. Phys. Rev. C 48, 2462 (1993)

Anti-nuclei/nuclei ratio

$\sqrt{s_{NN}} = 5.02 \text{ TeV}$

- At the LHC energies the **antiproton/proton** ratio [5] is compatible with the **unity**:
 - regime of **nuclear transparency** is reached \rightarrow evanescent baryo-chemical ($\mu_B \sim 0$) potential in the mid-rapidity region
- **Thermal** and **coalescence** models predict for a nucleus X with mass number A :
$$\frac{\bar{X}}{X} \approx \left(\frac{\bar{p}}{p} \right)^A$$
- Results of \bar{d}/d and ${}^3\bar{\text{He}}/{}^3\text{He}$ in Pb-Pb collisions confirm the prediction:
 - p_T and **centrality** independent

[5] ALICE Collaboration, Phys. Rev. C 88 (2013) 044910

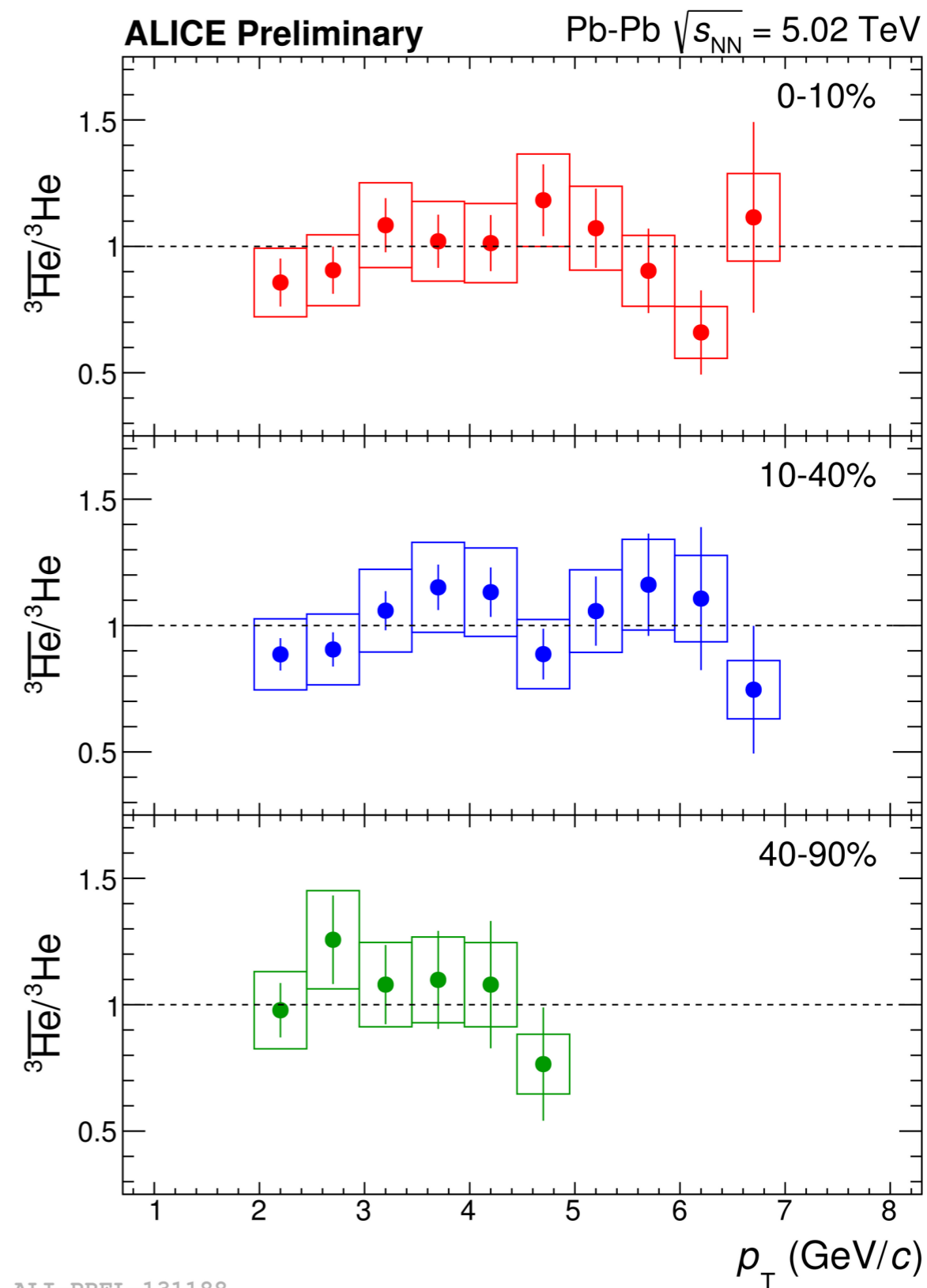


Anti-nuclei/nuclei ratio

$\sqrt{s_{NN}} = 5.02 \text{ TeV}$

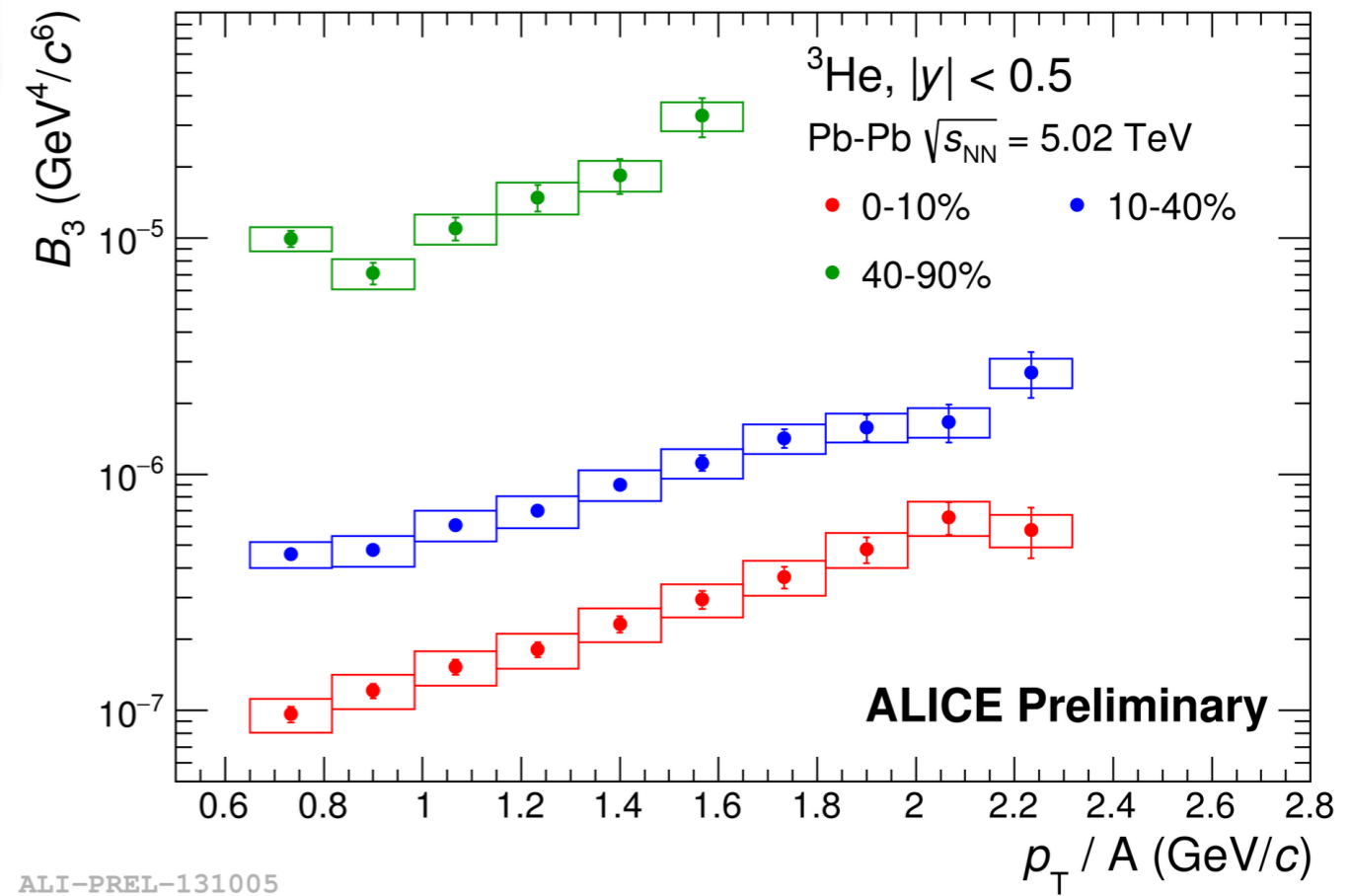
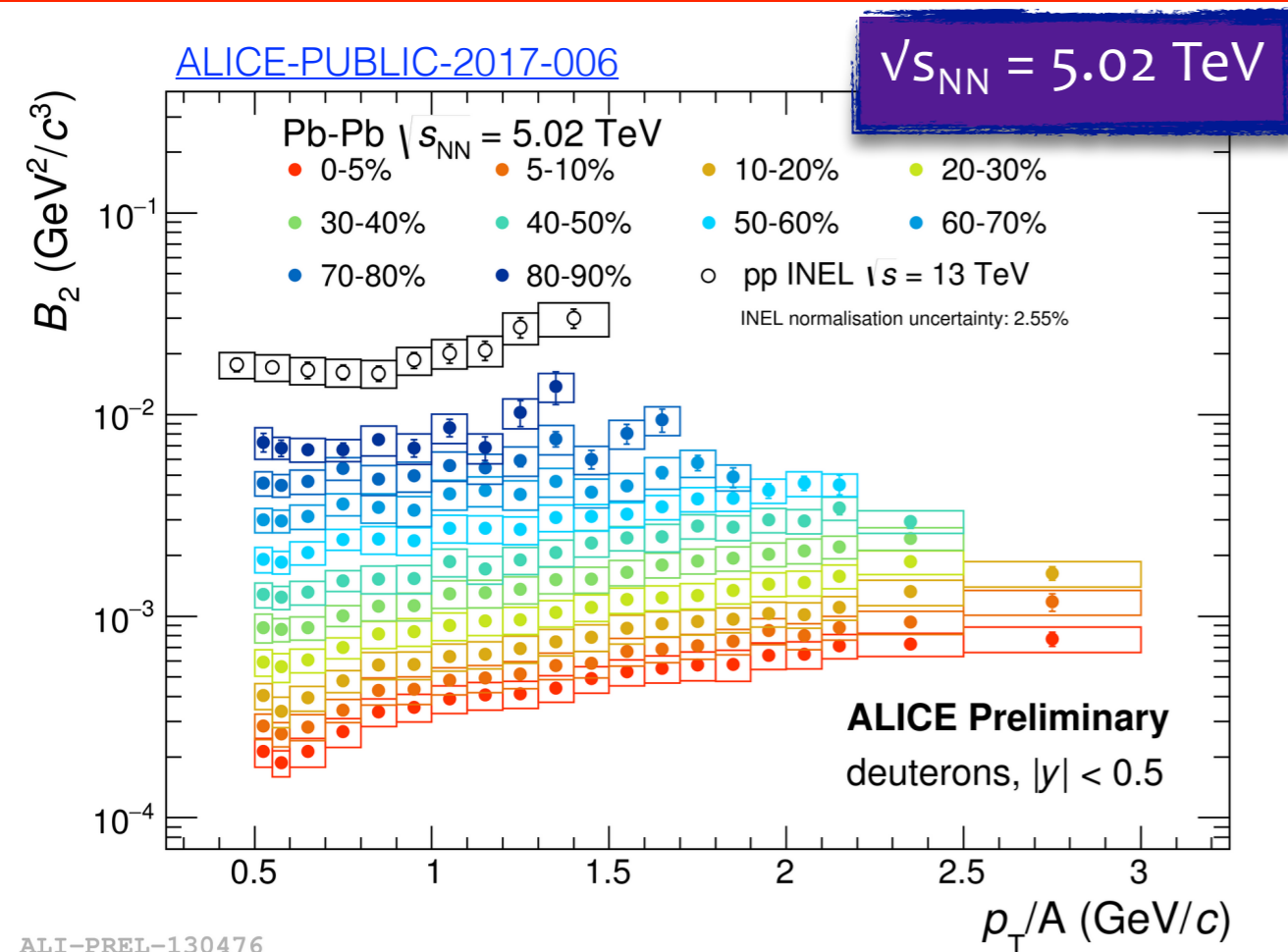
- At the LHC energies the **antiproton/proton** ratio [5] is compatible with the **unity**:
 - regime of **nuclear transparency** is reached \rightarrow evanescent baryo-chemical ($\mu_B \sim 0$) potential in the mid-rapidity region
- **Thermal** and **coalescence** models predict for a nucleus X with mass number A:
$$\frac{\bar{X}}{X} \approx \left(\frac{\bar{p}}{p} \right)^A$$
- Results of \bar{d}/d and $\bar{^3\text{He}}/^3\text{He}$ in Pb-Pb collisions confirm the prediction:
 - p_T and **centrality** independent

[5] ALICE Collaboration, Phys. Rev. C 88 (2013) 044910



ALI-PREL-131188

Coalescence parameter B_A



- The **probability** to form a nucleus via coalescence can be quantified by the **coalescence parameter B_A** :

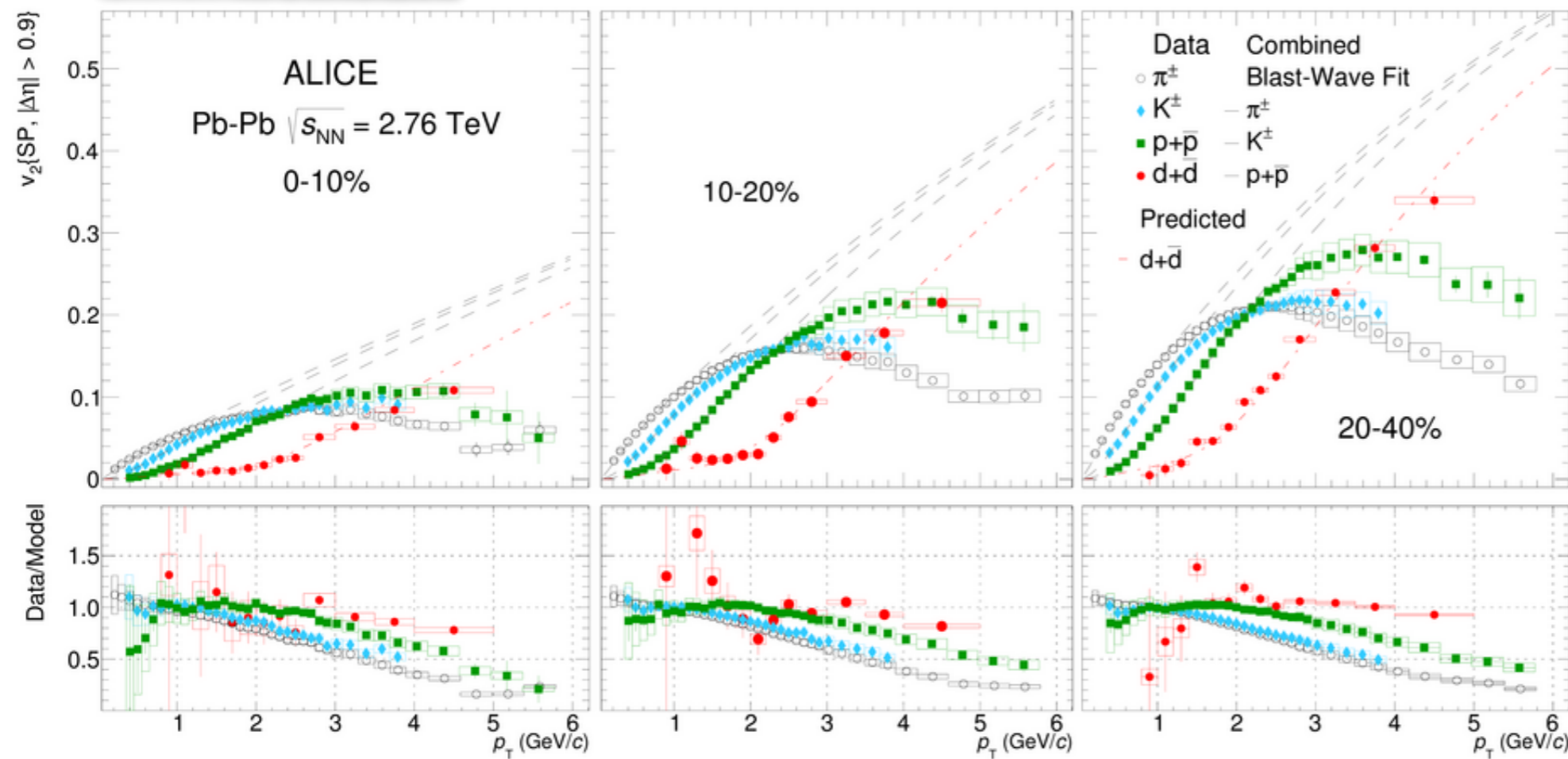
$$B_A = E_A \frac{d^3 N_A}{dp_A^3} / \left(E_p \frac{d^3 N_p}{dp_p^3} \right)^A$$

- A is the mass number
- $p_p = p_A/A$

- According to **simple coalescence** predictions B_A is **p_T flat**:
 - simple coalescence **does not describe** the trend observed in Pb-Pb collisions
- The **rise in p_T** becomes milder moving from central to peripheral collisions

Deuteron elliptic flow

$\sqrt{s_{NN}} = 2.76 \text{ TeV}$



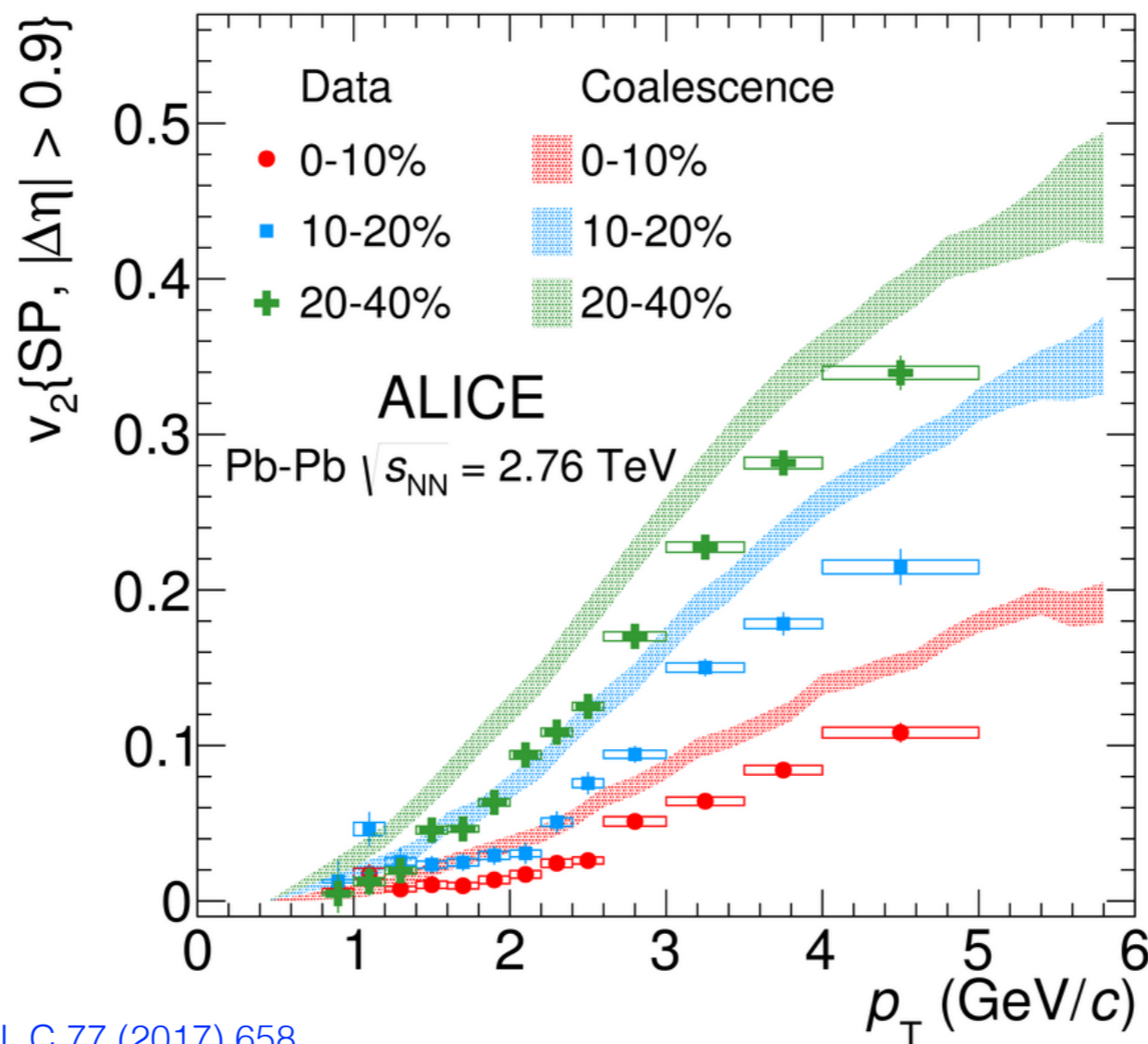
Elliptic flow measured with **scalar product** method

$$v_n\{SP\} = \frac{\langle u_{n,i}(p_T, \eta) \cdot \frac{Q_n^*}{M} \rangle}{\sqrt{\langle \frac{Q_{n,A}^*}{M_A} \cdot \frac{Q_{n,B}^*}{M_B} \rangle}}$$

- The v_2 of the deuteron is compatible with the prediction of the **Blast-Wave** model:
 - scale the BW fits to $\pi/K/p$ spectra to the deuteron mass \rightarrow hint of a common thermal production

Deuteron elliptic flow

$\sqrt{s_{NN}} = 2.76$ TeV



Elliptic flow measured with **scalar product** method

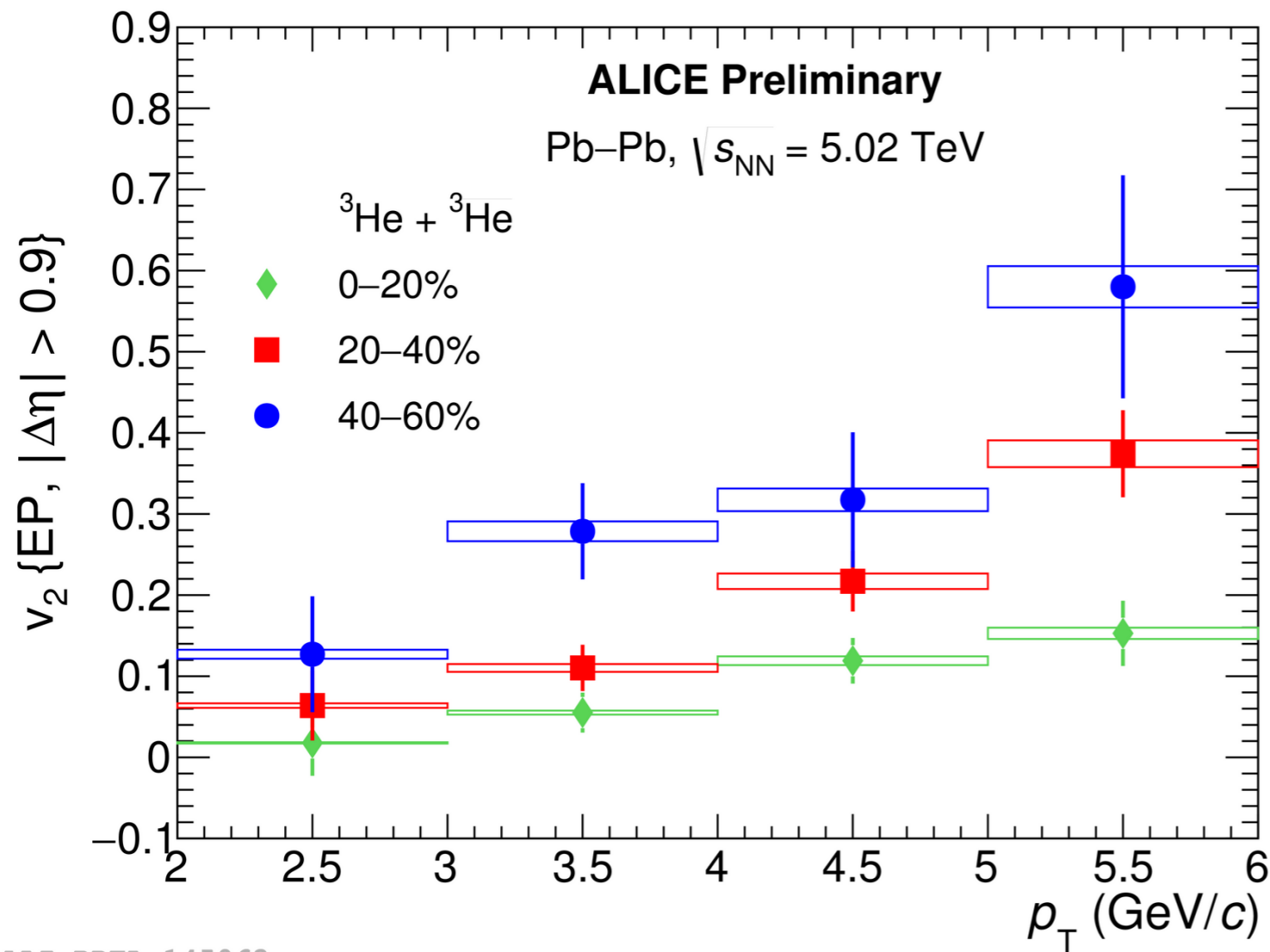
$$v_n\{SP\} = \frac{\langle u_{n,i}(p_T, \eta) \cdot \frac{Q_n^*}{M} \rangle}{\sqrt{\langle \frac{Q_{n,A}^*}{M_A} \cdot \frac{Q_{n,B}^*}{M_B} \rangle}}$$

[ALICE Collaboration, Eur. Phys. J. C 77 \(2017\) 658](#)

- The v_2 of the deuteron is compatible with the prediction of the **Blast-Wave** model:
 - scale the BW fits to $\pi/K/p$ spectra to the deuteron mass \rightarrow hint of a common thermal production
- The **simple coalescence** model **does not describe** the v_2 of the deuterons:
 - $v_2^d(p_T^d) = 2 \cdot v_2^p(2p_T^p) \rightarrow$ at lower energies able to describe deuteron v_2

^3He elliptic flow

$\sqrt{s_{\text{NN}}} = 5.02 \text{ TeV}$



ALI-PREL-145063

- v_2 of ^3He measured in three centrality classes:
 - increase while going to peripheral collisions
 - smooth rise with p_T

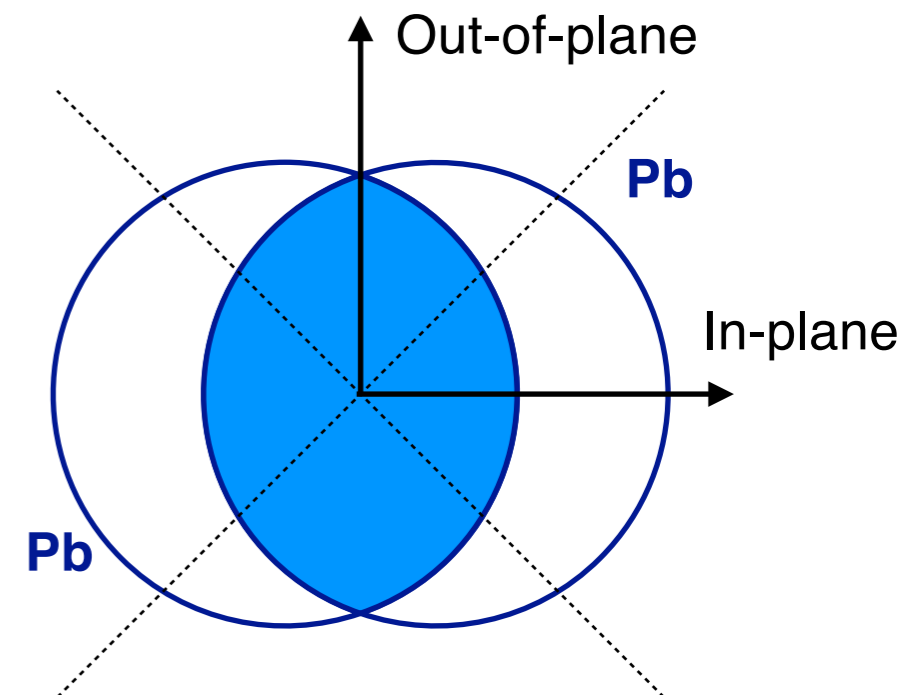
The v_2 of ^3He is measured using the **Event-Plane** method:

- Reconstruction of the Event Plane (estimator of the Reaction Plane)

- v_2 computed as:

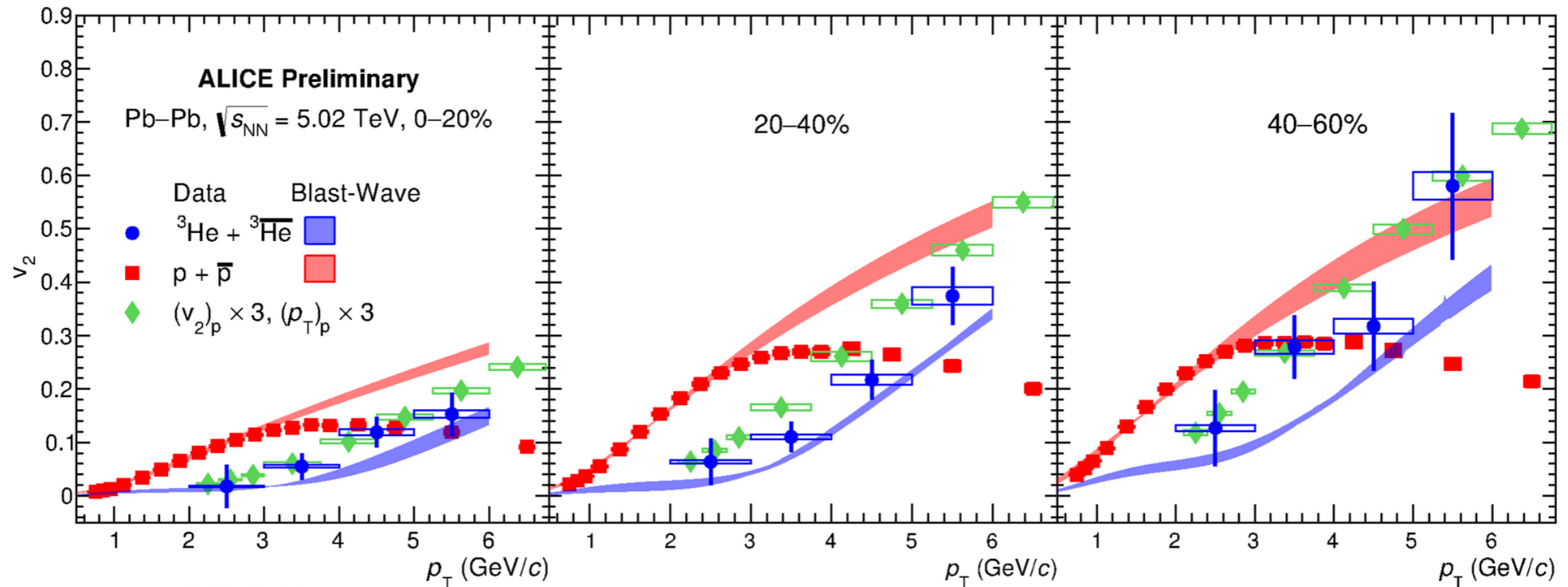
$$v_2 = \frac{1}{R_2} \frac{\pi}{4} \frac{N_{\text{in-plane}} - N_{\text{out-of-plane}}}{N_{\text{in-plane}} + N_{\text{out-of-plane}}}$$

R_2 is the event plane resolution



^3He elliptic flow

$\sqrt{s_{\text{NN}}} = 5.02 \text{ TeV}$

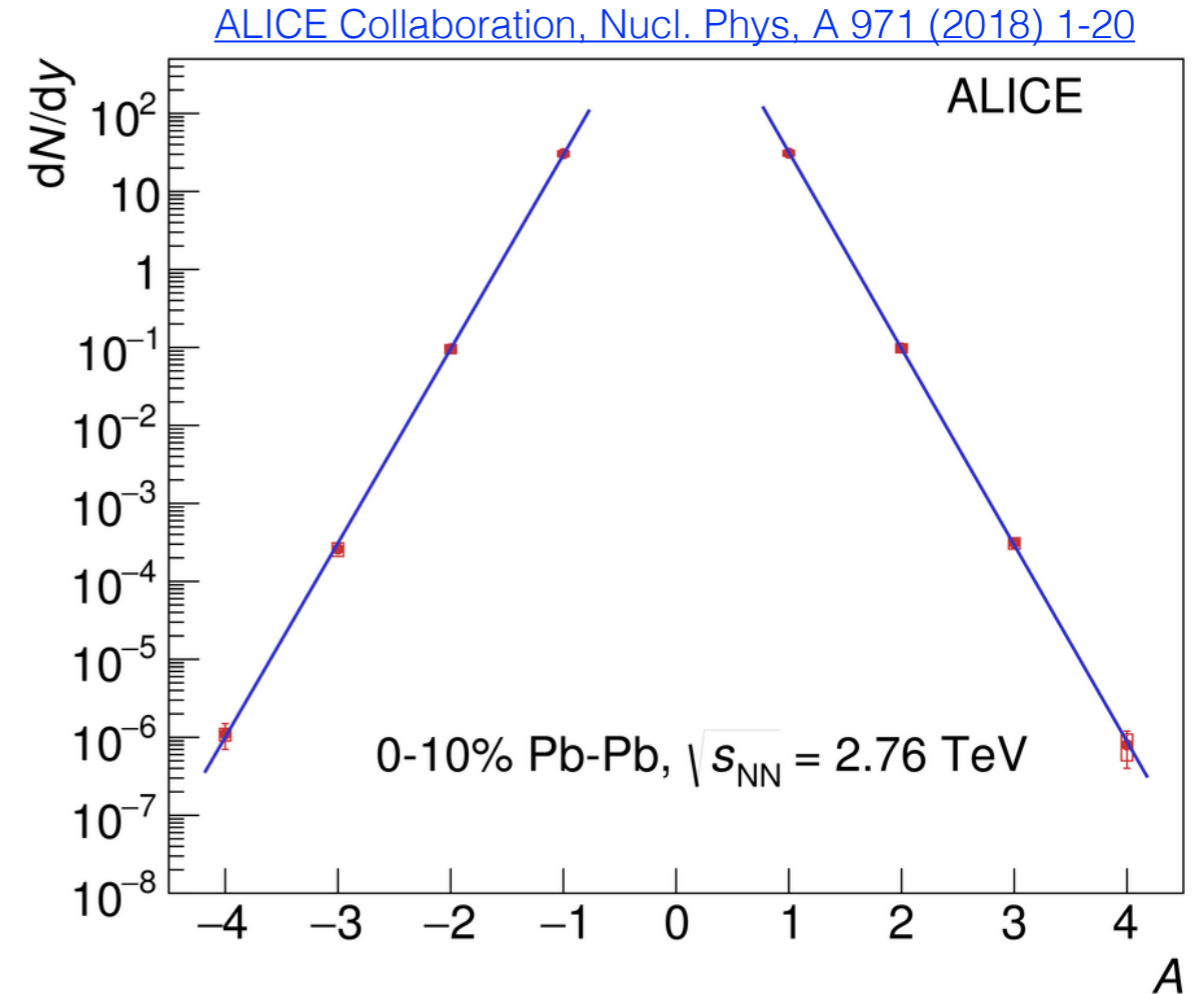
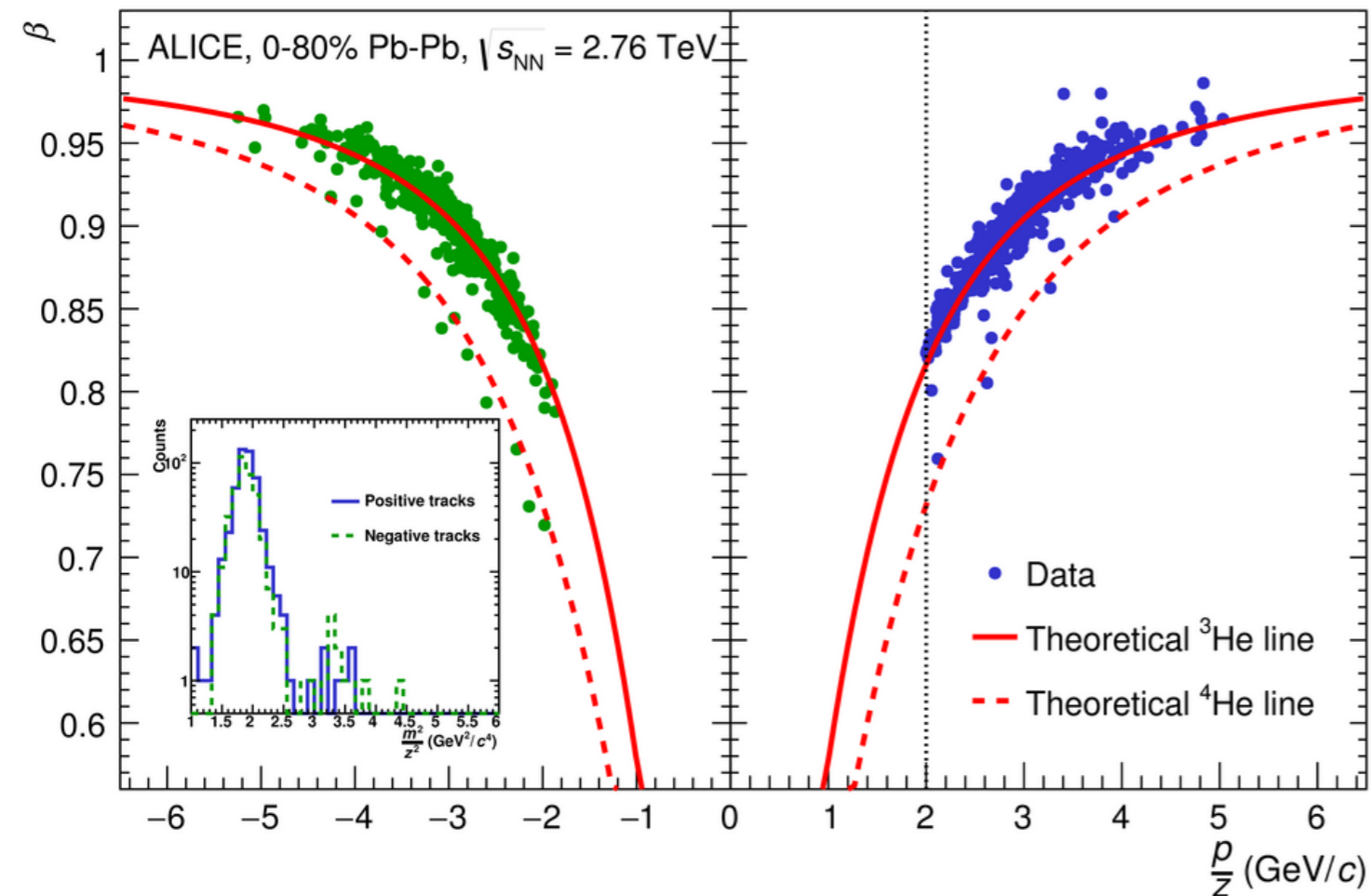


ALI-PREL-145075

- v_2 of ^3He shows a different behavior with respect to v_2 of deuteron
 - overall agreement of the prediction from **Blast-Wave fit** to lighter species is **better** in the **most central collisions**
 - **simple coalescence** expectation (green points) is closer for the results in **40-60% centrality**

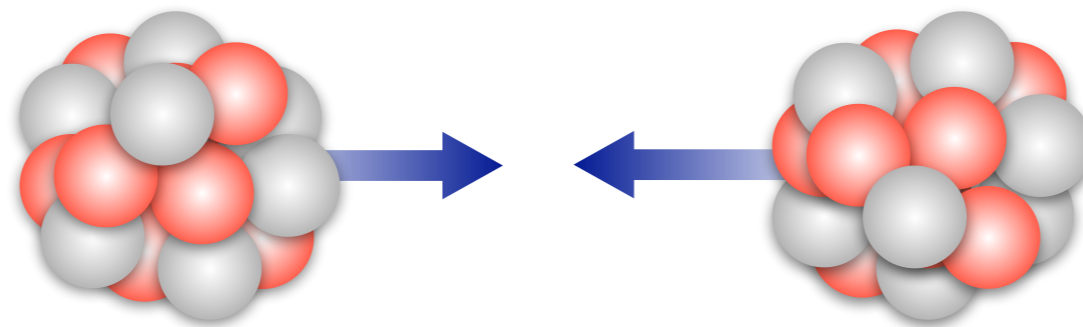
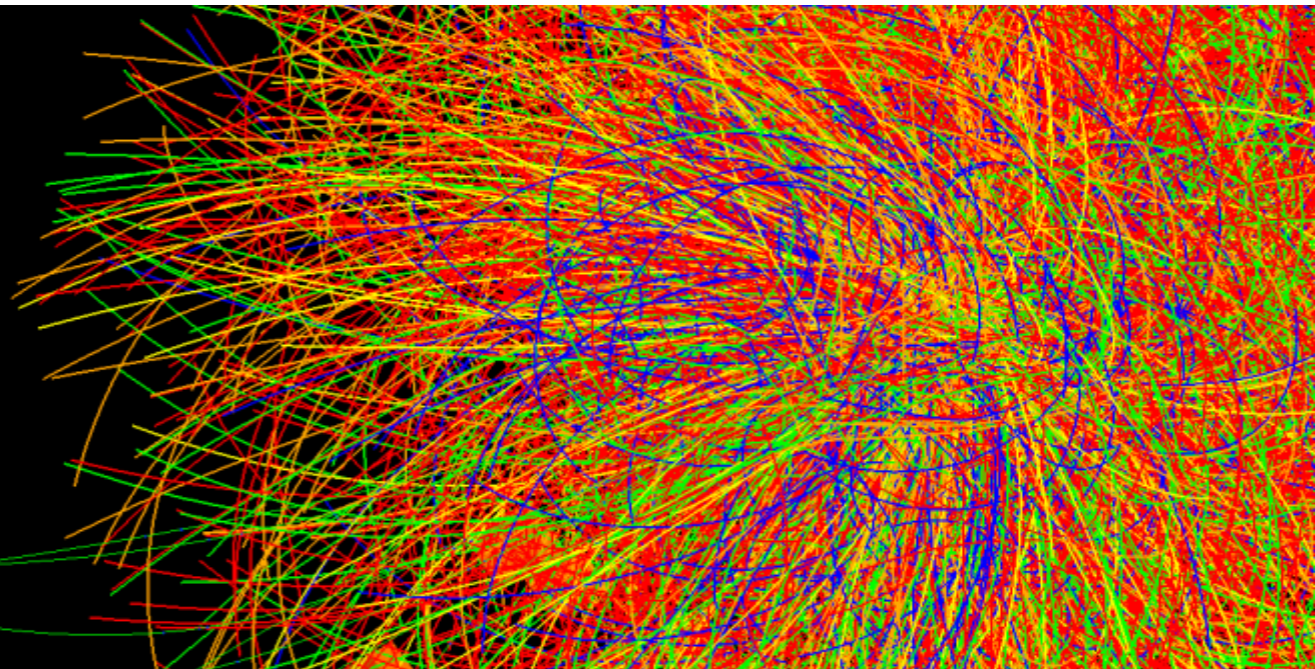
^4He production yields

$\sqrt{s_{\text{NN}}} = 2.76 \text{ TeV}$

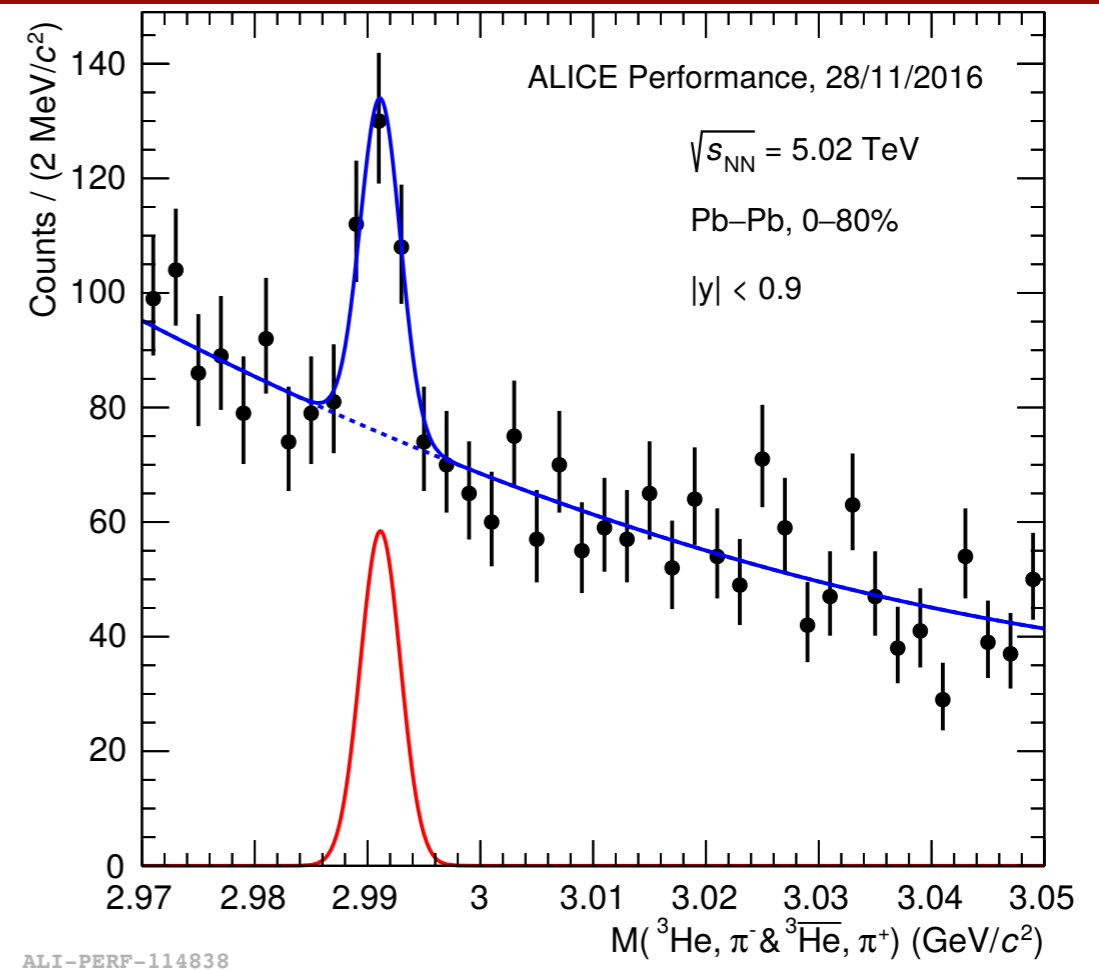
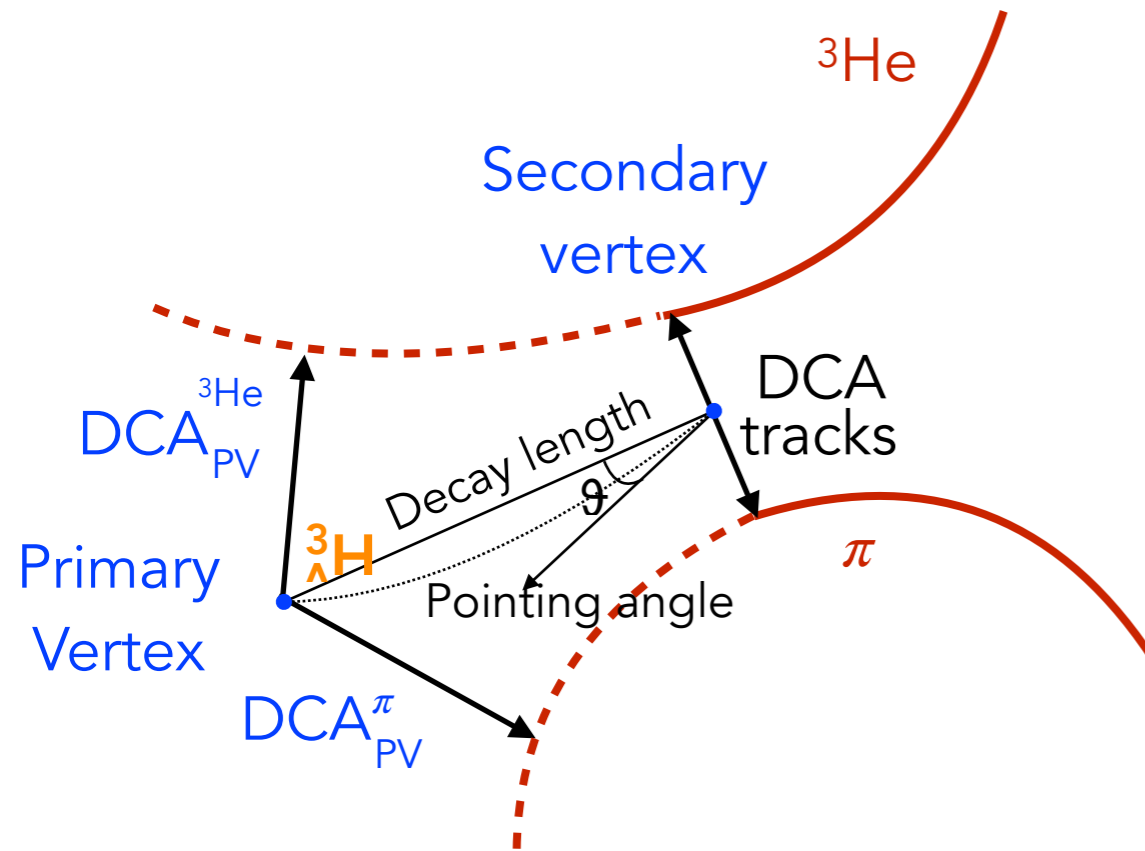


- the production of the **heaviest anti-nucleus** ever has been measured in **Pb-Pb at 2.76 TeV** and “rediscovered” also in **Pb-Pb at 5.02 TeV**
- the prediction by the **thermal model** of **exponential decrease** in nuclei production rate is **confirmed**
 - in Pb-Pb the **penalty factor** for adding one baryon is **~ 300**

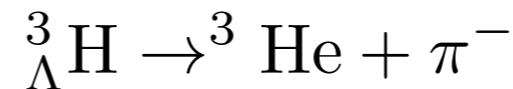
Production in Pb-Pb: *Hypertriton*



Hypertriton identification



- (Anti-)hypertriton **production** studies performed via two charged body decay channel



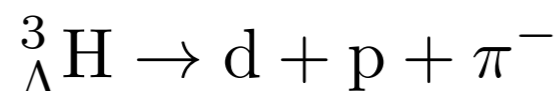
- ${}^3\text{He}$ and π tracks identified via specific energy loss in TPC
- **Secondary vertex** reconstructed exploiting the algorithm used for the V0 topology
- **Signal raw yields** extracted with a fit to the invariant mass distribution:

$$f(m) = N_{sig} \cdot f_{sig}(m) + N_{bkg} \cdot f_{bkg}(m)$$

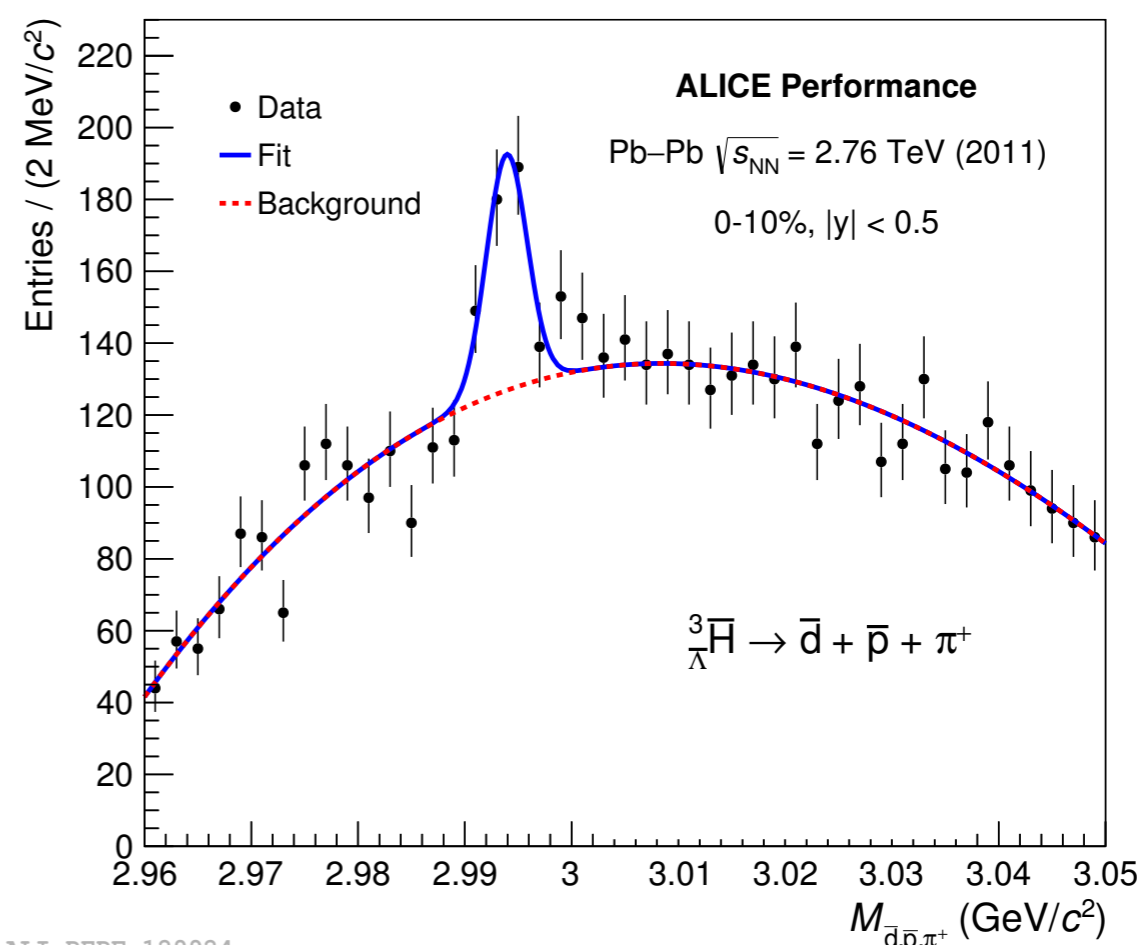
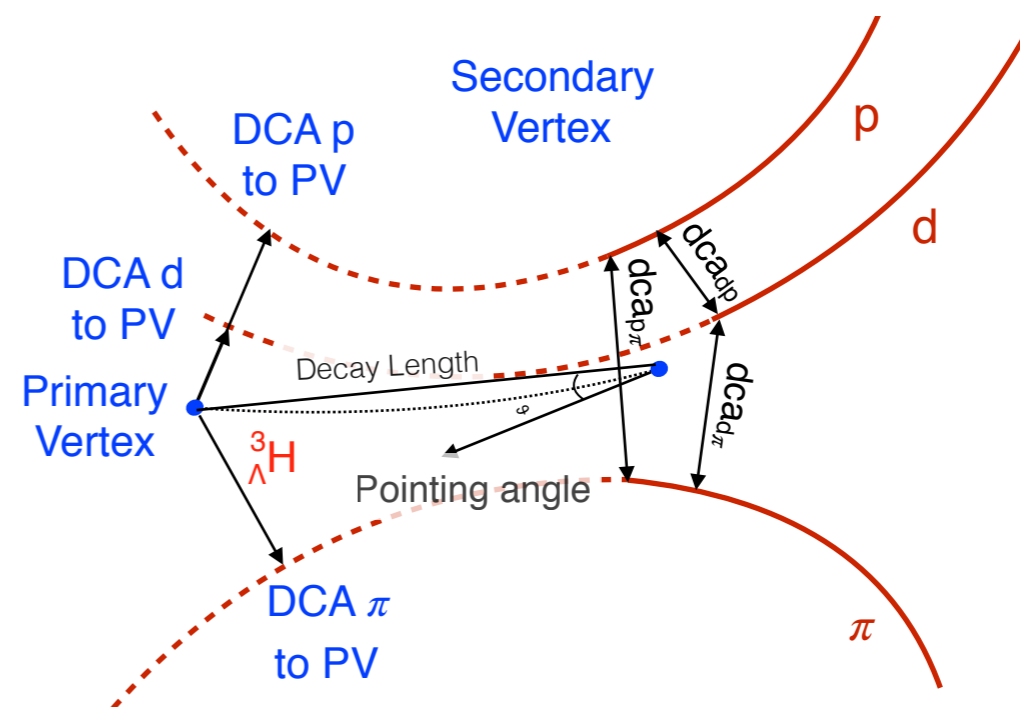
- Method used both for **production** and **lifetime** analysis

Hypertriton identification

- (Anti-)hypertriton **production** studies performed via **three charged body** decay channel



- higher **Branching Ratio** compared to the two body, but also larger **combinatorial background**
- **d**, **p** and **π** tracks identified via specific energy loss in TPC
- Topological and kinematical selections on the daughter tracks
- **Secondary vertex** reconstructed as the point at **minimum distance** to the selected tracks
- **Signal raw yields** extracted with a fit to the invariant mass distribution, as previously shown

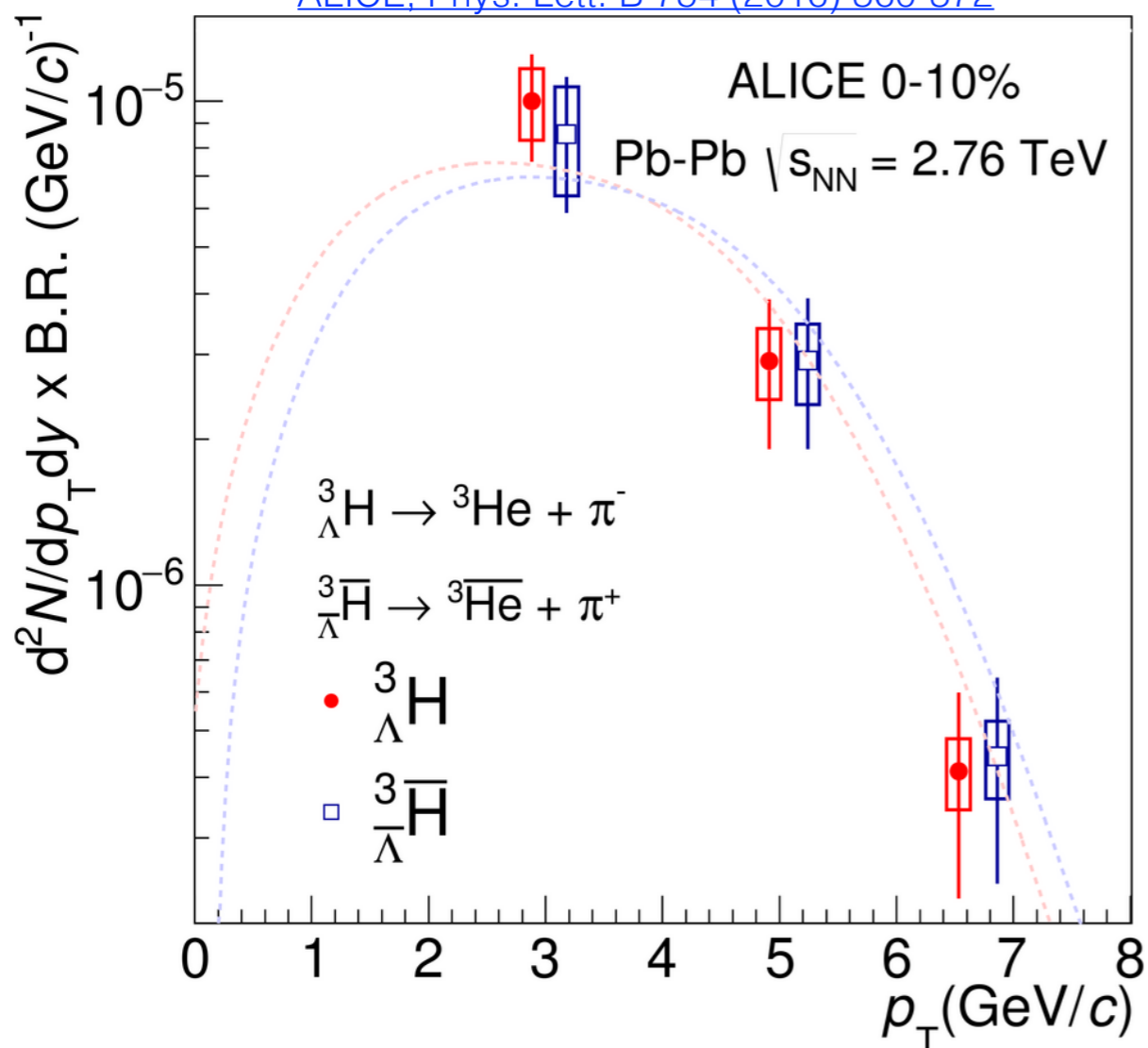


ALI-PERF-129924

${}^3_{\Lambda}\text{H}$ production

$\sqrt{s_{\text{NN}}} = 2.76 \text{ TeV}$

ALICE, Phys. Lett. B 754 (2016) 360-372

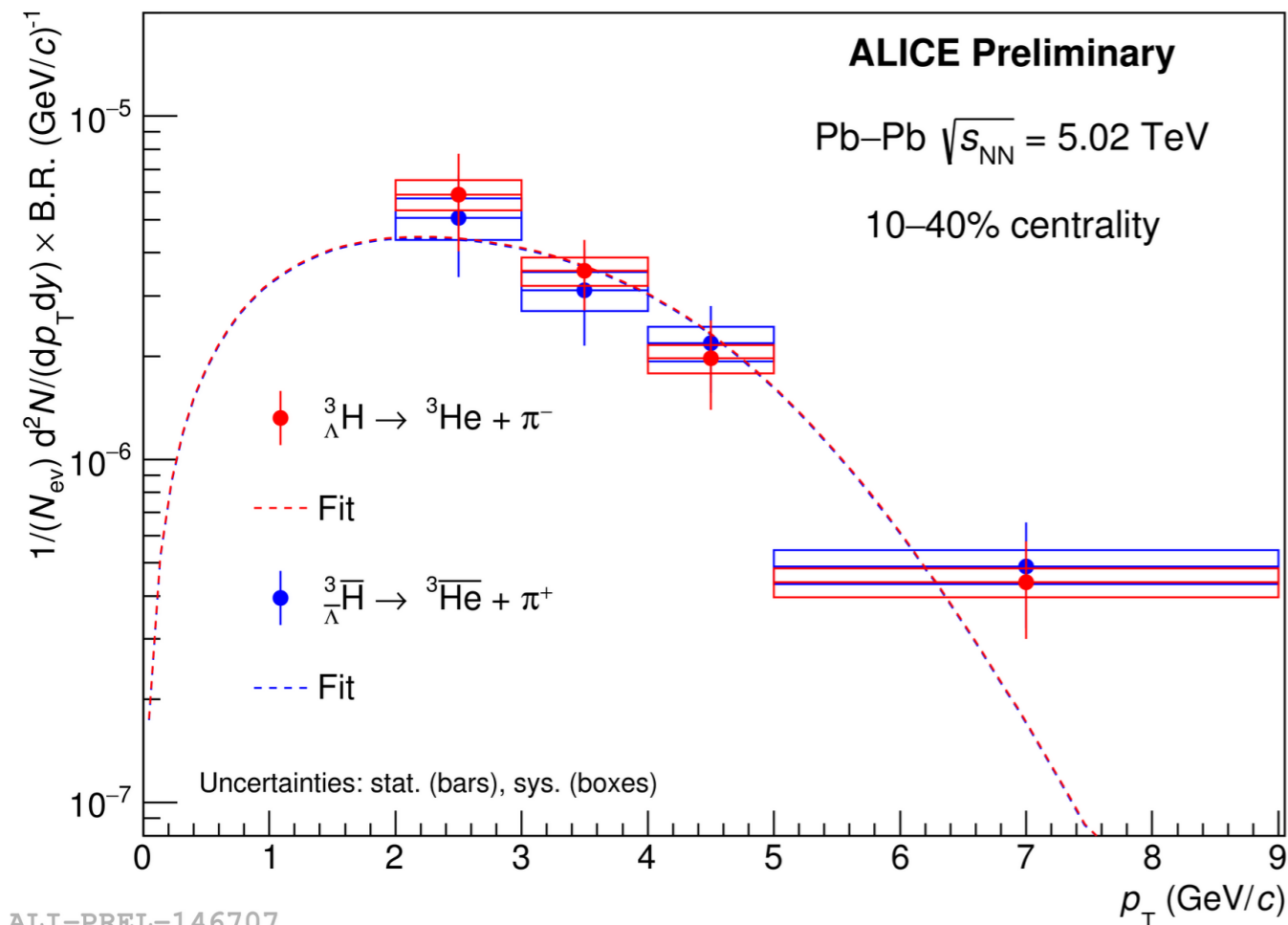


Antimatter-to-matter ratio in agreement with unity within the uncertainties

- p_T spectra were measured in **most central** collisions at **2.76 TeV**:
 - **Blast-Wave** fit to extrapolate yield in the unmeasured regions
- Similarly p_T spectra have been measured in **semi-central** collisions at **5.02 TeV**
- In Pb-Pb collisions at **5.02 TeV** yields measured as a function of the **charged particle multiplicity**:
 - dN/dy in three centrality classes
 - increasing trend can be interpreted in the thermal model as related to the volume of the created medium

${}^3_{\Lambda}\text{H}$ production

$\sqrt{s_{\text{NN}}} = 5.02 \text{ TeV}$

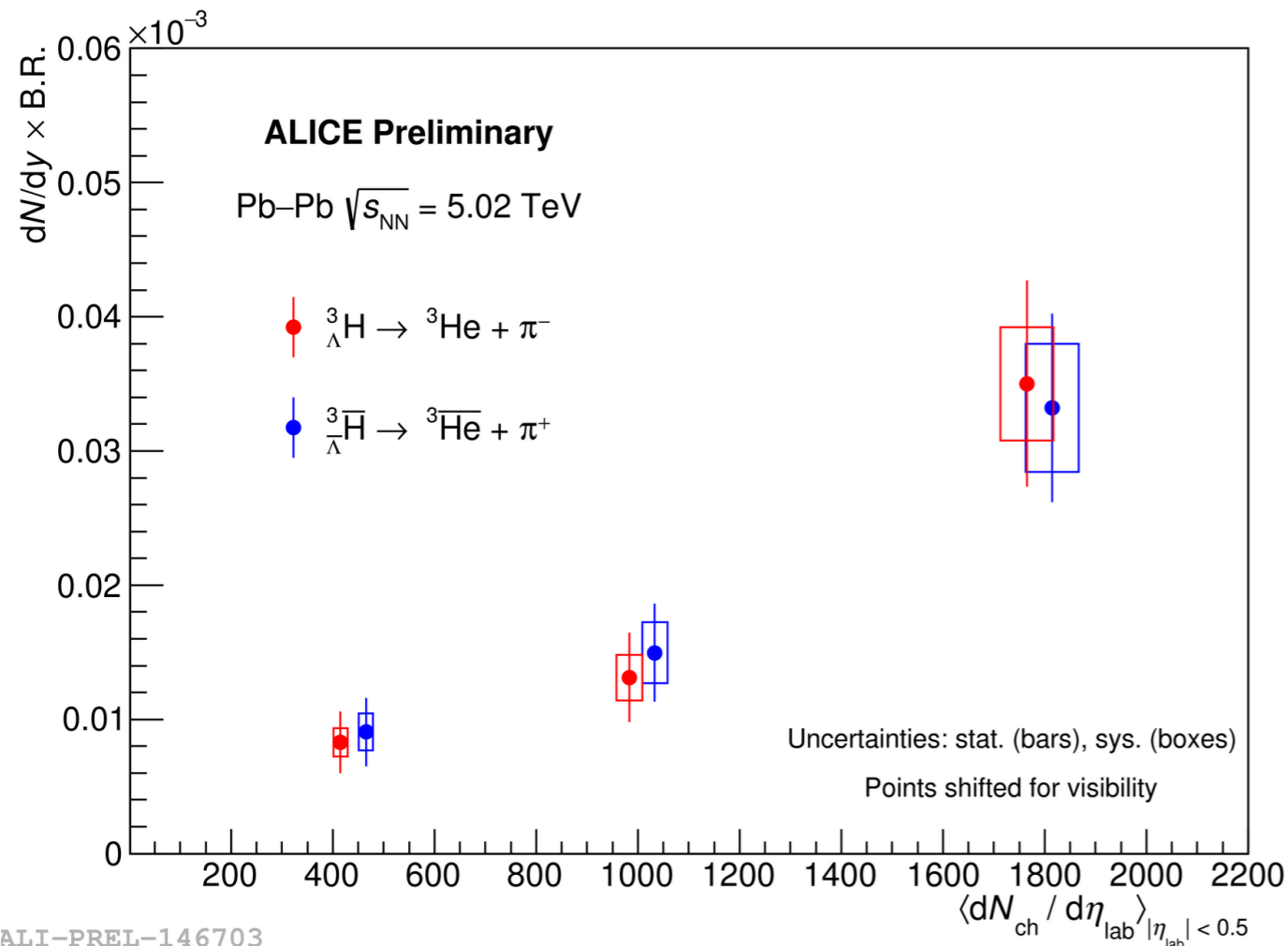


Antimatter-to-matter ratio in agreement with unity within the uncertainties

- p_T spectra were measured in **most central** collisions at **2.76 TeV**:
 - **Blast-Wave** fit to extrapolate yield in the unmeasured regions
- Similarly p_T spectra have been measured in **semi-central** collisions at **5.02 TeV**
- In Pb-Pb collisions at **5.02 TeV** yields measured as a function of the **charged particle multiplicity**:
 - dN/dy in three centrality classes
 - increasing trend can be interpreted in the thermal model as related to the volume of the created medium

${}^3_{\Lambda}\text{H}$ production

$$\sqrt{s_{\text{NN}}} = 5.02 \text{ TeV}$$



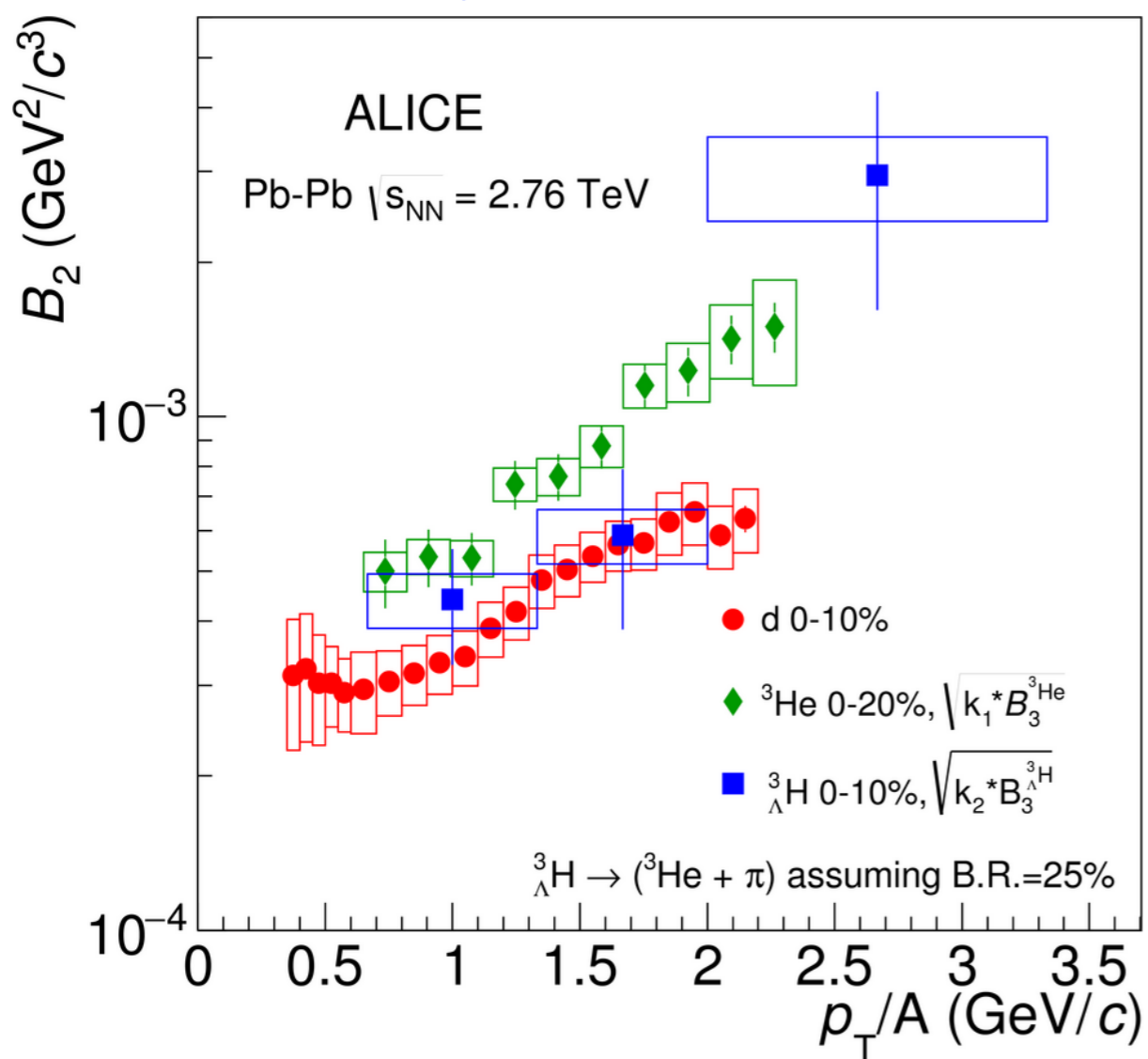
Antimatter-to-matter ratio in agreement with unity within the uncertainties

- p_{T} spectra were measured in **most central** collisions at **2.76 TeV**:
 - **Blast-Wave** fit to extrapolate yield in the unmeasured regions
- Similarly p_{T} spectra have been measured in **semi-central** collisions at **5.02 TeV**
- In Pb-Pb collisions at **5.02 TeV** yields measured as a function of the **charged particle multiplicity**:
 - dN/dy in three centrality classes
 - increasing trend can be interpreted in the thermal model as related to the volume of the created medium

${}^3_{\Lambda}\text{H}$ coalescence parameter

$$\sqrt{s_{\text{NN}}} = 2.76 \text{ TeV}$$

ALICE, Phys. Lett. B 754 (2016) 360-372

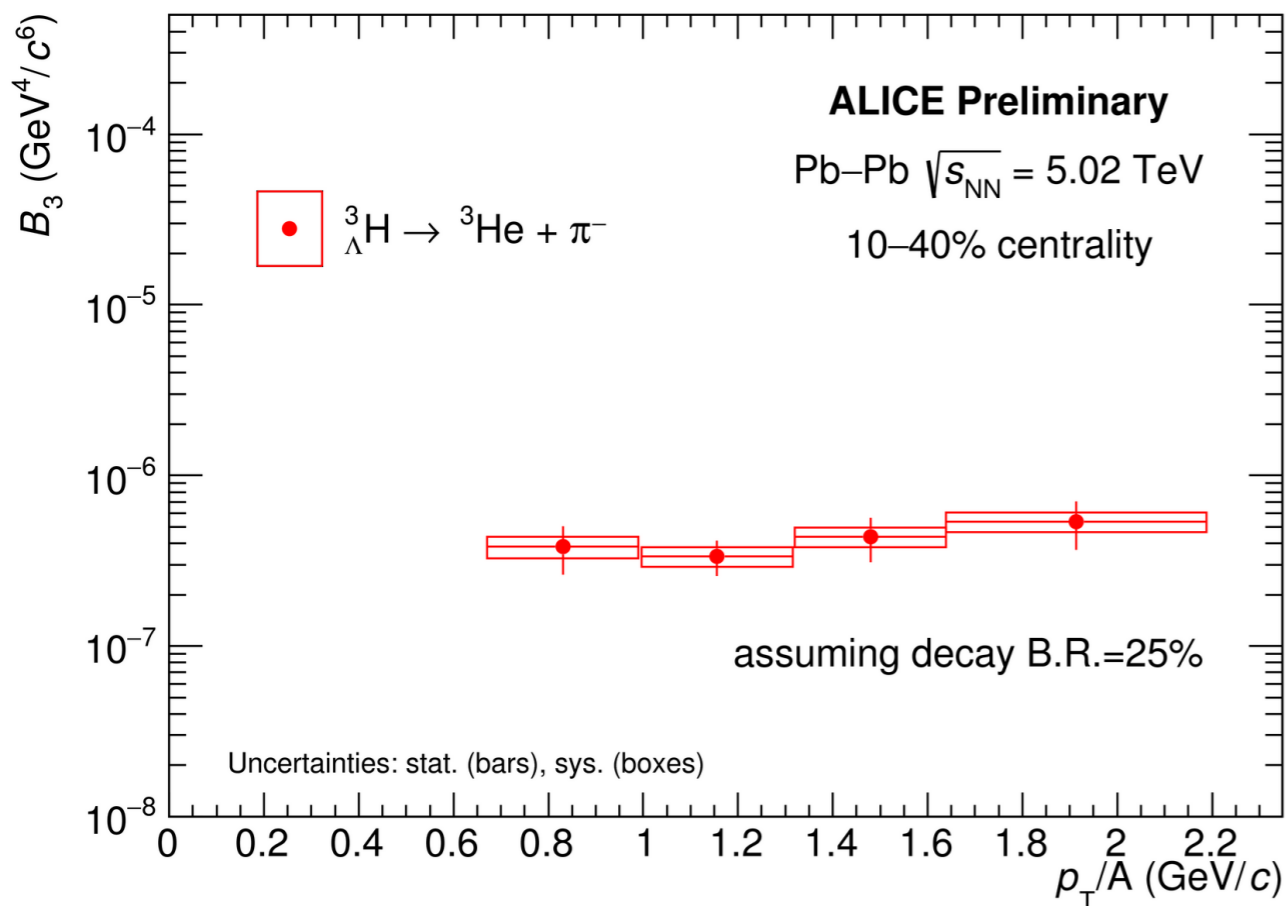


Proton and Λ spectra used the calculations are measured at the same energies

- (Anti-)hypertriton B_3 measured in central collisions at **2.76 TeV**:
 - rescaled for a comparison with deuteron B_2
 - rise with p_T not expected by simple coalescence
- In Pb-Pb collisions at **5.02 TeV** B_3 measured in **semi-central collisions**:
 - separately for matter and anti-matter
 - almost flat behavior as a function of p_T as supposed in coalescence picture
- Despite the different energies B_3 is higher in **semi-central** than in **central collisions**

${}^3_{\Lambda}\text{H}$ coalescence parameter

$$\sqrt{s_{\text{NN}}} = 5.02 \text{ TeV}$$

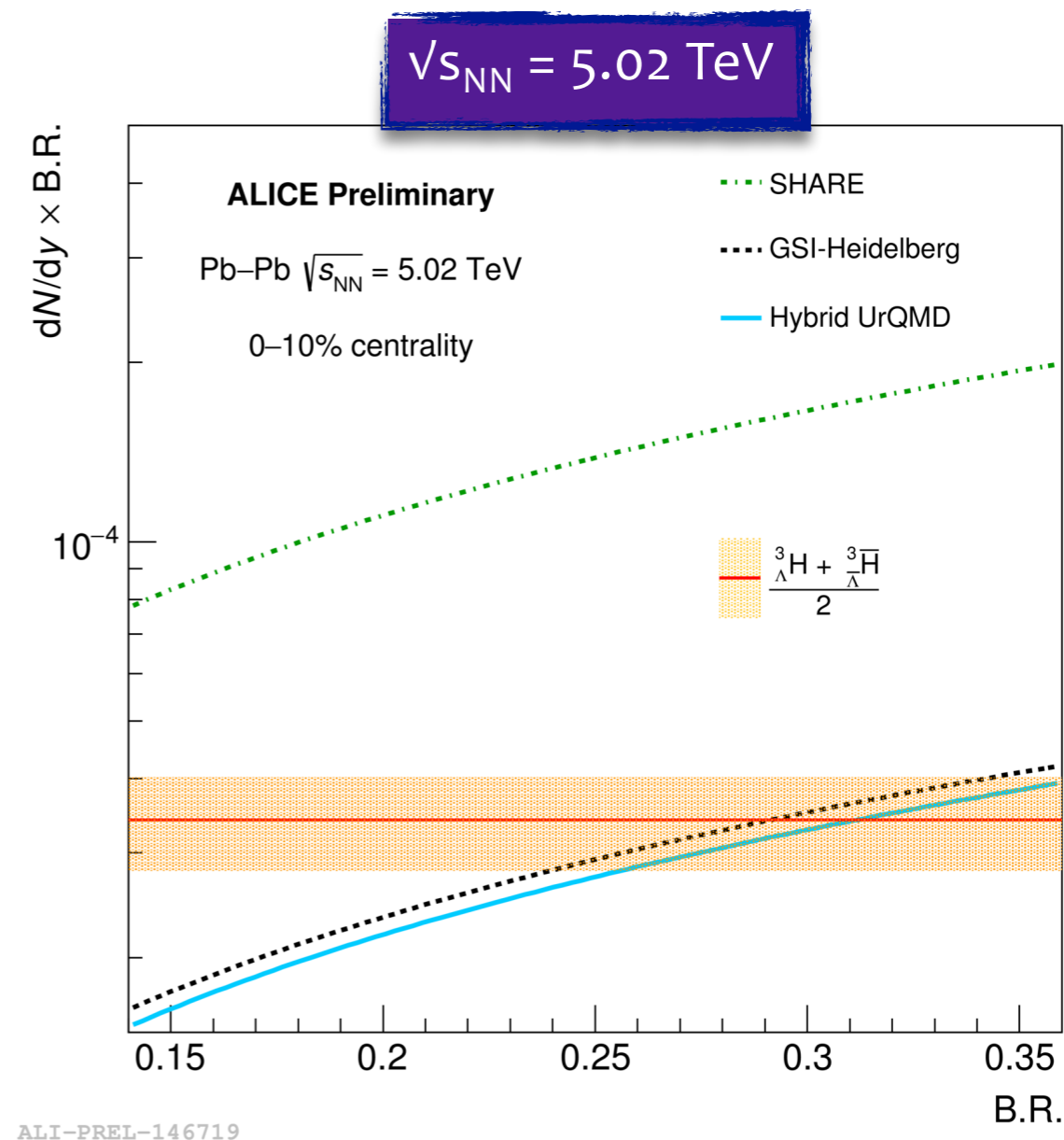
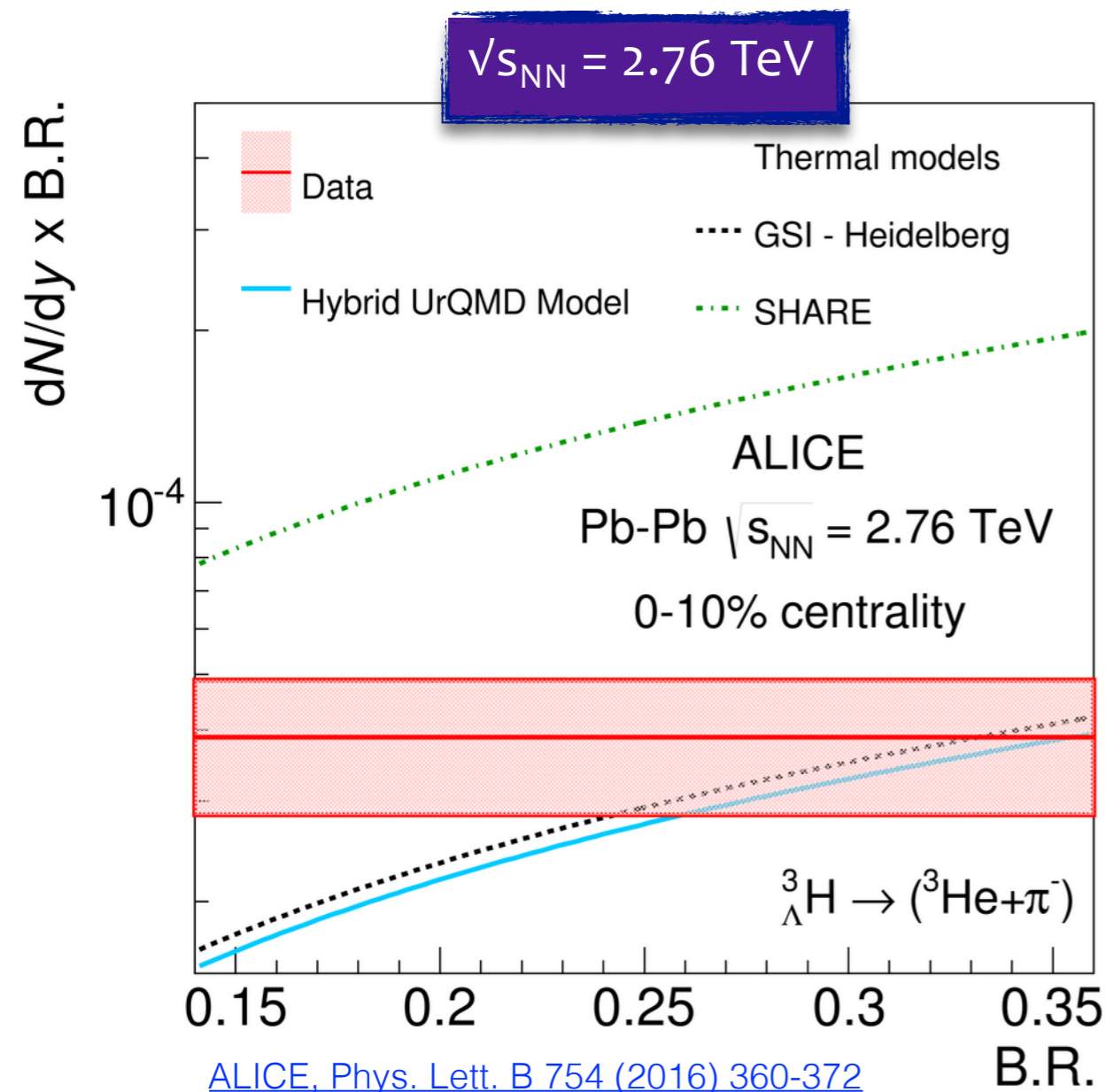


ALI-PREL-146743

Proton and Λ spectra used the calculations are measured at the same energies

- (Anti-)hypertriton B_3 measured in central collisions at **2.76 TeV**:
 - rescaled for a comparison with deuteron B_2
 - rise with p_T not expected by simple coalescence
- In Pb-Pb collisions at **5.02 TeV** B_3 measured in **semi-central collisions**:
 - separately for matter and anti-matter
 - almost flat behavior as a function of p_T as supposed in coalescence picture
- Despite the different energies B_3 is higher in **semi-central** than in **central collisions**

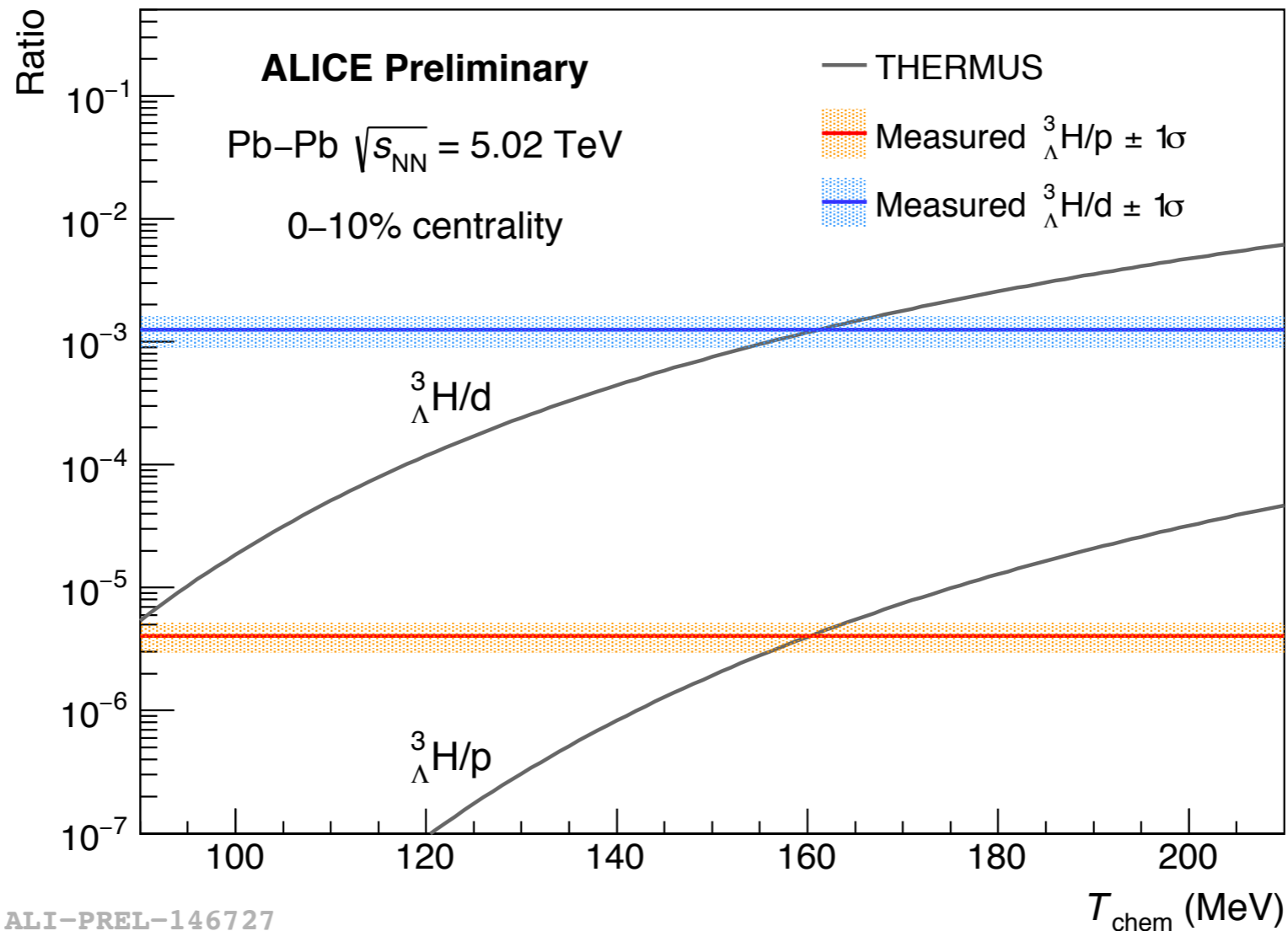
dN/dy vs B.R.



- (Anti-)hypertriton **Branching Ratio** is not precisely known
 - only constrained by the ratio between all charged channels containing a pion
- **Thermal model predictions** done for different **B.R.** values \rightarrow agreement in the range **0.24 - 0.35** with equilibrium thermal models

${}^3_{\Lambda}\text{H}$ ratios to light hadron yields

$\sqrt{s_{\text{NN}}} = 5.02 \text{ TeV}$



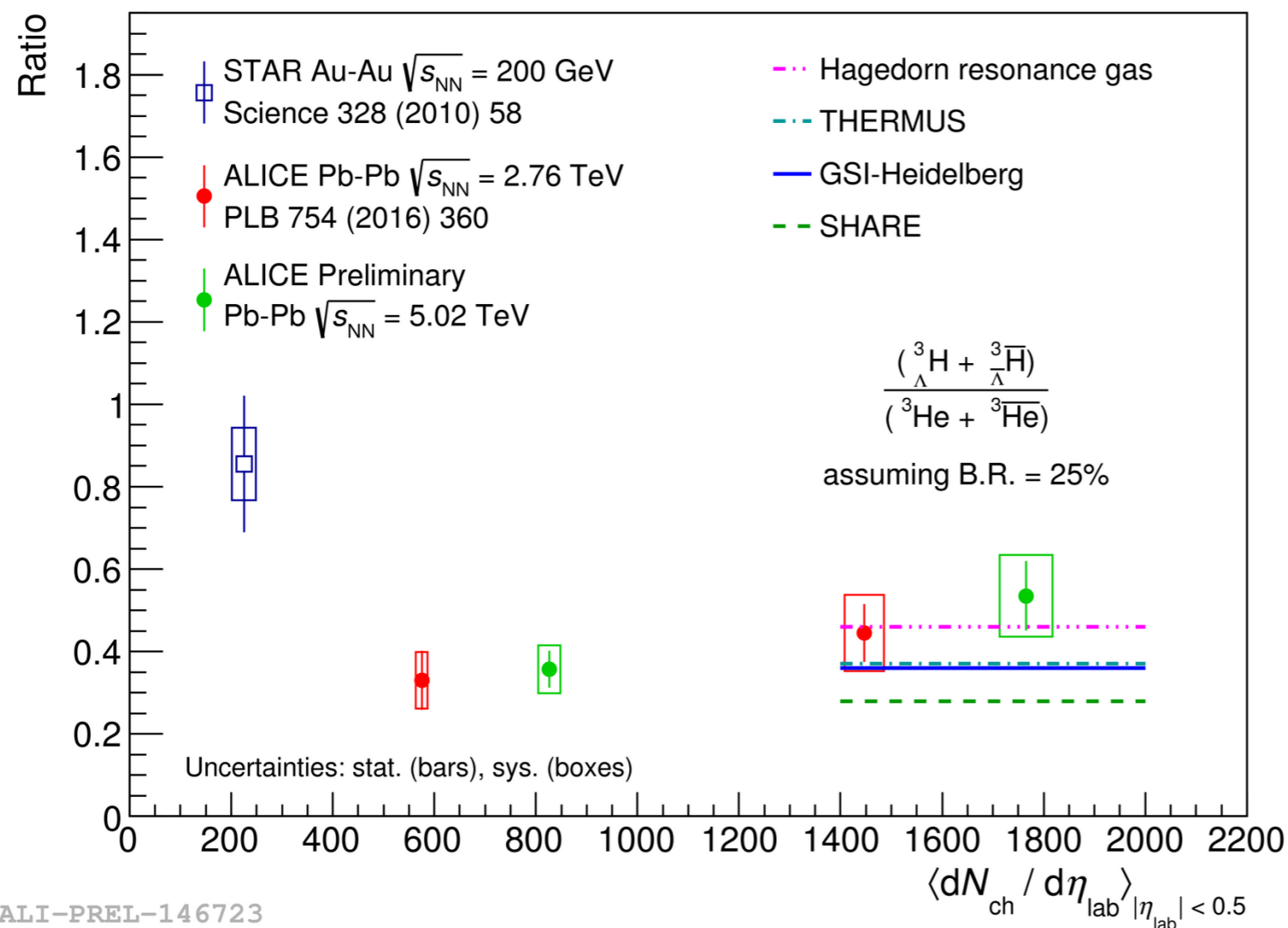
THERMUS:

[S. Wheaton, et al., CPC180, 84 \(2009\)](#)

- Ratio to **light hadron yields** more sensitive to the **chemical freeze-out temperature**
- ${}^3_{\Lambda}\text{H}/p$ and ${}^3_{\Lambda}\text{H}/d$ compared with THERMUS predictions as a function of T_{chem}
- Range $T_{\text{chem}} = 153\text{-}165 \text{ MeV}$ in agreement with $T_{\text{chem}} = 156 \text{ MeV}$ obtained at **2.76 TeV**

${}^3_{\Lambda}\text{H}$ -to- ${}^3\text{He}$ ratio

- Ratios for **most central collisions** ($\sqrt{s_{\text{NN}}} = 2.76 \text{ TeV}$ and $\sqrt{s_{\text{NN}}} = 5.02 \text{ TeV}$) are in agreement with predictions from **Hagedorn resonance gas (HRG)** and **thermal models**
- The new result at **5.02 TeV** might give a hint for an evolution with **charged particle multiplicity**
- Predictions from **coalescence** and for **lower multiplicities** are needed



THERMUS: [S. Wheaton, et al., CPC180, 84 \(2009\)](#)

GSI-Heidelberg: [A. Andronic, et al., PLB 697, 203 \(2011\); PLB 673, 142 \(2009\) 142](#)

SHARE3: [G. Torrieri, et al., CPC 167, 229 \(2005\); CPC 175, 635 \(2006\); CPC185, 2056 \(2014\)](#)

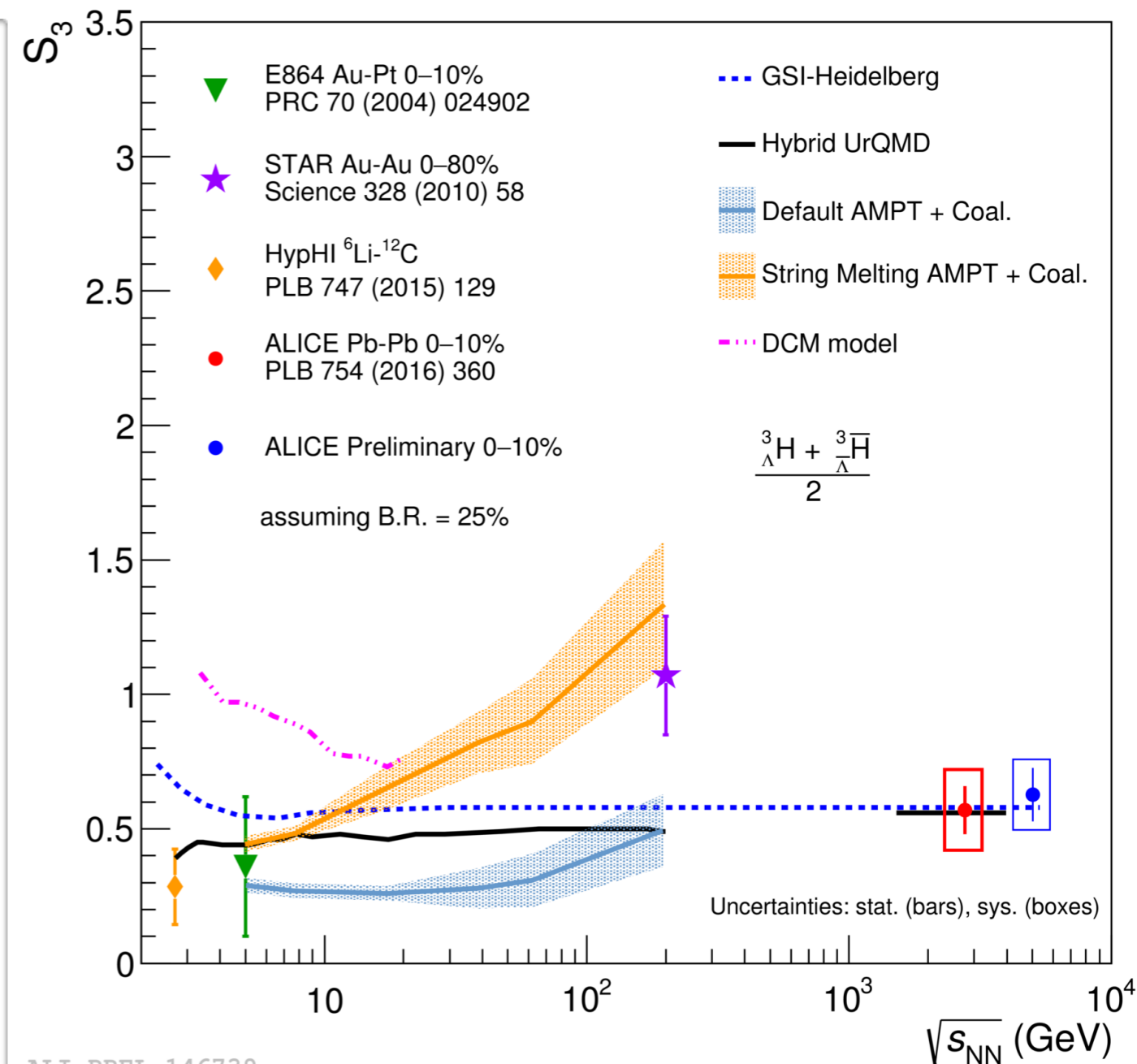
Strangeness population factor

Strangeness population factor S_3 [6,7]

is defined as:

$$S_3 = \frac{3 \text{H}}{3 \text{He}} \times \frac{p}{\Lambda}$$

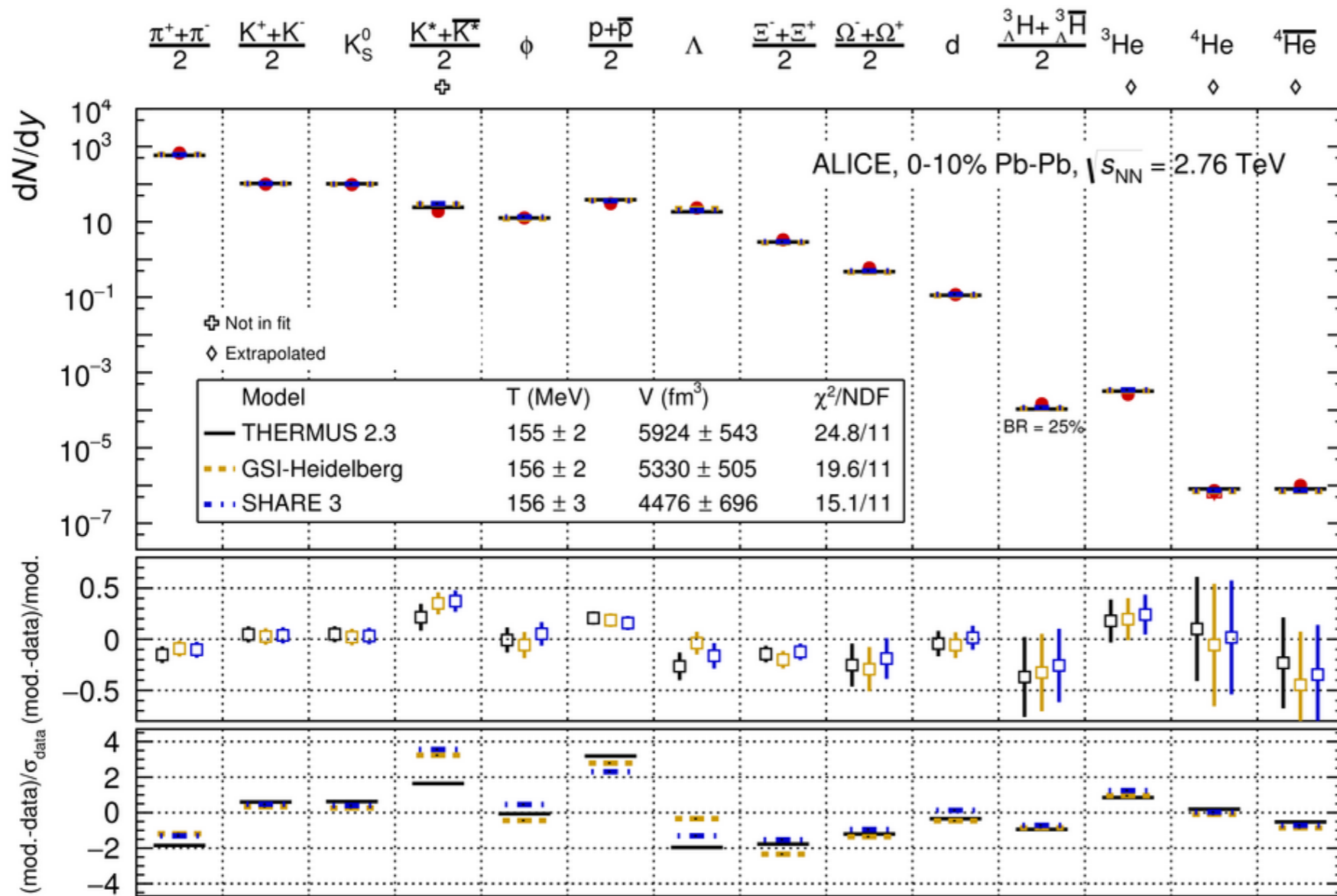
- **independent** on the **chemical potential** of the particles and additional canonical correction factor for **strangeness** is cancelled
- ALICE results at 5.02 TeV is:
 - **compatible** with the published results at 2.76 TeV and with those at lower energies
 - **in agreement** with the prediction of the equilibrium thermal model
- **Coalescence** predictions available only up to top RHIC energies



[6] [E864 Collaboration, T. A. Armstrong et al. Phys. Rev. C 70, 024902 \(2004\)](#)

[7] [S. Zhang et al. Phys. Lett. B 684, 224-227 \(2010\)](#)

The standard model for A-A collisions?



$\sqrt{s_{NN}} = 2.76$ TeV

[ALICE Collaboration, Nucl. Phys. A 971 \(2018\) 1-20](#)

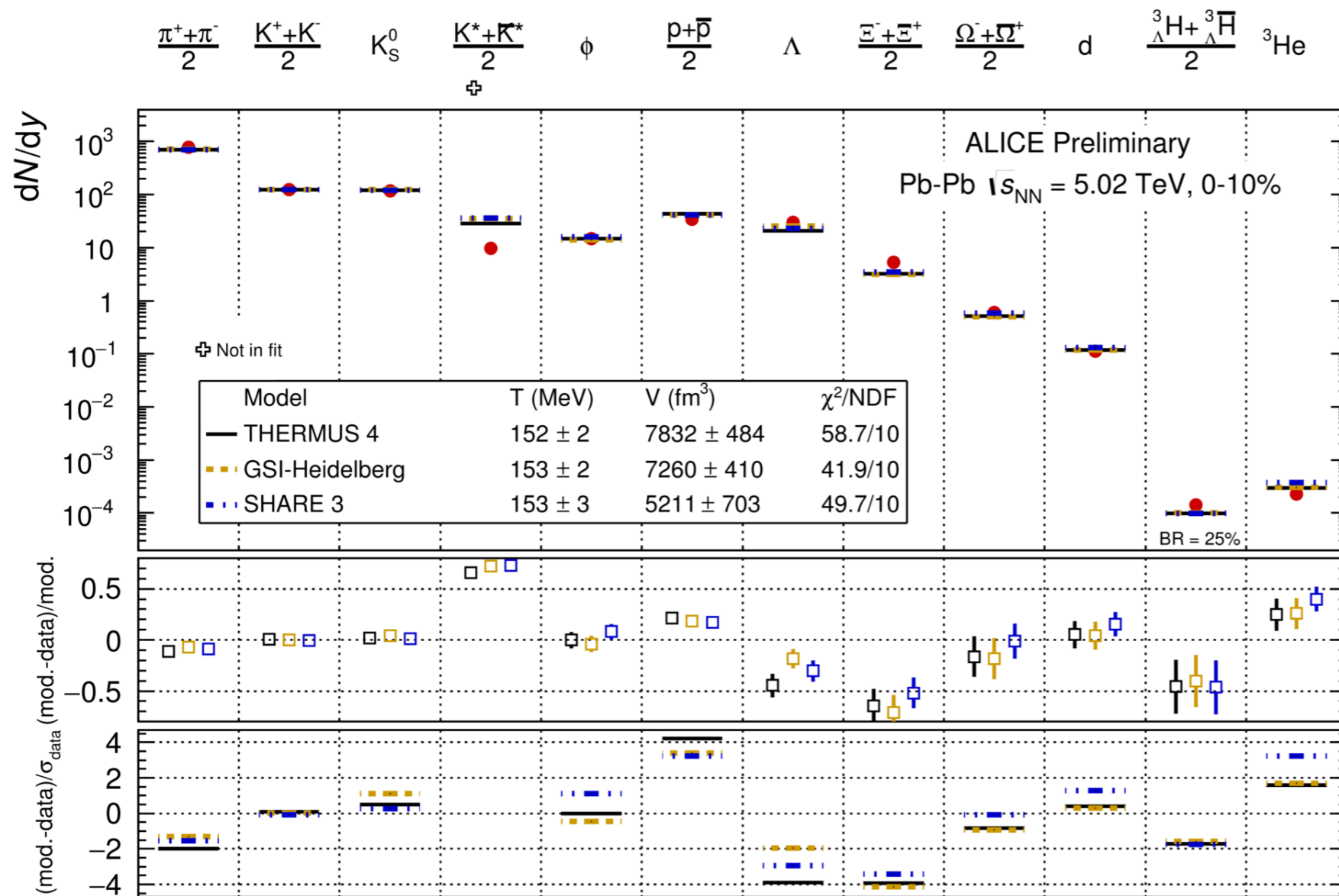
THERMUS: [S. Wheaton, et al., CPC180, 84 \(2009\)](#)

GSI-Heidelberg: [A. Andronic, et al., PLB 697, 203 \(2011\); PLB 673, 142 \(2009\) 142](#)

SHARE3: [G. Torrieri, et al., CPC 167, 229 \(2005\); CPC 175, 635 \(2006\); CPC185, 2056 \(2014\)](#)

- **Thermal model** successful in reproducing the **particle yields** measured in Pb-Pb collisions at $\sqrt{s_{NN}} = 2.76$ TeV → (anti-)(hyper-)nuclei included in the fit
- This result suggests that (hyper-)nuclei production happens at the **hadronisation**
- **The present formulation of thermal model seems to be the standard model of particle production in A-A collisions**

The standard model for A-A collisions?



$\sqrt{s_{NN}} = 5.02$ TeV

THERMUS: [S. Wheaton, et al., CPC180, 84 \(2009\)](#)

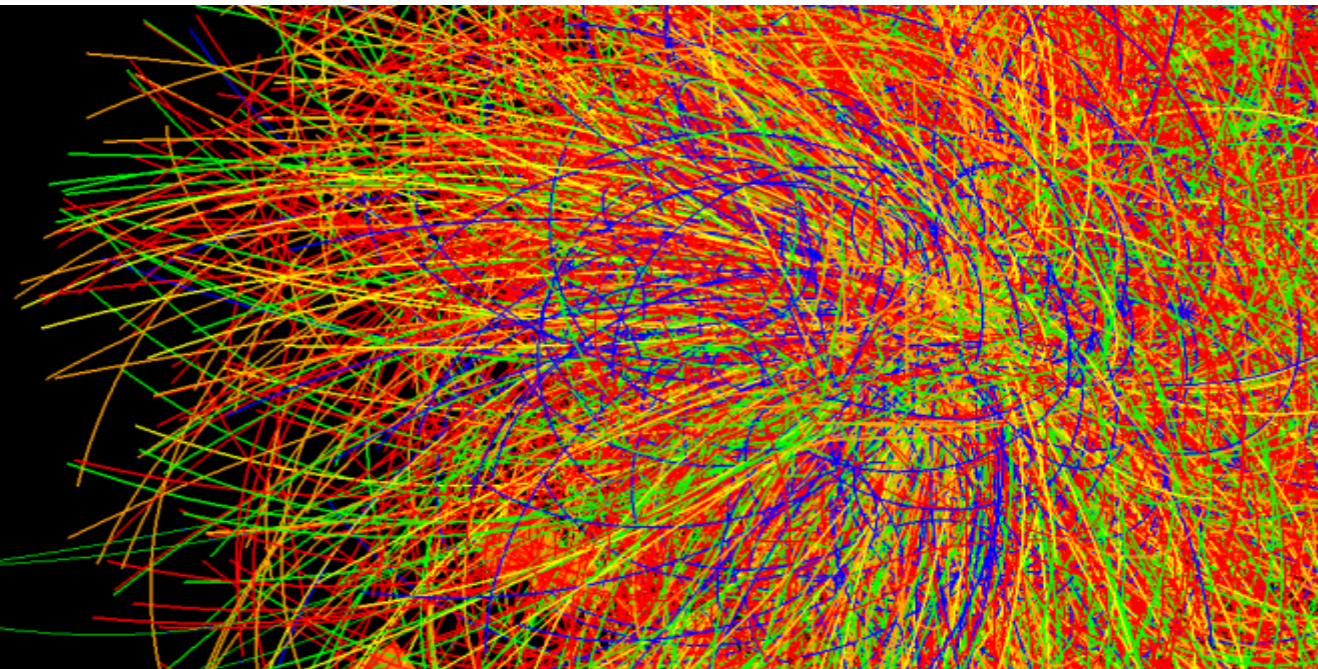
GSI-Heidelberg: [A. Andronic, et al., PLB 697, 203 \(2011\); PLB 673, 142 \(2009\) 142](#)

SHARE3: [G. Torrieri, et al., CPC 167, 229 \(2005\); CPC 175, 635 \(2006\); CPC185, 2056 \(2014\)](#)

ALI-PREL-148739

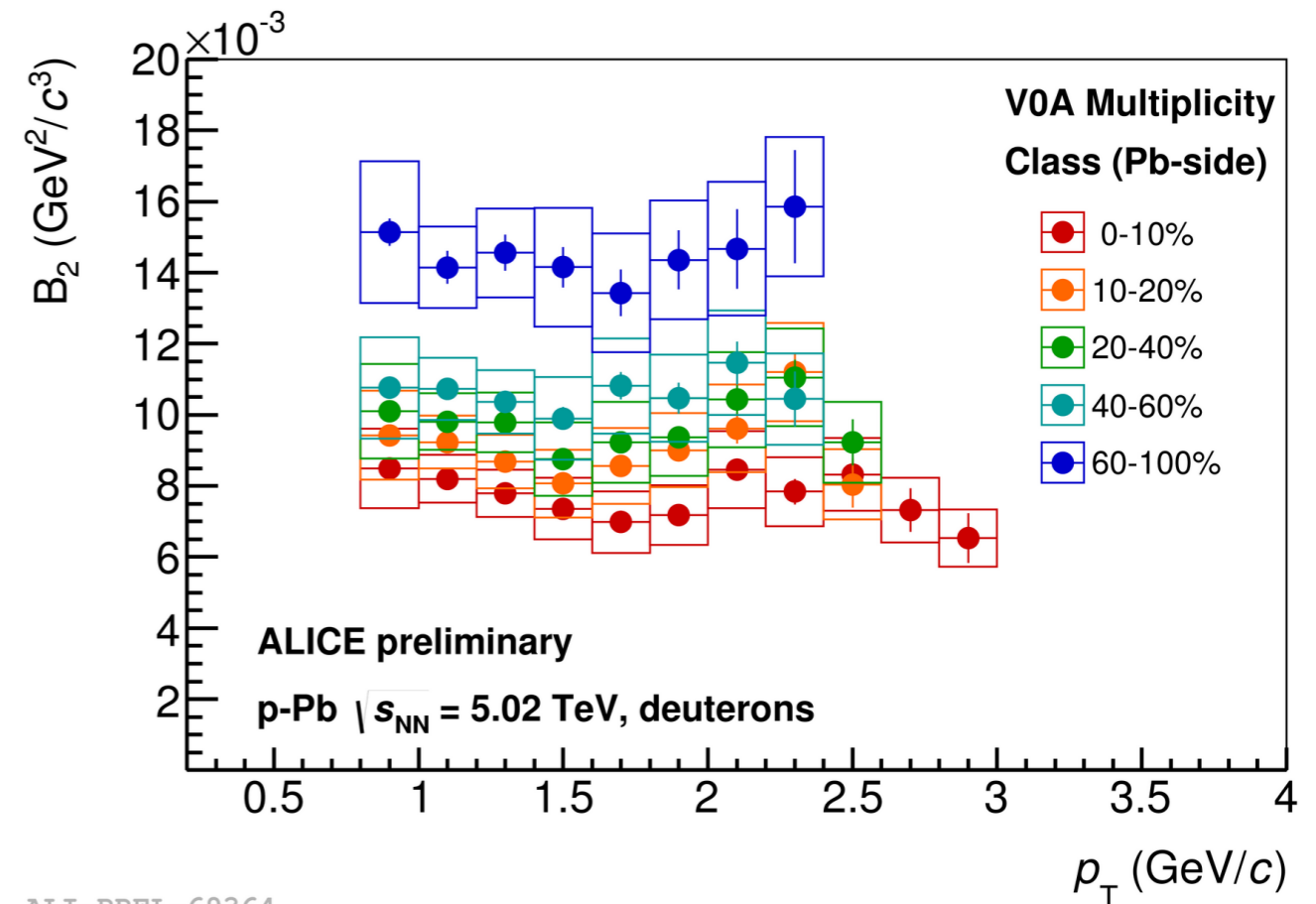
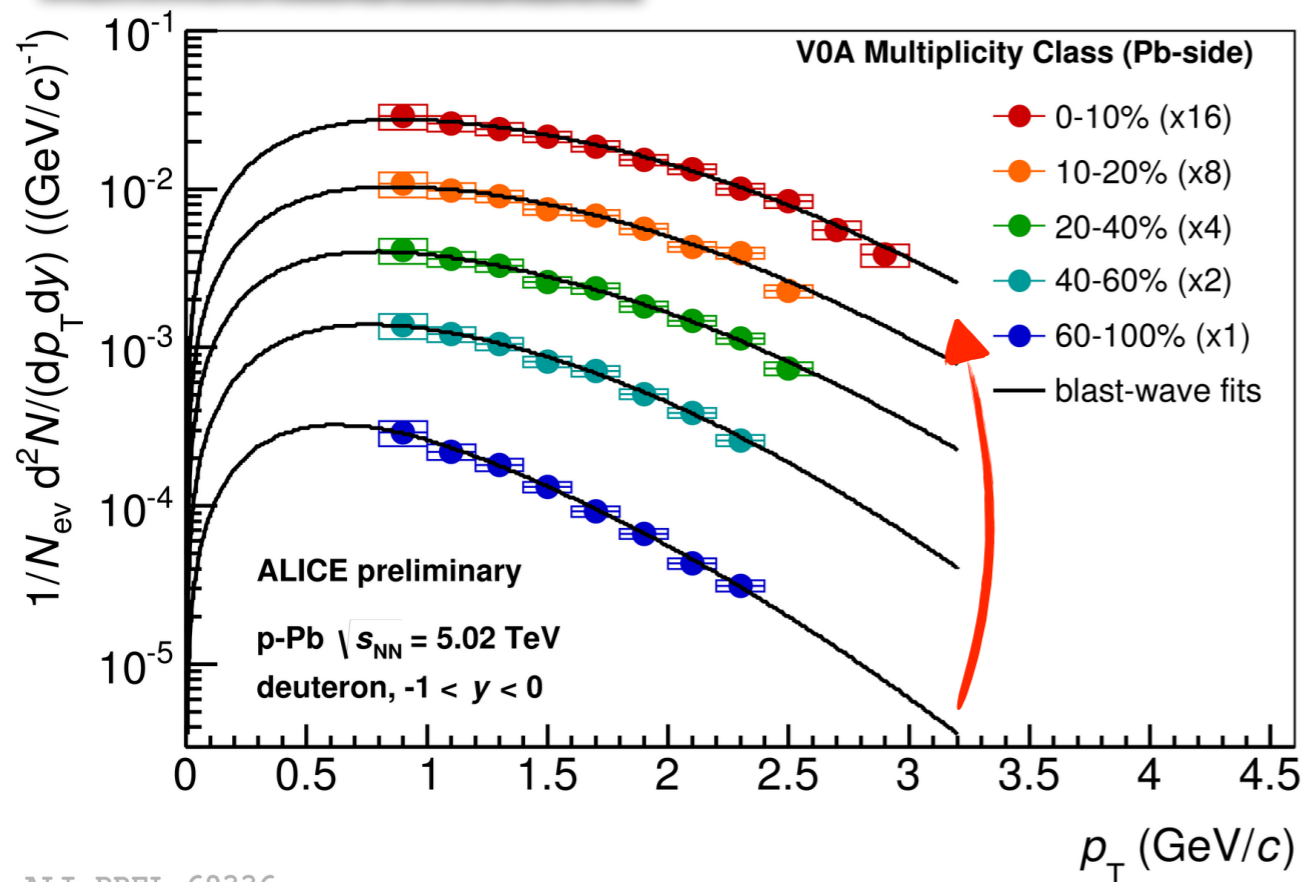
- **Larger** data sample collected in LHC Run2 and **improved** reconstruction and analysis techniques reduced the uncertainties.
- Although describing qualitatively well the particle yields, there is less agreement between the thermal model prediction and the particle yields
- **Does the model need further tuning and improvement?**

Production in small systems



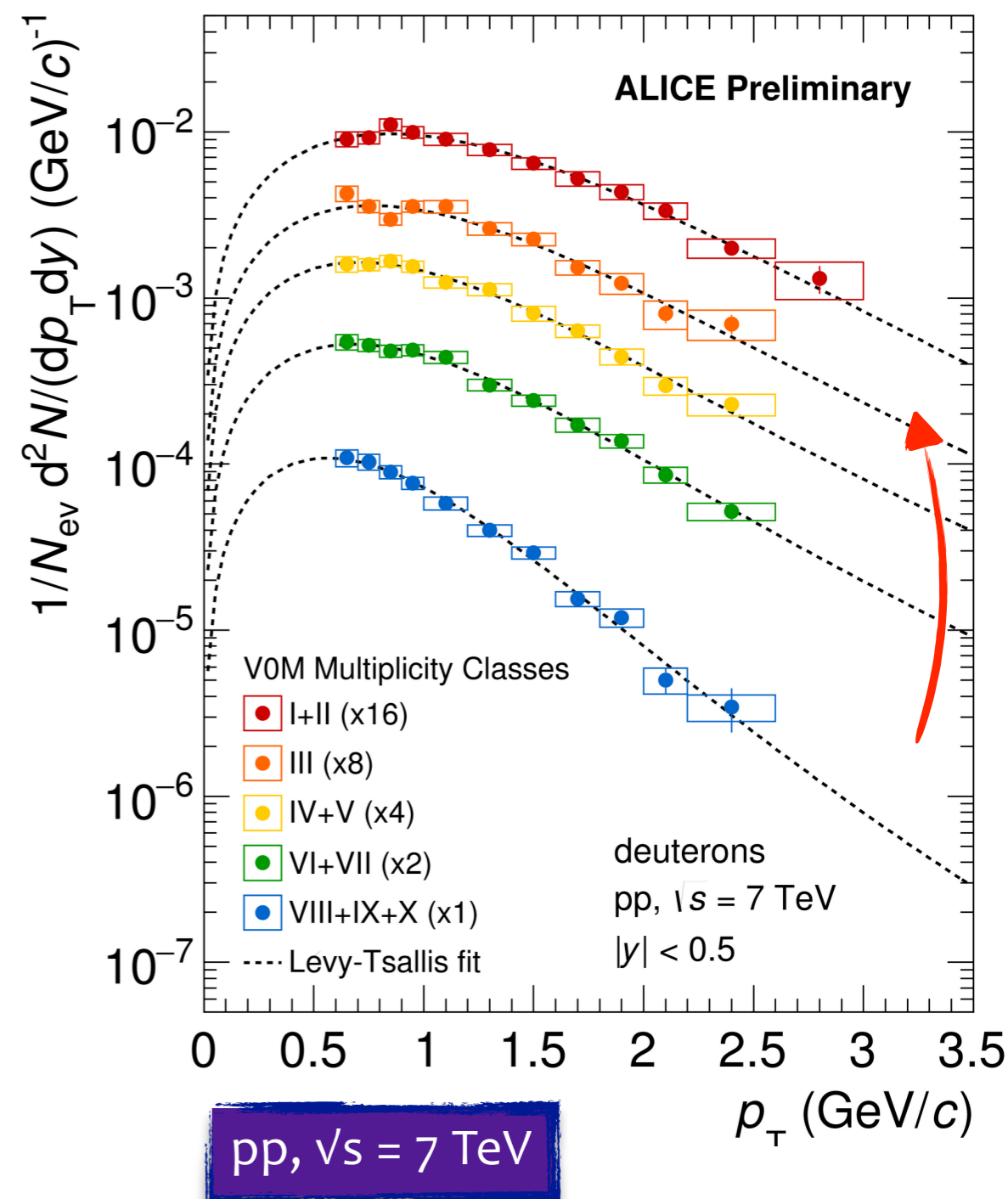
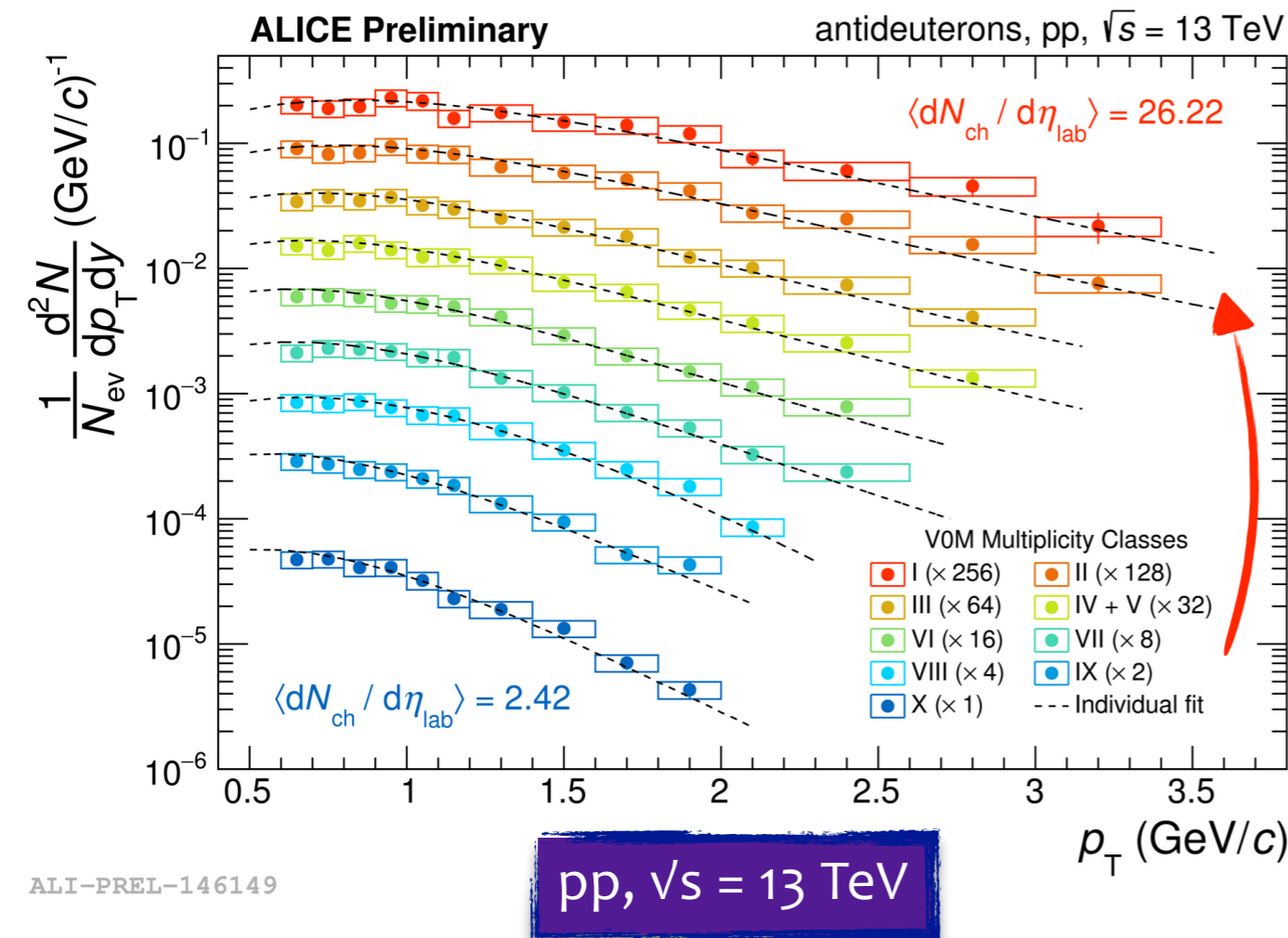
Deuteron production

p-Pb, $\sqrt{s_{NN}} = 5.02$ TeV



- p_T spectra becomes harder with increasing multiplicity in p-Pb → hint of **radial flow**
 - the **Blast-Wave** (BW) function describe the data well in p-Pb and is used for the yield extrapolation to the unmeasured regions
- deuteron B_2 is almost flat as a function of p_T while it increase while going to **lower multiplicity** in p-Pb → compatible with **simple coalescence** picture

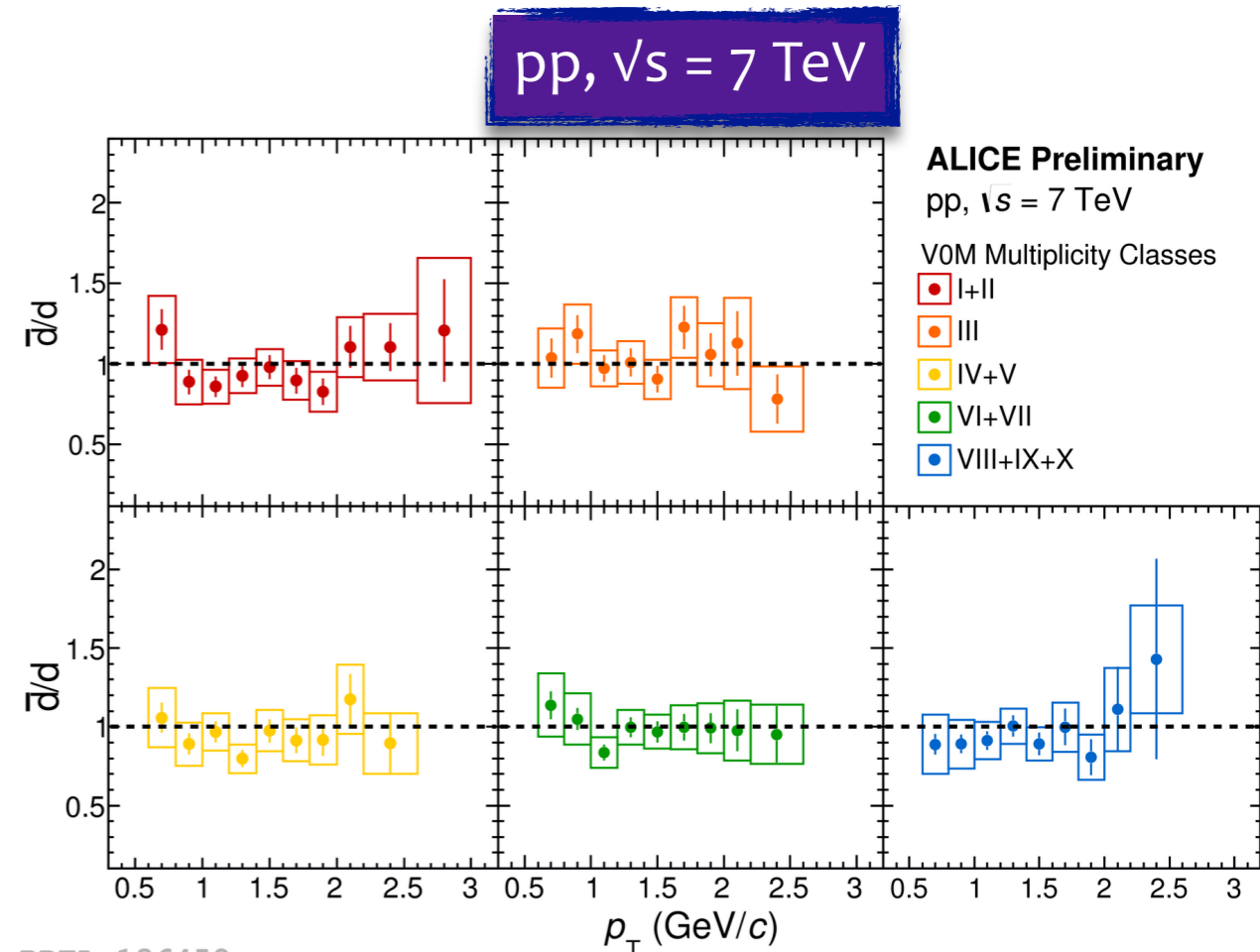
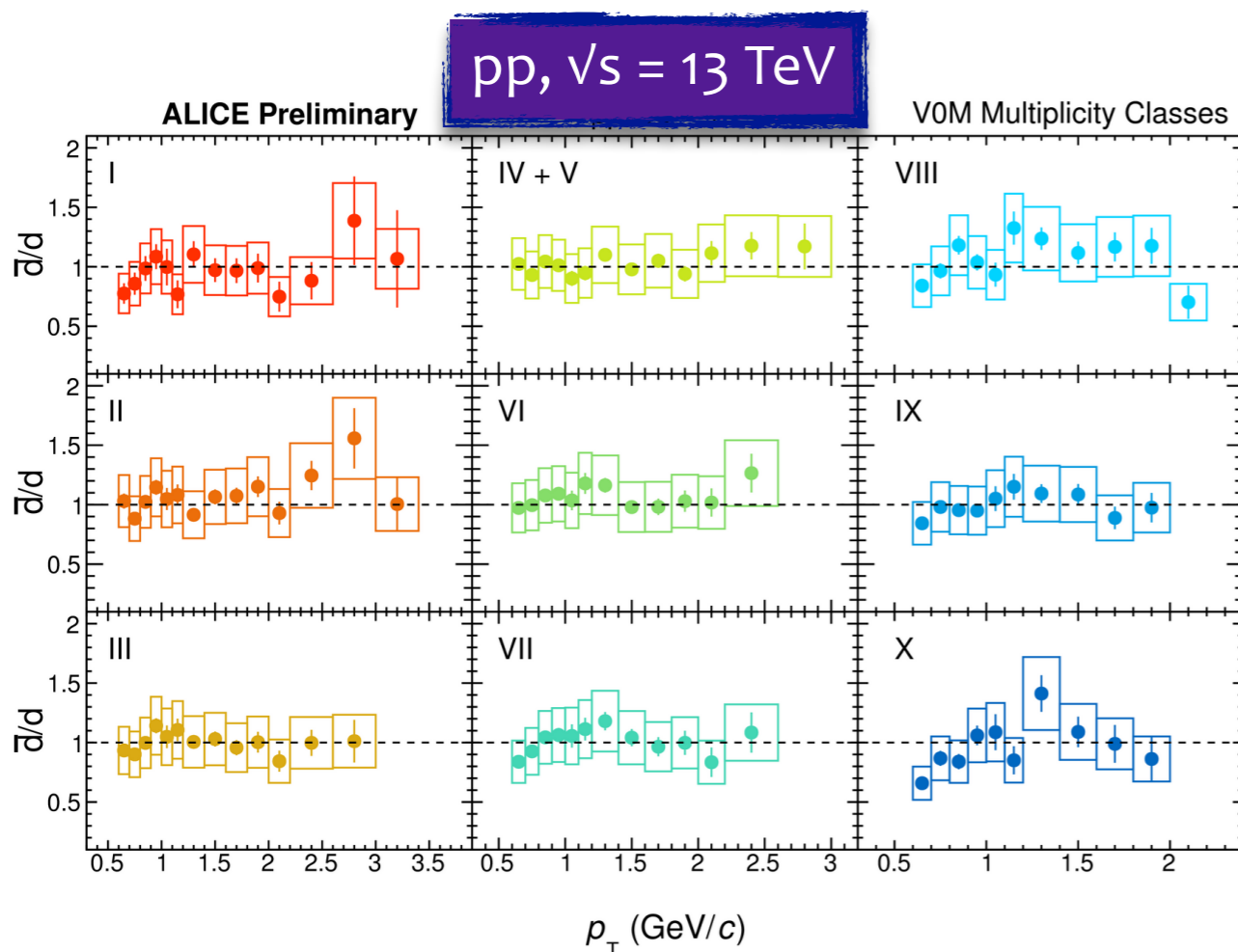
Deuteron production



- The fit is performed with a **Levy-Tsallis** function [8] used for the yield extrapolation to the unmeasured regions
- Also the **p_T spectra** as a function of **charged particle multiplicity** do not show a pronounced hardening

[8] C. Tsallis, J. Stat. Phys. 52 (1988) 479

Anti-deuteron/deuteron ratio



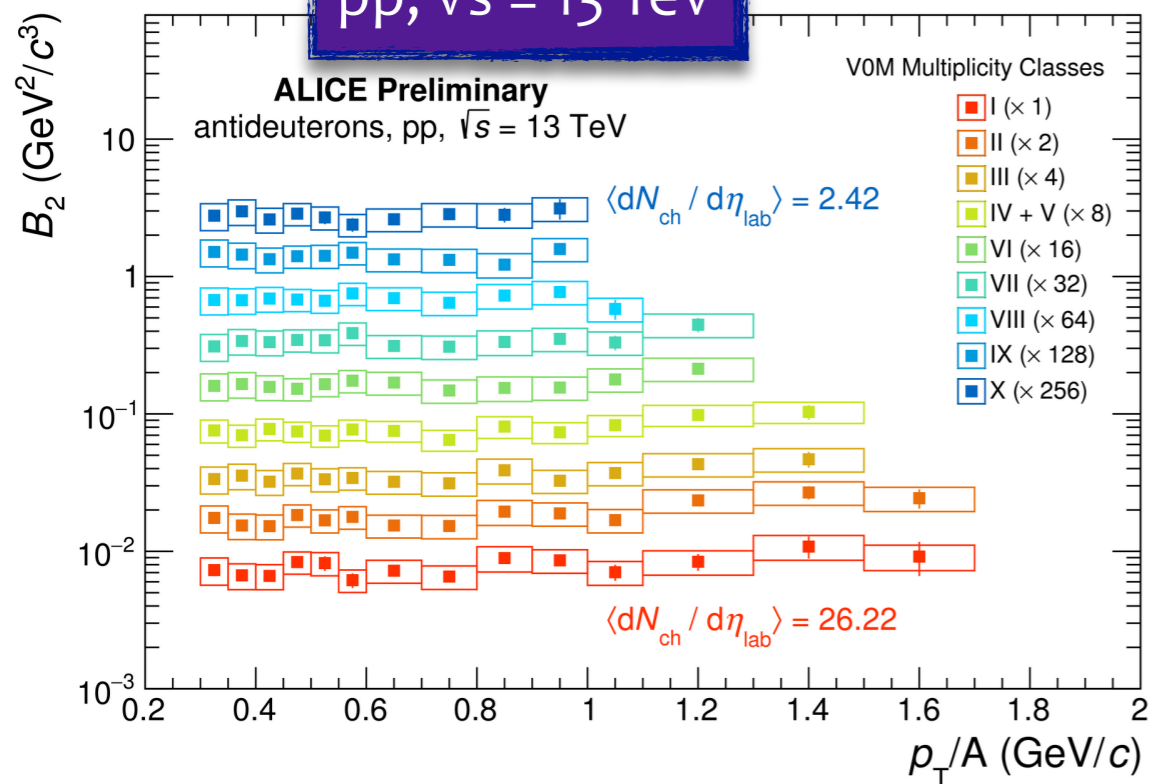
- In the regime of nuclear transparency **thermal** and **coalescence** models predict for a nucleus X with mass number A:

$$\frac{\bar{X}}{X} \approx \left(\frac{\bar{p}}{p} \right)^A$$

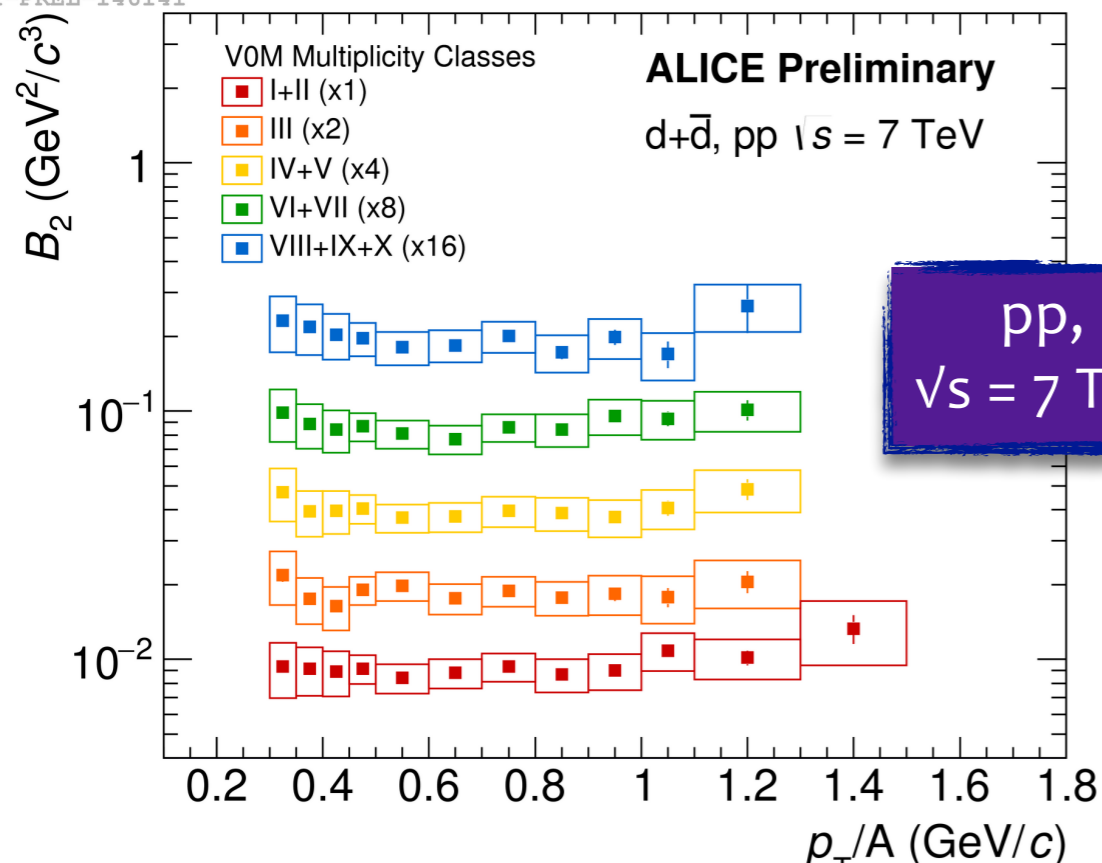
- Results of \bar{d}/d in p-p collisions confirm the prediction:
 - p_T and **multiplicity** independent

Coalescence parameter B_2

pp, $\sqrt{s} = 13$ TeV



ALI-PREL-146141



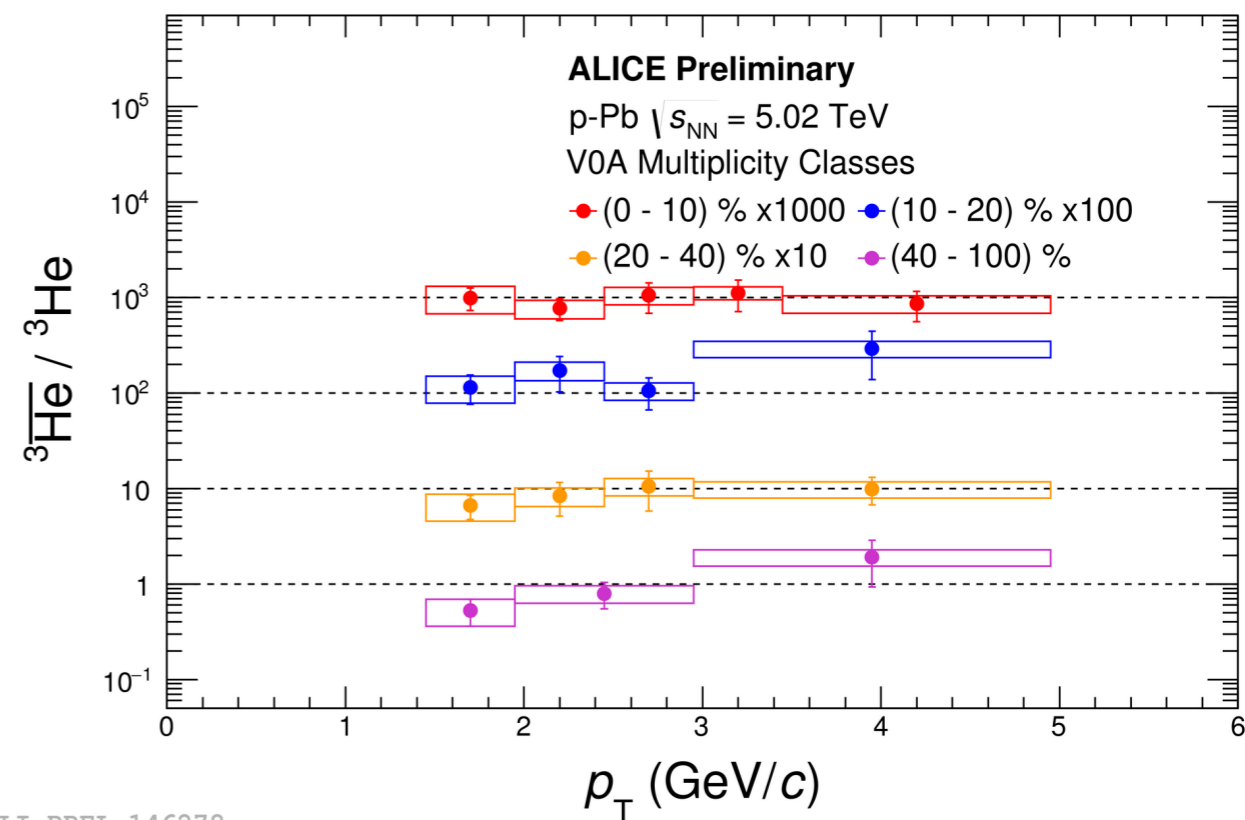
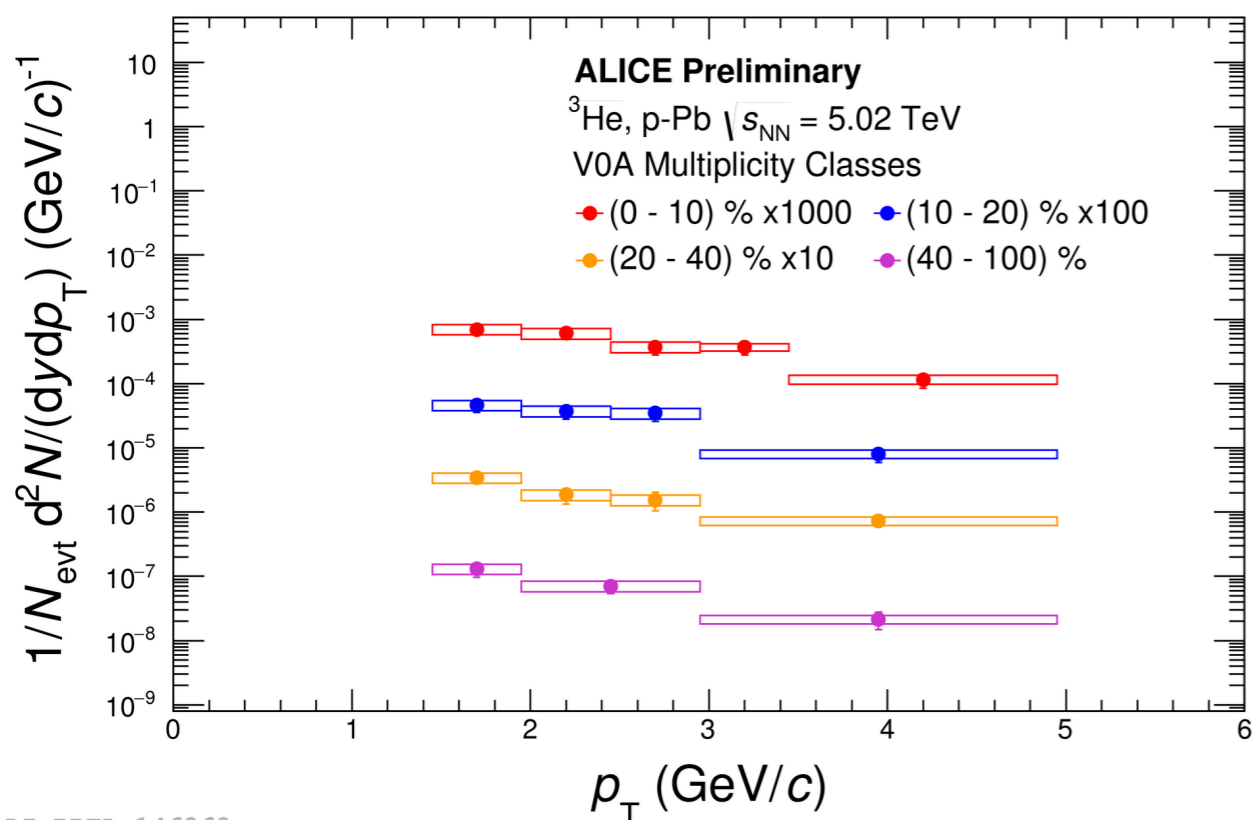
- The **probability** to form a (anti-)deuteron via coalescence can be quantified by the **coalescence parameter B_2** :

$$B_A = E_A \frac{d^3 N_A}{dp_A^3} / \left(E_p \frac{d^3 N_p}{dp_p^3} \right)^A$$

- B_2 measured in p-p collisions as a function of charged particle multiplicity:
 - B_2 is **flat** as a function of p_T
 - B_2 increases while going to lower multiplicities
- This behavior is in agreement with the simple **coalescence model**

^3He production

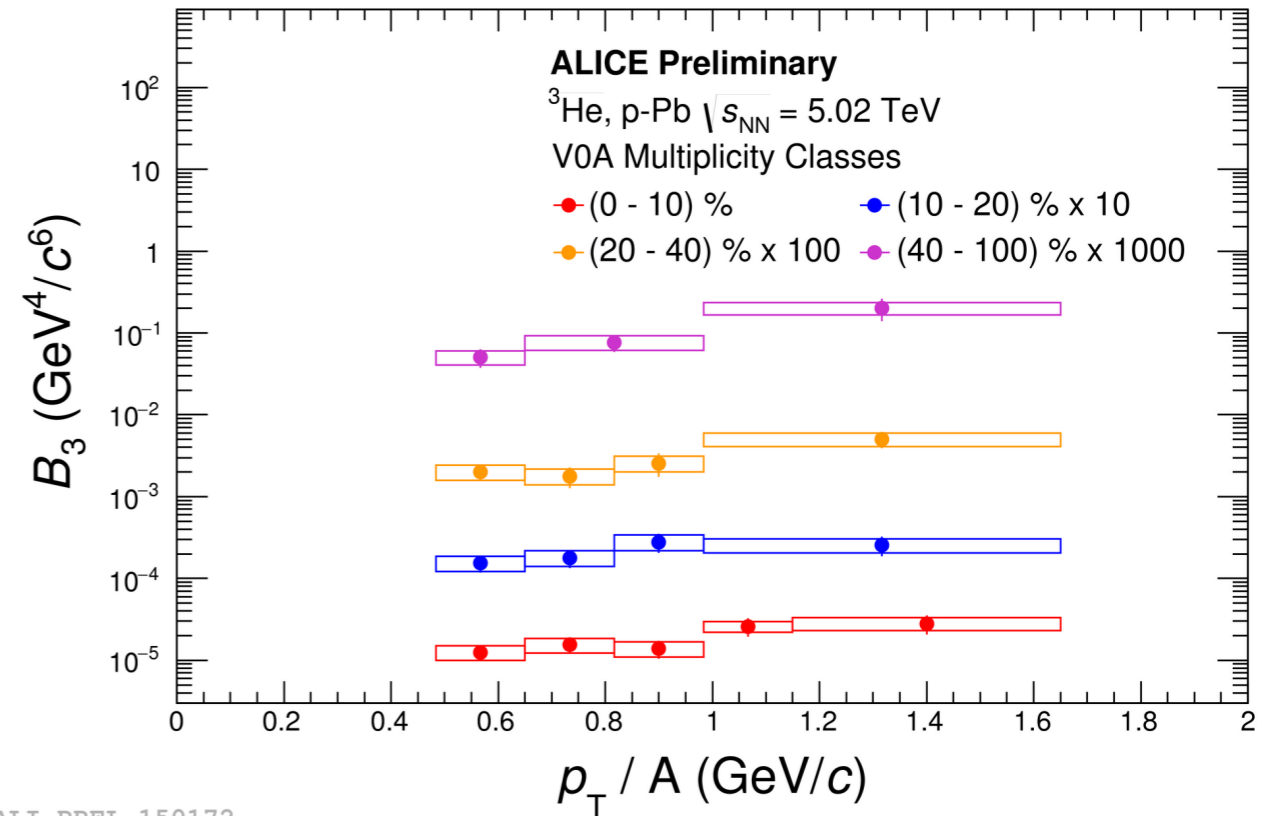
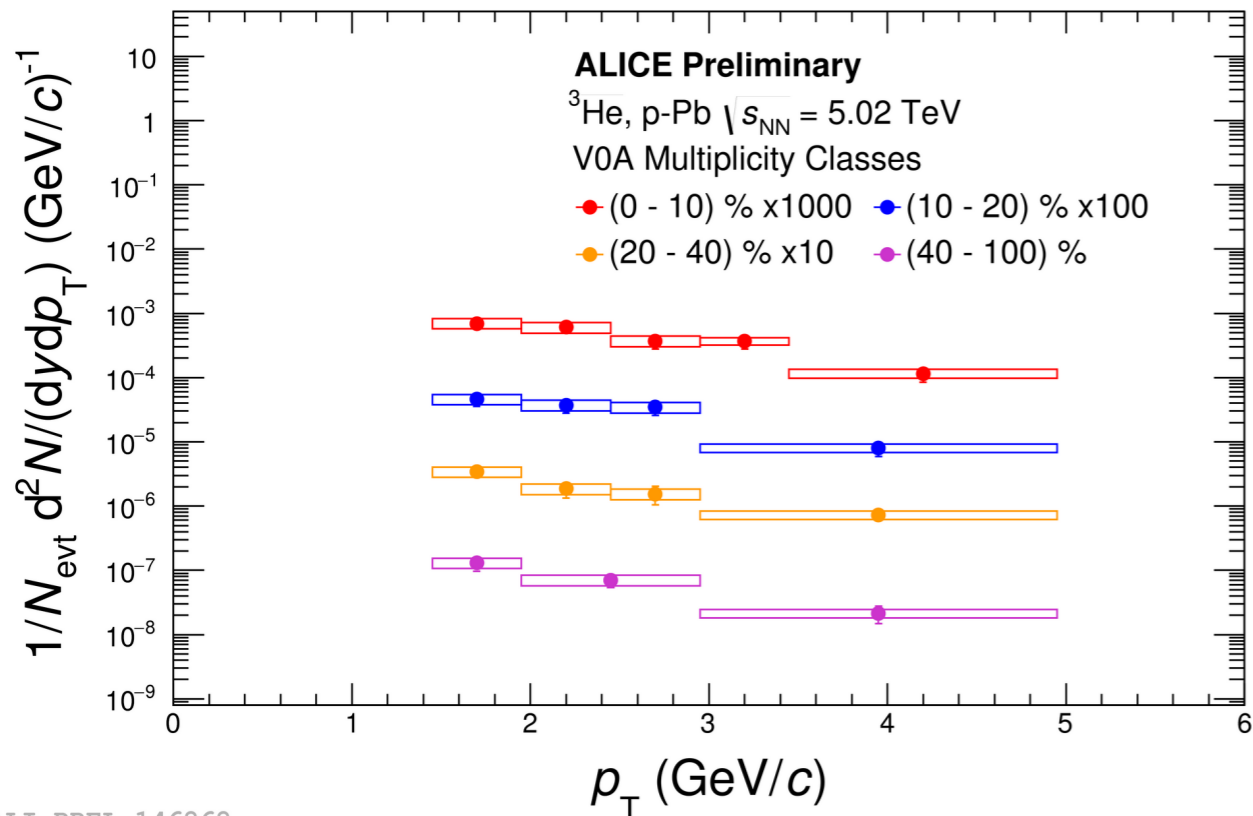
p-Pb, $\sqrt{s_{\text{NN}}} = 5.02$ TeV



- p_T spectra measured in 4 multiplicity bins in p-Pb
 - show a hardening with **increasing multiplicity**
- $^3\overline{\text{He}}/^3\text{He}$ ratio in agreement with unity as a function of p_T and **multiplicity**
- B_3 measured in p-Pb collisions as a function of charged particle multiplicity:
 - almost **flat** as a function of p_T , except for the lowest multiplicity class

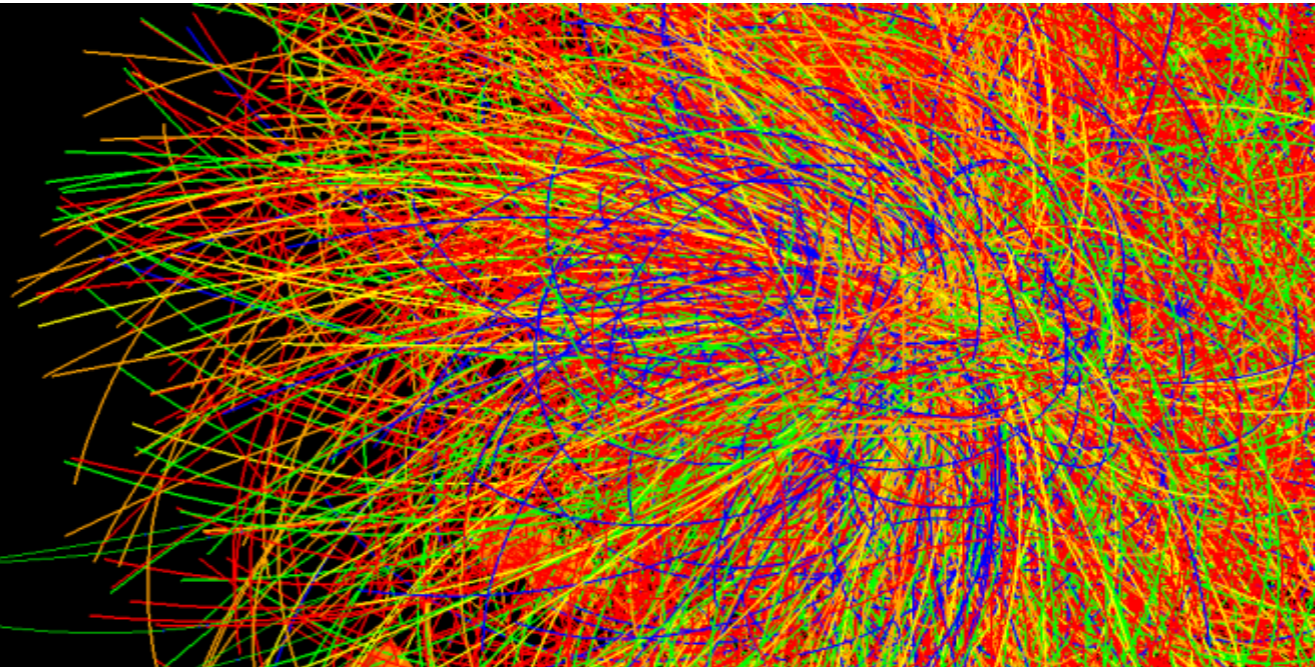
^3He production

p-Pb, $\sqrt{s_{\text{NN}}} = 5.02$ TeV



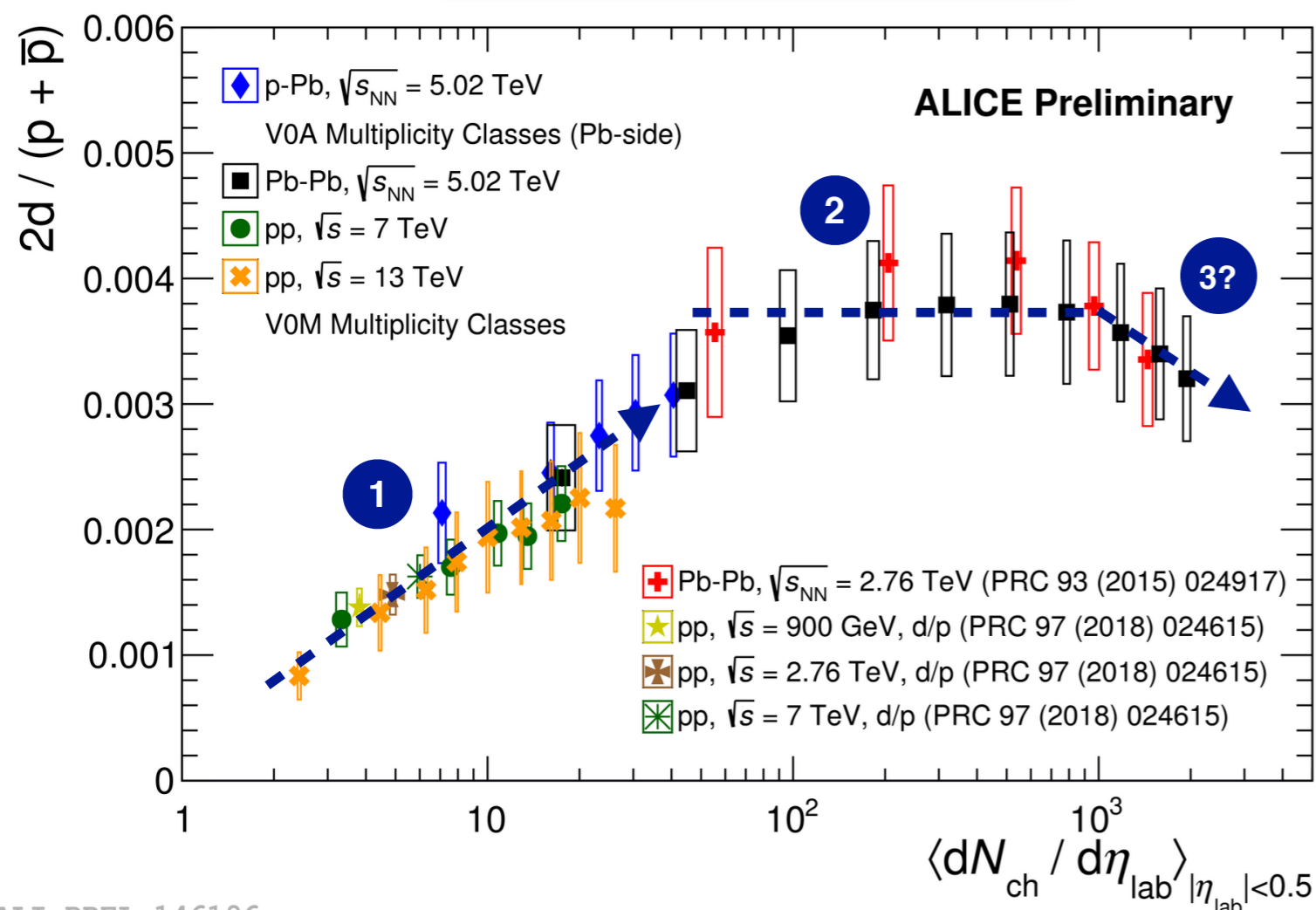
- p_T spectra measured in 4 multiplicity bins in p-Pb
 - show a hardening with **increasing multiplicity**
- $\overline{^3\text{He}}/^3\text{He}$ ratio in agreement with unity as a function of p_T and **multiplicity**
- B_3 measured in p-Pb collisions as a function of charged particle multiplicity:
 - almost **flat** as a function of p_T , except for the lowest multiplicity class

Unified description of nucleosynthesis?



Nucleus over proton ratio

deuteron-over-proton



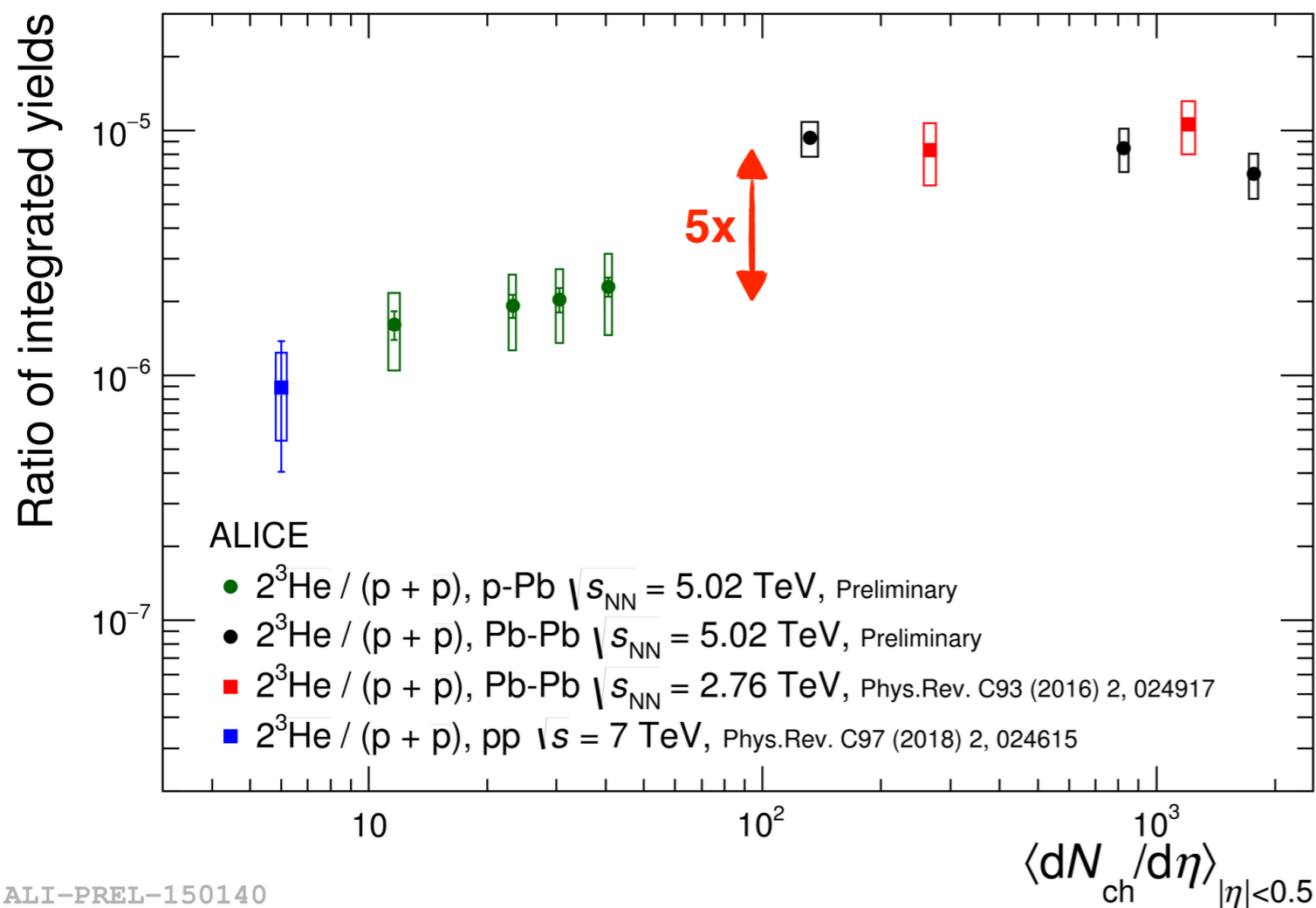
ALI-PREL-146196

Is there a unique production mechanism depending only on the system size?

- **d/p** ratio does not show discontinuity between different colliding systems
- Two different regimes:
 - 1. Increasing:** rise at low multiplicity compatible with the description of the **coalescence** models
 - 2. Flat:** at high multiplicity there is no dependence of the ratio on the multiplicity, in agreement with **thermal** model predictions
 - 3. Suppression(?):** still not significant with these uncertainties
- On the other hand **$^3\text{He}/p$ ratio** shows factor 5 step between small systems and Pb-Pb

Nucleus over proton ratio

^3He -over-proton



- d/p ratio does not show discontinuity between different colliding systems
- Two different regimes:
 1. **Increasing**: rise at low multiplicity compatible with the description of the **coalescence** models
 2. **Flat**: at high multiplicity there is no dependence of the ratio on the multiplicity, in agreement with **thermal** model predictions
 3. **Suppression(?)**: still not significant with these uncertainties
- On the other hand $^3\text{He}/p$ ratio shows factor 5 step between small systems and Pb-Pb

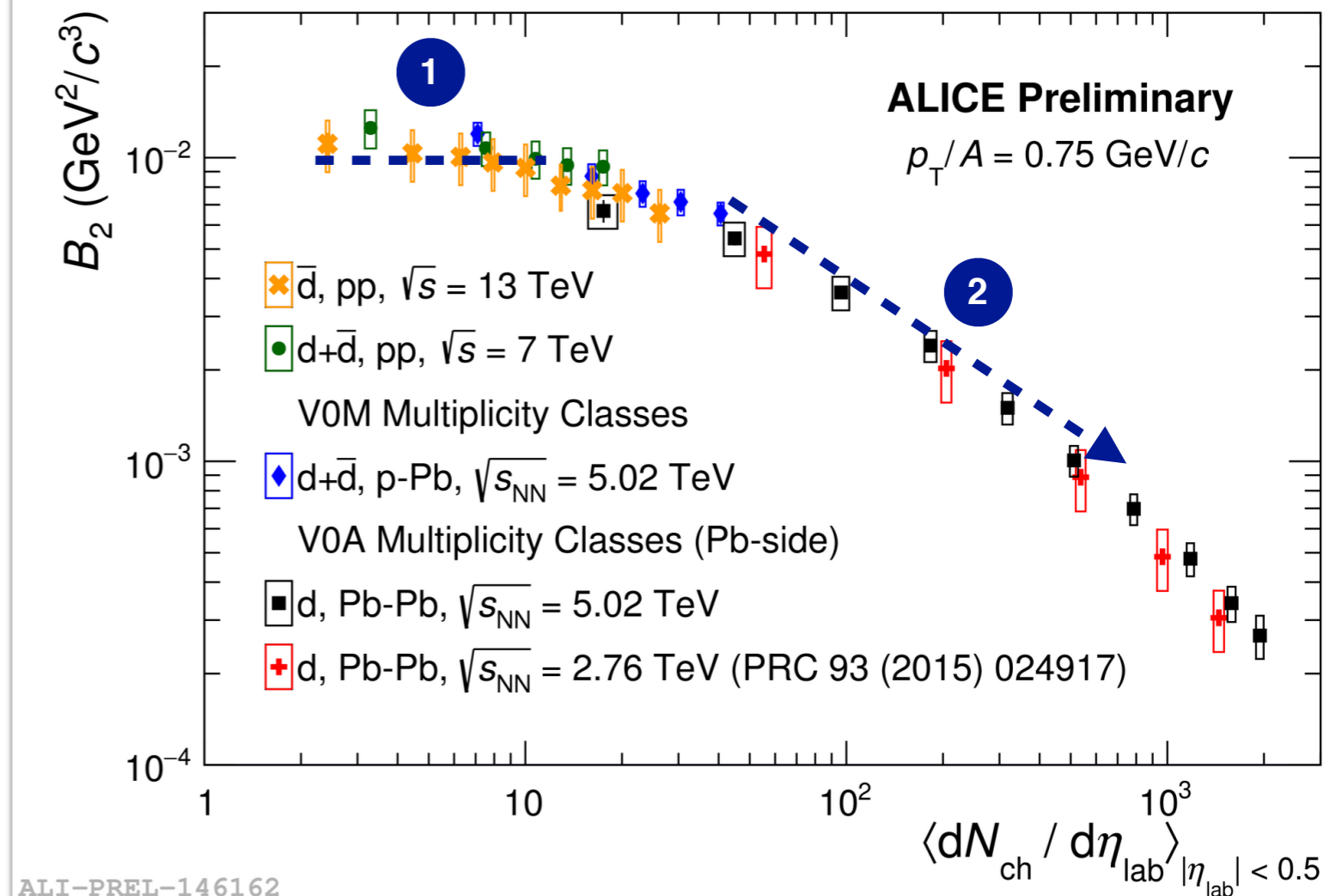
If the factor 5 is confirmed by studies on larger data samples, then a unified description will be more challenging

Multiplicity dependence of B_A

- The measurement of B_2 does not show discontinuity between different colliding systems
- Two different regimes:
 - Flat**: the system size is smaller than deuteron size
 - Decreasing**: the system size gets larger than the deuteron size
- This behavior has been **qualitatively** described by parametrizing the coalescence parameter using the **system HBT radius R** :

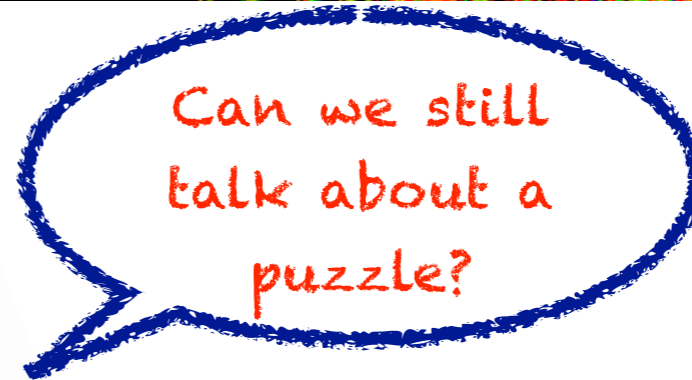
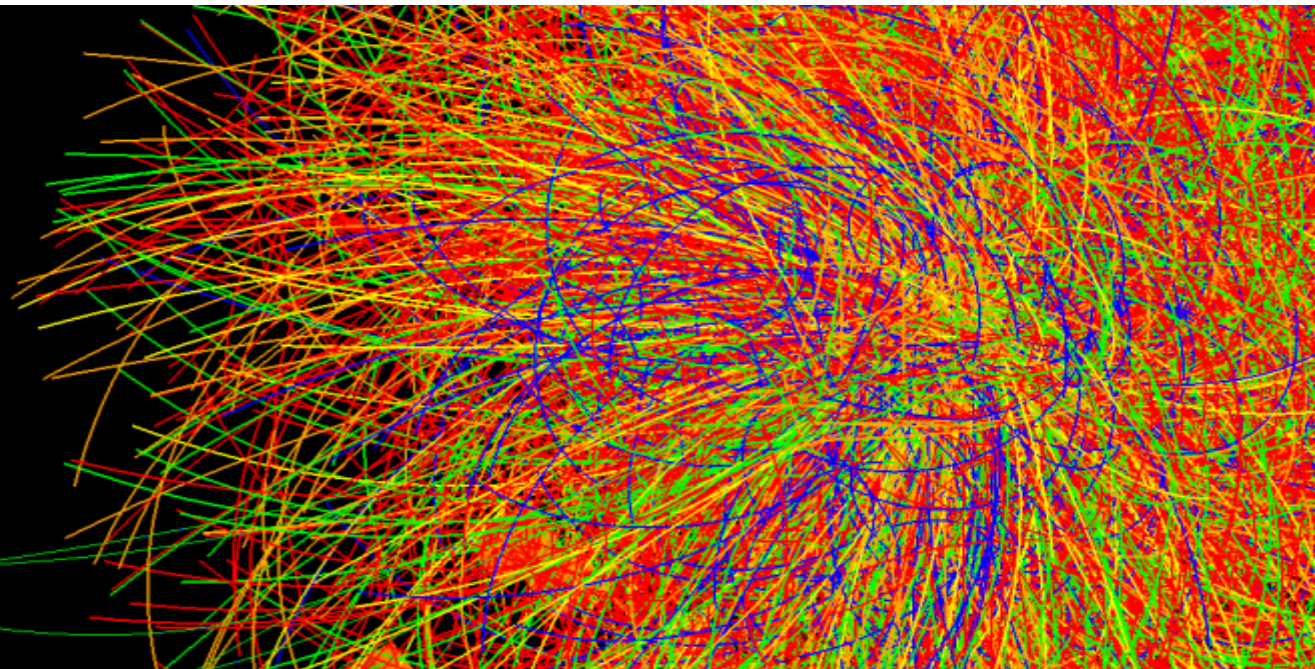
$$\frac{B_2}{\text{GeV}^2} \approx 0.068 \left[\left(\frac{R(p_T)}{1\text{fm}} \right)^2 + 2.6 \left(\frac{b_2}{3.2\text{fm}} \right)^2 \right]^{-3/2}$$

[K. Blum et al., Phys. Rev. D 96 \(2017\) 103021](#)



Is there a unique production mechanism depending only on the system size?

(Anti-)hypertriton lifetime



Hypertriton (${}^3_{\Lambda}\text{H}$): bound state of **p**, **n** and **Λ** , is the lightest known hypernucleus

- Mass = $2.99116 \pm 0.00005 \text{ GeV}/c^2$ [1]
- Λ binding energy = $0.13 \pm 0.05 \text{ MeV}$ [1]
- lifetime: world average = $216^{+16}_{-19} \text{ ps}$ [2]
- decay channels: \rightarrow Mesonic (MWD)
 \rightarrow Non Mesonic (NMWD)

Mesonic channels

| Channels | Branching Ratio [3] |
|--|---------------------|
| ${}^3\text{He}+\pi^-$ ${}^3\text{H}+\pi^0$ | 37,3% |
| $\text{d}+\text{p}+\pi^-$ $\text{d}+\text{n}+\pi^0$ | 60,1% |
| $\text{n}+\text{p}+\text{p}+\pi^-$ $\text{n}+\text{n}+\text{p}+\pi^0$ | 0,94% |

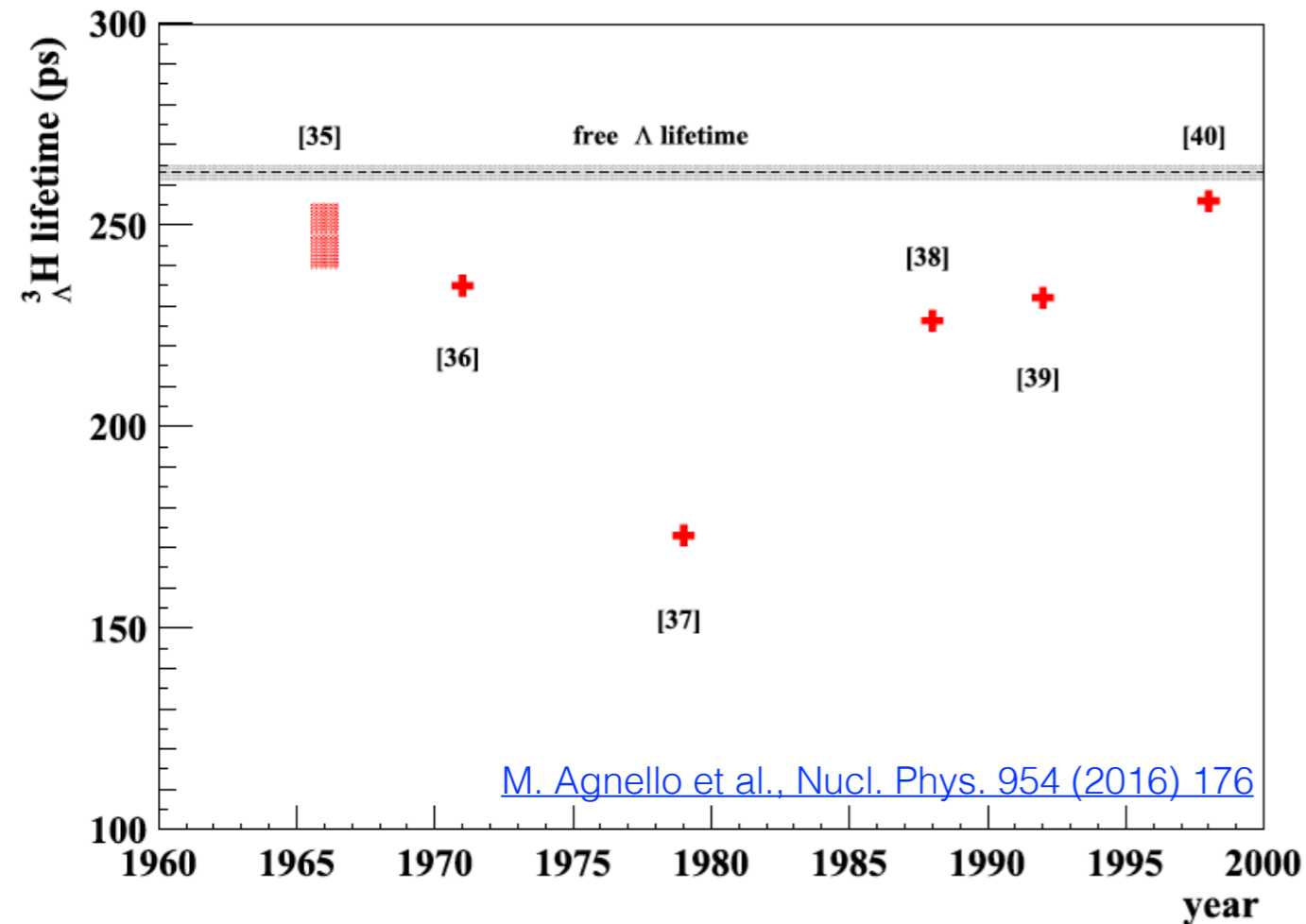
- Very small **Λ separation energy** led to the hypothesis that the ${}^3_{\Lambda}\text{H}$ lifetime is slightly below the free Λ hyperon lifetime ($263.2 \pm 2 \text{ ps}$ [3])
 - consequence of the fact that the Λ spends most of the time far from the **deuteron core** due to very small value of B_{Λ}
 - many theoretical calculations support this hypothesis

[1] [D.H. Davis., Nucl. Phys. A 754 \(2005\) 3-13](#)

[2] [C. Rappold et al., Phys. Lett. B 728, 543 \(2014\)](#)

[3] [H. Kamada et al., Phys. Rev. C 57 \(1998\) 1595-1603](#)

Theoretical predictions



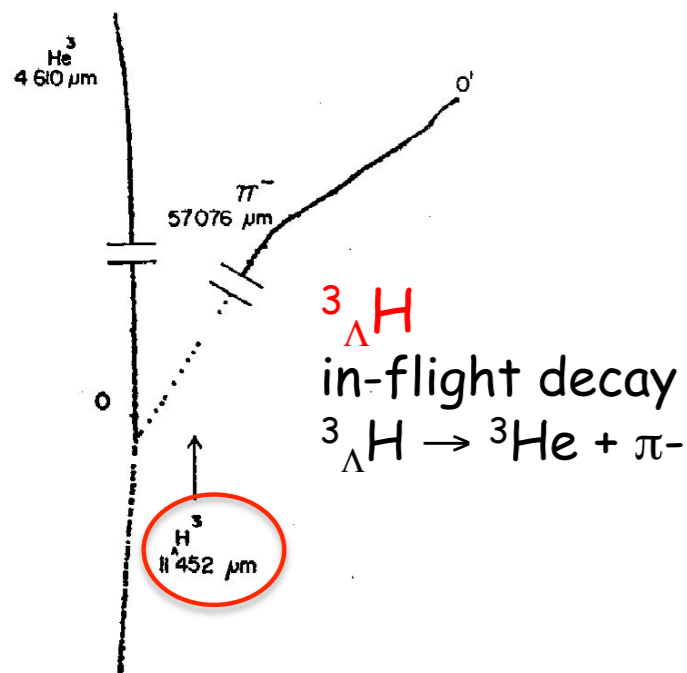
- [35] *M. Rayet, R.H. Dalitz, Il Nuovo Cim. A 46 (1966) 786*
 - values for τ in the range from **239.3 - 255.5 ps**
 - phase space factor, Pauli principle effect, corrections for final-state pion scattering and for NMWD included
- [36] *M. Ram, W. Williams, Nucl. Phys. B 28 (1971) 566*
 - calculated a value of **235 ps**
 - investigation whether hard core corrections in ΛN and NN potentials used to calculate the wave functions could affect the values of τ
- [37] *H. Manosur, K. Higgins, Il Nuovo Cim. A 51 (1979) 180*
 - lower value of **173 ps**
 - calculation based on explicit inclusion of the nucleon induced pionic emission

- [38] *N. Kolesnikov, V. Kopylov, Sov. Phys. J 31 (1988) 210*
 - values for τ of **226.3 ps**
 - Using wave functions found by multi-parameter variation calculations employing 5 different ΛN potential
- [39] *J.G. Congleton, J. Phys. G., Nucl. Part. Phys. 18 (1992) 339*
 - obtained a value of **232 ps**
 - using updated values for the NN and YN potentials to determine the wave functions
- [37] *H. Kamada et al., Phys. Rev. C 57 (1998) 1595*
 - prediction of a value of **256 ps**
 - calculation based on rigorous solution of three-body Faddeev equations for the hypernucleus wave function and for the $3N$ scattering states, where realistic NN and YN interactions were used.

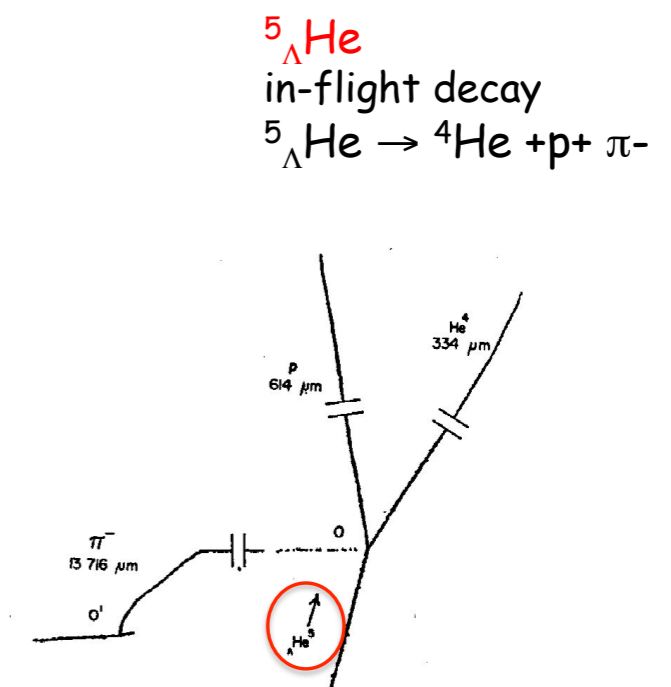
Lifetime measurements: *visualizing techniques*

Hypernuclei discovered 1953 in photographic emulsion, through the **MWD**

- At the beginning **light hypernuclei/hyperfragments** identified via their π^- MWD with **visualizing techniques**
 - emulsion/bubble chambers exposed to energetic K^- beams
 - observation of charged decay modes
- In the first experiments:
 - assignment of **spin/parity** to light hypernuclei ground state ($^3_\Lambda\text{H}$, $^4_\Lambda\text{H}$, $^4_\Lambda\text{He}$, $^8_\Lambda\text{Li}$, $^{11}_\Lambda\text{B}$ and $^{12}_\Lambda\text{B}$) through properties of π^- MWD ($^7_\Lambda\text{Li}$)
 - study of the **Λ -N spin dependent interaction** ($J_{\text{hyp g.s.}} = J_{\text{core}} - 1/2$)



First experiments:
Lifetime obtained from the spatial distribution of the π^- -MWD vertices around the formation point of the hypernucleus



Lifetime measurements: *visualizing techniques*

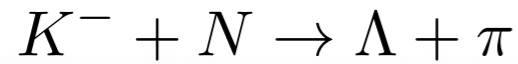
Hypernuclei discovered 1953 in photographic emulsion, through the **MWD**

- At the beginning **light hypernuclei/hyperfragments** identified via their π^- MWD with **visualizing techniques**
 - emulsion/bubble chambers exposed to energetic K^- beams
 - observation of charged decay modes
- In the first experiments:
 - assignment of **spin/parity** to light hypernuclei ground state ($^3_\Lambda\text{H}$, $^4_\Lambda\text{H}$, $^4_\Lambda\text{He}$, $^8_\Lambda\text{Li}$, $^{11}_\Lambda\text{B}$ and $^{12}_\Lambda\text{B}$) through properties of π^- MWD ($^7_\Lambda\text{Li}$)
 - study of the **Λ -N spin dependent interaction** ($J_{\text{hyp g.s.}} = J_{\text{core}} - 1/2$)
- **Limitations** of visualizing techniques:
 - ✗ no timing information
 - ✗ no neutron, γ detection \rightarrow only charged WD channels
 - ✗ number of formed hypernuclei not counted \rightarrow no Branching Ratio determination
 - ✗ spatial distribution of the π^- MWD vertices around the formation point

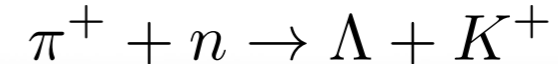
Lifetime measurements: counter experiment - I

Studies with **counter experiments** at accelerators (BNL AGS, KEK PS) from '80 on

- high intensity K^-/π^+ beams for hypernuclei production via:

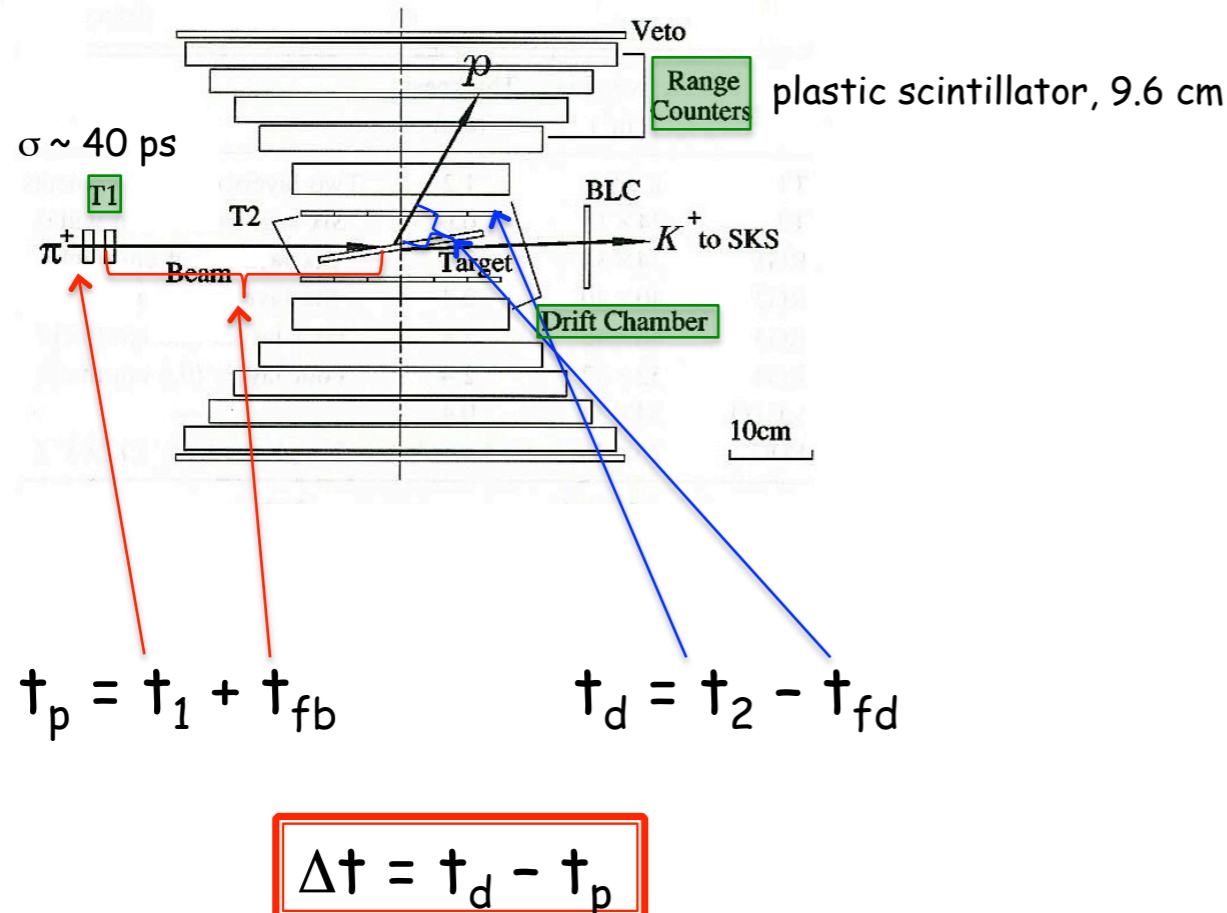


Strangeness exchange

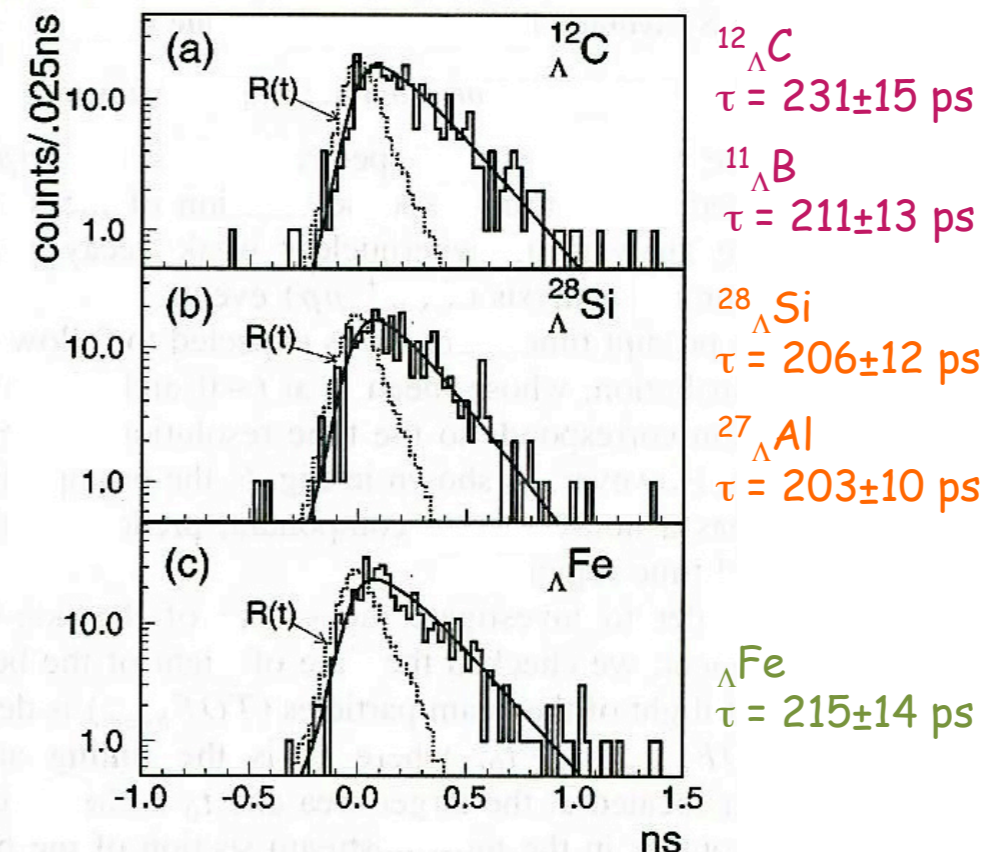


Associated production

- Coincidence measurements with large solid angle spectrometer and **direct timing** measurement techniques



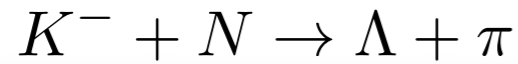
Medium Mass Number hypernuclei



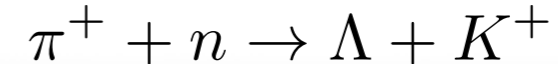
Lifetime measurements: counter experiment - I

Studies with **counter experiments** at accelerators (BNL AGS, KEK PS) from '80 on

- high intensity K^-/π^+ beams for hypernuclei production via:

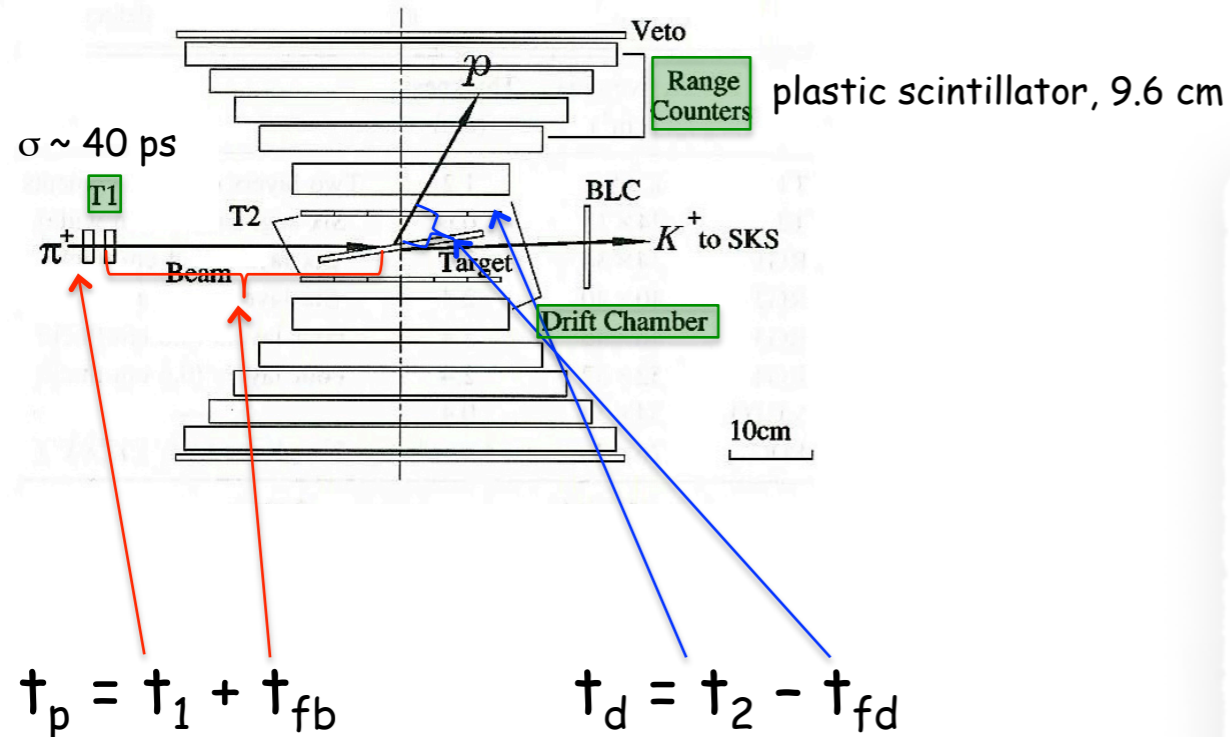


Strangeness exchange



Associated production

- Coincidence measurements with large solid angle spectrometer and **direct timing** measurement techniques



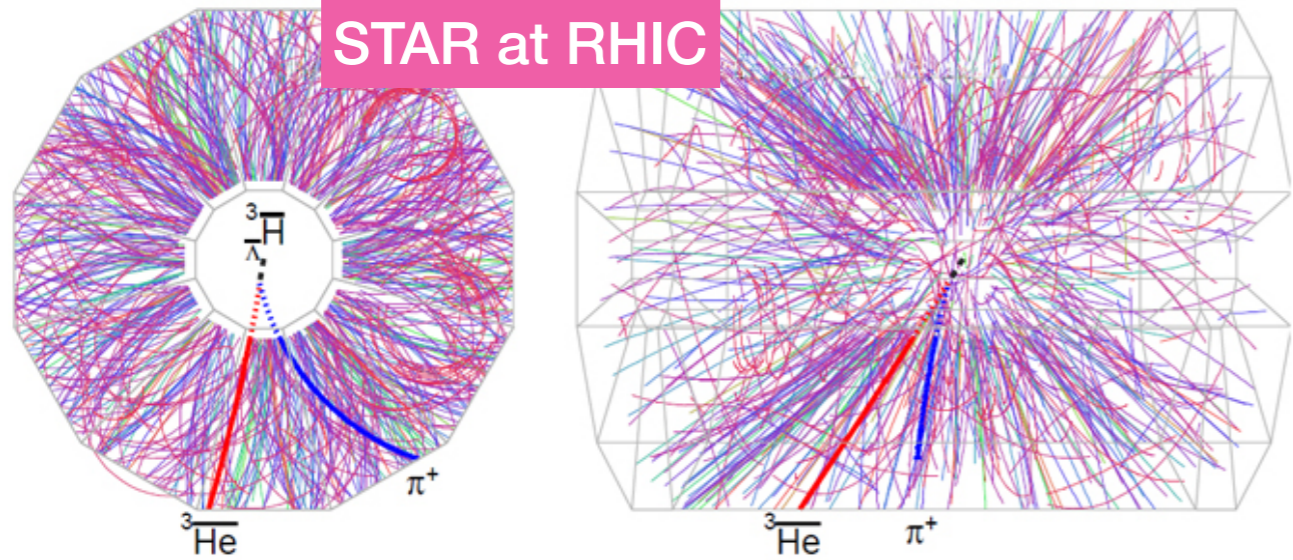
$$\Delta t = t_d - t_p$$

- X** This experimental technique **could not be applied** to the **hydrogen hyperisotopes**
- X** The two-body reactions require targets
 - ${}^3\text{H} \rightarrow$ radioactive, hard to deal with
 - ${}^4\text{H} \rightarrow$ does not exist

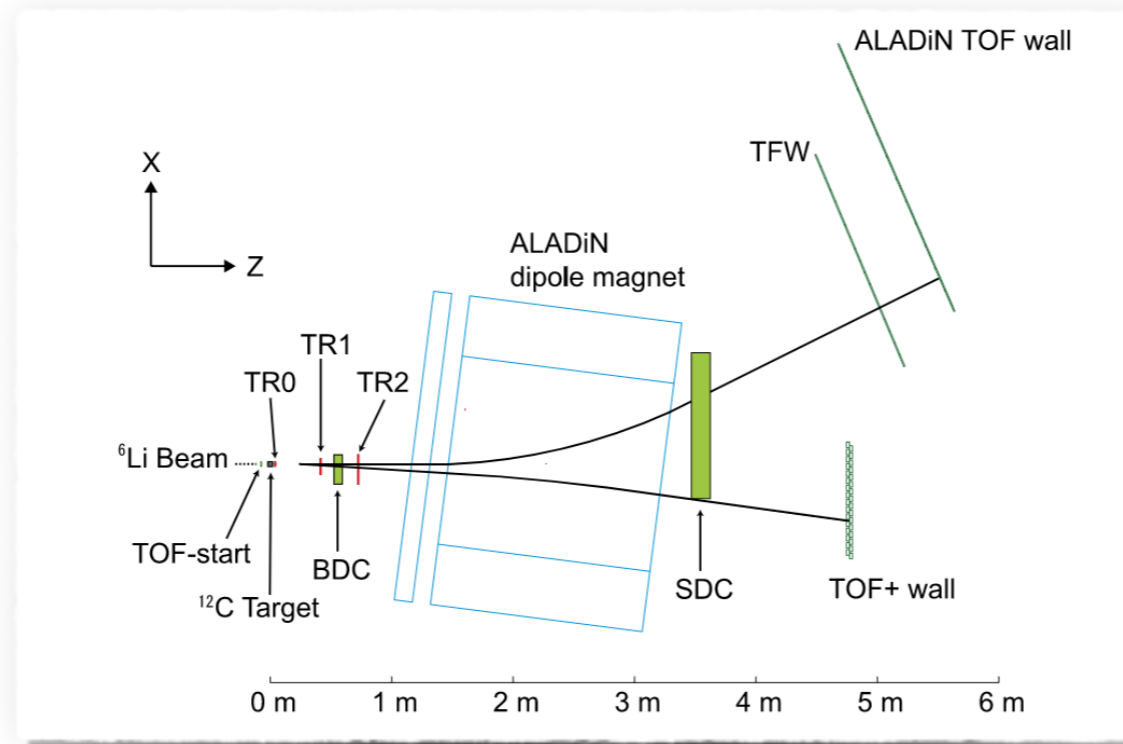
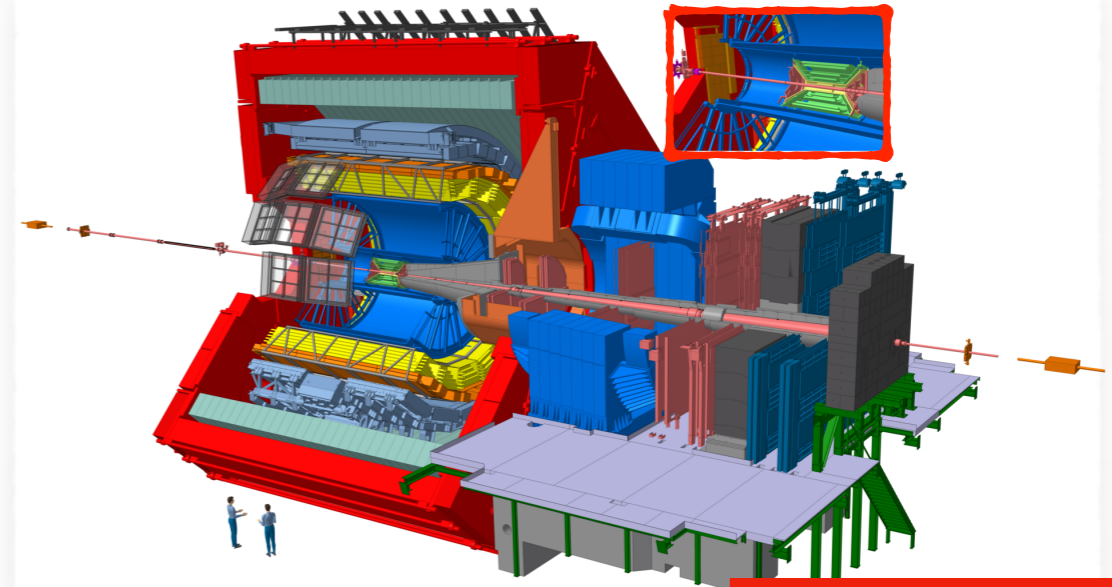
Lifetime measurements: counter experiment - II

Heavy ion collisions: production of light (anti-)hypernuclei measured via invariant mass of decay products in mesonic decay channels

Au-Au collisions (GeV regime)



Pb-Pb collisions (TeV regime)

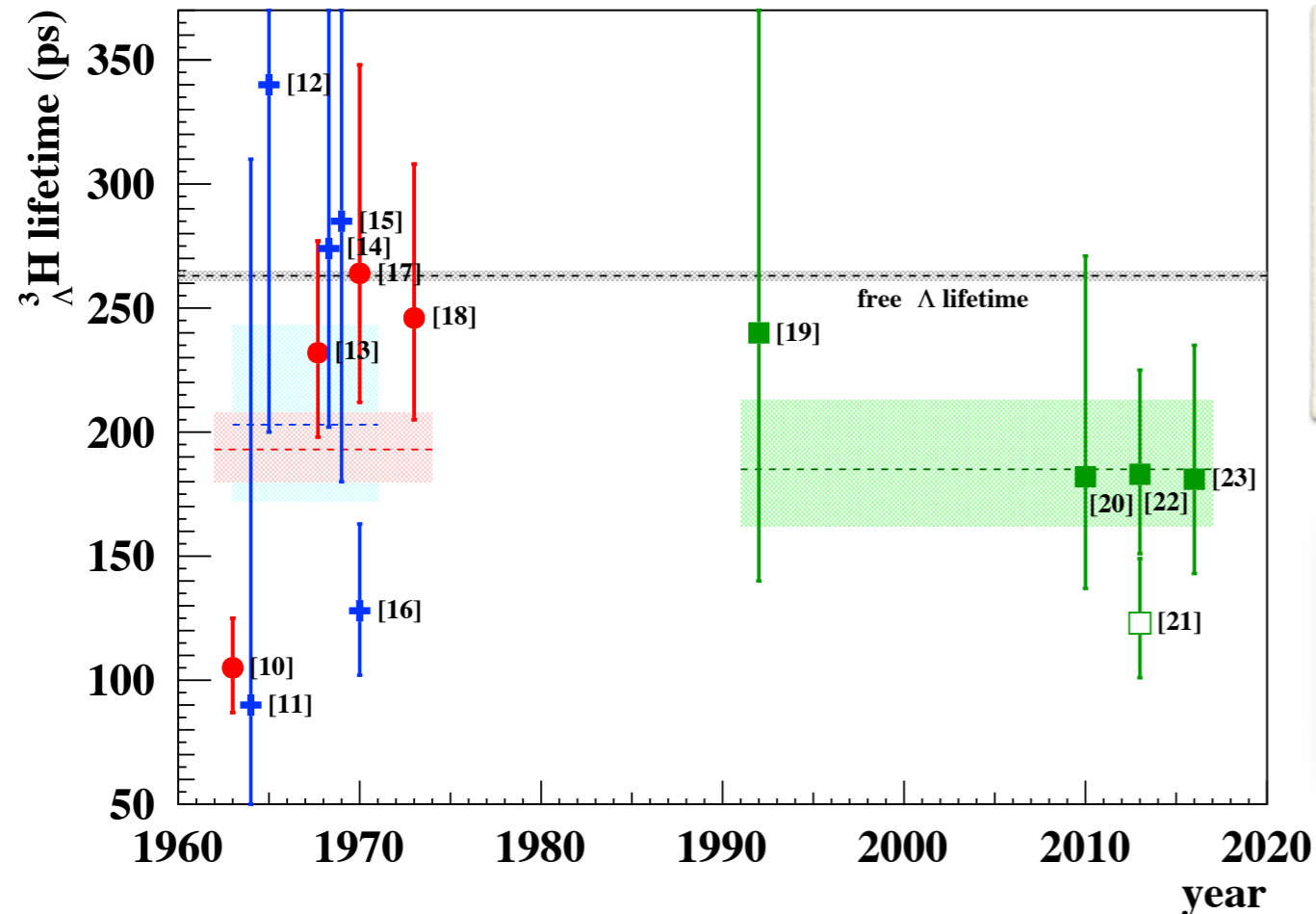


HypHI at GSI

projectile fragmentation reactions of ^6Li at 2 AGeV delivered on a carbon target.

Experimental knowledge

M. Agnello et al., Nucl. Phys. 954 (2016) 176



emulsion technique: 203^{+40}_{-31} ps

He Bubble Chamber: 195^{+15}_{-13} ps

Electronic techniques: 185^{+28}_{-23} ps without [21]

Electronic techniques: 163^{+18}_{-16} ps with [21]

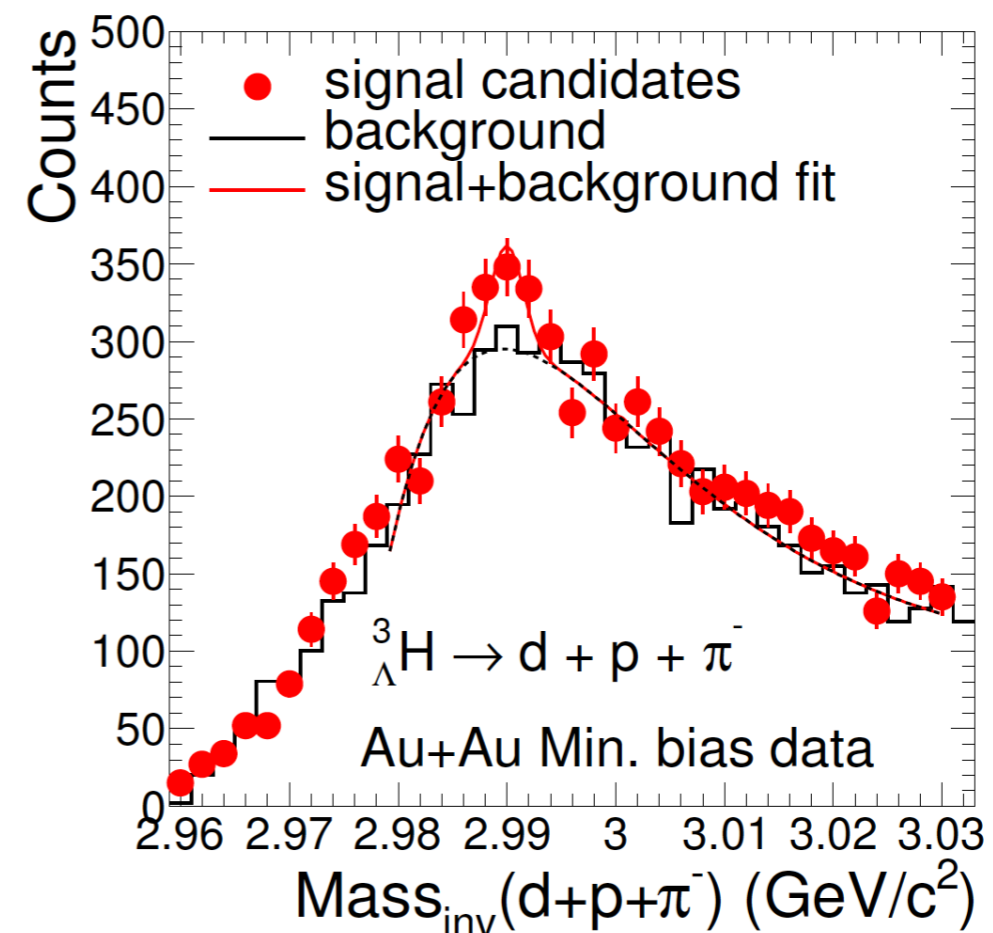
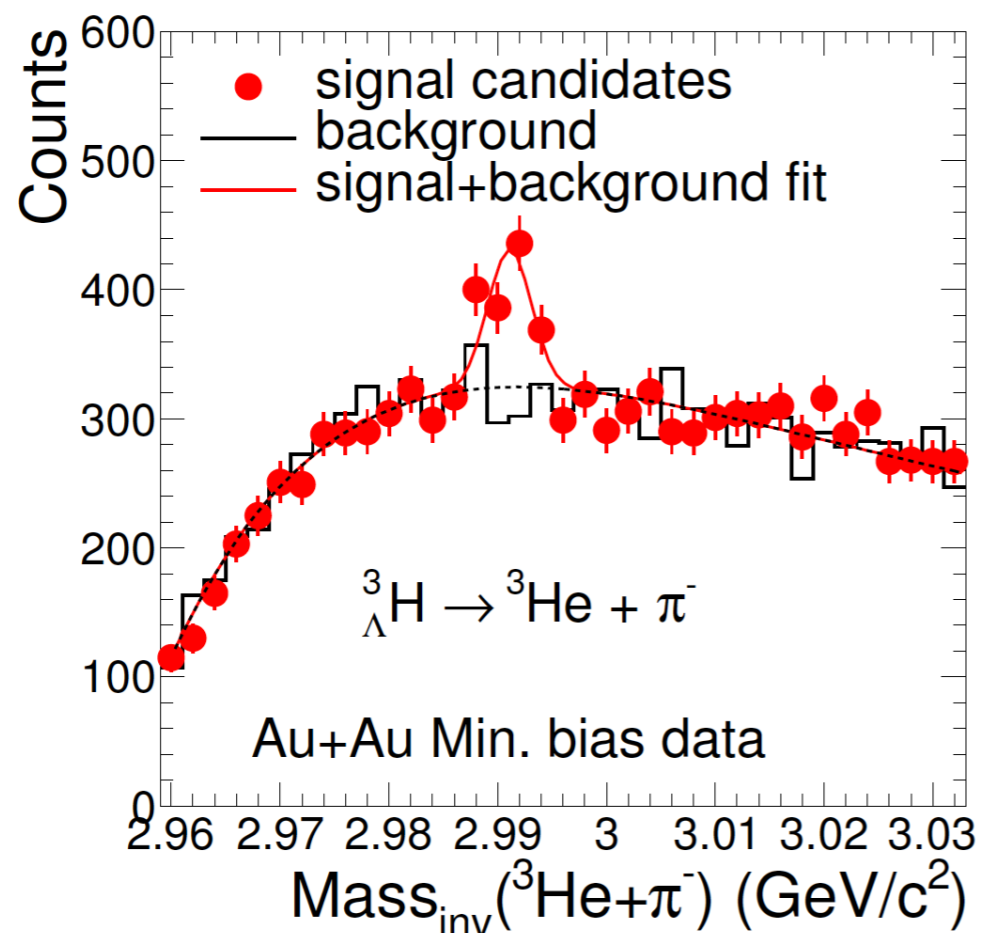
CAVEAT:

The citations close to each marker are related to the review where the plot is shown

- Visualizing techniques (emulsion and ^3He Bubble chamber):
 - values closer and in agreement with the free Λ lifetime
 - large uncertainties due to the limited data sample
- Electronic techniques (heavy-ion experiments):
 - larger data sample led to a reduction of the uncertainties
 - measured values are below the expectations

Latest results: STAR

- Invariant mass spectra from **2-** and **3-body decay**:
 - analysis of the **Au-Au collisions** data sample from beam energy scan (BES)
 - large uncertainties due to the limited data sample
- **Lifetime determination** with both decay modes



Latest results: STAR

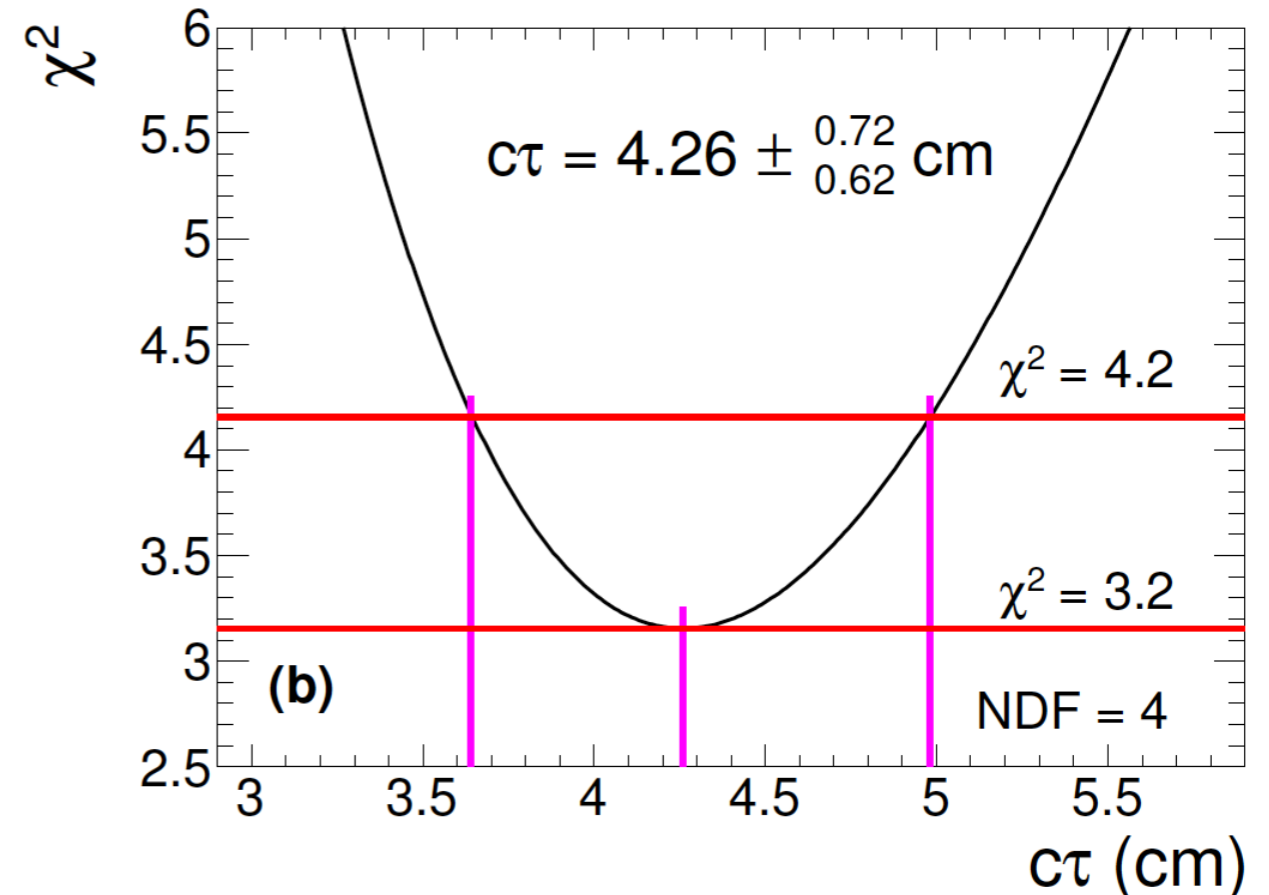
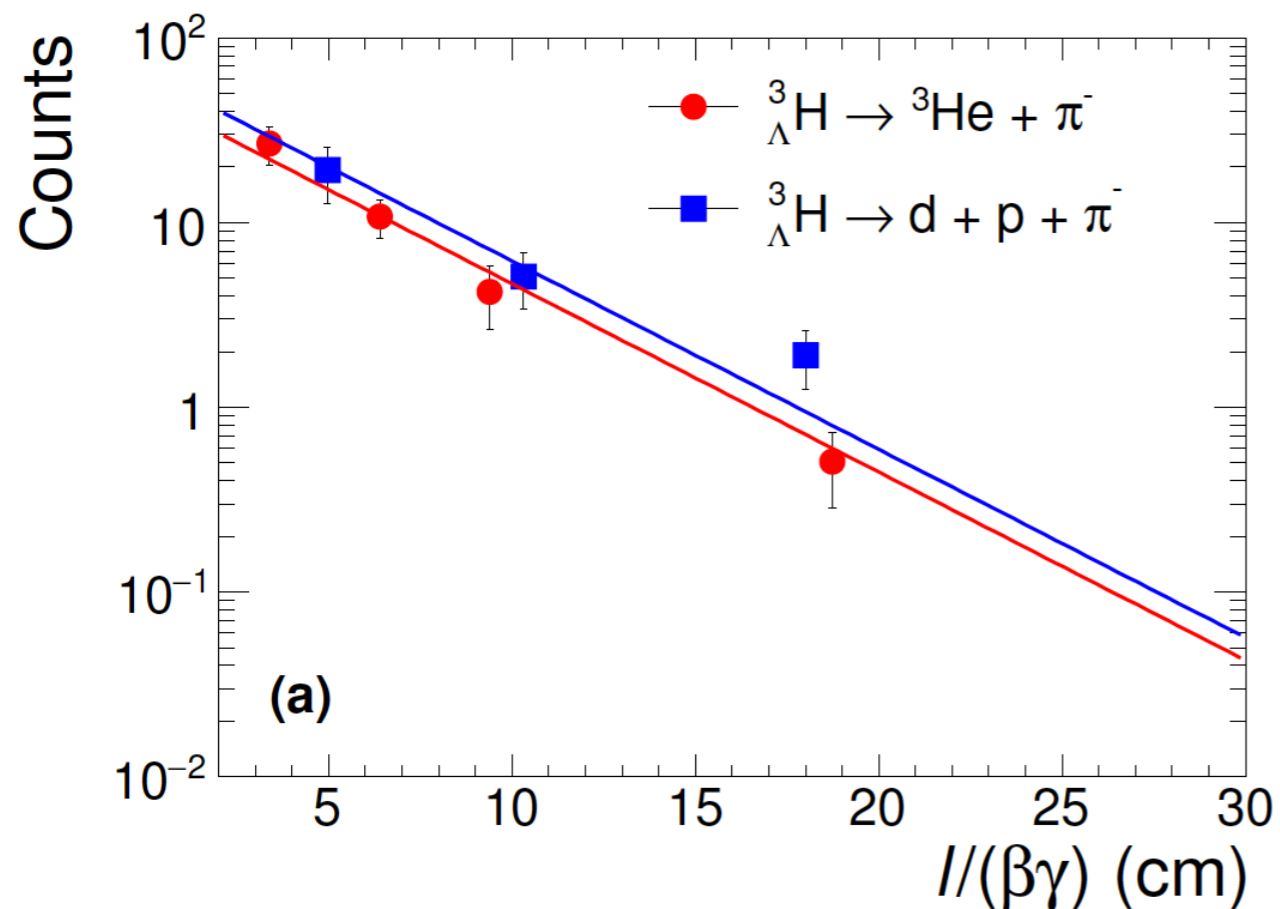
- Invariant mass spectra from **2-** and **3-body decay**:
 - analysis of the **Au-Au collisions** data sample from beam energy scan (BES)
 - large uncertainties due to the limited data sample
- **Lifetime determination** with both decay modes

2-body $\tau = 123_{-21}^{+26} (stat.) ps$

3-body $\tau = 193_{-48}^{+82} (stat.) ps$

Final value

$\tau = 142_{-21}^{+24} (stat.) \pm 29 (syst.) ps$



The lifetime estimate is performed:

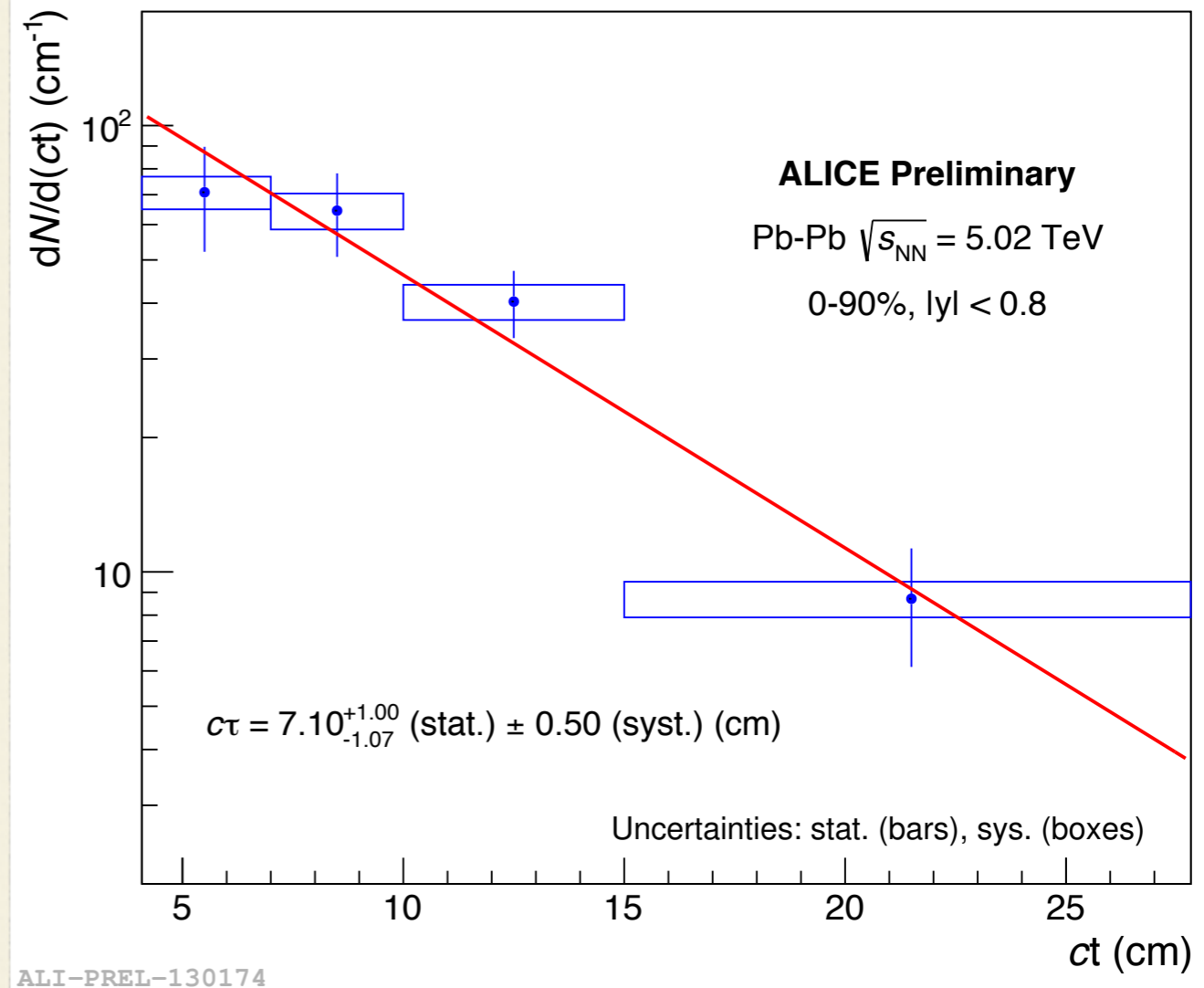
- using the **full data sample** of Pb-Pb collisions at $\sqrt{s_{NN}} = 5.02$ TeV collected in 2015
- selecting both hypertriton and anti-hypertriton **candidates**
- **using two methods: “ct spectra”** (default) and **unbinned fit** (crosscheck)

ct spectra (default)

- **Signal extraction** in four different ct bins
 - 4-7, 7-10, 10-15, 15-28 cm
- **Exponential fit** to the corrected dN/ct spectrum for the lifetime estimate

$$\tau = 237_{-36}^{+33}(\text{stat.}) \pm 17(\text{syst.})\text{ps}$$

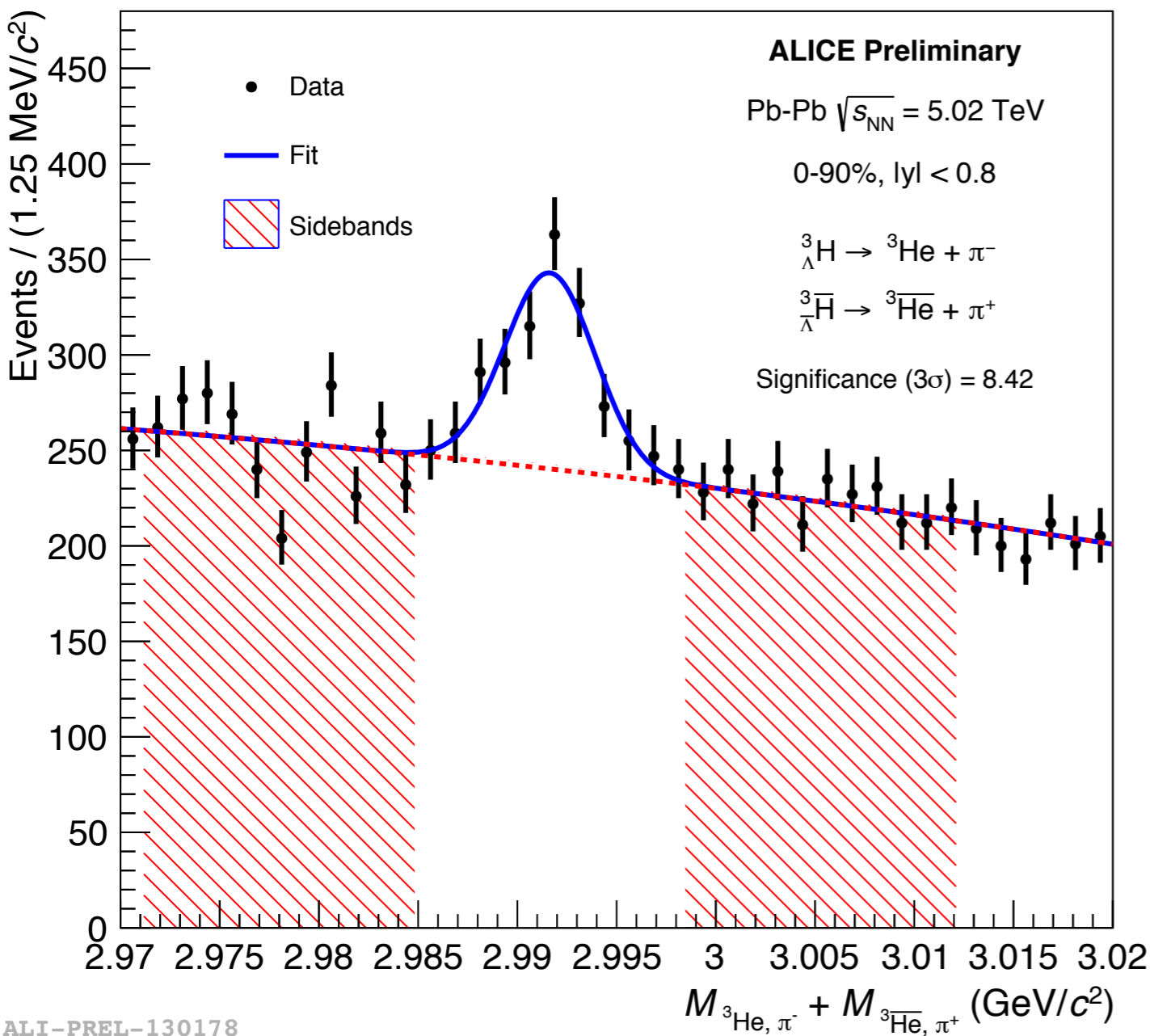
- **Result** with the highest precision at the moment
 - improved resolutions with respect to the previous result at 2.76 TeV
- Lifetime estimate with an alternative method as a **crosscheck**



ALICE results (Pb-Pb at 2.76 TeV)

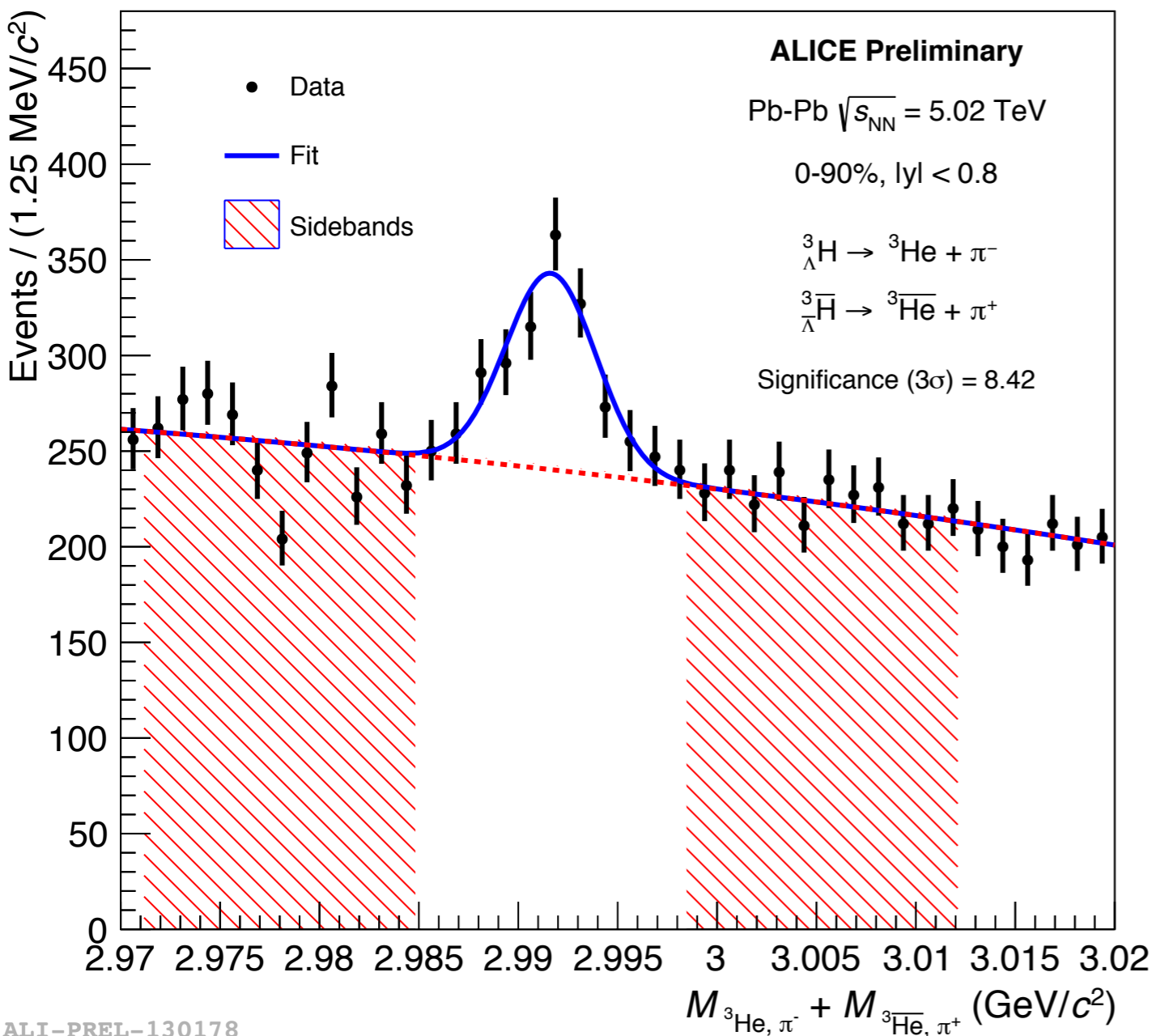
$$\tau = 181_{-38}^{+54}(\text{stat.}) \pm 33(\text{syst.})\text{ps}$$

Latest results: ALICE

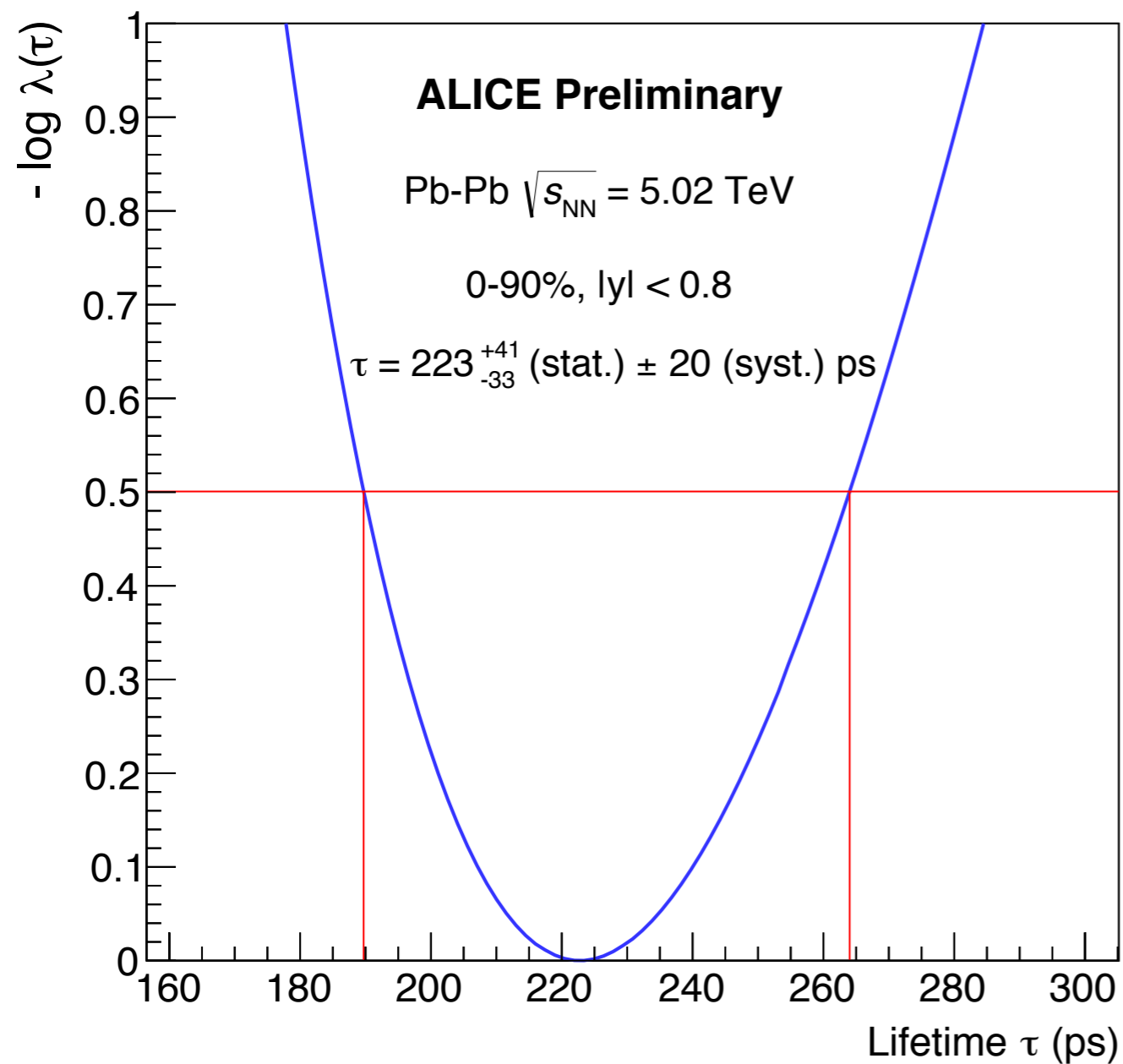


- Fit to the invariant mass distribution to define the **signal range** and the **sidebands**

Latest results: ALICE



- Fit to the invariant mass distribution to define the **signal range** and the **sidebands**
- Fit in the **sidebands** with two exponentials is performed (**background**)
- Fit in the **signal range** for the lifetime estimate
 - **signal**: exponential function multiplied for the efficiency
 - **background**: from the sidebands fit

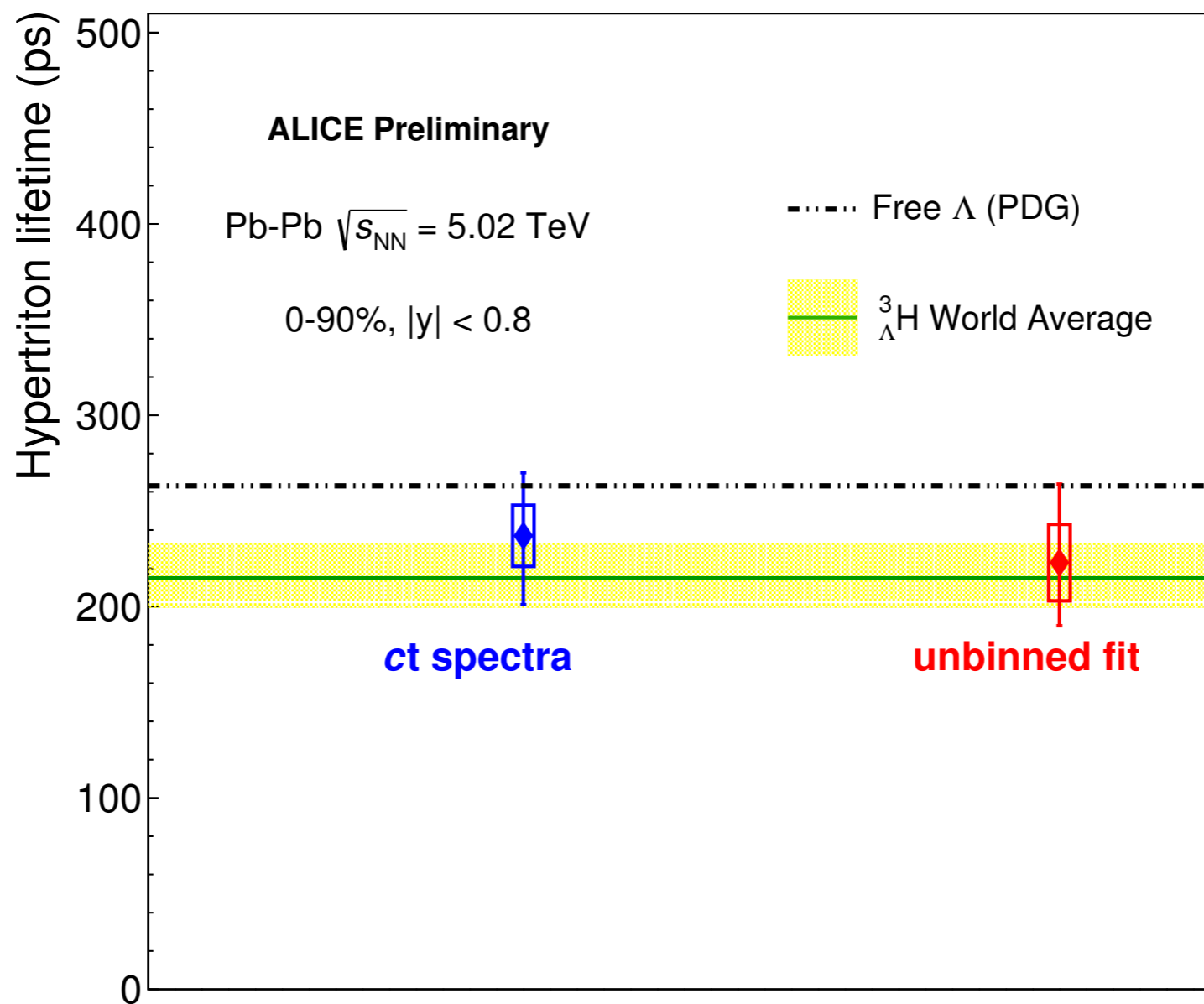
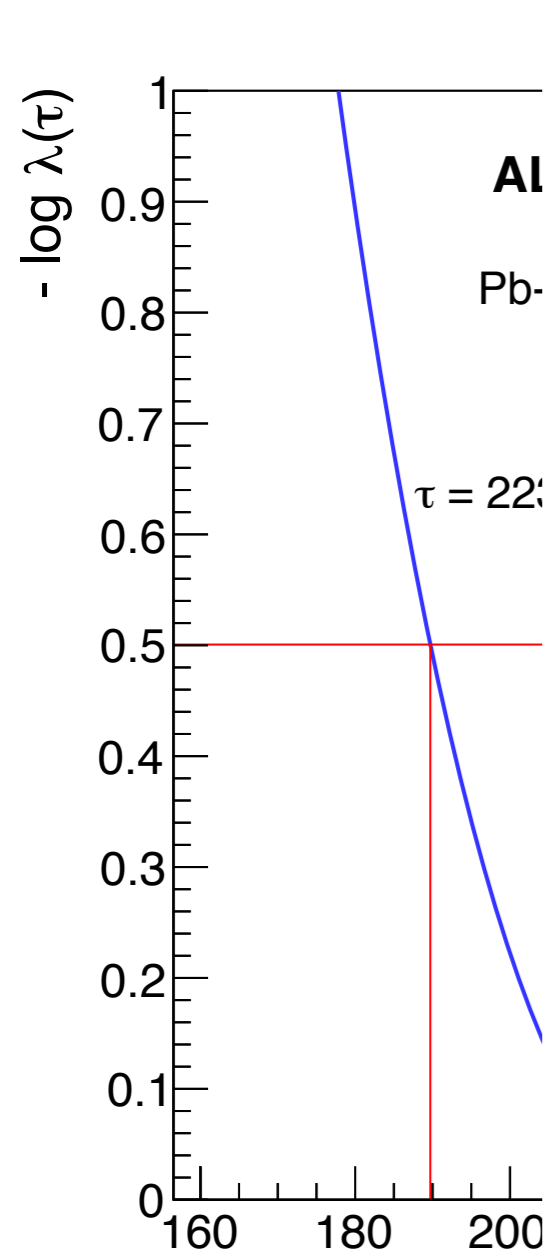


- Fit to the invariant mass distribution to define the **signal range** and the **sidebands**
- Fit in the **sidebands** with two exponential is performed (**background**)
- Fit in the **signal range** for the lifetime estimate
 - **signal**: exponential function multiplied for the efficiency
 - **background**: from the sidebands fit

Lifetime value estimate

$$\tau = 223^{+41}_{-33} (\text{stat.}) \pm 20 (\text{syst.}) \text{ps}$$

Latest results: ALICE



ALI-PREL-130199

$$\tau = 223_{-33}^{+33}(\text{stat.}) \pm 20(\text{syst.})\text{ps}$$

mass distribution
 range and the

with two
 rmed

e for the lifetime

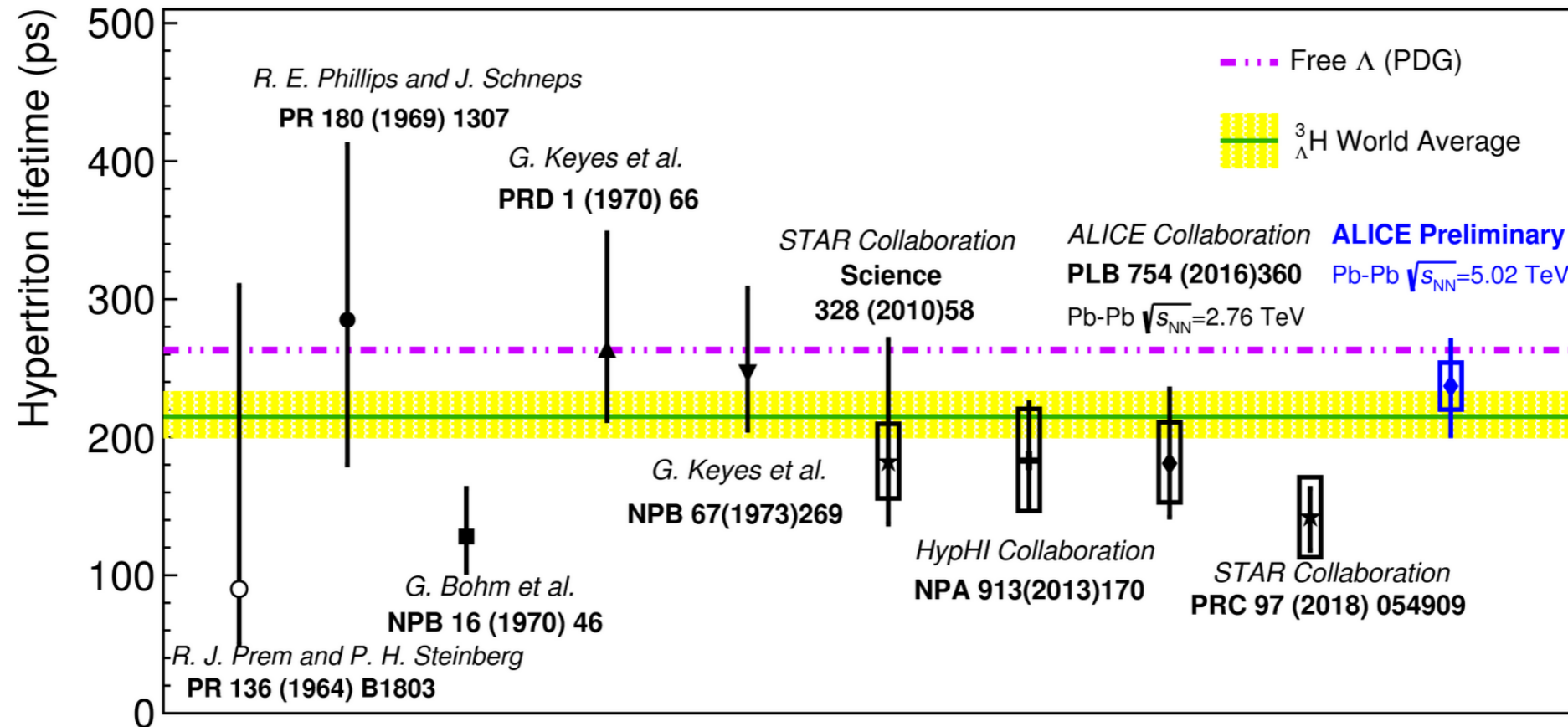
function
 efficiency

the sidebands

e estimate

ALI-PREL-130191

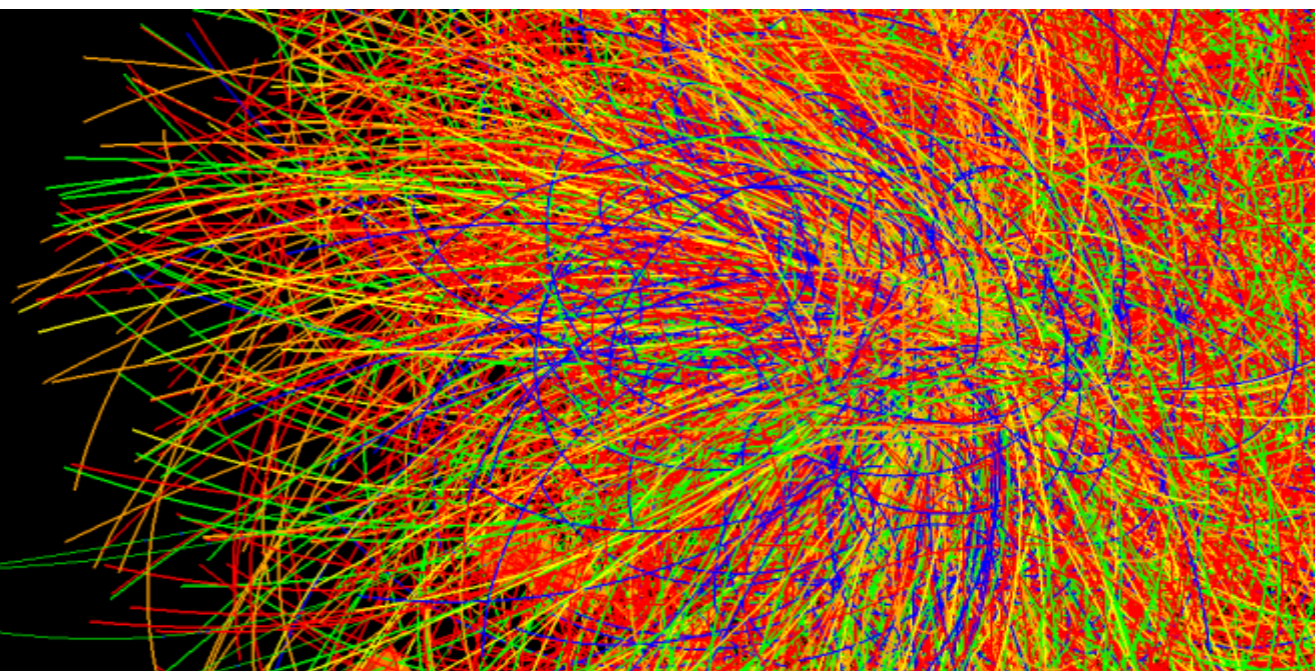
Lifetime collection



ALI-DER-161043

- ALICE result, obtained from the analysis Pb-Pb at $\sqrt{s_{NN}} = 5.02$ TeV data sample, show an **improved precision** with respect to previous heavy ion experiment
 - it is **compatible** with the world average and, in particular, with the free Λ hyperon lifetime
- **Further improvements** will come from:
 - from lifetime measured in the **3-body** decay channel
 - upgrade of the ALICE experiment for LHC Run3 and Run4

Conclusion and perspective



Conclusion and perspective

Production

- Both **thermal** and **coalescence** models can describe **particular aspects** of (hyper-)nuclei measurements in **three different collision systems**
- Huge **experimental effort** is going on to provide more precise results to investigate a possible **unified description of nucleosynthesis**
- **Theoretical predictions** are needed especially for comparison with **small systems**

Conclusion and perspective

☑ Production

- Both **thermal** and **coalescence** models can describe **particular aspects** of (hyper-)nuclei measurements in **three different collision systems**
- Huge **experimental effort** is going on to provide more precise results to investigate a possible **unified description of nucleosynthesis**
- **Theoretical predictions** are needed especially for comparison with **small systems**

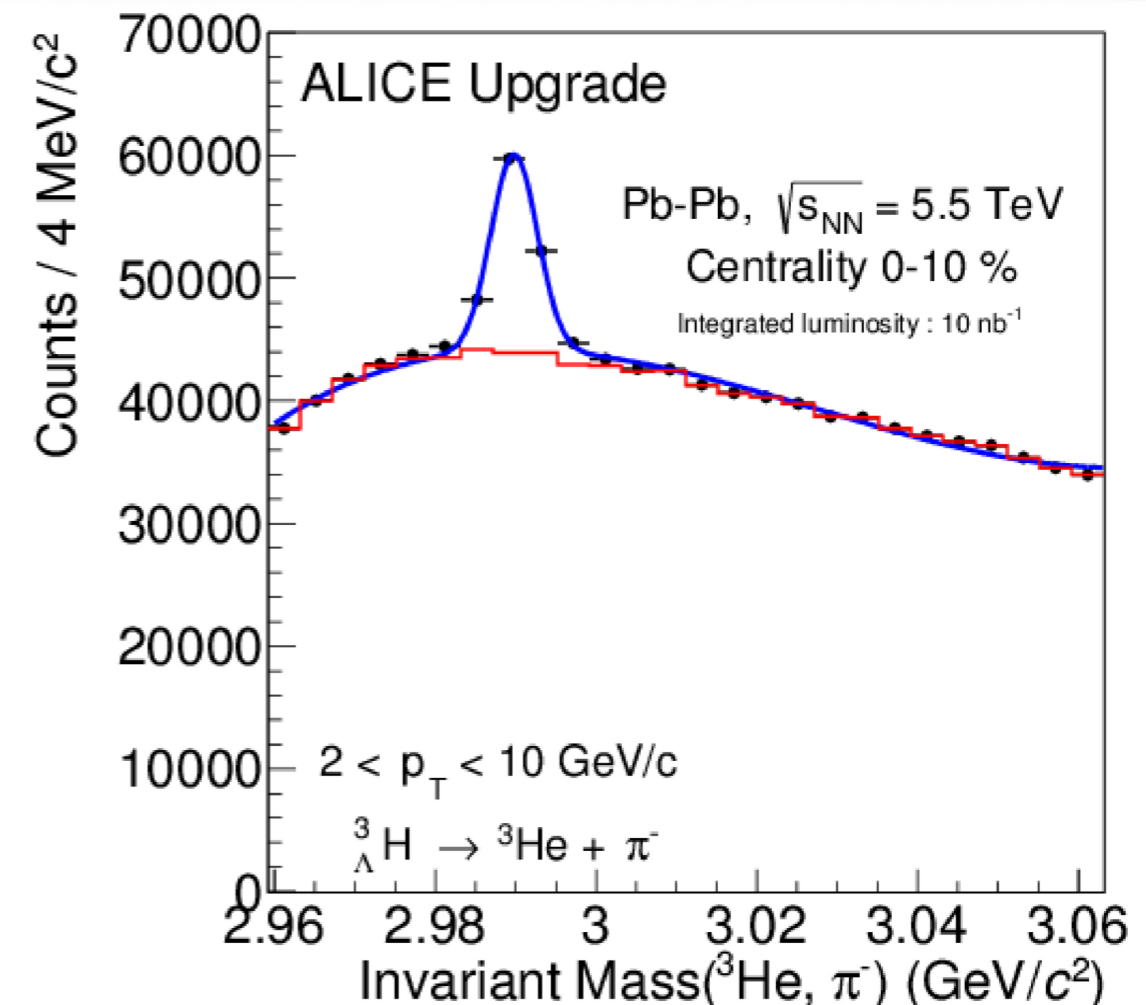
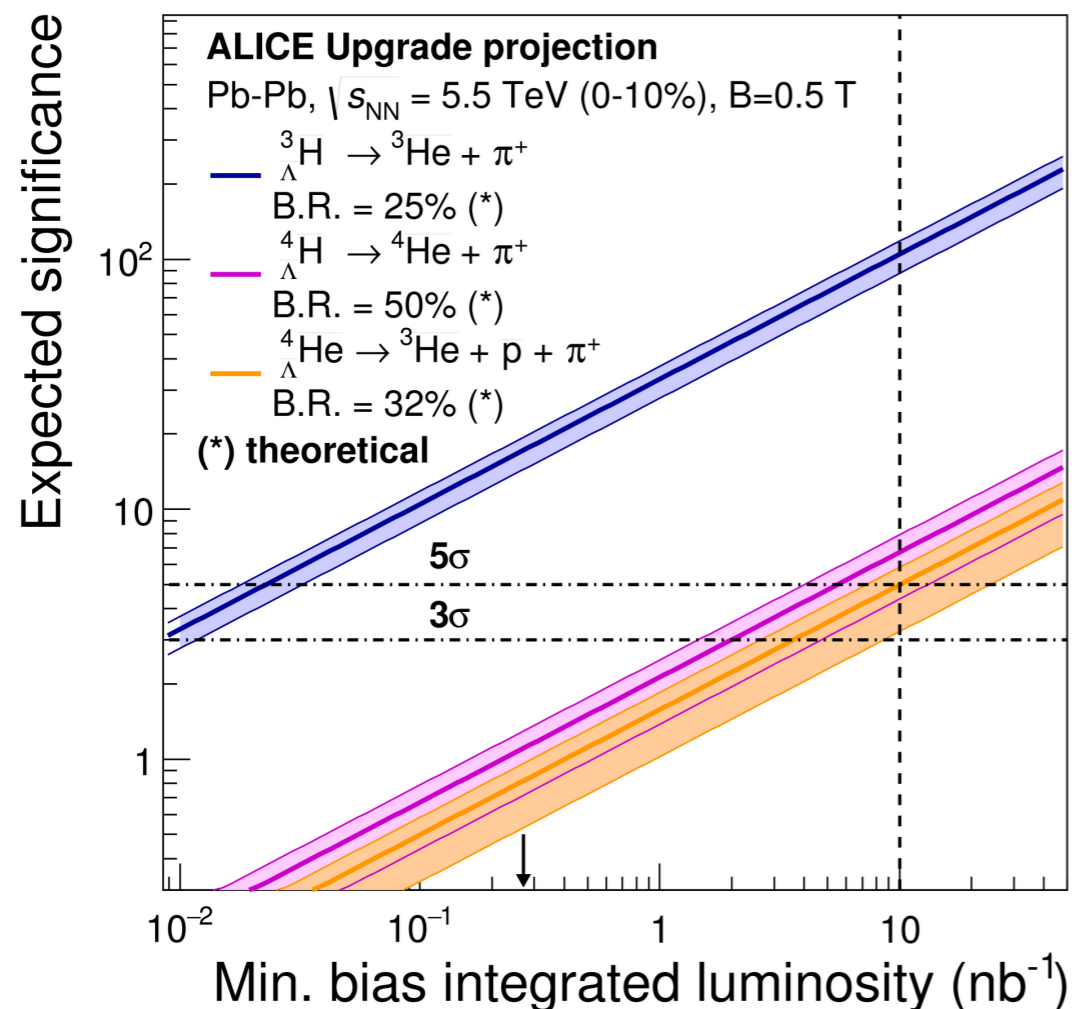
☑ Lifetime puzzle

- Latest **ALICE** result at 5.02 TeV is the **most precise** and is **closer** to the theoretical expectation → this raise the **question** “*can we still talk about a puzzle?*”
- Challenge faced by other experiments to measure the **lifetime** and also the **Λ binding energy** with higher precision
- In the next **LHC Run3** and **Run4** ALICE is expected to collect a larger data sample to reduce the uncertainties below 5%

Conclusion and perspective

✓ Outlook

- **ALICE** has started a huge **upgrade** of the main detectors in preparation of LHC **Run3** and **Run4** → expected Pb-Pb $\mathcal{L}_{\text{DEL}} = 13 \text{ nb}^{-1}$ at **50 kHz** collision rate
- Improvements on the **results for A=3** and possibility to investigate **A=4** (hyper-)nuclei production



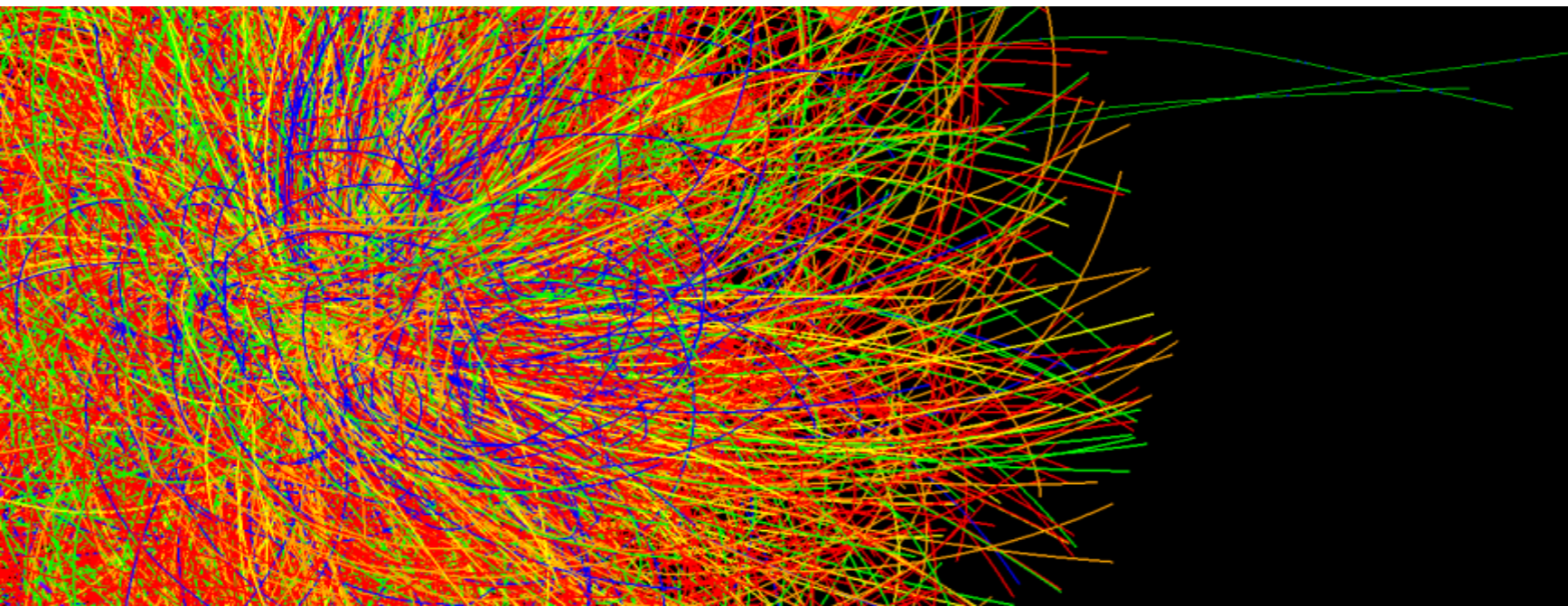
ALI-PUB-80396

ALI-SIMUL-312332

ALICE Collaboration, J. Phys. G 41, 087002 (2014)

*Thank you for
your attention
and
Best Wishes!*



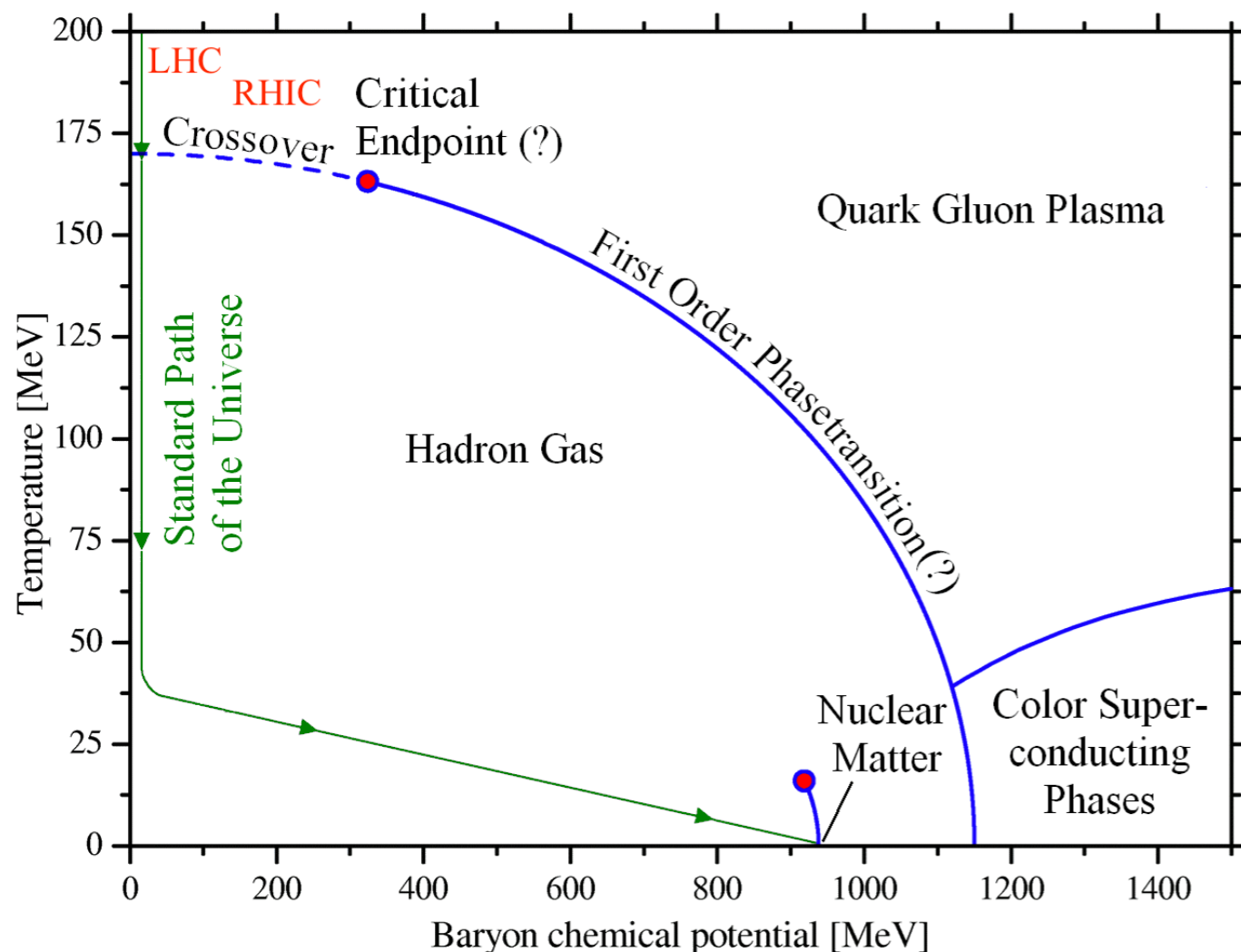


Backup

Why heavy ion collisions?

Everyday matter comes in various form and we distinguish between **solid**, **liquid** and **gas** phases...

[T. Boeckel and J. Schaffner-Bielich, Phys. Rev. D 85, 103506 \(2012\)](#)



QCD phase diagram

- Consequence of the running of α_s is the existence of a phase transition:
 - **Hadron gas** \Leftrightarrow **Quark Gluon Plasma**
- In the QGP **quarks** and **gluons** are no longer confined in colour singlets:
 - probably existed in the early universe, 10 μ s after the Big Bang
- The phase transition is expected to be:
 - **first order transition** at *high* μ_B (FAIR)
 - **crossover** at *small* μ_B and *high* T (LHC, RHIC)

- [E. Fermi, Prog. Theor. Phys. 5, 570 \(1950\)](#)

- [R. Stock, "Relativistic Nucleus-Nucleus Collisions and the QCD Matter Phase Diagram" \(2008\)](#)

- [J. Rafelski and J. Birrell, J. Phys. Conf. 509, 012014 \(2014\)](#)



Blast Wave distribution

- Distribution based on the phenomenological model for hadronic matter production in heavy collision, described in [E. Schnedermann, J. Sollfrank, and U. Heinz, Phys. Rev. C 48, 2462 \(1993\)](#)
- It describes particle production spectra both at RHIC and LHC energies
- Description for hadron spectra from HIC in terms of few collective variables

$$\frac{1}{p_T} \frac{dN}{dp_T} \propto \int_0^R r dr m_T I_0 \left(\frac{p_T \sinh \rho}{T_{kin}} \right) K_1 \left(\frac{m_T \cosh \rho}{T_{kin}} \right)$$

where

- $m_T = \sqrt{p_T^2 + m^2}$ is the transverse mass
- I_0, K_1 are the modified Bessel functions
- r is the radial distance on the transverse plane
- T_{kin} is the kinetic freeze-out temperature
- ρ is the velocity profile $\rightarrow \rho = \tanh^{-1} \left(\left(\frac{r}{R} \right)^n \beta_s \right)$
- β_s is the transverse expansion velocity at the system surface

Centrality class

- Centrality of a collision estimated using the particle multiplicities (N_{ch}) and correlated to the impact parameter using the Glauber model
- In literature, the centrality is defined as **percentage** of the total hadronic cross section σ_{AA}

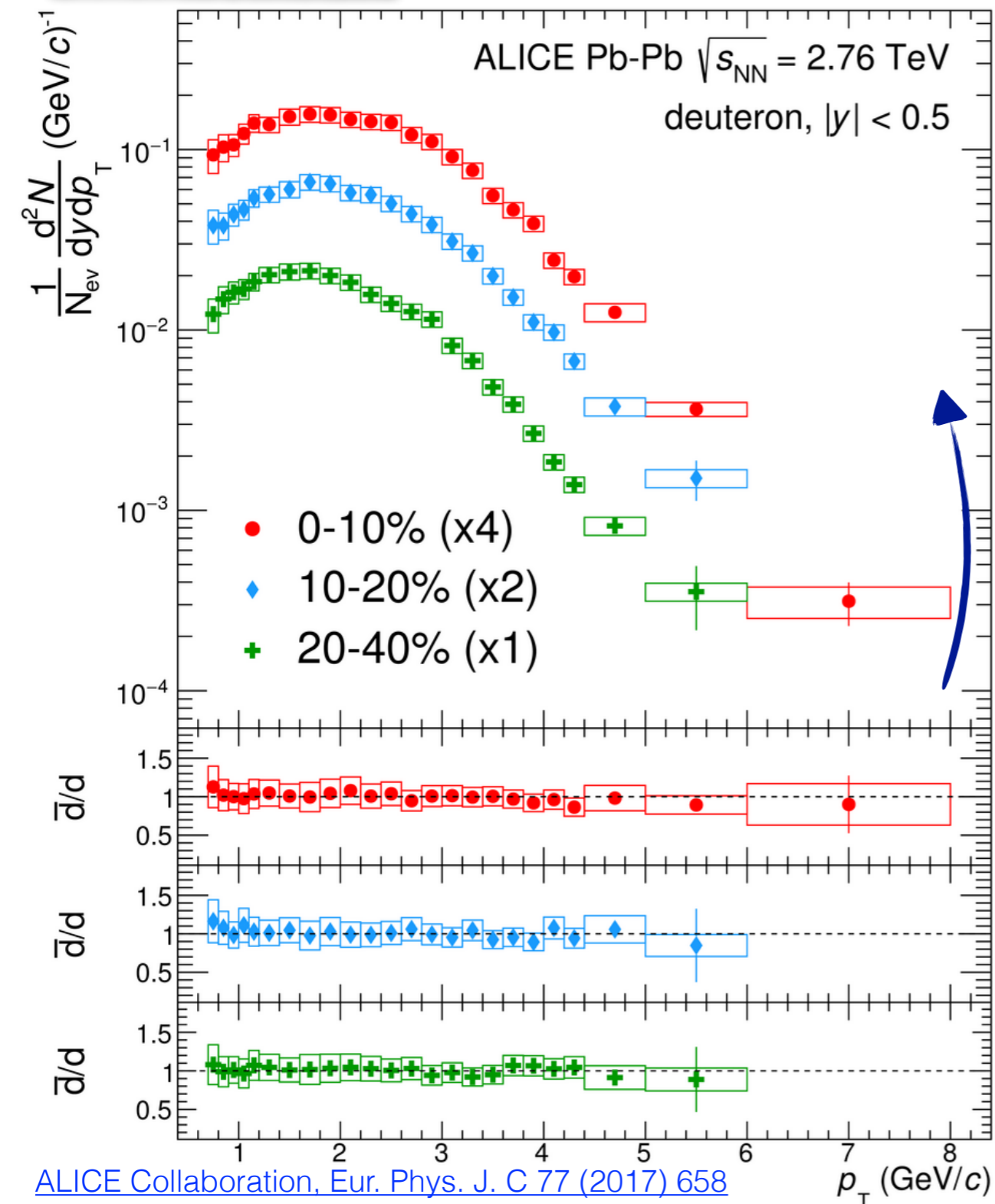
$$c(b) = \frac{\int_0^b \frac{d\sigma}{db'} db'}{\int_0^\infty \frac{d\sigma}{db'} db'} = \frac{1}{\sigma_{AA}} \int_0^b \frac{d\sigma}{db'} db'$$

- Assuming a monotonic dependence of the charged particle multiplicity on the overlap volume, the centrality can be expressed as:

$$c(b) \approx \frac{1}{\sigma_{AA}} \int_{N_{ch}}^\infty \frac{d\sigma}{dN'_{ch}} dN'_{ch}$$

Deuteron spectra

$\sqrt{s_{NN}} = 2.76 \text{ TeV}$



ALICE Collaboration, Eur. Phys. J. C 77 (2017) 658

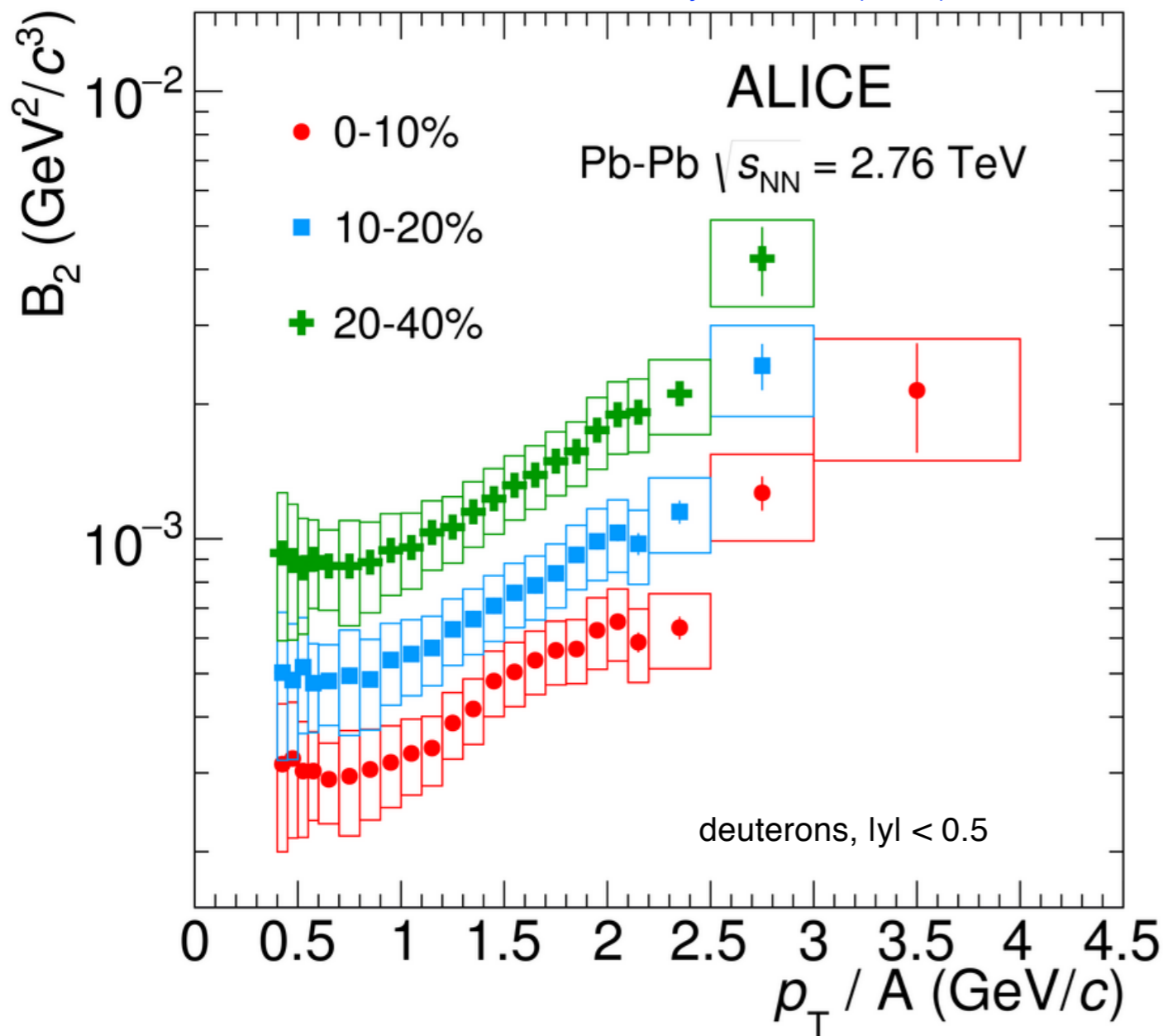
[4] E. Schnedermann et al. Phys. Rev. C 48, 2462 (1993)

- p_T spectra measured for deuteron and anti-deuteron in three different centrality classes
 - pronounced hardening of the spectra visible for increased centrality \rightarrow radial flow
- Integrated yield and mean p_T are extracted by fitting the spectra with the Blast-Wave [4] (BW) function
- Ratio \bar{d}/d in agreement with unity within the uncertainties
 - confirms equal production of matter and anti-matter at the LHC energies

Coalescence parameter B_A

$$\sqrt{s_{NN}} = 2.76 \text{ TeV}$$

ALICE Collaboration, Eur. Phys. J. C 77 (2017) 658



- The **probability** to form a nucleus via coalescence can be quantified by the **coalescence parameter B_A** :

$$B_A = E_A \frac{d^3 N_A}{dp_A^3} / \left(E_p \frac{d^3 N_p}{dp_p^3} \right)^A$$

- A is the mass number
- $\rho_p = p_A/A$
- According to **simple coalescence** predictions B_A is **p_T flat**:
 - simple coalescence **does not describe** the trend observed in Pb-Pb collisions
- The **rise in p_T** becomes milder moving from central to peripheral collisions

Coalescence parameter B_A

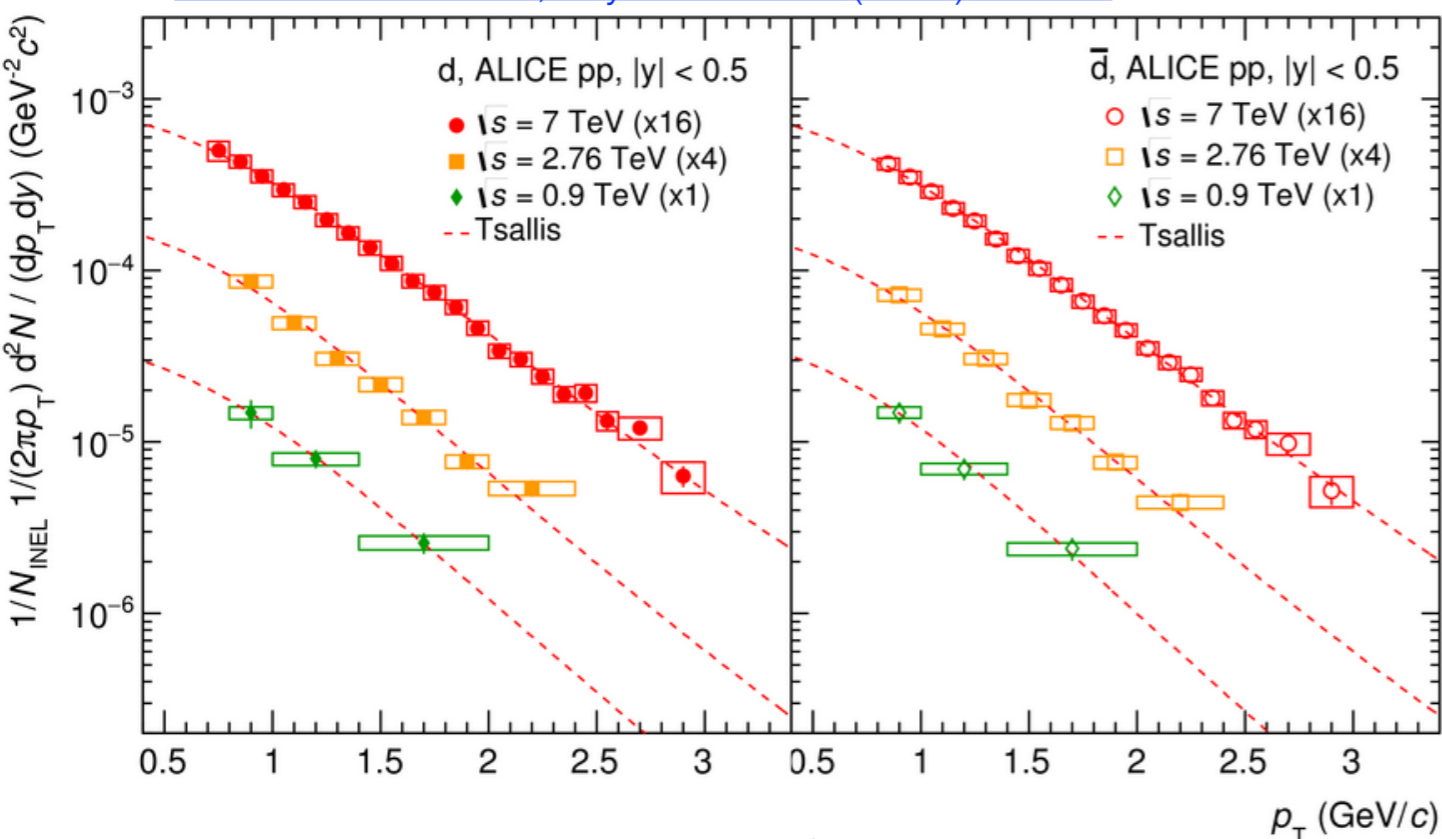
- The **probability** to form a nucleus via coalescence can be quantified by the **coalescence parameter B_A** :

$$B_A = E_A \frac{d^3 N_A}{dp_A^3} / \left(E_p \frac{d^3 N_p}{dp_p^3} \right)^A$$

- A is the mass number
- $\rho_p = \rho_A/A$
- According to **simple coalescence** predictions B_A is **ρ_T flat**:
 - simple coalescence **does not describe** the trend observed in Pb-Pb collisions
- The **rise in ρ_T** becomes milder moving from central to peripheral collisions

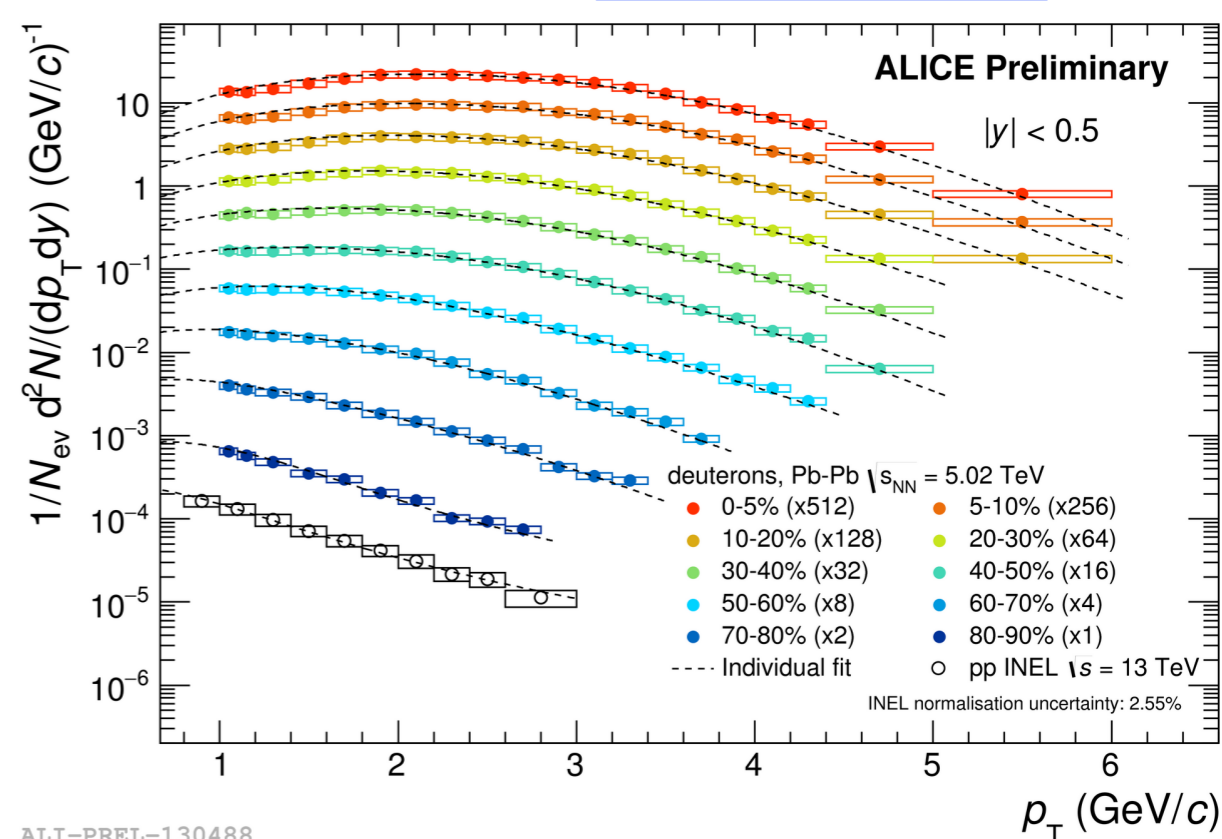
Deuteron production

ALICE Collaboration, Phys. Rev. C 97 (2018) 024615



pp, $\sqrt{s} = 0.9, 2.76, 7$ TeV

ALICE-PUBLIC-2017-006

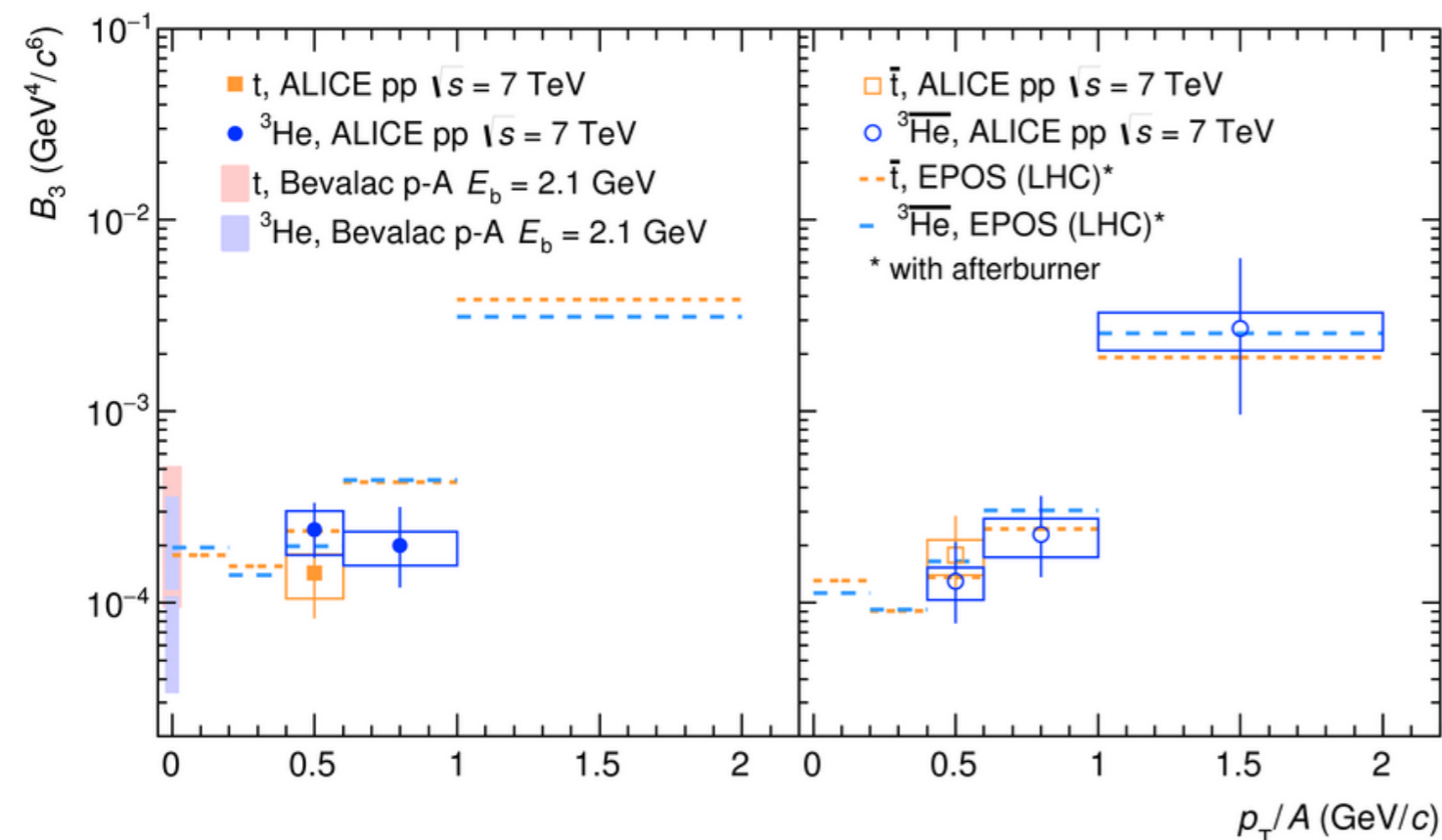
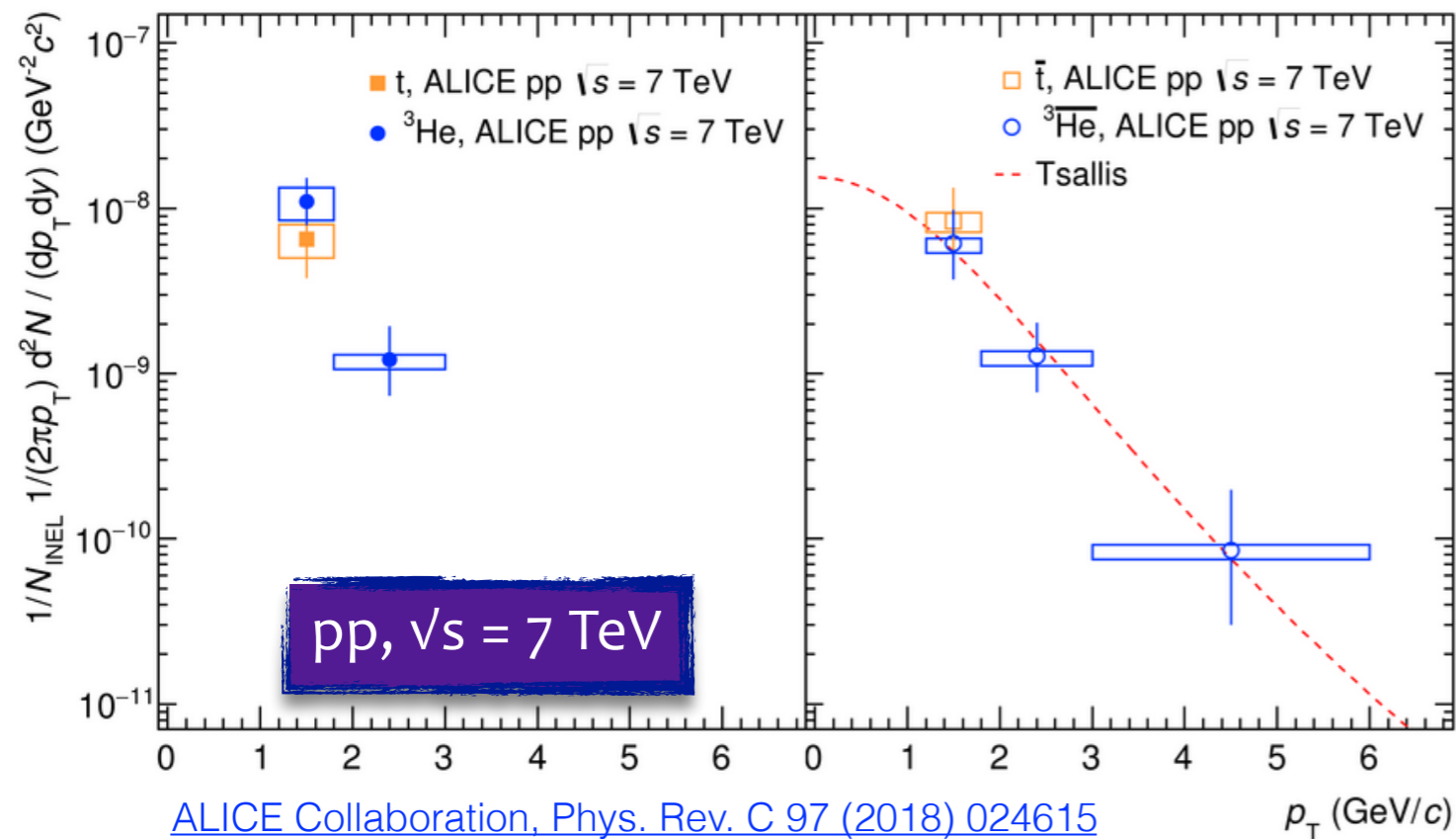


pp, $\sqrt{s} = 7$ TeV

- Minimum Bias p_T spectra in pp collisions show no sign of radial flow
- The fit is performed with a Tsallis function [8] used for the yield extrapolation to the unmeasured regions

[8] C. Tsallis, J. Stat. Phys. 52 (1988) 479



${}^3\text{He}$ and ${}^3\text{H}$ production



- **First (anti-) ${}^3\text{He}$** spectrum measured in pp collisions
 - fit performed with the **Levy-Tsallis** function
- **(anti-) ${}^3\text{H}$** measurement extremely difficult
- Antimatter-to-matter ratios agrees with unity
- **B_3** measured in p-p collisions and compared with:
 - predictions of **EPOS-LHC** with afterburner
 - Bevalac measurements, shown as vertical bands



Summary: thermal production

Nuclei and hypernuclei production

| | Pb-Pb | p-Pb | pp |
|-------------------------|---|--|--|
| Thermal (+hydro) | <ul style="list-style-type: none"> ✓ ρ_T spectra ✓ particle yields ✓ antinucleus/nucleus ✓ deuteron v_2 ✓ ^3He v_2 ✓ d/p and $^3\text{He}/p$ ✓ dN/dy mass depend. ✗ B_2 and B_3 factor | <ul style="list-style-type: none"> ✓ ρ_T spectra ✓ antinucleus/nucleus ✗ d/p and $^3\text{He}/p$ ✓ dN/dy mass depend. ✗ B_2 and B_3 factor | <ul style="list-style-type: none"> ✓ ρ_T spectra ✓ antinucleus/nucleus ✗ d/p and $^3\text{He}/p$ ✗ B_2 and B_3 factor |
| | <ul style="list-style-type: none"> ✓ ρ_T spectra ✓ particle yields ✓ $^3\text{H}/^3\text{H}$ ✓ $^3\text{H}/p$, $^3\text{H}/d$ and $^3\text{H}/^3\text{He}$ ✓ S_3 factor ✗ B_3 factor |  |  |

Legend: ✓ = well described; ✓ = described with some tension; ✗ = not described/missing prediction

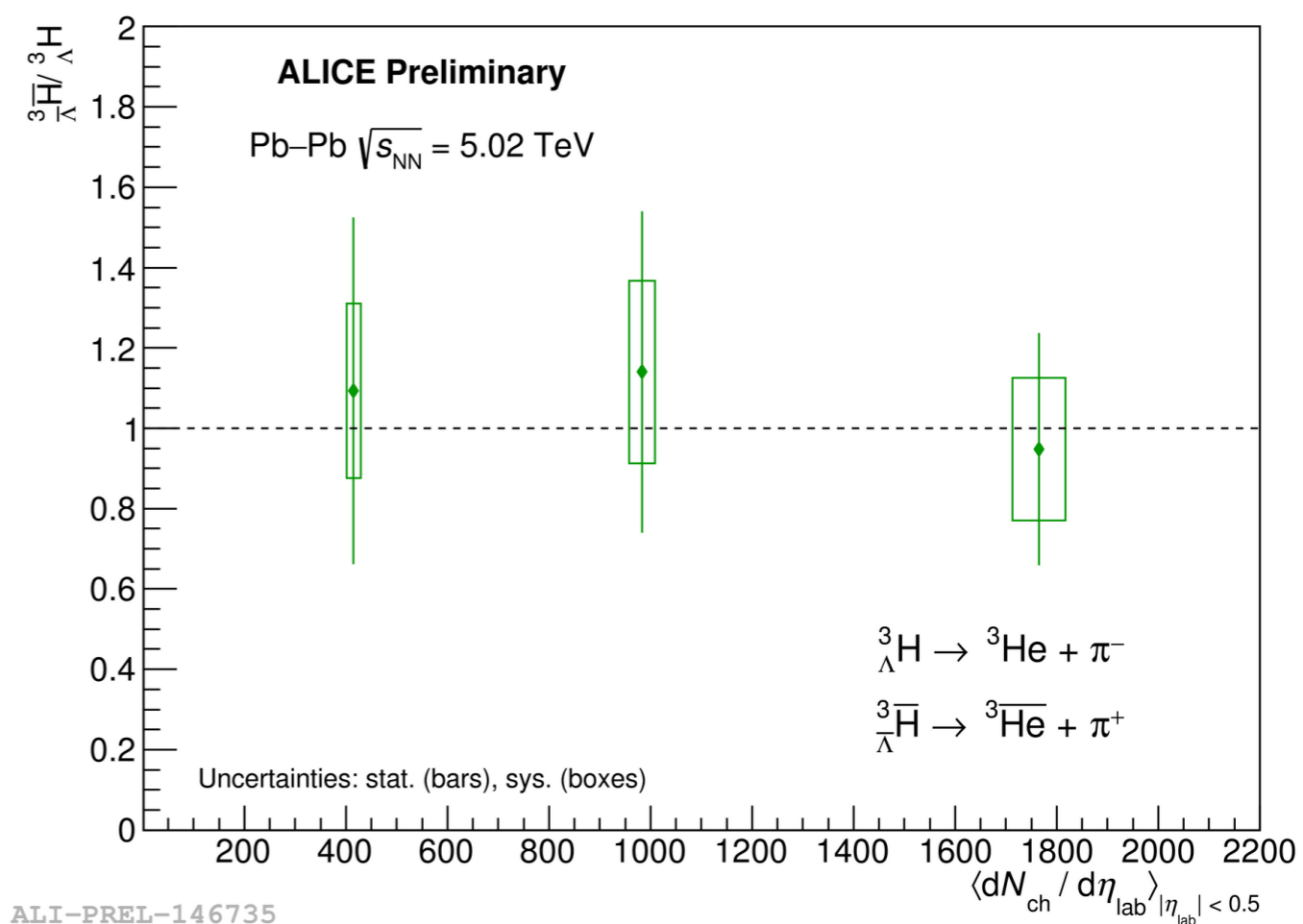
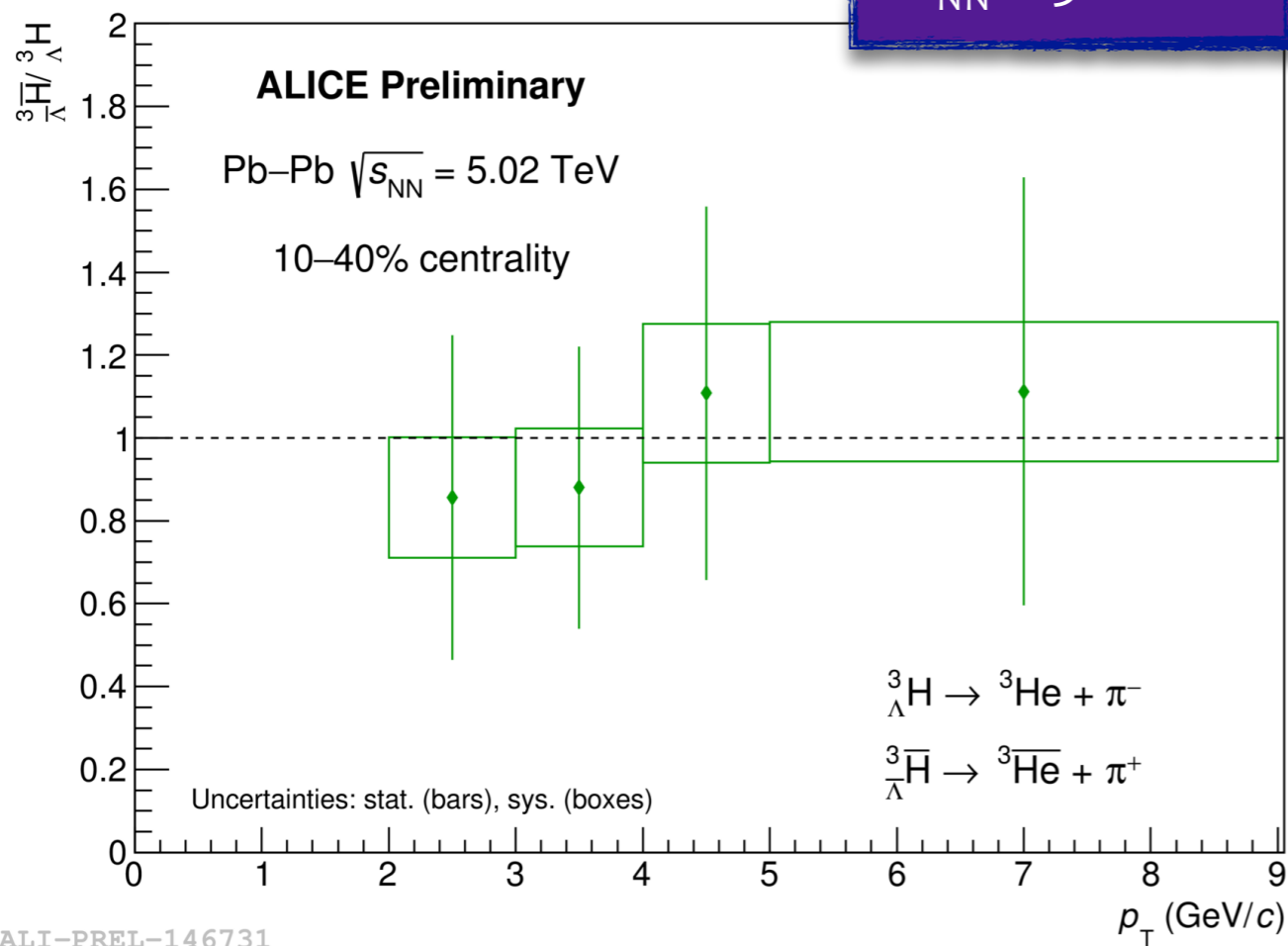
Summary: production via coalescence

| Nuclei and hypernuclei production | | | |
|-----------------------------------|---|--|--|
| | Pb-Pb | p-Pb | pp |
| Coalescence model | <ul style="list-style-type: none"> ✓ ρ_T spectra ✓ particle yields ✓ antinucleus/nucleus ✗ deuteron v_2 ✓ ^3He v_2 ✗ d/p and $^3\text{He}/p$ ✗ dN/dy mass depend. ✓ B_2 and B_3 factor | <ul style="list-style-type: none"> ✓ ρ_T spectra ✓ antinucleus/nucleus ✓ d/p and $^3\text{He}/p$ ✗ dN/dy mass depend. ✓ B_2 and B_3 factor | <ul style="list-style-type: none"> ✓ ρ_T spectra ✓ antinucleus/nucleus ✗ d/p and $^3\text{He}/p$ ✓ B_2 and B_3 factor |
| | <ul style="list-style-type: none"> ✓ ρ_T spectra ✓ particle yields ✓ $^3\text{H}/^3\text{H}$ ✗ $^3\text{H}/p$, $^3\text{H}/d$ and $^3\text{H}/^3\text{He}$ ✗ S_3 factor ✓ B_3 factor |  |  |

Legend: ✓ = well described; ✓ = described with some tension; ✗ = not described/missing prediction

$\frac{{}^3\bar{H}_{\Lambda}}{{}^3H_{\Lambda}}$ ratio

$\sqrt{s_{NN}} = 5.02 \text{ TeV}$



- The ratio has been measured as a function of p_T and of the **charged particle multiplicity**
- **Anti-hypertriton/hypertriton** ratio is in agreement with unity \rightarrow confirm the predictions from **thermal** and **coalescence models**

${}^3\Lambda$ H lifetime knowledge

[M. Agnello et al., Nucl. Phys. 954 \(2016\) 176](#)

| Year | Laboratory | Beam | Exp. method | Lifetime (ps) | Reference |
|------|-----------------------------|--|--------------------|---------------------|-----------|
| 1963 | LBL Bevatron | stopped K^- | He bubble chamber | 105^{+20}_{-18} | [10] |
| 1964 | BNL AGS | K^- , 2.3–2.5 GeV/c | ph. emulsions | 90^{+220}_{-40} | [11] |
| 1965 | BNL AGS and LBL Bevatron | K^- , 2.3 GeV/c K^- 790 MeV/c | ph. emulsions | 340^{+820}_{-140} | [12] |
| 1968 | ANL ZGS | stopped K^- | He bubble chamber | 232^{+45}_{-34} | [13] |
| 1968 | LBL Bevatron | K^- 1.1 GeV/c | ph. emulsions | 274^{+110}_{-72} | [14] |
| 1969 | BNL AGS | K^- 1.1 GeV/c | ph. emulsions | 285^{+127}_{-105} | [15] |
| 1970 | CERN PS | stopped K^- | ph. emulsions | 128^{+35}_{-26} | [16] |
| 1970 | ANL ZGS | stopped K^- | He bubble chamber | 264^{+84}_{-52} | [17] |
| 1973 | ANL ZGS | stopped K^- | He bubble chamber | 246^{+62}_{-41} | [18] |
| 1992 | Dubna Synchrophasotron | He, Li ions 2.2–5 AGeV rHIC | counter experiment | 240^{+170}_{-100} | [19] |
| 2010 | BNL RHIC | Au–Au $\sqrt{s_{NN}} = 200$ GeV central urHIC | counter experiment | 182^{+89}_{-45} | [20] |
| 2013 | BNL RHIC | Au–Au $\sqrt{s_{NN}} = 7.7$ –200 GeV central urHIC | counter experiment | 123^{+26}_{-22} | [21] |
| 2013 | GSI SIS | Li ions 2 AGeV peripheral rHIC | counter experiment | 183^{+42}_{-32} | [22] |
| 2016 | CERN LHC | Pb–Pb $\sqrt{s_{NN}} = 2.76$ TeV central urHIC | counter experiment | 181^{+54}_{-38} | [23] |

[10] M.M. Block, et al., in: Proc. of the International Conference on Hyperfragments, St. Cergue, 28–30 March 1963, p.63.

[11] R.J. Prem, P.H. Steinberg, Phys. Rev. 136 (1964) B1803.

[12] Y.V. Kang, et al., Phys. Rev. 139 (1965) B401.

[13] G. Keyes, et al., Phys. Rev. Lett. 20 (1968) 819.

[14] R.J. Phillips, J. Schneps, Phys. Rev. Lett. 20 (1968) 1383.

[15] R.J. Phillips, J. Schneps, Phys. Rev. 180 (1969) 1307.

[16] G. Bohm, et al., Nucl. Phys. B 16 (1970) 46.

[17] G. Keyes, et al., Phys. Rev. D 1 (1970) 66.

[18] G. Keyes, et al., Nucl. Phys. B 67 (1973) 269.

[19] S. Avramenko, et al., Nucl. Phys. A 547 (1992) 95c.

[20] STAR Collaboration, Science 328 (2010) 58.

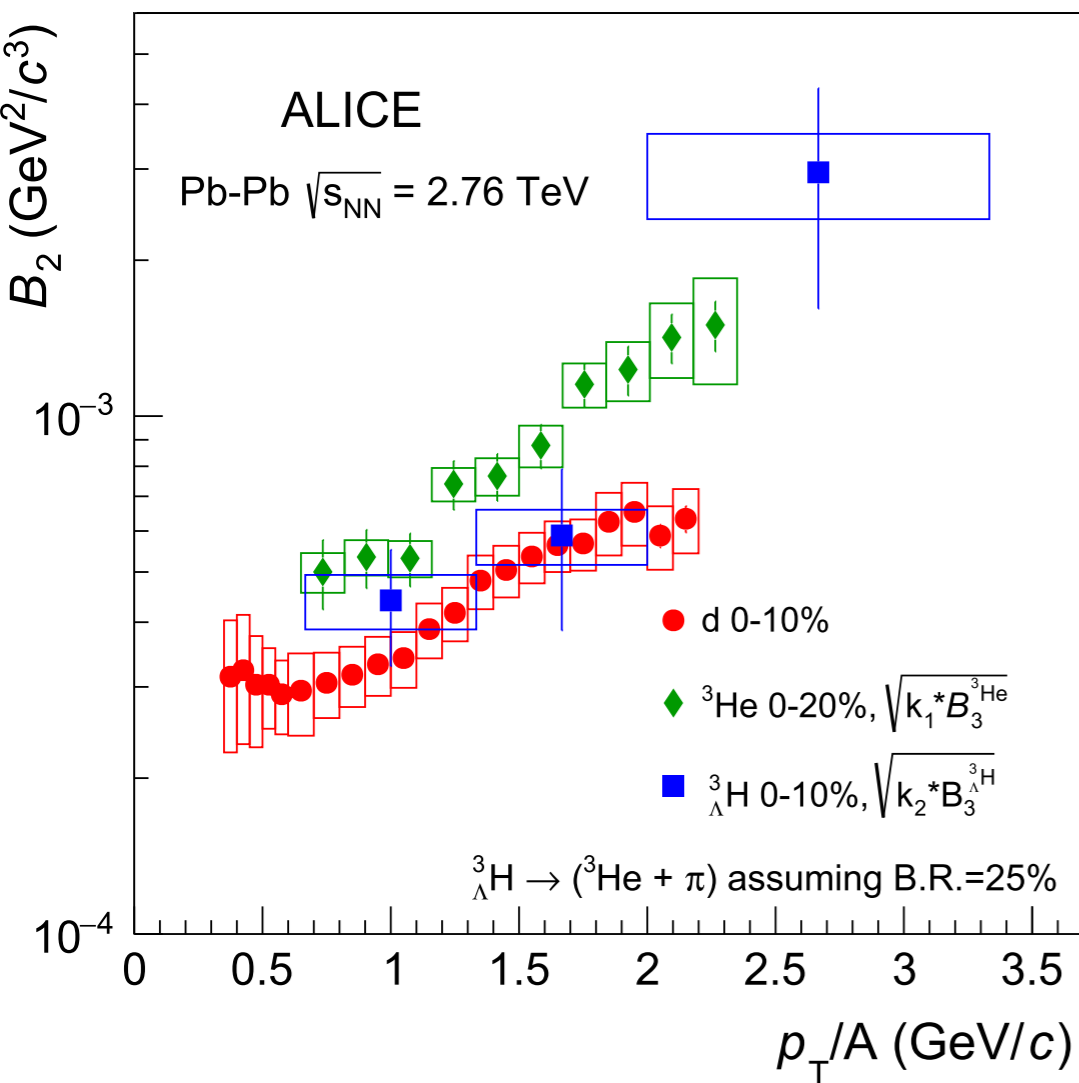
[21] J. Zhu, Nucl. Phys. A 904 (2013) 551c.

[22] C. Rappold, et al., Nucl. Phys. A 913 (2013) 170.

[23] ALICE Collaboration, J. Adam, et al., Phys. Lett. B 754 (2016) 360.

${}^3_{\Lambda}\text{H}$ coalescence parameter details

- Λ , p and n close in the phase space at the *kinetic freeze-out* can form a(n) (anti-)hypertriton
- B_A is expected to be independent from p_T and centrality



- B_3 is computed for ${}^3_{\Lambda}\text{H}$ according to the above equation
 - ${}^3\text{H}$ measured p_T spectra from this analysis
 - p and Λ spectra respectively from [9] and [10]
- $B_3^{3_{\Lambda}\text{H}}$ is compared with B_2^d and $B_3^{3\text{He}}$ obtained in [11]
 - ${}^3\text{He}$ B_3 is scaled to B_2 through the scaling factor k_1
 - ${}^3_{\Lambda}\text{H}$ B_3 is scaled to B_2 through the scaling factor k_2

$$k_1 = \frac{m_d^2}{M_{3\text{He}} m_p} \quad k_2 = \frac{m_d^2 m_{\Lambda}}{m_p^2 M_{3_{\Lambda}\text{H}}}$$

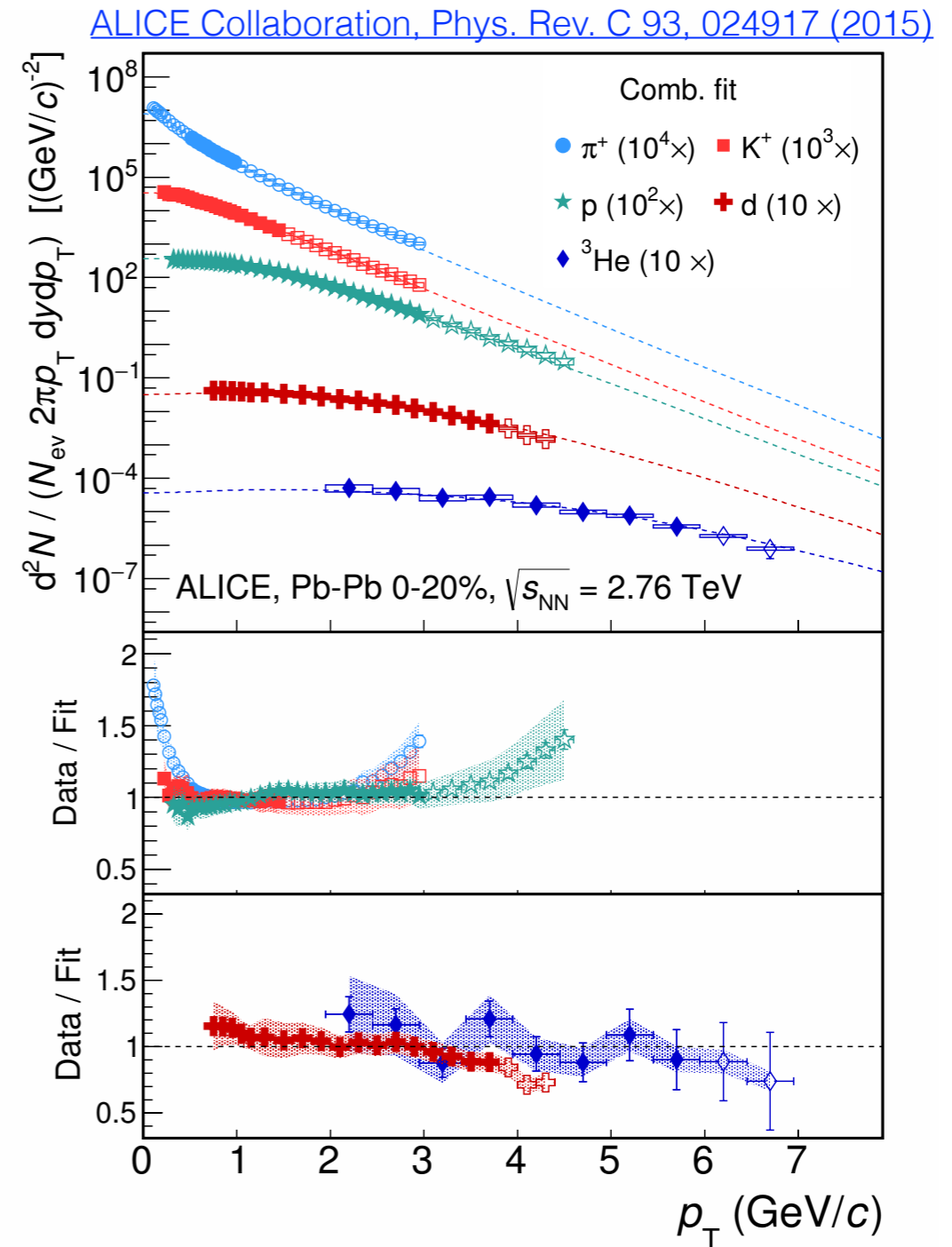
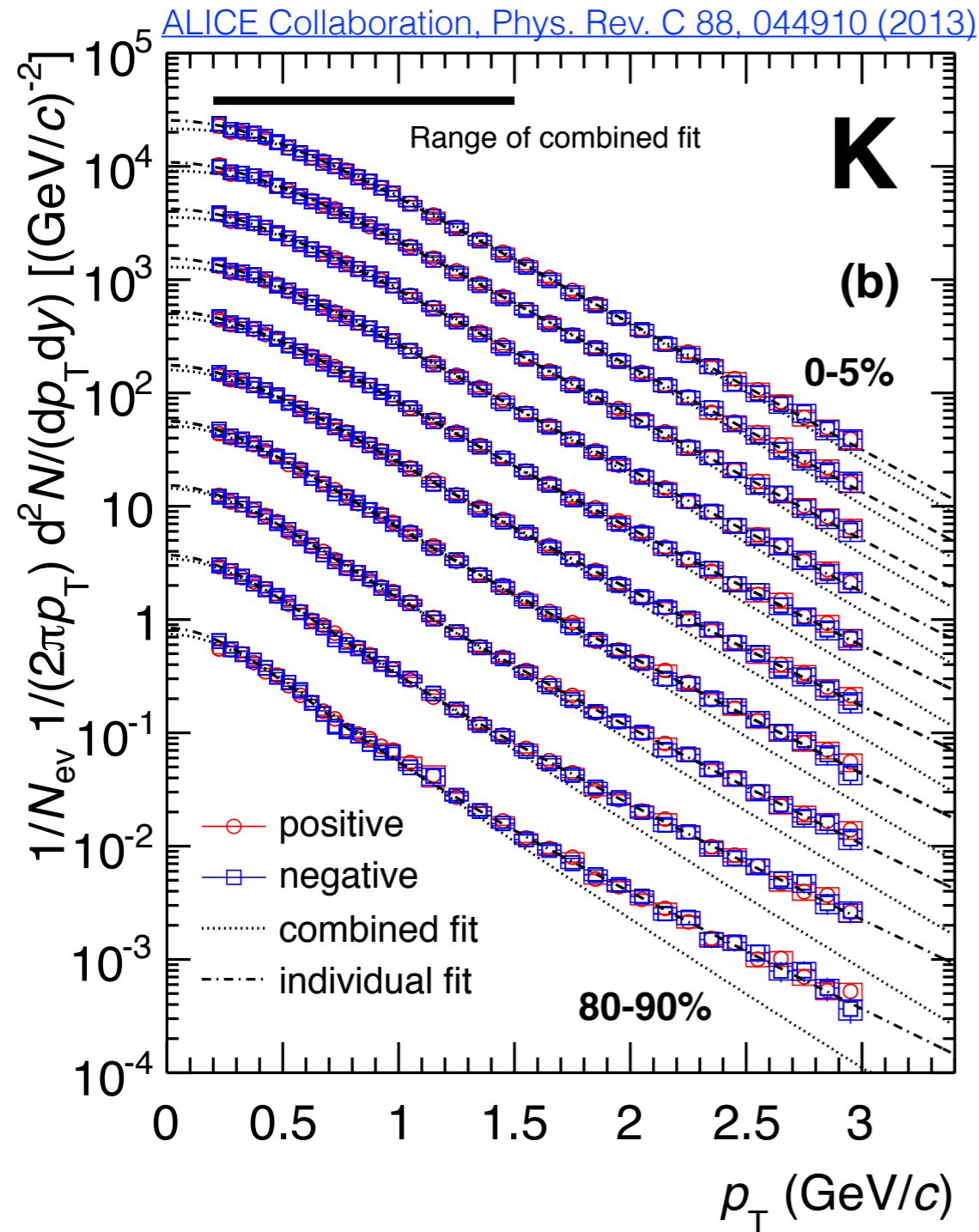
- ${}^3\text{H}$ coalescence parameter is not flat as function of p_T contrary to the simple coalescence model predictions
- Model does not take Λ into account characteristics of the emitting source
- Behaviour similar to the one observed for d and ${}^3\text{He}$

[9] ALICE Collaboration Phys. Rev. C 88, (2013) 044910

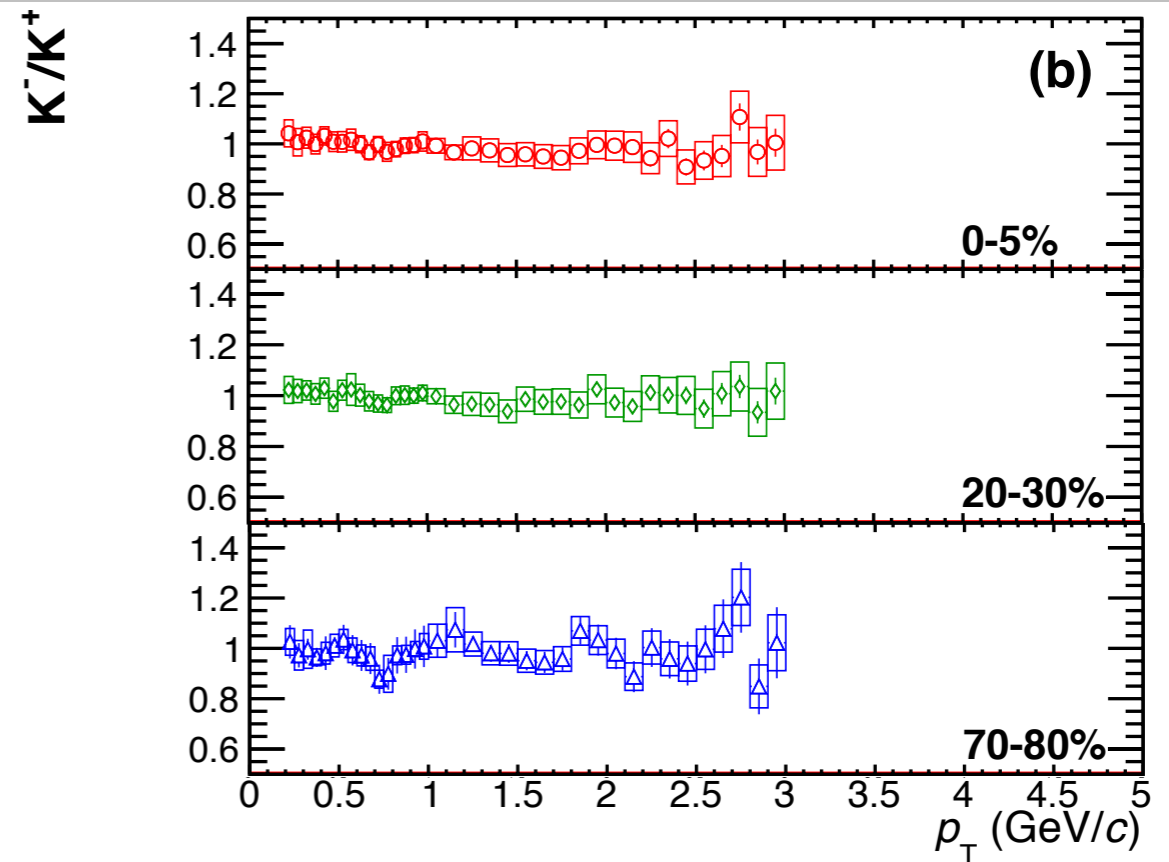
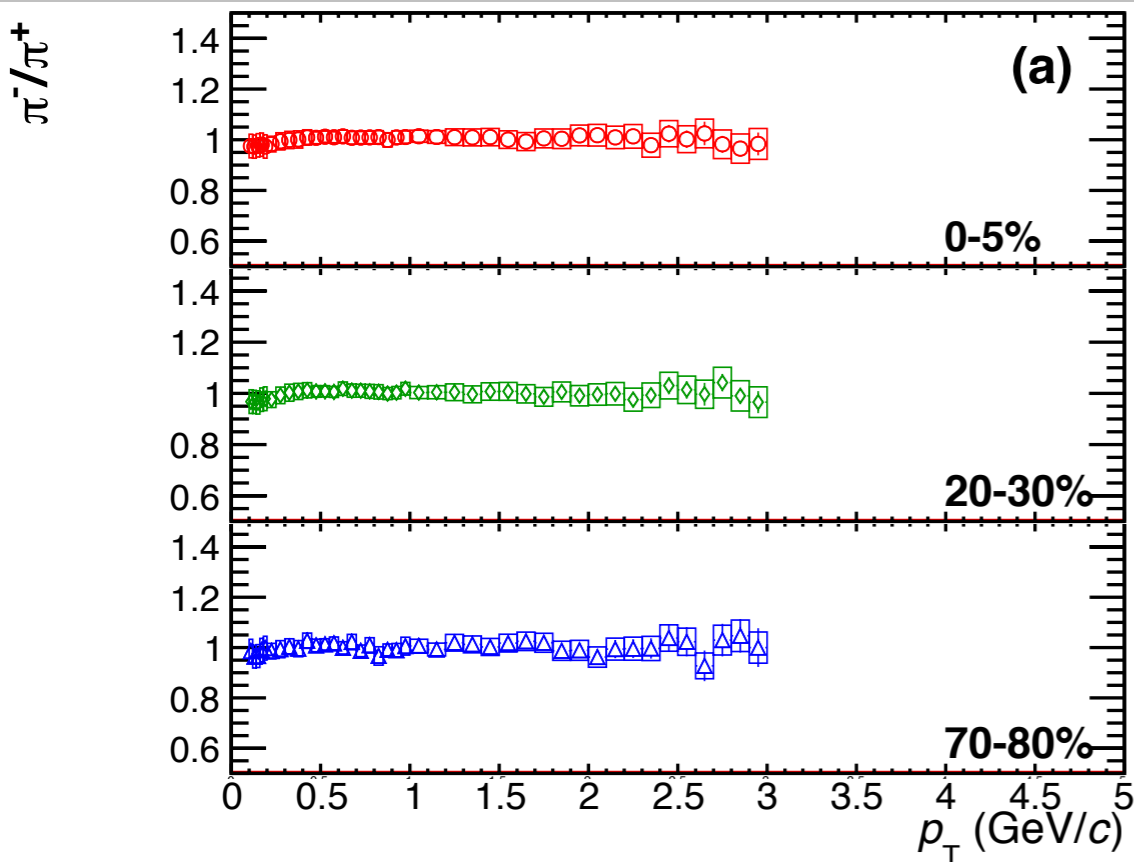
[10] ALICE Collaboration Phys. Rev. Lett. 111, (2013) 22301

[11] ALICE Collaboration Phys. Rev. C 93 (2016) 024917

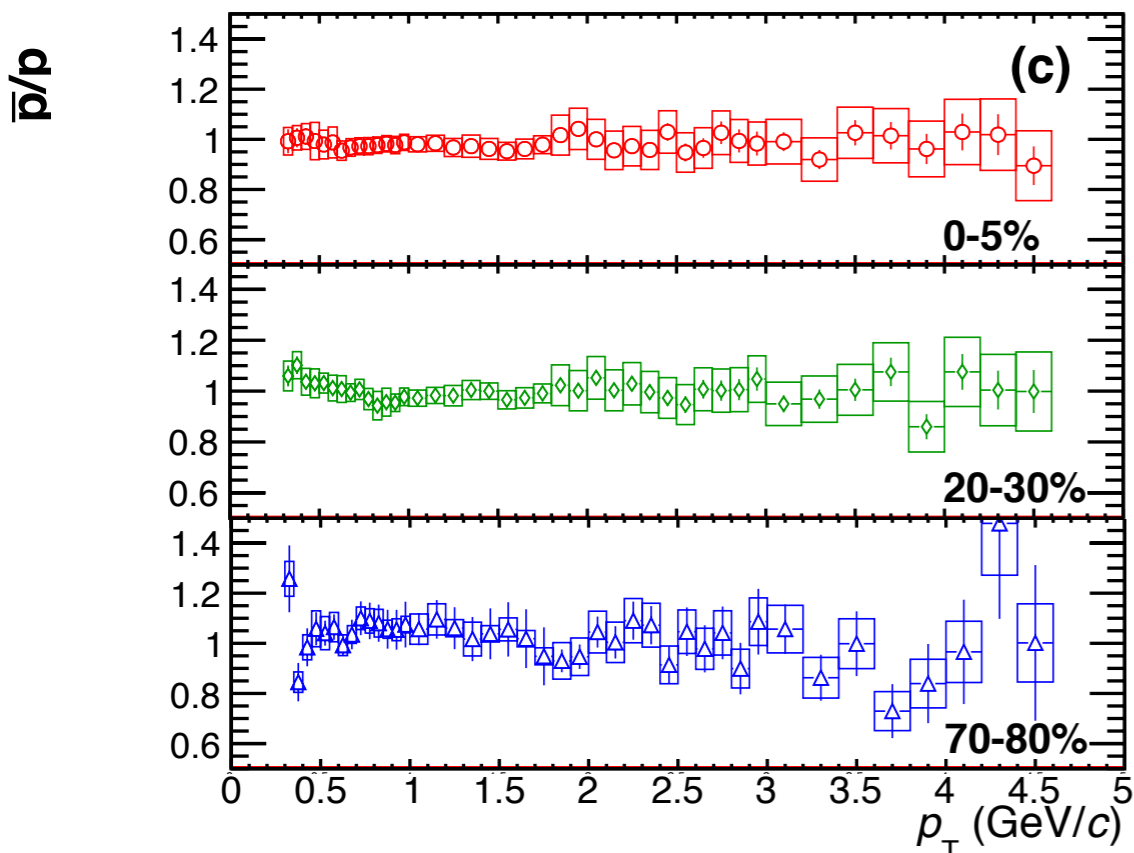
Blast Wave distribution



Antimatter-to-matter ratio

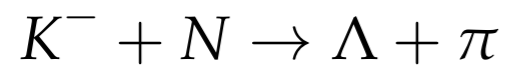


[ALICE Collaboration, Phys. Rev. C 88, 044910 \(2013\)](#)



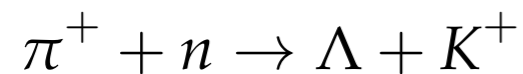
Hypernuclei production mechanisms

Strangeness exchange



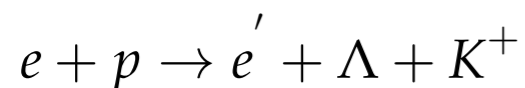
- A transfer of the s-quark from the incident meson to the struck baryon

Associated production



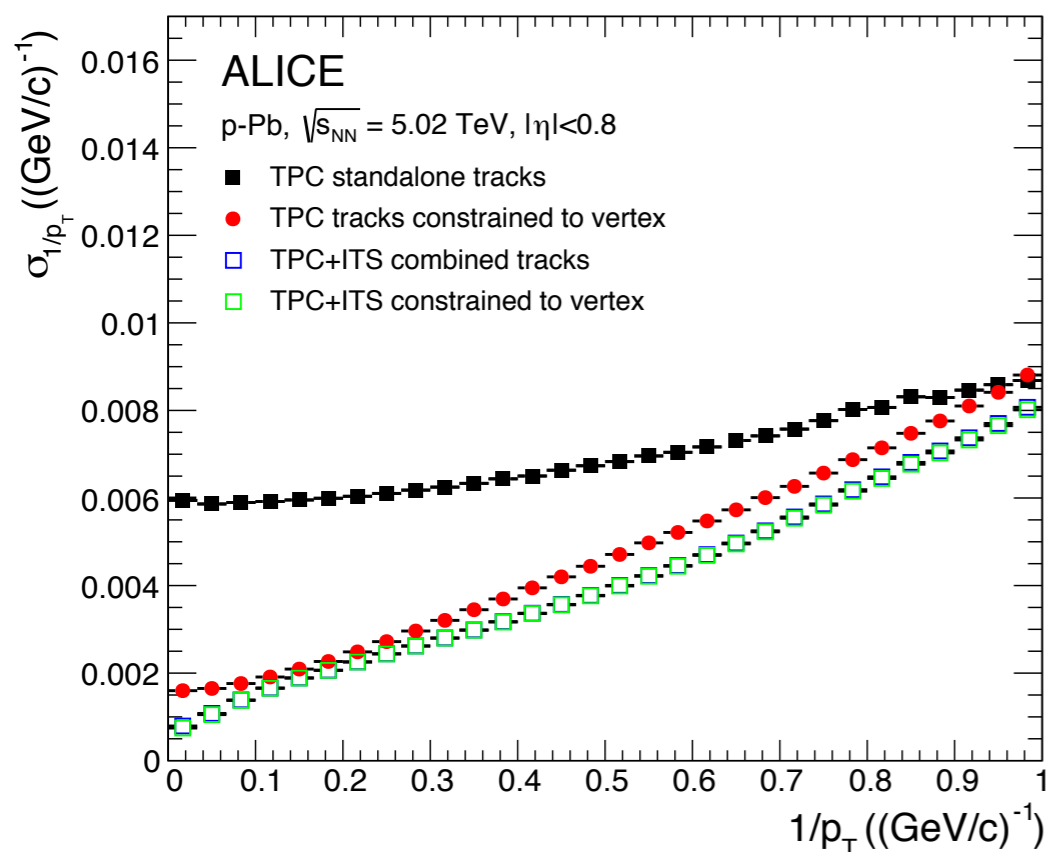
- Proceeds by the creation of $s\bar{s}$ pair by the incident meson

Electroproduction

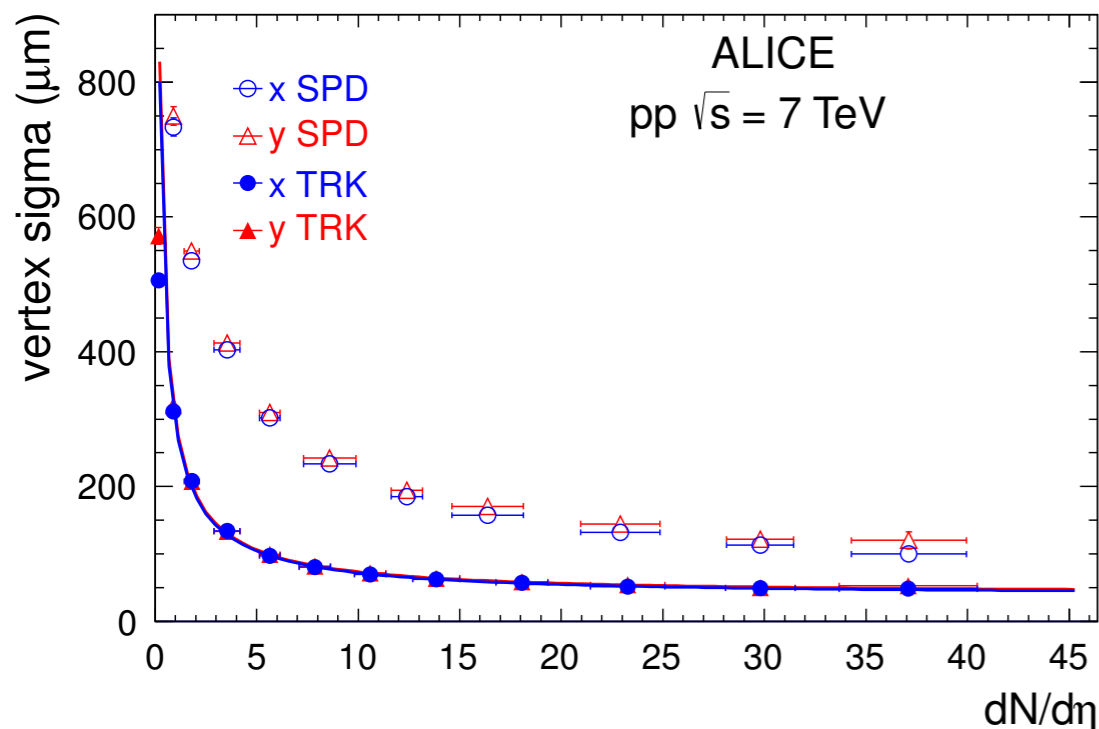


- Electroproduction of strangeness on protons in the very forward direction
- Virtual photon associated can be regarded as quasi-real

- Heavy ion collision as the superposition of the interactions between the constituent nucleons of colliding nuclei
- Key parameters:
 - N_{part} : number of nucleons participating in the interactions
 - N_{coll} : number of binary collisions between nucleons
 - ➔ correlated with impact parameter of the collision
- Assumptions:
 - nucleons point like and independent inside the colliding nuclei
 - only hadronic interactions are considered
 - each interaction does not deflect the trajectories of colliding nucleons
- It allows to calculate:
 - the interaction probability
 - N_{coll} and N_{part}
 - Size of the overlap region between the colliding nuclei



- Momentum resolution $\frac{\sigma_{p_T}}{p_T} = p_T \sigma_{1/p_T}$
 - TPC standalone tracks 1-6% (1-10 GeV/c)
 - resolution improved when constraining the tracks to the primary vertex and when requiring the ITS



- Primary vertex resolution
 - better resolution with full tracks than using only SPD
 - scale with the charged particle multiplicity